TOPICS IN STABILITY ANALYSIS OF MULTI-LAYER HELE-SHAW AND POROUS MEDIA FLOWS

A Dissertation

by

CRAIG ROBERT GIN

Submitted to the Office of Graduate and Professional Studies of
Texas A&M University
in partial fulfillment of the requirements for the degree of

DOCTOR OF PHILOSOPHY

Chair of Committee,	Prabir Daripa
Committee Members,	Harold Boas
	Stephen Fulling
	Peter Howard
	Vivek Sarin
Head of Department,	Emil Straube

August 2015

Major Subject: Mathematics

ABSTRACT

We study the linear stability of multi-layer Hele-Shaw flows. This topic has many useful applications including the design of efficient enhanced oil recovery techniques. We study four problems: two in a rectilinear flow geometry and two in a radial flow geometry. The first of these involves a characterization of the eigenvalues and eigenfunctions of the eigenvalue problem which results from the stability analysis of three-layer rectilinear flows in which the middle layer has variable viscosity. The resulting eigenvalue problem is a Sturm-Liouville problem in which the eigenvalues appear in the boundary conditions. For the case of an increasing viscous profile, we find that there is an infinite number of eigenvalues that increase without bound. By connecting the problem to a related regular Sturm-Liouville problem, we are able to prove the completeness of the eigenfunctions in a certain Sobolev space. We then provide an in-depth analysis of the case where the viscous profile of the middle layer is exponential. We find an explicit sequence of numbers which alternate with the eigenvalues.

The second problem involves the stability of three-layer rectilinear Hele-Shaw flows in which there is diffusion of polymer within the middle layer of fluid. We first reformulate the eigenvalue problem using dimensionless quantities. We then revisit an old theorem about the stabilizing effect of diffusion and give a new proof. An efficient and accurate pseudo-spectral Chebyshev method is used to show that the stabilizing effect of diffusion is, in fact, drastic.

We proceed to consider the stability of multi-layer Hele-Shaw flows in a radial flow geometry. We first study the case of an arbitrary number of fluid layers with constant viscosity. We provide upper bounds on the growth rate of disturbances

and use them to provide conditions for stabilization of the flow. We also show that the equations for rectilinear flow can be obtained as a certain limit of radial flow. For the specific case of three-layer flows, we give exact expressions for the growth rate and explore the asymptotic limits of a thick and thin intermediate layer. We finish by using these exact expressions to study the effects of important parameters of the problem. We conclude that large values of interfacial tension can completely stabilize the flow and that decreasing the curvature of the interfaces by pumping in additional fluid has a non-monotonic effect on stability.

We then consider three-layer radial flows in which the intermediate layer has variable viscosity. In order to use a similar analysis to that which is done in the previous problems, we define a change of variables that fixes the basic solution. In this new coordinate system, we are able to formulate the eigenvalue problem that governs the growth rate of disturbances. We define a measure based on the eigenvalue problem which leads to a Hilbert space in which the problem is self-adjoint. We also derive upper bounds on the growth rate, analogous to ones previously found for variable viscosity rectilinear flows. We then undertake a numerical study of the eigenvalue problem and find that variable viscosity flows, if chosen properly, can be less unstable than constant viscosity flows.

Finally, we give details on our numerical method which is used throughout.

DEDICATION

I would like to dedicate this to my wife, Taylor, who stood beside me the entire time that I worked on this dissertation. When the work was difficult for me, she felt it just as much. I am extremely grateful for her encouragement. I would also like to thank my parents who have supported me throughout my academic career.

ACKNOWLEDGEMENTS

First and foremost, I would like to thank my advisor, Dr. Daripa, for all of his help and guidance. I would also like to thank my committee members for their helpful comments. Finally, I would like to thank the TAMU Department of Mathematics for supporting me the last several years.

TABLE OF CONTENTS

Page

LIST OF FIGURES

FIGURE Page

LIST OF TABLES

TABLE Page

1. INTRODUCTION

1.1 Motivation

Hydrodynamic stability is a broad subject that makes use of many areas of mathematics and is applicable to a vast array of physical problems. The study of different types of instabilities can provide a framework with which to understand many important phenomena that occur in fluid flows. One such type of instability is Saffman-Taylor instability (or viscous fingering), which occurs when a less viscous fluid drives a more viscous fluid. This type of instability is most often studied in the context of porous media or Hele-Shaw flows. My research aims to further the understanding of this subject.

Viscous fingering is important in many different applications. These include sugar refinement [44], the underground storage of gas [60], fixed bed regeneration in chemical processing, hydrology, filtration [45], petrology [8], cell fragmentation, the growth of tumors, mixing in multi-phase flow, crystal growth, and flow in granular media [40]. However, the main application that drives my research is oil recovery. The primary oil recovery process relies on the natural pressure in the reservoir. However, typically only 5-15% of the oil in the reservoir is recovered through primary recovery. Secondary recovery processes use some type of external source to create pressure to drive out additional oil. Typically, this consists of pumping water into the reservoir. Because water is less viscous than oil, this process is subject to viscous fingering, which is one of the primary mechanisms that limits the amount of oil that can be recovered through water-flooding. After secondary recovery, still only 30-50% of the oil is recovered [73].

Due to factors such as increases in oil prices and a desire for domestic sources

of oil, there has been a resurgence in seeking novel ways to increase the amount of oil we can recover from existing wells. One approach is chemical enhanced oil recovery (EOR), which consists of pumping a series of complex fluids of varying rheological properties (such as viscosity, etc.) into the reservoir (see Figure 1.1). An understanding of this process and the underlying stability can help engineers to choose fluids with properties that can maximize the amount of recovered oil. This process is much more complicated than that of secondary recovery and is worthy of in-depth study.

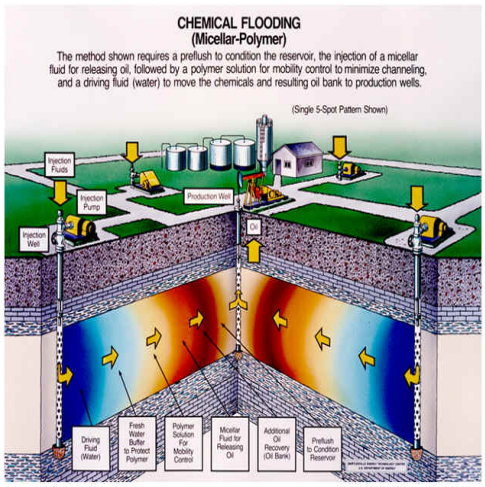

Figure 1.1: Chemical flooding (drawing courtesy of the Department of Energy National Energy Technology Laboratory)

1.2 Hele-Shaw Flows

It is common practice to study Saffman-Taylor instability through Hele-Shaw flows, which are flows between two fixed plates with a thin gap between them [63] (see Figure 1.2a and Figure 1.2b). It is customary to average across the thin gap and consider the average velocity of the fluid in a two-dimensional domain. The averaged

velocity, $\mathbf{u}$, satisfies

$$\nabla p = -\frac{12\mu}{b^2}\mathbf{u}, \tag{1.1}$$

where p is the pressure, μ the viscosity, and b the width of the gap between the plates. Equation (1.1) is known as Darcy's Law [15], and also holds for homogeneous porous media flows with constant permeability $K = b^2/12$. Therefore, Hele-Shaw flows are a good model of porous media flows. For more discussion on the similarity of these flows, see [17].

Beyond just their applicability to porous media flows, Hele-Shaw flows have long been studied as an interesting mathematical object in their own right. In the absence of interfacial tension between different fluids, the problem is well-studied using conformal mappings and the tools of complex analysis [13, 14, 39, 46, 62, 66]. However, the problem becomes much more challenging for the physically relevant case of non-zero interfacial tension. A strong mathematical understanding of this problem is of great practical importance. Some work has been done on various aspects of the well-posedness of the problem [4, 35, 36, 38, 78, 79] as well as asymptotic analysis in the case of small interfacial tension [61, 67, 69, 70]. There are also important numerical studies [9, 49, 50, 57, 58].

The linear stability analysis of two fluids of different viscosities in a Hele-Shaw cell was first investigated by Saffman and Taylor [64] and in porous media by Chuoke, van Meurs, and van der Poel [10]. Both of these groups studied the stability of flows with a linear displacement and an initially planar interface. This configuration is shown in Figure 1.2a and will be referred to as rectilinear flow. However, for oil recovery, the fluid is injected into the reservoir and moves outward radially from the injection well. The stability of this system, with an initially circular interface, was first studied by Bataille [3] and Wilson [76] and later by Paterson [60]. This

configuration, which we refer to as radial flow, is shown in Figure 1.2b.

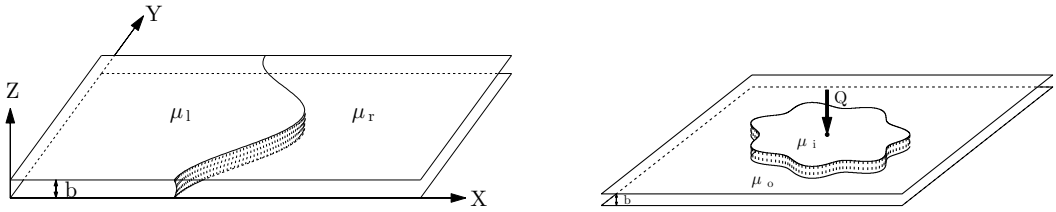

(a) (b)

Figure 1.2: Fluid flow in a Hele-Shaw cell. The two flow configurations are (a) rectilinear flow and (b) radial flow.

Recently there have been many studies of the stability of Hele-Shaw flows with more complex physics. These include tapered Hele-Shaw cells [1], the effects of viscous normal stresses, viscous pressure and/or wetting effects at the interface [2, 32, 33, 48, 56], inertial effects [31], and flows of chemically reactive [43] or non-Newtonian fluids [12, 37], but almost all involve two layers of fluids separated by one interface initially.

1.3 Multi-layer Hele-Shaw Flows

Recall that in chemical EOR, a series of fluids is pumped into the reservoir. Therefore, it is practical to consider the stability of Hele-Shaw flows with more than two different regions of fluid. Additionally, the fluids used are often complicated chemical mixtures such as in alkali-surfactant-polymer (ASP) flooding. In such methods, polymer is used in the driving fluid in order to increase its viscosity. If the concentration of polymer varies throughout the fluid, the viscosity of the fluid can also vary. We will consider such flows below within Newtonian flow approximation and will refer to them as variable viscosity flows. However, the fluids used in ASP flood-

ing are non-Newtonian and experience diffusion of the polymer species. All of these aspects lead to new challenges in the modeling process and change the stability of the system.

In this work, we study the linear stability of multi-layer (i.e. more than two-layer) and/or variable viscosity Hele-Shaw flows. In order to provide a basis for understanding the content below, we begin with a brief description of the linear stability analysis of Hele-Shaw flows from Daripa [16].

The purpose of linear stability analysis is to study the stability of some solution to a differential equation to small perturbations. The analysis starts with some "basic" solution, typically an equilibrium solution, to the equations. Denote this solution by F_0. We then consider a solution which is an asymptotic expansion of the form

$$F = F_0 + \epsilon F_1 + \epsilon^2 F_2 + ... \tag{1.2}$$

Plugging this into the equations and keeping only terms which are linear with respect to ϵ (hence the term **linear** stability), we have an equation for F_1 which depends on the basic solution. We study the growth or decay of F_1.

For the case of variable viscosity Hele-Shaw flows (neglecting the effects of diffusion), the governing equations, which hold within each layer of fluid, are (see [16])

$$\nabla \cdot \mathbf{u} = 0, \qquad \nabla\, p = -\mu\, \mathbf{u}, \qquad \frac{\partial \mu}{\partial t} + \mathbf{u} \cdot \nabla \mu = 0, \tag{1.3}$$

where $\mathbf{u}$ denotes the averaged velocity of the fluid, p the pressure, and μ the viscosity. The first equation $(1.3)_1$ is the continuity equation for incompressible flow, the second equation $(1.3)_2$ is Darcy's law, and the third equation $(1.3)_3$ is an advection equation for viscosity. This last equation comes from the advection equation

for the concentration of polymer and the assumption that viscosity is an invertible function of concentration. Note that, with a slight abuse of notation, we have scaled the viscosity by $b^2/12$. Therefore, equation $(1.3)_2$ agrees with equation (1.1). At an interface between two immiscible fluids with position given by η, there are two conditions:

$$\frac{D\eta}{Dt} = \mathbf{u} \cdot \hat{n}, \qquad [p] = T \nabla \cdot \hat{n}, \tag{1.4}$$

where D/Dt denotes the material derivative, $[p]$ the jump in pressure across the interface, and T the interfacial tension. Equation $(1.4)_1$ is called the kinematic boundary condition and ensures that fluid particles on the interface remain on the interface. Equation $(1.4)_2$ is the dynamic boundary condition and requires that the pressure jump across the interface is proportional to the curvature.

For rectilinear flow, our basic solution consists of all fluid moving with constant velocity U in the positive x-direction (see Figure 1.2a) with planar interfaces separating the fluids. In a moving frame with velocity $(U, 0)$, this solution is stationary. If we denote the velocity by $\mathbf{u} = (u, v)$, then the basic solution in the moving frame can be written as $(u_0 = 0, v_0 = 0, p_0, \mu_0)$ where μ_0 is the initial viscous profile and p_0 is obtained by integrating $(1.3)_2$. As stated above, we perturb this solution and plug in the asymptotic expansion. For the first-order solution, which we denote by F_1 above, we use the ansatz

$$(u_1, v_1, p_1, \mu_1) = (f(x), \tau(x), \psi(x), \phi(x))e^{iky+\sigma t}. \tag{1.5}$$

Here, we have decomposed the solution into its Fourier modes in the y-direction, and we may study each mode separately. Therefore, the disturbance with wavenumber k grows (or decays) exponentially like $e^{\sigma t}$. If σ is negative for all k, we say that

the basic solution is stable, but if σ is positive for some wavenumber, the solution is unstable.

For radial flow, the process is similar except that the basic solution consists of fluid being pumped into the cell at the origin with flow rate Q, all the fluid moving outward radially with velocity $Q/(2\pi r)$, and the fluids separated by circular interfaces. Additionally, the ansatz (1.5) becomes

$$(u_1, v_1, p_1, \mu_1) = (f(r), \tau(r), \psi(r), \phi(r))e^{in\theta + \int_0^t \sigma(s)ds}, \tag{1.6}$$

for an integer, n. Here, we use polar coordinates and u and v denote the r and θ components of velocity, respectively.

In both cases, the use of the ansatz (1.5) or (1.6) results in an eigenvalue problem with the growth rate σ as the eigenvalue. Therefore, the understanding of this eigenvalue problem results in an understanding of the stability of the flow. For multi-layer Hele-Shaw flows, there will be multiple eigenvalues for each wavenumber, and for variable viscosity flows there will be infinitely many. Of particular importance is the maximum value of σ over all eigenvalues and all wavenumbers, which is called the most dangerous mode. The wavenumber associated with this mode is called the most dangerous wavenumber. These two numbers are of great practical importance.

To show the importance of these two values, we consider the case of two-layer rectilinear Hele-Shaw flow with constant viscosity fluids. The growth rate in this scenario, which we refer to as the Saffman-Taylor growth rate and denote by σ_{ST}, is well-known and found in standard books on Hydrodynamic Stability (see [34]). The growth rate is given by the formula

$$\sigma_{ST} = \frac{Uk(\mu_r - \mu_l) - Tk^3}{\mu_r + \mu_l}, \tag{1.7}$$

where μ_l and μ_r are the viscosities of the left fluid and right fluid, respectively, U is the velocity of the basic flow, and T is the interfacial tension. Note that when $\mu_r > \mu_l$, that is, the less viscous fluid is driving the more viscous fluid, the Saffman-Taylor growth rate will be positive for small values of k (i.e. long waves). Therefore, the flow will be unstable. However, the presence of interfacial tension stabilizes short waves (large k) and causes σ_{ST} to have a maximum value for positive k. The maximum value of σ_{ST}, which we denote by σ^*_{ST} and the corresponding wavenumber k^* are

$$\sigma^*_{ST} = \frac{2T}{\mu_r + \mu_l}\left(\frac{U(\mu_r - \mu_l)}{3T}\right)^{3/2}, \qquad k^* = \sqrt{\frac{U(\mu_r - \mu_l)}{3T}}. \tag{1.8}$$

In unstable Hele-Shaw flows, the interface, which begins as nearly planar, eventually forms long finger-like structures (see Figure 1.3). Hence, this instability is called viscous fingering. Because a disturbance with wavenumber k^* grows the fastest, the number of fingers that form initially is k^*. Eventually, nonlinear effects begin to dominate and the fingers can break up or merge, resulting in very complicated dynamics of the interface (see Figure 1.4). The amount of time it takes for these nonlinear effects to take over is given by the linear growth rate. In oil recovery, it is useful to suppress the growth of the fingers, which can be achieved by reducing the value of σ^*_{ST}.

For radial Hele-Shaw flows, the growth rate for two-layer flows with constant viscosity is given by

$$\sigma_{ST} = \frac{Qn}{2\pi R^2}\frac{\mu_o - \mu_i}{\mu_o + \mu_i} - \frac{Q}{2\pi R^2} - \frac{T}{\mu_o + \mu_i}\frac{n\,(n^2-1)}{R^3}, \tag{1.9}$$

where μ_i and μ_o are the viscosities of the inner and outer fluid, respectively, R is the distance from the circular interface to the origin, and Q is the injection rate. This

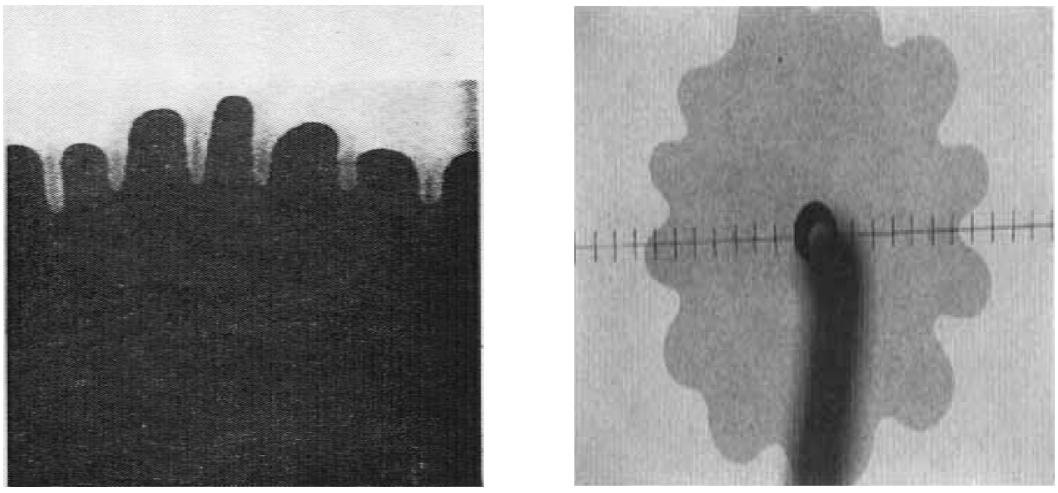

(a) (b)

Figure 1.3: (a) Viscous fingering in rectilinear Hele-Shaw flow (photo from Chuoke et. al. [10]). (b) Viscous fingering in radial Hele-Shaw flow (photo from Cardoso and Woods [8]).

term is similar to the rectilinear Saffman-Taylor growth rate, but it contains an extra term due to the curvature of the interface of the basic flow. Again, the wavenumber n which maximizes the growth rate predicts the number of fingers that form.

1.3.1 Previous Work

There are some recent studies of the linear stability of multi-layer Hele-Shaw flows. For rectilinear flow, Gorell and Homsy studied the case of three layers of fluid in which the intermediate fluid has variable viscosity [42]. They considered the case in which there is no interfacial tension acting on the trailing interface and also no viscous jump at the trailing interface. Therefore, there was only one interface between immiscible fluids. In this paper, they formulated the eigenvalue problem and investigated optimal viscous profiles for the middle layer given N, the total amount of polymer added. They were able to find some asymptotic results for small N and provided numerical results for larger values of N.

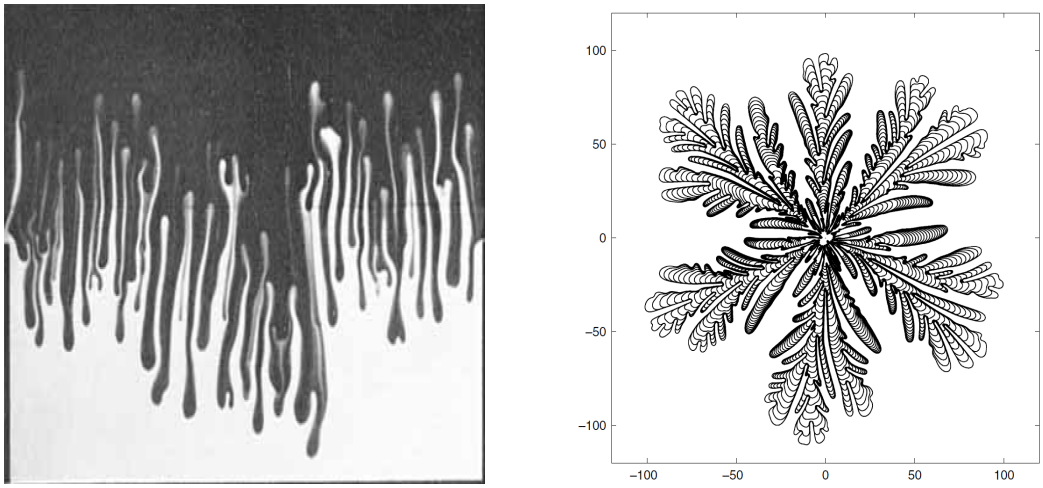

(a) (b)

Figure 1.4: (a) Tip-splitting in rectilinear Hele-Shaw flow (photo from Wooding [77]). (b) Tip-Splitting in radial Hele-Shaw flow (figure from Lowengrub [50]).

This work was followed by several others about three-layer rectilinear variable viscosity flows in which only the leading interface has a viscous jump and interfacial tension. In [59], Pasa proved the existence of an optimal viscous profile by using properties of weakly continuous functionals on Hilbert spaces. This optimal profile was found using a finite difference method in [6]. The convergence of this finite difference method was proven in [7]. In [26], Daripa and Pasa used the finite difference method to obtain upper bounds on the growth rate. Using these upper bounds, they got lower bounds on the length of the middle layer and total amount of polymer required to make the flow more stable than a Hele-Shaw flow without the middle layer.

In [8], Cardoso and Woods studied three-layer constant viscosity Hele-Shaw flows in both the rectilinear and radial geometries. For rectilinear flow, they were able to write the growth rate as a solution to a quadratic equation. This was the first paper that considered Hele-Shaw flows with two interfaces that have viscous jumps

and interfacial tension. Daripa performed more in-depth studies of this problem in [17] and [18]. In [17], Daripa found a formula for a critical value of the viscosity of the middle layer that minimizes the bandwidth of unstable waves. He also provided upper bounds on the growth rate and investigated the effect of the length of the middle layer on the instability. In [18], Daripa investigated long and short waves separately in order to obtain both upper and lower bounds for stable and unstable waves.

Daripa and Pasa [27] were the first to study variable viscosity Hele-Shaw flows in which there were two interfaces with viscous jumps and interfacial tension. They found an upper bound on the growth rate by using a finite difference discretization of the eigenvalue problem and using techniques from numerical analysis. They also provided an upper bound for three-layer constant viscosity flows using the variational form of the problem. In [28], Daripa and Pasa used the variational form to find an upper bound for three-layer variable viscosity flows. It is important, here, to examine the form of these upper bounds. Let μ_l and μ_r denote the viscosities of the left-most and right-most fluids and let $\mu(x)$ for $x \in [-L, 0]$ denote the viscosity of the fluid in the middle layer. Let T_0 denote the interfacial tension of the leading interface and T_1 the interfacial tension of the trailing interface. Let U denote the velocity of the basic flow. Then, for a fixed wavenumber k, the upper bound given in [28] is

$$\sigma < \max\left\{\frac{Uk(\mu_r - \mu(0)) - T_0k^3}{\mu_r}, \frac{Uk(\mu(-L) - \mu_l) - T_1k^3}{\mu_l}, \frac{U}{\mu_l}\max_x \mu'(x)\right\}. \quad (1.10)$$

Compare the first term of this upper bound with the Saffman-Taylor growth rate (1.7). It is not the Saffman-Taylor growth rate of the leading interface because the denominator term is not $\mu_r + \mu(0)$, but it can be thought of as an "effective" Saffman-Taylor growth rate because it is comparable to the Saffman-Taylor growth rate and

contains only terms that pertain to the leading interface. Likewise, the second term is an effective Saffman-Taylor growth rate of the trailing interface. The last term represents the instability that can come from a middle layer with an increasing (in the direction of the flow) viscous profile. Therefore, the upper bound has decoupled the instability due to the leading interface, the trailing interface, and the middle layer itself.

In (1.10), only the first two terms depend on the wavenumber. Recall that we are interested in the maximum value of σ over all wavenumbers. An upper bound on this value can easily be found from (1.10) by maximizing each term over all k. This expression is given by

$$\sigma < \max\left\{ \frac{2T_0}{\mu_r}\left(\frac{U(\mu_r-\mu(0))}{3T_0}\right)^{3/2}, \frac{2T_1}{\mu_l}\left(\frac{U(\mu(-L)-\mu_l)}{3T_1}\right)^{3/2}, \frac{U}{\mu_l}\max_x \mu'(x)\right\}. \tag{1.11}$$

These upper bounds are useful because their dependence on the parameters of the problem is explicit and clear. Therefore, they provide simple principles to design improved oil recovery techniques.

In [16], Daripa extended the previous upper bounds results to flows with an arbitrary number of fluid layers, both of constant and variable viscosity. In addition, he improved upon previous upper bounds in the three-layer case. Using these new upper bounds, he found some necessary conditions (see [19] also) on the middle layer viscosity and the interfacial tensions at the interfaces of three-layer constant viscosity flows in order for the flow to be less unstable than a corresponding two-layer flow. He also gave conditions on the number of intermediate layers of equal length with equal viscous jumps at the interfaces that are required in order to obtain an arbitrary level of stability. In [19], Daripa produced similar results for Hele-Shaw flows in which the fluids have different densities and gravity acts in the direction of the flow.

This couples the effect of Saffman-Taylor instability with the famous Rayleigh-Taylor instability, which occurs when a more dense fluid is above a less dense fluid. In [22], Daripa and Ding extended the results of [17] to an arbitrary number of layers. They found critical values of the viscosities of all intermediate fluids in order to minimize the unstable bandwidth.

In recent years, Daripa and Ding have published a series of papers about choosing an optimal viscous profile for the intermediate layer of three-layer Hele-Shaw flows. In [21], Daripa and Ding used numerical methods to investigate optimal viscous profiles. First, they found the optimal constant viscosity for the middle layer. Then they proceeded to find the optimal increasing viscous profile among a selection of four different types: linear, exponential, sinusoidal, and quadratic. They found that for a very thin middle layer, a linear viscous profile is best, while an exponential viscous profile was optimal for moderate and large middle layers. Finally, they considered some non-monotonic viscous profiles. In [20], Daripa used the previously found upper bounds to predict the optimal viscous profile. This method is much easier than the one used in [21], but yields the same results. In [24], Daripa and Ding found optimal viscous profiles for two intermediate variable viscosity layers in four-layer Hele-Shaw flows. They used these optimal profiles to show that almost complete stabilization can be obtained by large values of interfacial tension at the external interfaces.

In chemical EOR, a fluid with variable concentration of polymer in which the concentration profile is not linear would experience diffusion of the polymer species. Two recent works have addressed this practical issue. In [29], Daripa and Pasa formulated the linear stability problem for three-layer Hele-Shaw flows with variable viscosity middle layer and diffusion of the polymer species. They found some upper bounds on the growth rate and proved that diffusion made the flow less unstable. Then, in [30], Daripa and Pasa used a finite difference discretization of the problem

to produce upper bounds on the growth rate and again prove the stabilizing effect of diffusion.

The subject is much less developed for the case of radial flows of multiple fluid regions. The stability of three-layer radial Hele-Shaw flows of constant viscosity was studied by Cardoso and Woods [8], but only in the restricted case when the inner interface is completely stable. They were able to find an explicit formula for the growth rate of the unstable outer interface. For such flows, when the disturbances of the outer interface become large enough, the inner interface reaches the outer interface and the intermediate layer breaks up into drops. Using the formula for the growth rate to find the most dangerous wavenumber at the time of break up, Cardoso and Woods were able to predict the number of drops that formed.

1.4 Outline

The purpose of our work is to advance the study of the linear stability of multi-layer Hele-Shaw flows. This dissertation includes four projects, each a separate chapter. We give an outline below.

1.4.1 Three-layer Rectilinear Hele-Shaw Flows with an Exponential Viscous Profile

Recall that in Daripa and Ding [21], it was found that for most three-layer rectilinear variable viscosity Hele-Shaw flows, an exponential viscous profile was the optimal choice for the middle layer. Additionally, Mungan [55] showed experimentally that an exponential viscous profile easily outperforms a constant viscosity middle layer which uses the same amount of polymer. Uzoigwe et. al. [74] confirmed this with numerical simulations. Therefore, it is important to better understand the stability of flows with an exponential viscous profile in the middle layer.

We undertake this study in chapter 2. We start by giving some results which hold for any variable viscosity flow in which the viscous profile of the middle layer is

increasing in the direction of flow. We are able to show that, for certain wavenumbers and increasing viscous profiles, there is an infinite set of discrete eigenvalues and that the corresponding eigenfunctions are complete in a certain Hilbert space. We then apply this theory to the case of an exponential viscous profile. Not only are we able to verify the theoretical results for this specific case, but also provide a sequence of numbers that alternate with the eigenvalues of the system, thereby giving both upper and lower bounds for the eigenvalues. We verify this with numerical computation of the eigenvalues using a pseudo-spectral method. Finally, we investigate several limiting cases. The first is when the viscous profile of the middle layer approaches a constant viscosity, both in the case of a fixed-length middle layer and also as the length of the middle layer goes to infinity. The second limiting case is when the length of the middle layer approaches zero.

1.4.2 Three-layer Rectilinear Hele-Shaw Flows with Diffusion in the Middle Layer

In chapter 3, we also study the linear stability analysis of three-layer rectilinear Hele-Shaw flows in which the middle layer has variable viscosity due to varying concentration of polymer. In this case, however, we consider the diffusion of polymer in the middle layer and its effect on the stability of the system. Recall that there are two previous papers on diffusion in Hele-Shaw flows ([29] and [30]). However, there are still many open questions related to this problem so we attempt to address some of them in chapter 3.

To begin, we reformulate the eigenvalue problem in a non-dimensional form. The dimensionless quantities of interest are the Peclet number, which is a ratio of the advection rate and the diffusion rate, and the Capillary number, which is a ratio of viscous forces and interfacial tension. In the previous papers, a linear relationship between the viscosity and the concentration of polymer was assumed. We broaden the

range of the model to include both a linear and exponential dependence of viscosity on polymer concentration. In [29], upper bounds were used to prove the stabilizing effects of diffusion. However, the assumption was made that the eigenfunctions are independent of the diffusion coefficient. We strengthen this theorem by proving it without this assumption.

In an unpublished manuscript by Daripa and Ding [23], they use a finite difference method to solve the eigenvalue problem and find that even a small amount of diffusion can significantly stabilize the flow. However, their numerical method is slow and the low order of accuracy results in numerical diffusion. Therefore, we conclude this chapter by doing a numerical study of the eigenvalue problem using an improved numerical method. To achieve a high order of accuracy, we use a pseudo-spectral Chebyshev method. We are able to confirm the results of Daripa and Ding [23] and show that if optimal viscous profiles are used, a moderate amount of diffusion can reduce the instability of the flow by several factors.

1.4.3 Multi-layer Radial Hele-Shaw Flows

The next two chapters deal with the linear stability analysis of multi-layer radial Hele-Shaw flows, a subject which is largely unexplored. In chapter 4, we study multi-layer flows in which each layer has a constant viscosity. We formulate the eigenvalue problem for an arbitrary number of fluid regions. Additionally, we provide rigorous upper bounds for the eigenvalues using a variational approach. Using these upper bounds, we are able to show that a flow can be reduced to an arbitrary level of instability by adding a prescribed number of intermediate layers of fluid with small positive viscous jumps at the interfaces. For the case of three-layer flows, exact expressions for the growth rates are given. We find that unlike for rectilinear flows, the growth rate can be complex for radial flows. Using these expressions for

the growth rate, we explore the dependence of the growth rate on several different physically relevant parameters. Finally, we show that the results on rectilinear flow obtained by Daripa [16, 17] can be recovered as a limiting case of the results on radial flow.

1.4.4 Three-layer Radial Hele-Shaw Flows with Variable Viscosity

In chapter 5, we study the linear stability of three-layer radial Hele-Shaw flows in which the intermediate layer of fluid has variable viscosity. This problem is more difficult than the corresponding problem for rectilinear flow because the basic flow is time-dependent. We remedy this situation by using an appropriate change of variables that makes the basic solution independent of time. In these new coordinates, we derive the eigenvalue problem that governs the stability of the flow. We investigate the limiting case of constant viscosity and use it to compare the growth rate in our new coordinate system to the physical growth rate, which we obtained for constant viscosity in chapter 4. We use variational principles to find upper bounds on the growth rate that are analogous to those found by Daripa and Pasa in [28]. We then characterize the eigenvalues and eigenfunctions of the problem and identify an appropriate Hilbert space in which to work.

Finally, we use a pseudo-spectral method to numerically compute the eigenvalues. Through numerical computation of the eigenvalues, we investigate the relationship between the growth rate in the new coordinate system and the growth rate in the physical coordinate system. We also study the change in the growth rate over time for a given viscous profile. Finally, we investigate optimal viscous profiles and give a strategy to decrease the instability by using a variable viscous profile.

1.4.5 Numerical Method

In chapter 6, we describe the numerical method that we use throughout the previous chapters to compute the eigenvalues. This method is a pseudo-spectral Chebyshev method and we find that it performs favorably to some previous alternatives. Finally, we conclude in chapter 7.

2. A STUDY OF A NON-STANDARD EIGENVALUE PROBLEM AND ITS APPLICATION TO THREE-LAYER IMMISCIBLE POROUS MEDIA AND HELE-SHAW FLOWS WITH EXPONENTIAL VISCOUS PROFILE*

2.1 Introduction

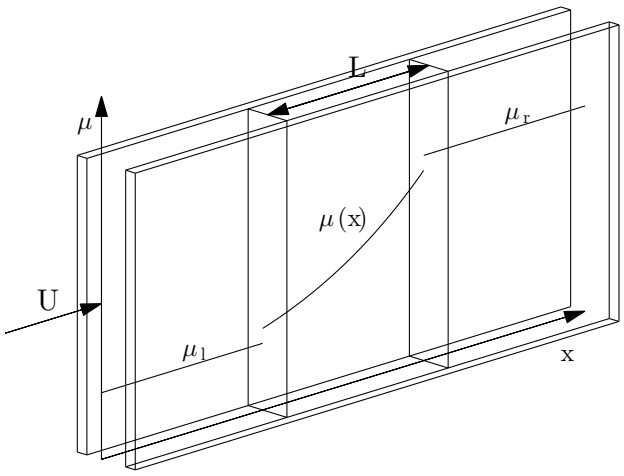

Figure 2.1: Three layer rectilinear Hele-Shaw flow in which the middle layer has a smooth viscous profile.

Numerous studies have been done on three-layer rectilinear Hele-Shaw flows in which the intermediate layer has variable viscosity. These include the derivation of upper bounds on the growth rate ([28]) and numerical studies of optimal profiles ([21]). However, two things that have not been done are a characterization of the eigenvalues and eigenfunctions of the associated eigenvalue problem and in-depth studies of particular viscous profiles. We tackle both of these issues here.

*The findings of this chapter have been adapted and reprinted with permission from "A Study of a Non-Standard Eigenvalue Problem and its Application to Three-Layer Immiscible Porous Media and Hele-Shaw Flows with Exponential Viscous Profile" by C. Gin and P. Daripa, 2015. *J. Math. Fluid Mech.*, **17**: pp.155-181, Copyright 2015 Springer Science and Business Media.

In this chapter, we briefly describe the three-layer case from [16] before moving onto our studies of the associated eigenvalue problem. In section 2.3, we characterize the eigenvalues and eigenfunctions for arbitrary increasing viscous profiles. Then, in section 2.4, we turn to the specific case of an exponential viscous profile. We find some analytical results about the size of the eigenvalues and then verify them with numerical results.

2.2 Preliminaries

The following derivation is taken from Daripa [16]. Three regions of fluid in the Hele-Shaw cell (Fig. 2.1) are separated by sharp interfaces that are initially at $x = -L$ and $x = 0$ along which there is interfacial tension given by the values T_1 and T_0, respectively. The fluid upstream ($-\infty < x < -L$) has a constant viscosity μ_l and a velocity $\mathbf{u} = (U, 0)$ as $x \to -\infty$. The fluid downstream ($0 < x < \infty$) has a constant viscosity μ_r. The middle layer, which has length L, contains a fluid of viscosity $\mu(x,t)$ where $\mu_l < \mu(x,t) < \mu_r$ for all $x \in (-L, 0)$. We assume here that $\mu(x,t)$ and its spatial derivative are continuous.

The governing equations for the system are

$$\nabla \cdot \mathbf{u} = 0, \quad \nabla p = -\mu\,\mathbf{u}, \quad \frac{\partial \mu}{\partial t} + \mathbf{u} \cdot \nabla \mu = 0. \tag{2.1}$$

Equation $(2.1)_1$ is the continuity equation for incompressible flow, equation $(2.1)_2$ is Darcy's Law, and equation $(2.1)_3$ is an advection equation for viscosity, which holds when viscosity is an invertible function of the concentration of polymer.

This system admits a simple basic solution in which all of the fluid moves with constant velocity $\mathbf{u} = (U, 0)$ and the interfaces remain planar. The pressure, $p(x)$, of the basic solution is found by integrating $(2.1)_2$. In a moving frame with velocity U, the basic solution is stationary. We perturb the basic solution by $(\tilde{u}, \tilde{v}, \tilde{p}, \tilde{\mu})$. The

linearized equations for $\tilde{\mathbf{u}} = (\tilde{u}, \tilde{v})$, $\tilde{p}$ and $\tilde{\mu}$ are

$$\nabla \cdot \tilde{\mathbf{u}} = 0, \quad \nabla \tilde{p} = -\mu \tilde{\mathbf{u}} - \tilde{\mu}(U, 0), \quad \frac{\partial \tilde{\mu}}{\partial t} + \tilde{u}\frac{d\mu}{dx} = 0. \tag{2.2}$$

We decompose the disturbances into normal modes. They take the form

$$(\tilde{u}, \tilde{v}, \tilde{p}, \tilde{\mu}) = (f(x), \tau(x), \psi(x), \phi(x))e^{iky+\sigma t}, \tag{2.3}$$

where k is the wavenumber and σ is the growth rate of the disturbances. This ansatz is used in the linearized equations (2.2) along with linearized kinematic and dynamic boundary conditions to derive an eigenvalue problem for $f(x)$. The eigenvalue problem is

$$\left.\begin{aligned} &(\mu f')' - (k^2\mu - \tfrac{k^2 U}{\sigma}\mu')f = 0, && -L < x < 0 \\ &\mu(-L)f'(-L) = \left(\mu_l k - \tfrac{E_1}{\sigma}\right) f(-L) \\ &-\mu(0)f'(0) = \left(\mu_r k - \tfrac{E_0}{\sigma}\right) f(0), \end{aligned}\right\} \tag{2.4}$$

where $E_0 = k^2 U(\mu_r - \mu(0)) - T_0 k^4$ and $E_1 = k^2 U(\mu(-L) - \mu_l) - T_1 k^4$.

In order to simplify our analysis of these equations, we use the variable $\lambda = \frac{1}{\sigma}$. Then, the above equations can be written as

$$\left.\begin{aligned} &(\mu f')' - (k^2\mu - k^2 U\mu'\lambda)f = 0, && -L < x < 0 \\ &\mu(-L)f'(-L) = (\mu_l k - E_1\lambda)f(-L) \\ &-\mu(0)f'(0) = (\mu_r k - E_0\lambda)f(0). \end{aligned}\right\} \tag{2.5}$$

Equation $(2.5)_1$ looks like a typical Sturm-Liouville problem, but note that the boundary conditions $(2.5)_2$ and $(2.5)_3$ contain the spectral parameter, λ. Therefore, much of the classical theory does not apply.

The maximum value of the growth rate, σ, determines the stability of the system. Therefore, it is of physical significance to understand the minimum value of λ and its dependence on the parameters. To this end, we study the nature of the spectrum of the above differential operator. A complete understanding of the eigenvalues and eigenfunctions can shed light on strategies to stabilize the flow through control of the physical quantities.

2.3 Characterization of the Eigenvalues and Eigenfunctions

We now investigate the nature of the eigenvalues and eigenfunctions associated with the eigenvalue problem (2.5). This section follows the techniques of Churchill [11].

Theorem 1. *Let $f(x)$ solve (2.5). Let E_0, E_1, U, k, μ_l, $\mu_r > 0$. Let $\mu(x)$ be a positive, strictly increasing function in $C^1([-L, 0])$. Then the eigenvalue problem has a countably infinite number of real eigenvalues that can be ordered*

$$0 < \lambda_0 < \lambda_1 < \lambda_2 < ...$$

with the property that for the corresponding eigenfunctions, $\{f_i\}_{i=0}^{\infty}$, f_i has exactly i zeros in the interval $(-L, 0)$. Additionally, the eigenfunctions are continuous with a continuous derivative.

Proof. The fact that there are a countably infinite number of real eigenvalues that can be ordered and corresponding eigenfunctions with the prescribed number of zeros is proven by Ince [47, p. 232-233] in Theorem I and Theorem II using

$$a = -L, \qquad b = 0, \qquad K(x, \lambda) = \mu(x), \qquad G(x, \lambda) = k^2 \left(\mu(x) - U\mu'(x)\lambda\right),$$
$$\alpha = \mu(-L), \qquad \alpha' = \mu_l k - E_1\lambda, \qquad \beta = \mu(0), \qquad \beta' = \mu_r k - E_0\lambda.$$

The regularity of the eigenfunctions comes from the existence theorem of Ince [47, p. 73]. It remains to show that all of the eigenvalues are both real and positive. Let (f, λ) satisfy the eigenvalue problem. We take the inner product of $(2.5)_1$ with $f^*(x)$, the complex conjugate of $f(x)$.

$$\int_{-L}^{0} (\mu(x) f'(x))' f^*(x) dx - k^2 \int_{-L}^{0} (\mu(x) - U\mu'(x)\lambda) |f(x)|^2 dx = 0.$$

We then perform integration by parts on the first integral and use the boundary conditions $(2.5)_2$ and $(2.5)_3$ to get

$$\begin{aligned} &- (\mu_r k - E_0 \lambda) |f(0)|^2 - (\mu_l k - E_1 \lambda) |f(-L)|^2 - \int_{-L}^{0} \mu(x) |f'(x)|^2 dx \\ &- k^2 \int_{-L}^{0} (\mu(x) - U\mu'(x)\lambda) |f(x)|^2 dx = 0. \end{aligned}$$

Solving for λ,

$$\lambda = \frac{\mu_r k |f(0)|^2 + \mu_l k |f(-L)|^2 + \int_{-L}^{0} \mu(x) \left\{ |f'(x)|^2 + k^2 |f(x)|^2 \right\} dx}{E_0 |f(0)|^2 + E_1 |f(-L)|^2 + k^2 U \int_{-L}^{0} \mu'(x) |f(x)|^2}. \tag{2.6}$$

Note that all terms are real and positive. Therefore, $\lambda > 0$ [28]. □

2.3.1 An Orthogonality Property of the Eigenfunctions

We now note the following property of the eigenfunctions for later use. Let f_i and f_j be eigenfunctions of (2.5). Then

$$\begin{aligned}\left(\mu f_i' f_j - \mu f_i f_j'\right)' &= (\mu f_i')' f_j + \mu f_i' f_j' - (\mu f_j')' f_i - \mu f_i' f_j' \\ &= (\mu f_i')' f_j - (\mu f_j')' f_i \\ &= (k^2\mu - k^2 U\mu'\lambda_i) f_i f_j - (k^2\mu - k^2 U\mu'\lambda_j) f_i f_j \\ &= (\lambda_j - \lambda_i) k^2 U\mu' f_i f_j. \end{aligned} \tag{2.7}$$

Therefore,

$$\begin{aligned}(\lambda_j - \lambda_i)\int_{-L}^{0} f_i f_j (k^2 U\mu')dx &= \int_{-L}^{0} \left(\mu f_i' f_j - \mu f_i f_j'\right)' dx \\ &= \left(\mu f_i' f_j - \mu f_i f_j'\right)\Big|_{-L}^{0} \\ &= (\mu(0) f_i'(0) f_j(0) - \mu(0) f_i(0) f_j'(0)) - \\ &\quad (\mu(-L) f_i'(-L) f_j(-L) - \mu(-L) f_i(-L) f_j'(-L)) \\ &= [-(\mu_r k - E_0\lambda_i) f_i(0) f_j(0) + (\mu_r k - E_0\lambda_j) f_i(0) f_j(0)] - \\ &\quad [(\mu_l k - E_1\lambda_i) f_i(-L) f_j(-L) - (\mu_l k - E_1\lambda_j) f_i(-L) f_j(-L)] \\ &= (\lambda_i - \lambda_j) E_0 f_i(0) f_j(0) + (\lambda_i - \lambda_j) E_1 f_i(-L) f_j(-L). \end{aligned}$$

And therefore, if $\lambda_i \neq \lambda_j$,

$$\int_{-L}^{0} f_i f_j (k^2 U\mu')dx + E_0 f_i(0) f_j(0) + E_1 f_i(-L) f_j(-L) = 0. \tag{2.8}$$

2.3.2 Transformation to a Regular Sturm-Liouville Problem

We now wish to connect the eigenvalue problem (2.5) to a related eigenvalue problem whose properties are known. Since $f_0(x)$ is non-zero on $[-L, 0]$, we can define the function, for each integer $i \geq 1$,

$$F_i(x) = \mu(x)\frac{d}{dx}\left(\frac{f_i(x)}{f_0(x)}\right). \tag{2.9}$$

We use the following lemma.

Lemma 1. *Let E_0, E_1, U, k, μ_l, $\mu_r > 0$ and $\mu(x)$ be a positive, strictly increasing function in $C^1([-L, 0])$. Additionally, let $\mu(x)$ be twice differentiable. Let $\{F_i\}_{i=1}^{\infty}$ be the set of functions defined by (2.9) where $\{f_i\}_{i=0}^{\infty}$ is the set of eigenfunctions of (2.5) corresponding to the eigenvalues $\{\lambda_i\}_{i=0}^{\infty}$. Then for each $i \in \mathbb{N}$, (F_i, λ_i) is a solution to the regular Sturm-Liouville problem*

$$\begin{cases} \left(\frac{f_0^2}{\mu'}F'\right)' + \left\{\frac{2}{(\mu')^2}(\mu' f_0 f_0'' - \mu'(f_0')^2 + \mu'' f_0 f_0') + \frac{k^2 U f_0^2}{\mu}(\lambda - \lambda_0)\right\} F = 0 \\ E_1 f_0(-L)F'(-L) = \{k^2 U \mu'(-L) f_0(-L) - 2E_1 f_0'(-L)\}F(-L) \\ -E_0 f_0(0)F'(0) = \{k^2 U \mu'(0) f_0(0) + 2E_0 f_0'(0)\}F(0). \end{cases} \tag{2.10}$$

Furthermore, there are no other solutions to (2.10).

Proof. Let $i \in \mathbb{N}$. By using the quotient rule on equation (2.9) as well as equation (2.7), we get

$$(f_0^2 F_i)' = (\mu f_0 f_i' - \mu f_i f_0')' = (\lambda_0 - \lambda_i)k^2 U \mu' f_0 f_i. \tag{2.11}$$

Therefore,

$$\left(\frac{1}{k^2 U \mu' f_0^2}(f_0^2 F_i)'\right)' = \left((\lambda_0 - \lambda_i)\frac{f_i}{f_0}\right)',$$

which can be rewritten as

$$\left(\frac{1}{k^2U\mu' f_0^2}(f_0^2F_i)'\right)' + (\lambda_i - \lambda_0)\frac{F_i}{\mu} = 0. \tag{2.12}$$

But note that for any twice differentiable function $F(x)$ and constant λ,

$$\begin{aligned}
&\left(\frac{1}{k^2U\mu' f_0^2}(f_0^2F)'\right)' + (\lambda - \lambda_0)\frac{F}{\mu} \\
=&\left(\frac{1}{k^2U\mu'}F' + \frac{2f_0'}{k^2U\mu' f_0}F\right)' + (\lambda - \lambda_0)\frac{F}{\mu} \\
=&\frac{1}{k^2U\mu'}F'' - \frac{\mu''}{k^2U(\mu')^2}F' + \frac{2f_0'}{k^2U\mu' f_0}F' \\
&+ \frac{2}{k^2U}\left(\frac{\mu' f_0 f_0'' - f_0'(\mu' f_0' + \mu'' f_0)}{(\mu')^2 f_0^2}\right)F + (\lambda - \lambda_0)\frac{F}{\mu} \\
=&\frac{f_0^2}{\mu'}F'' + \left(\frac{2f_0 f_0'}{\mu'} - \frac{\mu'' f_0^2}{(\mu')^2}\right)F' \\
&+ \frac{2}{(\mu')^2}(\mu' f_0 f_0'' - \mu'(f_0')^2 + \mu'' f_0 f_0')F + k^2U f_0^2(\lambda - \lambda_0)\frac{F}{\mu} \\
=&\left(\frac{f_0^2}{\mu'}F'\right)' + \left\{\frac{2}{(\mu')^2}(\mu' f_0 f_0'' - \mu'(f_0')^2 + \mu'' f_0 f_0') + \frac{k^2U f_0^2}{\mu}(\lambda - \lambda_0)\right\}F.
\end{aligned}$$

Therefore

$$\left(\frac{f_0^2}{\mu'}F_i'\right)' + \left\{\frac{2}{(\mu')^2}(\mu' f_0 f_0'' - \mu'(f_0')^2 + \mu'' f_0 f_0') + \frac{k^2U f_0^2}{\mu}(\lambda_i - \lambda_0)\right\}F_i = 0, \tag{2.13}$$

which is the equation $(2.10)_1$. Next, we find the boundary conditions satisfied by the F_i. It follows from relation (2.9) that

$$F_i = \mu\left(\frac{f_i}{f_0}\right)' = \frac{\mu f_0 f_i' - \mu f_i f_0'}{f_0^2},$$

and therefore

$$\mu f_i' = f_0 F_i + f_i\frac{\mu f_0'}{f_0}. \tag{2.14}$$

Replacing the left-hand side of (2.14) with the boundary condition $(2.5)_2$, we obtain

$$(\mu_l k - E_1\lambda_i)f_i(-L) = f_0(-L)F_i(-L) + f_i(-L)\frac{\mu(-L)f_0'(-L)}{f_0(-L)}.$$

Adding and subtracting the term $E_1\lambda_0 f_i(-L)$ and rearranging terms,

$$f_0(-L)F_i(-L) + \left\{\frac{\mu(-L)f_0'(-L)}{f_0(-L)} - (\mu_l k - E_1\lambda_0)\right\} f_i(-L) - E_1(\lambda_0 - \lambda_i)f_i(-L) = 0.$$

The term inside the brackets is zero due to the boundary condition $(2.5)_2$ for f_0. Therefore,

$$f_0(-L)F_i(-L) - E_1(\lambda_0 - \lambda_i)f_i(-L) = 0. \tag{2.15}$$

Using (2.11), we have that

$$(\lambda_0 - \lambda_i)k^2 U\mu' f_0 f_i = (f_0^2 F_i)' = f_0^2 F_i' + 2f_0 f_0' F_i.$$

Therefore,

$$(\lambda_0 - \lambda_i)f_i(-L) = \frac{1}{k^2 U\mu'(-L)}\{f_0(-L)F_i'(-L) + 2f_0'(-L)F_i(-L)\}. \tag{2.16}$$

Combining equations (2.15) and (2.16),

$$f_0(-L)F_i(-L) - \frac{E_1}{k^2 U\mu'(-L)}\{f_0(-L)F_i'(-L) + 2f_0'(-L)F_i(-L)\} = 0,$$

and therefore

$$E_1 f_0(-L)F_i'(-L) = \{k^2 U\mu'(-L)f_0(-L) - 2E_1 f_0'(-L)\}F_i(-L), \tag{2.17}$$

which is the boundary condition $(2.10)_2$. We repeat this process for the boundary condition at $x = 0$. Replacing the left-hand side of (2.14) with the boundary condition $(2.5)_3$,

$$f_0(0)F_i(0) + \left\{ \frac{\mu(0)f_0'(0)}{f_0(0)} + (\mu_r k - E_0\lambda_i) \right\} f_i(0) = 0.$$

Using the boundary condition $(2.5)_3$ for f_0,

$$f_0(0)F_i(0) + E_0(\lambda_0 - \lambda_i)f_i(0) = 0. \tag{2.18}$$

From (2.11), we get

$$(\lambda_0 - \lambda_i)f_i(0) = \frac{1}{k^2 U\mu'(0)}\{f_0(0)F_i'(0) + 2f_0'(0)F_i(0)\}. \tag{2.19}$$

Combining equations (2.18) and (2.19),

$$f_0(0)F_i(0) + \frac{E_0}{k^2 U\mu'(0)}\{f_0(0)F_i'(0) + 2f_0'(0)F_i(0)\} = 0,$$

and therefore

$$-E_0 f_0(0)F_i'(0) = \{k^2 U\mu'(0)f_0(0) + 2E_0 f_0'(0)\}F_i(0), \tag{2.20}$$

which is the boundary condition $(2.10)_3$. Therefore, from (2.13), (2.17), and (2.20), F_i and λ_i satisfy the system (2.10).

It remains to show that the set $\{(F_i, \lambda_i)\}_{i=1}^{\infty}$ defined by (2.9) is all of the solutions to (2.10). Let $(G(x), \alpha)$ solve (2.10). We will show that $(G, \alpha) = (F_i, \lambda_i)$ for some i.

Define the function

$$g(x) = f_0(x)\left[\int_{-L}^{x} \frac{G(t)}{\mu(t)}dt + C\right], \tag{2.21}$$

where C is given by the expression

$$C = \frac{f_0^2(-L)G'(-L) + 2f_0(-L)f_0'(-L)G(-L)}{(\lambda_0 - \alpha)k^2 U\mu'(-L)f_0^2(-L)}, \qquad \alpha \neq \lambda_0. \tag{2.22}$$

Claim: $g(x)$ and α satisfy (2.5). We prove this below.

Note that

$$g' = f_0\frac{G}{\mu} + f_0'\left[\int_{-L}^{x} \frac{G(t)}{\mu(t)}dt + C\right]. \tag{2.23}$$

Therefore,

$$\begin{aligned}(\mu g')' &= \left(f_0 G + \mu f_0'\left[\int_{-L}^{x} \frac{G(t)}{\mu(t)}dt + C\right]\right)' \\ &= f_0 G' + f_0' G + \mu f_0'\frac{G}{\mu} + (\mu f_0')'\left[\int_{-L}^{x} \frac{G(t)}{\mu(t)}dt + C\right] \\ &= f_0 G' + 2f_0' G + (\mu f_0')'\left[\int_{-L}^{x} \frac{G(t)}{\mu(t)}dt + C\right]. \end{aligned} \tag{2.24}$$

Using (2.21),

$$\begin{aligned}(\mu g')' &= \frac{1}{f_0}(f_0^2 G' + 2f_0 f_0' G) + (\mu f_0')'\frac{g}{f_0} \\ &= \frac{1}{f_0}\left\{(f_0^2 G)' + g(\mu f_0')'\right\}.\end{aligned}$$

We wish to show that $\frac{(\mu g')' - (k^2\mu - k^2 U\mu'\alpha)g}{k^2 U\mu' f_0}$ is a constant. Using the above equality,

$$\begin{aligned}
&\frac{(\mu g')' - (k^2\mu - k^2 U\mu'\alpha)g}{k^2 U\mu' f_0} \\
&= \frac{1}{k^2 U\mu'}\left\{\frac{1}{f_0^2}(f_0^2 G)' + \frac{g}{f_0^2}(\mu f_0')' - \frac{g}{f_0}(k^2\mu - k^2 U\mu'\alpha)\right\} \\
&= \frac{1}{k^2 U\mu' f_0^2}(f_0^2 G)' + \frac{1}{k^2 U\mu' f_0}\left\{\frac{1}{f_0}(\mu f_0')' - (k^2\mu - k^2 U\mu'\alpha)\right\} g \\
&= \frac{1}{k^2 U\mu' f_0^2}(f_0^2 G)' + \frac{1}{k^2 U\mu' f_0}\left\{\frac{1}{f_0}(\mu f_0')' - (k^2\mu - k^2 U\mu'\lambda_0) - k^2 U\mu'(\lambda_0 - \alpha)\right\} g.
\end{aligned}$$

Since (f_0, λ_0) satisfies $(2.5)_1$, we obtain

$$\begin{aligned}
\frac{(\mu g')' - (k^2\mu - k^2 U\mu'\alpha)g}{k^2 U\mu' f_0} &= \frac{1}{k^2 U\mu' f_0^2}(f_0^2 G)' + \frac{1}{k^2 U\mu' f_0}\left\{k^2 U\mu'(\alpha - \lambda_0)\right\} g \\
&= \frac{1}{k^2 U\mu' f_0^2}(f_0^2 G)' + (\alpha - \lambda_0)\frac{g}{f_0}.
\end{aligned}$$

If we take the derivative of this expression, we see that

$$\begin{aligned}
&\left(\frac{1}{k^2 U\mu' f_0^2}(f_0^2 G)' + (\alpha - \lambda_0)\frac{g}{f_0}\right)' = \\
&= \left(\frac{1}{k^2 U\mu' f_0^2}(f_0^2 G)'\right)' + (\alpha - \lambda_0)\left(\frac{g}{f_0}\right)' \\
&= \left(\frac{1}{k^2 U\mu' f_0^2}(f_0^2 G)'\right)' + (\alpha - \lambda_0)\frac{G}{\mu}.
\end{aligned}$$

But this is zero by the equivalence of (2.12) and (2.13) and the fact that (G, α) solves $(2.10)_1$. Therefore, the original expression is equal to some constant, D. That is,

$$\frac{(\mu g')' - (k^2\mu - k^2 U\mu'\alpha)g}{k^2 U\mu' f_0} = D,$$

and therefore,

$$(\mu g')' - (k^2\mu - k^2 U\mu'\alpha)g = Dk^2 U\mu' f_0, \qquad \forall x \in [-L, 0]. \tag{2.25}$$

We now show that $D = 0$ and therefore $g(x)$ and α solve $(2.5)_1$. We replace g in this equation by using our original definition of g, (2.21), along with equation (2.24).

$$\begin{aligned} &f_0 G' + 2f_0' G + (\mu f_0')' \left[\int_{-L}^{x} \frac{G(t)}{\mu(t)} dt + C\right] \\ &- (k^2\mu - k^2 U\mu'\alpha) f_0 \left[\int_{-L}^{x} \frac{G(t)}{\mu(t)} dt + C\right] = Dk^2 U\mu' f_0. \end{aligned}$$

Through some algebraic manipulation and adding and subtracting the term $k^2 U\mu'\lambda_0 f_0$,

$$\begin{aligned} &f_0 G' + 2f_0' G + \left\{(\mu f_0')' - (k^2\mu - k^2 U\mu'\lambda_0) f_0 - k^2 U\mu'(\lambda_0 - \alpha) f_0\right\} \\ &* \left[\int_{-L}^{x} \frac{G(t)}{\mu(t)} dt + C\right] = Dk^2 U\mu' f_0. \end{aligned}$$

Since (f_0, λ_0) solves $(2.5)_1$,

$$f_0 G' + 2f_0' G - k^2 U\mu'(\lambda_0 - \alpha) f_0 \left[\int_{-L}^{x} \frac{G(t)}{\mu(t)} dt + C\right] = Dk^2 U\mu' f_0.$$

Solving for D,

$$D = \frac{1}{k^2 U\mu'} \left(G' + 2\frac{f_0'}{f_0} G\right) - (\lambda_0 - \alpha) \left[\int_{-L}^{x} \frac{G(t)}{\mu(t)} dt + C\right]. \tag{2.26}$$

This expression holds for all values of $x \in [-L, 0]$, so we may choose $x = -L$. Then

$$D = \frac{1}{k^2 U\mu'(-L)} \left(G'(-L) + 2\frac{f_0'(-L)}{f_0(-L)} G(-L)\right) - (\lambda_0 - \alpha) C. \tag{2.27}$$

Using our choice of C from (2.22), we get $D = 0$ as long as $\alpha \neq \lambda_0$.

We now show that $\alpha \neq \lambda_0$ by contradiction. Assume that $\alpha = \lambda_0$. Then, by (2.26)

$$D = \frac{f_0^2(x)G'(x) + 2f_0(x)f_0'(x)G(x)}{k^2U\mu'(x)f_0^2(x)}, \qquad \forall x \in [-L, 0]. \tag{2.28}$$

Note that the numerator above can be expressed as $(f_0^2(x)G(x))'$. Recall that $E_0, E_1 \geq 0$. Therefore, we can consider four separate cases:

1. $E_0, E_1 \neq 0$

   First note that equation $(2.10)_1$ along with the initial conditions $F(c) = \alpha$ and $F'(c) = \beta$ for some point $c \in [-L, 0]$ and some constants α and β has a unique solution [47, p. 73]. By boundary condition $(2.10)_2$, if $G(-L) = 0$ and $E_1 \neq 0$, then $G'(-L) = 0$. Therefore, $G(x) \equiv 0$, which contradicts that G is an eigenfunction of (2.10). Therefore, we can conclude that since $E_1 \neq 0$, $G(-L) \neq 0$. Likewise, since $E_0 \neq 0$, $G(0) \neq 0$.

   When $E_1 \neq 0$, we can rearrange the boundary condition $(2.10)_2$ to get

   $$\frac{f_0^2(-L)G'(-L) + 2f_0(-L)f_0'(-L)G(-L)}{k^2U\mu'(-L)f_0^2(-L)} = \frac{G(-L)}{E_1}.$$

   But by (2.28), the left-hand side of the above equation is D. Therefore, for all $x \in [-L, 0]$,

   $$\frac{(f_0^2(x)G(x))'}{k^2U\mu'(x)f_0^2(x)} = \frac{G(-L)}{E_1}. \tag{2.29}$$

   Multiplying by $k^2U\mu'(x)f_0^2(x)$ and integrating from $-L$ to 0, we get

   $$\int_{-L}^{0} \left(f_0^2(x)G(x)\right)' dx = \int_{-L}^{0} k^2U\mu'(x)f_0^2(x)\frac{G(-L)}{E_1}dx.$$

Evaluating the first term,

$$f_0^2(0)G(0) - f_0^2(-L)G(-L) = k^2U\frac{G(-L)}{E_1}\int_{-L}^{0}\mu'(x)f_0^2(x)dx,$$

and therefore

$$f_0^2(0)G(0) = G(-L)\left\{f_0^2(-L) + \frac{k^2U}{E_1}\int_{-L}^{0}\mu'(x)f_0^2(x)dx\right\}. \tag{2.30}$$

Note that the coefficients of $G(-L)$ and $G(0)$ are both positive. Therefore, $G(-L)$ and $G(0)$ must have the same sign.

When $E_0 \neq 0$, we can rearrange the boundary condition $(2.10)_3$ to get

$$\frac{f_0^2(0)G'(0) + 2f_0(0)f_0'(0)G(0)}{k^2U\mu'(0)f_0^2(0)} = -\frac{G(0)}{E_0}.$$

Again, the left-hand side is equal to D. Therefore, we can combine this with (2.29) to get

$$\frac{G(-L)}{E_1} = -\frac{G(0)}{E_0}. \tag{2.31}$$

This tells us that $G(-L)$ and $G(0)$ have opposite signs, which is a contradiction.

2. $E_0 = 0$ and $E_1 \neq 0$

   When $E_0 = 0$, the boundary condition $(2.10)_3$ for $G(x)$ becomes

$$k^2U\mu'(0)f_0(0)G(0) = 0,$$

which can only be true if $G(0) = 0$. Since $E_1 \neq 0$, equations (2.29) and (2.30) still hold. Also, as seen in the previous case, $E_1 \neq 0$ implies that $G(-L) \neq 0$. However, (2.30) cannot be true if $G(0) = 0$ and $G(-L) \neq 0$. Thus, we have a

contradiction.

3. $E_0 \neq 0$ and $E_1 = 0$

When $E_1 = 0$, the boundary condition $(2.10)_2$ for $G(x)$ becomes

$$k^2 U\mu'(-L)f_0(-L)G(-L) = 0,$$

which can only be true if $G(-L) = 0$. Using this fact along with equation (2.28), we get that for all $x \in [-L, 0]$,

$$\frac{(f_0^2(x)G(x))'}{k^2 U\mu'(x)f_0^2(x)} = \frac{f_0^2(-L)G'(-L) + 2f_0(-L)f_0'(-L)G(-L)}{k^2 U\mu'(-L)f_0^2(-L)} = \frac{G'(-L)}{k^2 U\mu'(-L)}.$$

Multiplying by $k^2 U\mu'(x)f_0^2(x)$ and integrating from $-L$ to 0, we get

$$f_0^2(0)G(0) - f_0^2(-L)G(-L) = \frac{G'(-L)}{\mu'(-L)} \int_{-L}^{0} \mu'(x)f_0^2(x)dx,$$

and therefore

$$f_0^2(0)G(0) = \frac{G'(-L)}{\mu'(-L)} \int_{-L}^{0} \mu'(x)f_0^2(x)dx. \tag{2.32}$$

Note that by the uniqueness theorem stated in Case 1 and the fact that $G(x) \not\equiv 0$, $G'(-L) \neq 0$.

Since $E_0 \neq 0$, we know from Case 1 that $G(0) \neq 0$. Also, for all $x \in [-L, 0]$

$$\frac{f_0^2(x)G'(x) + 2f_0(x)f_0'(x)G(x)}{k^2 U\mu'(x)f_0^2(x)} = -\frac{G(0)}{E_0}.$$

In particular, this is true at $x = -L$. Therefore,

$$\frac{G'(-L)}{k^2 U\mu'(-L)} = -\frac{G(0)}{E_0}. \tag{2.33}$$

However, equation (2.32) implies that $G(0)$ and $G'(-L)$ are of the same sign and equation (2.33) implies that $G(0)$ and $G'(-L)$ have opposite signs, which is a contradiction.

4. $E_0 = E_1 = 0$

   When $E_0 = E_1 = 0$, $G(-L) = G(0) = 0$. Since $E_1 = 0$, equation (2.32) still holds. Therefore, $G'(-L) = 0$. But then, by the uniqueness theorem, $G(x) \equiv 0$ which is a contradiction.

Therefore, since all cases lead to a contradiction, we have shown that $\alpha \neq \lambda_0$. Therefore, $(g(x), \alpha)$ solves $(2.5)_1$.

We claim that $(g(x), \alpha)$ also satisfies the boundary conditions $(2.5)_2$ and $(2.5)_3$. From $(2.10)_2$, we know that

$$E_1 f_0(-L)G'(-L) = \{k^2 U\mu'(-L)f_0(-L) - 2E_1 f_0'(-L)\}G(-L),$$

and therefore

$$f_0(-L)G(-L) - \frac{E_1}{k^2 U\mu'(-L)}\{f_0(-L)G'(-L) + 2f_0'(-L)G(-L)\} = 0. \qquad (2.34)$$

Since $G(x) = \mu\left(\frac{g(x)}{f_0(x)}\right)$ and $g(x)$ solves $(2.5)_1$, we can follow the steps used to derive (2.11) to get

$$(f_0^2 G)' = (\mu f_0 g' - \mu g f_0')' = (\lambda_0 - \alpha)k^2 U\mu' f_0 g.$$

Dividing by f_0 and evaluating at $x = -L$ yields

$$f_0(-L)G'(-L) + 2f_0'(-L)G(-L) = (\lambda_0 - \alpha)k^2 U\mu'(-L)g(-L).$$

Substituting this into (2.34), we get

$$f_0(-L)G(-L) - E_1(\lambda_0 - \alpha)g(-L) = 0.$$

We use the boundary condition $(2.5)_2$ for the function f_0 to get that

$$\frac{\mu(-L)f_0'(-L)}{f_0(-L)} - (\mu_l k - E_1\lambda_0) = 0.$$

Multiplying this by $g(-L)$ and adding to the previous expression gives

$$f_0(-L)G(-L) - E_1(\lambda_0 - \alpha)g(-L) + \left\{\frac{\mu(-L)f_0'(-L)}{f_0(-L)} - (\mu_l k - E_1\lambda_0)\right\} g(-L) = 0.$$

Canceling terms and rearranging,

$$(\mu_l k - E_1\alpha)g(-L) = f_0(-L)G(-L) + \frac{\mu(-L)f_0'(-L)}{f_0(-L)}g(-L).$$

Using expressions (2.23) and (2.21) evaluated at $x = -L$,

$$(\mu_l k - E_1\alpha)g(-L) = \mu(-L)g'(-L).$$

Therefore, $(g(x), \alpha)$ satisfies $(2.5)_2$. Following the same process, we can see that $(g(x), \alpha)$ also satisfies $(2.5)_3$. Therefore, $(g(x), \alpha)$ satisfies (2.5), which proves our claim.

Since $(g(x), \alpha)$ solves (2.5), $g \equiv f_i$ for some i and $\alpha = \lambda_i$. This means that $G \equiv F_i$. □

Lemma 1 shows us that the set $\{(F_i, \lambda_i)\}_{i=1}^{\infty}$ is the set of solutions to a regular Sturm-Liouville problem. Therefore, the set $\{F_i\}_{i=1}^{\infty}$ forms an orthonormal basis of

the space

$$L^2_w(-L,0) = \left\{ f(x) \,\middle|\, \int_{-L}^{0} |f(x)|^2 w(x)dx < \infty \right\},$$

where $w(x) = \frac{k^2 U f_0^2(x)}{\mu(x)}$. In addition, it verifies the fact that the eigenvalues $\{\lambda_i\}_{i=1}^{\infty}$ are real and only have a limit point at infinity.

We now wish to show that a certain class of functions can be written as a linear combination of the eigenfunctions, $\{f_i\}_{i=0}^{\infty}$. Since $\{(F_i, \lambda_i)\}_{i=1}^{\infty}$ is an orthonormal basis of $L^2_w(-L,0)$, any function $f(x) \in L^2_w(-L,0)$ can be expanded as

$$f(x) = \sum_{i=1}^{\infty} c_i F_i,$$

where $c_i = \int_{-L}^{0} f(x)F_i(x)w(x)dx$.

We define the bilinear form

$$B(f,g) = \int_{-L}^{0} fg(k^2 U\mu')dx + E_0 f(0)g(0) + E_1 f(-L)g(-L). \tag{2.35}$$

Recall from (2.8) that for any distinct eigenfunctions f_i and f_j of (2.5), $B(f_i, f_j) = 0$. Using this bilinear form, we may now expand any function in terms of the eigenfunctions using the following theorem.

Theorem 2. *Let E_0, E_1, U, k, μ_l, $\mu_r > 0$ and $\mu(x)$ be a twice differentiable, positive, strictly increasing function in $C^1([-L,0])$. Let $\{f_i\}_{i=0}^{\infty}$ be the eigenfunctions of (2.5). Let $w(x) = \frac{k^2 U f_0^2(x)}{\mu(x)}$. Let*

$$H^1_w(-L,0) = \left\{ f(x) \in L^2_w(-L,0) | f'(x) \in L^2_w(-L,0) \right\}.$$

Then for any function $f(x) \in H^1_w(-L, 0)$,

$$f(x) = \sum_{i=0}^{\infty} A_i f_i(x), \tag{2.36}$$

where equality is in the sense of $L^2_w(-L, 0)$ *and the constants* A_i *are given by*

$$A_i = \frac{B(f, f_i)}{B(f_i, f_i)}. \tag{2.37}$$

Proof. Let $f \in H^1_w(-L, 0)$. Then, since μ and f_0 are in $C^1([-L, 0])$, $\mu\left(\frac{f}{f_0}\right)' \in L^2_w(-L, 0)$. Since the set $\{F_i\}_{i=1}^{\infty}$ is complete in $L^2_w(-L, 0)$, we can write

$$\mu\left(\frac{f}{f_0}\right)' = \sum_{i=1}^{\infty} A_i F_i, \tag{2.38}$$

where

$$A_i = \int_{-L}^{0} \mu\left(\frac{f}{f_0}\right)' F_i w(x) dx. \tag{2.39}$$

Dividing (2.38) by μ and integrating gives us that for any $x \in [-L, 0]$,

$$\int_{-L}^{x} \left(\frac{f}{f_0}\right)' dt = \sum_{i=1}^{\infty} A_i \int_{-L}^{x} \frac{F_i}{\mu} dt.$$

Using that $\frac{F_i}{\mu} = \left(\frac{f_i}{f_0}\right)'$, we get

$$\frac{f(x)}{f_0(x)} - \frac{f(-L)}{f_0(-L)} = \sum_{i=1}^{\infty} A_i \left[\frac{f_i(x)}{f_0(x)} - \frac{f_i(-L)}{f_0(-L)}\right],$$

and therefore

$$f(x)f_0(-L) - f(-L)f_0(x) = \sum_{i=1}^{\infty} A_i[f_i(x)f_0(-L) - f_i(-L)f_0(x)] \quad \forall x \in [-L, 0]. \tag{2.40}$$

Let $\tilde{w}(x) = k^2 U\mu'(x)$. Multiply the above equation by $f_0\tilde{w}$ and integrate from $-L$ to 0. Then

$$\begin{aligned}
&\int_{-L}^{0} f(x)f_0(-L)f_0(x)\tilde{w}(x)dx - \int_{-L}^{0} f(-L)f_0^2(x)\tilde{w}(x)dx \\
&\quad = \sum_{i=1}^{\infty} A_i \left[\int_{-L}^{0} f_i(x)f_0(-L)f_0(x)\tilde{w}(x)dx - \int_{-L}^{0} f_i(-L)f_0^2(x)\tilde{w}(x)dx\right].
\end{aligned}$$

Recall the bilinear form (2.35)

$$B(f, g) = \int_{-L}^{0} fg\tilde{w}dx + E_0 f(0)g(0) + E_1 f(-L)g(-L),$$

and, from (2.8), that for all $i \neq j$

$$B(f_i, f_j) = 0.$$

If we replace the integral above using that

$$\int_{-L}^{0} fg\tilde{w}dx = B(f, g) - E_0 f(0)g(0) - E_1 f(-L)g(-L),$$

then

$$\begin{aligned}
&f_0(-L)[B(f,f_0) - E_0 f(0) f_0(0) - E_1 f(-L) f_0(-L)] \\
&- f(-L)[B(f_0,f_0) - E_0 f_0^2(0) - E_1 f_0^2(-L)] \\
&= \sum_{i=1}^{\infty} A_i \{ f_0(-L)[-E_0 f_i(0) f_0(0) - E_1 f_i(-L) f_0(-L)] \\
&- f_i(-L)[B(f_0,f_0) - E_0 f_0^2(0) - E_1 f_0^2(-L)] \}.
\end{aligned}$$

Canceling like terms, we get

$$\begin{aligned}
&f_0(-L)B(f,f_0) - f(-L)B(f_0,f_0) - E_0 f_0(0)\left[f(0)f_0(-L) - f(-L)f_0(0)\right] \\
&= -B(f_0,f_0)\sum_{i=1}^{\infty} A_i f_i(-L) - E_0 f_0(0)\sum_{i=1}^{\infty} A_i \left[f_i(0)f_0(-L) - f_i(-L)f_0(0)\right]. \quad (2.41)
\end{aligned}$$

Equation (2.40) with $x = 0$ gives

$$f(0)f_0(-L) - f(-L)f_0(0) = \sum_{i=1}^{\infty} A_i [f_i(0)f_0(-L) - f_i(-L)f_0(0)].$$

Plug this into (2.41) to get

$$\begin{aligned}
&f_0(-L)B(f,f_0) - f(-L)B(f_0,f_0) - E_0 f_0(0)\left[f(0)f_0(-L) - f(-L)f_0(0)\right] \\
&= -B(f_0,f_0)\sum_{i=1}^{\infty} A_i f_i(-L) - E_0 f_0(0)\left[f(0)f_0(-L) - f(-L)f_0(0)\right],
\end{aligned}$$

and therefore

$$f_0(-L)B(f,f_0) - f(-L)B(f_0,f_0) = -B(f_0,f_0)\sum_{i=1}^{\infty} A_i f_i(-L).$$

Solving for $f(-L)$,

$$f(-L) = \sum_{i=1}^{\infty} A_i f_i(-L) + f_0(-L)\frac{B(f, f_0)}{B(f_0, f_0)}.$$

If we define

$$A_0 = \frac{B(f, f_0)}{B(f_0, f_0)},$$

then

$$f(-L) = \sum_{i=0}^{\infty} A_i f_i(-L). \tag{2.42}$$

If we now plug this into equation (2.40), we get that $\forall x \in [-L, 0]$

$$f(x)f_0(-L) - \sum_{i=0}^{\infty} A_i f_i(-L) f_0(x) = \sum_{i=1}^{\infty} A_i [f_i(x) f_0(-L) - f_i(-L) f_0(x)].$$

Splitting the sum on the left-hand side and canceling like terms,

$$f(x)f_0(-L) - A_0 f_0(-L) f_0(x) = \sum_{i=1}^{\infty} A_i f_i(x) f_0(-L).$$

Rearranging,

$$f(x)f_0(-L) = f_0(-L) \sum_{i=0}^{\infty} A_i f_i(x).$$

Therefore,

$$f(x) = \sum_{i=0}^{\infty} A_i f_i(x). \tag{2.43}$$

It remains to show that

$$A_i = \frac{B(f, f_i)}{B(f_i, f_i)}, \qquad \text{for } i \neq 0.$$

Recall that these coefficients came from the expression (2.39). Consider a function

$h \in H^1_w(-L,0)$. Using integration by parts and (2.11), we have that

$$\begin{aligned}\int_{-L}^{0}\left(\frac{h}{f_0}\right)' f_0^2 F_i dx &= \left[\frac{h}{f_0} f_0^2 F_i\right]_{-L}^{0} - \int_{-L}^{0}(f_0^2 F_i)'\frac{h}{f_0}dx \\ &= \left[\frac{h}{f_0}(\mu f_0 f_i' - \mu f_0' f_i)\right]_{-L}^{0} + (\lambda_i - \lambda_0)\int_{-L}^{0} h f_i k^2 U \mu' dx. \quad (2.44)\end{aligned}$$

Using the boundary conditions $(2.5)_2$ and $(2.5)_3$,

$$\begin{aligned}&\left[\frac{h}{f_0}(\mu f_0 f_i' - \mu f_0' f_i)\right]_{-L}^{0} \\ &= \frac{h(0)}{f_0(0)}\left\{\mu(0) f_0(0) f_i'(0) - \mu(0) f_0'(0) f_i(0)\right\} \\ &- \frac{h(-L)}{f_0(-L)}\left\{\mu(-L) f_0(-L) f_i'(-L) - \mu(-L) f_0'(-L) f_i(-L)\right\} \\ &= \frac{h(0)}{f_0(0)}\left\{-f_0(0)(\mu_r k - E_0\lambda_i) f_i(0) + (\mu_r k - E_0\lambda_0) f_0(0) f_i(0)\right\} \\ &- \frac{h(-L)}{f_0(-L)}\left\{f_0(-L)(\mu_l k - E_1\lambda_i) f_i(-L) - (\mu_l k - E_1\lambda_0) f_0(-L) f_i(-L)\right\} \\ &= \frac{h(0)}{f_0(0)}\left\{E_0(\lambda_i - \lambda_0) f_0(0) f_i(0)\right\} + \frac{h(-L)}{f_0(-L)}\left\{E_1(\lambda_i - \lambda_0) f_0(-L) f_i(-L)\right\} \\ &= (\lambda_i - \lambda_0)\left\{E_0 h(0) f_i(0) + E_1 h(-L) f_i(-L)\right\}.\end{aligned}$$

Therefore, using this in (2.44),

$$\int_{-L}^{0}\left(\frac{h}{f_0}\right)' f_0^2 F_i dx = (\lambda_i - \lambda_0)\left\{\int_{-L}^{0} h f_i k^2 U \mu' dx + E_0 h(0) f_i(0) + E_1 h(-L) f_i(-L)\right\},$$

or

$$\int_{-L}^{0}\left(\frac{h}{f_0}\right)' f_0^2 F_i dx = (\lambda_i - \lambda_0) B(h, f_i). \quad (2.45)$$

In particular, using $h = f$,

$$\int_{-L}^{0}\left(\frac{f}{f_0}\right)' f_0^2 F_i dx = (\lambda_i - \lambda_0) B(f, f_i). \quad (2.46)$$

On the other hand, it follows from (2.38) that

$$\int_{-L}^{0} \mu \left(\frac{f}{f_0}\right)' \frac{f_0^2 F_i}{\mu} dx = \sum_{j=1}^{\infty} A_j \int_{-L}^{0} \frac{f_0^2 F_i F_j}{\mu} dx.$$

But since $\{F_i\}_{i=1}^{\infty}$ is orthonormal in $L_w^2(-L, 0)$,

$$\int_{-L}^{0} F_i F_j \frac{k^2 U f_0^2}{\mu} dx = \delta_{i,j},$$

where $\delta_{i,j}$ is the Kronecker delta. In particular, when $i \neq j$,

$$\int_{-L}^{0} F_i F_j \frac{f_0^2}{\mu} dx = 0.$$

Therefore,

$$\int_{-L}^{0} \mu \left(\frac{f}{f_0}\right)' \frac{f_0^2 F_i}{\mu} dx = A_i \int_{-L}^{0} \frac{f_0^2 F_i^2}{\mu} dx.$$

Equating this with (2.46) yields

$$A_i \int_{-L}^{0} \frac{f_0^2 F_i^2}{\mu} dx = (\lambda_i - \lambda_0) B(f, f_i). \tag{2.47}$$

But using (2.45) with $h = f_i$ and recalling from the definition of F_i that $\frac{F_i}{\mu} = \left(\frac{f_i}{f_0}\right)'$,

$$\int_{-L}^{0} \frac{f_0^2 F_i^2}{\mu} dx = \int_{-L}^{0} \left(\frac{f_i}{f_0}\right)' f_0^2 F_i dx = (\lambda_i - \lambda_0) B(f_i, f_i).$$

Combining this with (2.47), we get

$$A_i (\lambda_i - \lambda_0) B(f_i, f_i) = (\lambda_i - \lambda_0) B(f, f_i).$$

which leads to our desired result, (2.37). This concludes the proof of Theorem 2.

2.4 Exponential Viscous Profile

We now apply the above theory to the case where the viscosity of the middle layer follows an exponential profile where $\mu(-L) < \mu(0)$. Note that this meets the condition of the previous section since $\mu(x)$ is positive, strictly increasing, and smooth. So for all k such that $E_0, E_1 > 0$, there are infinitely many positive values of σ which can be ordered $\sigma_1 > \sigma_2 > ...$ with a limit point at 0 and any function in $H^1_w(-L, 0)$ can be expanded in terms of the eigenfunctions. The viscous profile can be written as

$$\mu(x) = \mu(-L)e^{\alpha(x+L)}, \quad -L < x < 0, \tag{2.48}$$

where $\alpha = \frac{1}{L}\ln\left(\frac{\mu(0)}{\mu(-L)}\right)$. Therefore, $\mu'(x) = \alpha\mu(x)$. Plugging this into equation $(2.5)_1$, for $-L < x < 0$,

$$(\mu(x)f'(x))' - (k^2\mu(x) - k^2U\alpha\mu(x)\lambda)f(x) = 0.$$

Therefore,

$$\mu(x)f''(x) + \alpha\mu(x)f'(x) - (k^2\mu(x) - k^2U\alpha\mu(x)\lambda)f(x) = 0,$$

and

$$f''(x) + \alpha f'(x) + k^2\left(U\alpha\lambda - 1\right)f(x) = 0.$$

This is a homogeneous, constant coefficient, second order differential equation. Therefore, the fundamental solutions are $e^{r_1(\lambda)x}$ and $e^{r_2(\lambda)x}$ where $r_1(\lambda)$ and $r_2(\lambda)$ are roots of the equation $x^2 + \alpha x + k^2\left(U\alpha\lambda - 1\right) = 0$. Therefore,

$$r_1(\lambda) = \frac{-\alpha}{2} + i\beta, \qquad r_2(\lambda) = \frac{-\alpha}{2} - i\beta, \tag{2.49}$$

where

$$\beta^2 = k^2(U\alpha\lambda - 1) - \frac{\alpha^2}{4}. \tag{2.50}$$

The general solution can be written as

$$f(x) = e^{-\frac{\alpha x}{2}}(A\cos(\beta x) + B\sin(\beta x)). \tag{2.51}$$

This holds except when $r_1 = r_2$ (i.e. when $\beta = 0$). We will consider this special case later. For now, assume that $\beta \neq 0$. Then

$$f'(x) = -\frac{\alpha}{2}f(x) + \beta e^{-\frac{\alpha x}{2}}(-A\sin(\beta x) + B\cos(\beta x)). \tag{2.52}$$

Therefore

$$f(0) = A, \qquad f(-L) = e^{\frac{\alpha L}{2}}(A\cos(\beta L) - B\sin(\beta L)),$$

and

$$f'(0) = -\frac{\alpha}{2}f(0) + \beta B, \qquad f'(-L) = -\frac{\alpha}{2}f(-L) + \beta e^{\frac{\alpha L}{2}}(A\sin(\beta L) + B\cos(\beta L)).$$

Plugging these into the boundary condition $(2.5)_3$,

$$\left(\frac{\mu_r k - E_0\lambda}{\mu(0)} - \frac{\alpha}{2}\right)A + \beta B = 0.$$

Likewise, from the boundary condition $(2.5)_2$,

$$\begin{aligned}&\left\{-\left(\frac{\mu_l k - E_1\lambda}{\mu(-L)} + \frac{\alpha}{2}\right)\cos(\beta L) + \beta\sin(\beta L)\right\}A \\ &+\left\{\left(\frac{\mu_l k - E_1\lambda}{\mu(-L)} + \frac{\alpha}{2}\right)\sin(\beta L) + \beta\cos(\beta L)\right\}B = 0.\end{aligned}$$

This gives us a matrix equation of the form $\mathbf{Mx} = \mathbf{0}$ where

$$\mathbf{M} = \begin{pmatrix} \frac{\mu_r k - E_0\lambda}{\mu(0)} - \frac{\alpha}{2} & \beta \\ -\left(\frac{\mu_l k - E_1\lambda}{\mu(-L)} + \frac{\alpha}{2}\right)\cos(\beta L) + \beta\sin(\beta L) & \left(\frac{\mu_l k - E_1\lambda}{\mu(-L)} + \frac{\alpha}{2}\right)\sin(\beta L) + \beta\cos(\beta L) \end{pmatrix},$$

and

$$\mathbf{x} = \begin{pmatrix} A \\ B \end{pmatrix}.$$

This equation has a nontrivial solution if and only if the determinant of $\mathbf{M}$ is zero. Let $H(\lambda, k) = \det(\mathbf{M})$. Then

$$H(\lambda, k) = H_1(\lambda, k)\sin(\beta L) + \beta H_2(\lambda, k)\cos(\beta L), \tag{2.53}$$

where

$$H_1(\lambda, k) = \left(\frac{\mu_r k - E_0\lambda}{\mu(0)} - \frac{\alpha}{2}\right)\left(\frac{\mu_l k - E_1\lambda}{\mu(-L)} + \frac{\alpha}{2}\right) - \beta^2, \tag{2.54}$$

and

$$H_2(\lambda, k) = \left\{\frac{\mu_l k - E_1\lambda}{\mu(-L)} + \frac{\mu_r k - E_0\lambda}{\mu(0)}\right\}. \tag{2.55}$$

The roots of $H(\lambda, k)$ are the values of λ that are solutions to the eigenvalue problem. However, note that $\beta = 0$ implies $H(\lambda, k) = 0$. As stated above, the analysis used to derive H does not hold when $\beta = 0$. We treat this case next.

We define the number

$$\gamma_0 := \frac{\alpha^2 + 4k^2}{4k^2 U\alpha}. \tag{2.56}$$

By examining (2.50), it is seen that $\beta = 0 \iff \lambda = \gamma_0$. Since the characteristic equation now has repeated roots, the eigenfunctions will be of the form

$f(x) = Ae^{-\frac{\alpha}{2}x} + Bxe^{-\frac{\alpha}{2}x}$. Then

$$\begin{aligned} f'(x) &= -\frac{\alpha}{2}e^{-\frac{\alpha}{2}x}(A + Bx) + Be^{-\frac{\alpha}{2}x} \\ &= e^{-\frac{\alpha}{2}x}\left\{-\frac{\alpha}{2}A + \left(1 + -\frac{\alpha}{2}x\right)B\right\}. \end{aligned}$$

Therefore,

$$f(0) = A, \qquad f(-L) = e^{\frac{\alpha L}{2}}(A - BL),$$

and

$$f'(0) = -\frac{\alpha}{2}A + B, \qquad f'(-L) = e^{\frac{\alpha L}{2}}\left\{-\frac{\alpha}{2}A + \left(1 + \frac{\alpha L}{2}\right)B\right\}.$$

Plugging these into the boundary condition $(2.5)_2$,

$$\left(\frac{\mu_l k - E_1\lambda}{\mu(-L)} + \frac{\alpha}{2}\right)A - \left\{L\left(\frac{\mu_l k - E_1\lambda}{\mu(-L)}\right) + 1 + \frac{\alpha L}{2}\right\}B = 0.$$

Likewise, using the boundary condition $(2.5)_3$,

$$\left(\frac{\mu_r k - E_0\lambda}{\mu(0)} - \frac{\alpha}{2}\right)A + B = 0.$$

This gives us a matrix equation of the form $\widetilde{\mathbf{M}}\mathbf{x} = \mathbf{0}$ where

$$\widetilde{\mathbf{M}} = \begin{pmatrix} \frac{\mu_l k - E_1\lambda}{\mu(-L)} + \frac{\alpha}{2} & -\left\{L\left(\frac{\mu_l k - E_1\lambda}{\mu(-L)}\right) + 1 + \frac{\alpha L}{2}\right\} \\ \frac{\mu_r k - E_0\lambda}{\mu(0)} - \frac{\alpha}{2} & 1 \end{pmatrix}.$$

Again, solutions occur when $\det(\widetilde{\mathbf{M}}) = 0$. Let $\widetilde{H}(\lambda, k) = det(\widetilde{\mathbf{M}})$. Then

$$\begin{aligned}\widetilde{H}(\lambda,k) =& \frac{\mu_l k - E_1\lambda}{\mu(-L)} + \frac{\alpha}{2} + \left(\frac{\mu_r k - E_0\lambda}{\mu(0)} - \frac{\alpha}{2}\right)\left(L\left(\frac{\mu_l k - E_1\lambda}{\mu(-L)}\right) + 1 + \frac{\alpha L}{2}\right) \\ =& \frac{\mu_l k - E_1\lambda}{\mu(-L)} + \frac{\alpha}{2} + L\left(\frac{\mu_r k - E_0\lambda}{\mu(0)}\right)\left(\frac{\mu_l k - E_1\lambda}{\mu(-L)}\right) \\ &+ \left(1 + \frac{\alpha L}{2}\right)\left(\frac{\mu_r k - E_0\lambda}{\mu(0)}\right) - \frac{\alpha L}{2}\left(\frac{\mu_l k - E_1\lambda}{\mu(-L)}\right) - \frac{\alpha}{2}\left(1 + \frac{\alpha L}{2}\right).\end{aligned}$$

After some algebraic manipulation,

$$\widetilde{H}(\lambda,k) = \left\{\frac{\mu_l k - E_1\lambda}{\mu(-L)} + \frac{\mu_r k - E_0\lambda}{\mu(0)} + L\left(\frac{\mu_r k - E_0\lambda}{\mu(0)} - \frac{\alpha}{2}\right)\left(\frac{\mu_l k - E_1\lambda}{\mu(-L)} + \frac{\alpha}{2}\right)\right\}. \tag{2.57}$$

Recall that when $\beta \neq 0$, we seek values of λ such that $H(\lambda, k) = 0$. However, when $\beta = 0$, λ is fixed ($\lambda = \gamma_0$). Therefore, this is only an eigenvalue of the problem for a wavenumber k such that $\widetilde{H}(\gamma_0, k) = 0$.

We now return to the case when $\beta \neq 0$. Note that when $\lambda > \gamma_0$, β is real-valued, but when $\lambda < \gamma_0$, β is imaginary. In the latter case, using that $\sinh(ix) = i\sin(x)$ and $\cosh(ix) = \cos(x)$,

$$H(\lambda,k) = i\left\{H_1(\lambda,k)\sinh(|\beta|L) + |\beta|H_2(\lambda,k)\cosh(|\beta|L)\right\}, \tag{2.58}$$

and H is purely imaginary. Therefore, when $\lambda < \gamma_0$ we can find the zeros of $Im(H)$. In summary, we have that

$$H(\lambda,k) = \begin{cases}\text{real, if } \lambda > \gamma_0 \\ \\ \text{imaginary, if } \lambda < \gamma_0.\end{cases} \tag{2.59}$$

In order to investigate the zeros of H, we define the sequence of positive numbers

$\{\gamma_n\}_{n=0}^{\infty}$ by

$$\gamma_n := \frac{4n^2\pi^2 + \alpha^2 L^2 + 4k^2 L^2}{4k^2 L^2 U \alpha}. \tag{2.60}$$

Here, the definition of γ_0 coincides with (2.56). Note that $\gamma_n > \gamma_0$ for any $n \geq 1$, which implies that β will be real when $\lambda = \gamma_n$. Also, for any $n \geq 1$, if $\lambda = \gamma_n$, then

$$\begin{aligned}
\beta &= \sqrt{k^2 \left(U\alpha\gamma_n - 1\right) - \frac{\alpha^2}{4}} \\
&= \sqrt{k^2 \left(\frac{4n^2\pi^2 + \alpha^2 L^2 + 4k^2 L^2}{4k^2 L^2} - 1\right) - \frac{\alpha^2}{4}} \\
&= \sqrt{\frac{4n^2\pi^2 + \alpha^2 L^2}{4L^2} - \frac{\alpha^2}{4}} \\
&= \sqrt{\frac{n^2\pi^2}{L^2}} \\
&= \frac{n\pi}{L}.
\end{aligned}$$

Therefore $\sin(\beta L) = 0$ and

$$H(\gamma_n, k) = \begin{cases} -\frac{n\pi}{L} H_2(\gamma_n, k), & n \text{ odd} \\ \frac{n\pi}{L} H_2(\gamma_n, k), & n \text{ even.} \end{cases} \tag{2.61}$$

Therefore, if $H_2(\gamma_n, k) = 0$, then γ_n is an eigenvalue of the system (2.5). More generally, if $n \geq 1$ and $H_2(\gamma_n, k)$ and $H_2(\gamma_{n+1}, k)$ have the same sign, then $H(\gamma_n, k)$ and $H(\gamma_{n+1}, k)$ will have opposite signs. Therefore, $H(\lambda, k) = 0$ for some $\gamma_n < \lambda < \gamma_{n+1}$.

This knowledge allows us to understand the behavior of H. In particular, we will show that for any k, H has infinitely many zeros with a limit point at infinity.

Consider the function H_2. Using (2.55), $H_2 = 0$ when

$$\frac{\mu_l k - E_1 \lambda}{\mu(-L)} + \frac{\mu_r k - E_0 \lambda}{\mu(0)} = 0,$$

which occurs if

$$\lambda = \frac{\frac{\mu_l}{\mu(-L)} + \frac{\mu_r}{\mu(0)}}{\frac{E_1}{\mu(-L)} + \frac{E_0}{\mu(0)}} k. \tag{2.62}$$

Note that for a fixed k, there is only one value of λ such that $H_2 = 0$. Let $\lambda^*(k)$ denote this value. Note that

$$\begin{aligned} \frac{E_1}{\mu(-L)} + \frac{E_0}{\mu(0)} &= \frac{k^2 U(\mu(-L) - \mu_l) - T_1 k^4}{\mu(-L)} + \frac{k^2 U(\mu_r - \mu(0)) - T_0 k^4}{\mu(0)} \\ &= k^2 U \left(\frac{\mu_r}{\mu(0)} - \frac{\mu_l}{\mu(-L)} \right) - k^4 \left(\frac{T_1}{\mu(-L)} + \frac{T_0}{\mu(0)} \right). \end{aligned}$$

Therefore,

$$\lambda^*(k) = \frac{\frac{\mu_l}{\mu(-L)} + \frac{\mu_r}{\mu(0)}}{kU \left(\frac{\mu_r}{\mu(0)} - \frac{\mu_l}{\mu(-L)} \right) - k^3 \left(\frac{T_1}{\mu(-L)} + \frac{T_0}{\mu(0)} \right)}. \tag{2.63}$$

There will be at most one value of n such that $\lambda^*(k) \in [\gamma_n, \gamma_{n+1})$. For all values of n such that $\lambda^*(k) \notin [\lambda_n, \lambda_{n+1}]$, we have the following lemma.

Lemma 2. *Fix k and let $\lambda^*(k)$ be defined by (2.63). For all $n \geq 1$ such that $\lambda^*(k) \notin [\gamma_n, \gamma_{n+1}]$, problem (2.5) has an eigenvalue λ such that*

$$\gamma_n < \lambda < \gamma_{n+1}, \tag{2.64}$$

and the corresponding eigenfunction f has either n or $n+1$ zeros on the interval $(0, L)$.

Proof. Since $\lambda^*(k) \notin [\gamma_n, \gamma_{n+1}]$, $H_2(\lambda, k)$ has no zeros in $[\gamma_n, \gamma_{n+1}]$. Therefore, $H_2(\gamma_n, k)$ and $H_2(\gamma_{n+1}, k)$ have the same sign. By (2.61), $H(\gamma_n, k)$ and $H(\gamma_{n+1}, k)$

have opposite signs, and therefore, $H(\lambda, k) = 0$ for some $\lambda \in (\gamma_n, \gamma_{n+1})$. So λ is an eigenvalue of (2.5).

Recall that the eigenfunctions are of the form $f(x) = e^{-\frac{\alpha x}{2}}(A\cos(\beta x) + B\sin(\beta x))$ for some constants A and B. If $\lambda \in (\gamma_n, \gamma_{n+1})$, then $\frac{n\pi}{L} < \beta < \frac{(n+1)\pi}{L}$. Therefore, the oscillatory part of f has between $\frac{n}{2}$ and $\frac{n+1}{2}$ periods on the interval $(-L, 0)$. Therefore, f must have either n or $n+1$ zeros in the interval. □

This provides an infinite sequence of unbounded, increasing eigenvalues, as predicted by Theorem 1.

We now wish to characterize the relationship between the wavenumber, k, and the value of n such that $\lambda^*(k) \in [\gamma_n, \gamma_{n+1})$. If we add a condition to the parameters $\mu_r, \mu(0), \mu(-L), \mu_l, T_0$, and T_1, then we get the following fact.

Lemma 3. *Let μ_r, $\mu(0)$, $\mu(-L)$, μ_l, T_0, and T_1 be such that there exists a value k_c such that E_0 and E_1 are positive for $k < k_c$ and $E_0 = E_1 = 0$ when $k = k_c$. Then there is a sequence of wavenumbers $\{k_n\}_{n=1}^{\infty}$ such that*

1. *For all n, k_n is the maximum wavenumber such that $0 < k_n < k_c$ and $H_2(\gamma_n, k_n) = 0$.*

2. *$k_1 < k_2 < k_3 < k_4 < ...$*

3. *$lim_{n\to\infty} k_n = k_c$.*

4. *For all n such that $k_n \geq \frac{k_c}{\sqrt{3}}$ and all k such that $k_n \leq k < k_{n+1}$, $\gamma_n \leq \lambda^*(k) < \gamma_{n+1}$ (where $\gamma_n = \lambda^*(k) \iff k_n = k$).*

5. *For all n such that $k_n \geq \frac{k_c}{\sqrt{3}}$ and all k such that $k_n < k < k_{n+1}$, there is an eigenvalue λ such that $\gamma_j < \lambda < \gamma_{j+1}$ for all $j \neq n$.*

Proof. 1. Fix a value of n. Recall (2.63) which gives the value $\lambda^*(k)$ such that $H_2(\lambda^*(k), k) = 0$. Also recall that γ_n depends on k and is given by (2.60) as $\gamma_n(k) = \frac{4n^2\pi^2+\alpha^2L^2+4k^2L^2}{4k^2L^2U\alpha}$. Therefore, we must show that there is a value $k_n \in (0, k_c)$ such that $\gamma_n(k_n) = \lambda^*(k_n)$. Note that $\gamma_n(k) = \mathcal{O}(\frac{1}{k^2})$ as $k \to 0$, and $\lambda^*(k) = \mathcal{O}(\frac{1}{k})$ as $k \to 0$. Therefore, $\lambda^*(k) < \gamma_n(k)$ for small enough k. However, as $k \to k_c$, $\lambda^*(k) \to \infty$. This comes from the expression (2.62) for $\lambda^*(k)$ along with the fact that $E_0, E_1 \to 0$ as $k \to k_c$. In contrast, $\gamma_n(k)$ has a finite limit as $k \to k_c$. Therefore, $\lambda^*(k) > \gamma_n(k)$ when k is sufficiently close to k_c and there must be at least one value of $k \in (0, k_c)$ such that $\lambda^*(k) = \gamma_n(k)$. Since both $\lambda^*(k)$ and $\gamma_n(k)$ are rational functions of k, there will be finitely many such points. Therefore, we choose k_n to be the maximum number in the interval $(0, k_c)$ such that $\lambda^*(k) = \gamma_n(k)$.

2. Note that $\gamma_{n+1}(k) > \gamma_n(k)$ for all n and k. Therefore, $\gamma_{n+1}(k_n) > \gamma_n(k_n) = \lambda^*(k_n)$ for all n. But as we saw above, $\lambda^*(k) > \gamma_{n+1}(k)$ for k sufficiently close to k_c. Therefore, there is a $k \in (k_n, k_c)$ such that $\gamma_{n+1}(k) = \lambda^*(k)$. This proves that $k_n < k_{n+1}$.

3. Fix $k < k_c$. Since $lim_{n\to\infty}\gamma_n = \infty$, we may choose an N large enough so that $\gamma_n(k) > \lambda^*(k)$ for all $n > N$. Let $n > N$. Since $\lim_{k\to k_c} \lambda^*(k) = \infty$ and $\lim_{k\to k_c} \gamma_n(k)$ is finite, there is a $\tilde{k} \in (k, k_c)$ such that $\gamma_n(\tilde{k}) = \lambda^*(\tilde{k})$, and therefore, $k_n > k$. Therefore, we have shown that $k_n > k$ for all $n > N$.

4. Let $k_n \geq \frac{k_c}{\sqrt{3}}$ and $k_n \leq k < k_{n+1}$. The fact that $\gamma_n \leq \lambda^*(k)$ with equality only when $k = k_n$ holds for all values of n (not just when $k_n \geq \frac{k_c}{\sqrt{3}}$) and follows from our choice of k_n as a maximum in item 1. It remains to show that $\lambda^*(k) < \gamma_{n+1}$. Note that $\gamma_{n+1}(k_n) > \gamma_n(k_n) = \lambda^*(k_n)$. Also note that γ_{n+1} is a decreasing function of wavenumber. For wavenumbers in $[\frac{k_c}{\sqrt{3}}, k_c)$, λ^* is an increasing

function of wavenumber. Therefore, there is at most one wavenumber in (k_n, k_c) such that $\gamma_{n+1} = \lambda^*$. k_{n+1} is this unique value. Therefore, $\lambda^*(k) < \gamma_{n+1}$.

5. This follows from item 4 and Lemma 2.

□

2.4.1 Numerical Results

We now choose values for the parameters and investigate the behavior of the system. Let

$$\mu_l = 2, \quad \mu(-L) = 4, \quad \mu(0) = 8, \quad \mu_r = 10, \quad U = 1, \quad L = 1, \quad T_0 = T_1 = 1.$$

Using these values, E_0 and E_1 are positive for $0 < k < \sqrt{2}$. Therefore, these are the wavenumbers for which our theory in Section 2.3 holds. In particular, for each k there are infinitely many values of σ which are positive, can be put in decreasing order, and have zero as a limit point. Figure 2.2 shows a plot of the fifteen largest values of σ using a pseudo-spectral method (see Chapter 6). For $0 < k < \sqrt{2}$, the values of σ behave as expected. Starting near $k = \sqrt{2}$, some values of σ become negative. The values of σ are given for several different values of k in Table 2.1.

Our choice of parameters satisfies the assumptions of Lemma 3 with $k_c = \sqrt{2}$. Therefore, Lemma 3 ensures a sequence $\{k_n\}_{n=1}^{\infty}$. There is also a unique wavenumber $k_0 \in (0, \sqrt{2})$ such that $\widetilde{H}(\gamma_0, k_0) = 0$. The first several values of k_n are given below. Note that $k_1 > \frac{k_c}{\sqrt{3}}$. Therefore, parts 4 and 5 of Lemma 3 hold for all $n \geq 1$.

$$k_0 = 0.126, k_1 = 1.282, k_2 = 1.375, k_3 = 1.396. \tag{2.65}$$

The eigenvalues exhibit different behaviors depending on the wavenumber relative

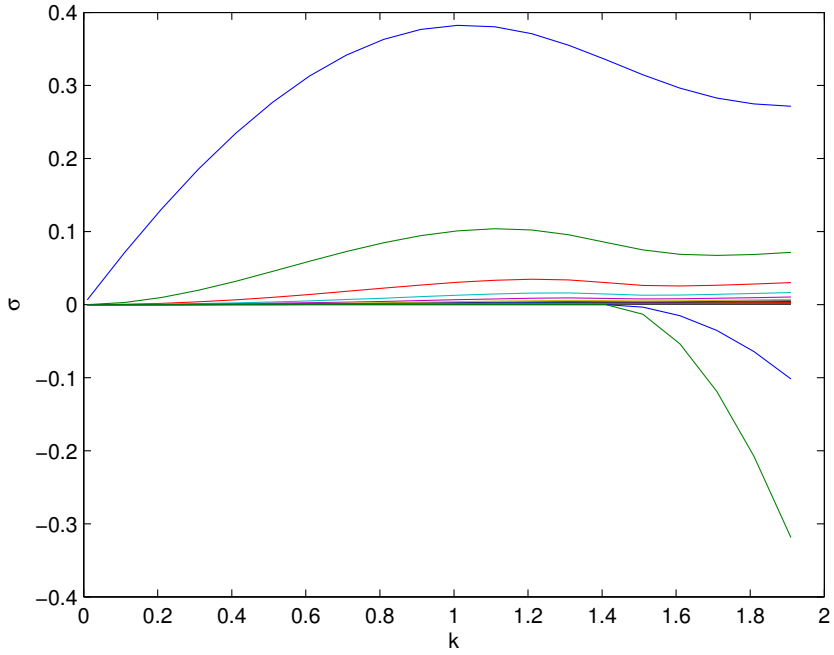

Figure 2.2: A plot of the dispersion curves for the fifteen largest values of σ.

to these values. We will now explain the behavior in each region and plot the function $H(\lambda, k)$ for some particular k in that region.

First consider when $k < k_0$. This is the only region for which there is an eigenvalue λ such that $\lambda < \gamma_0$. Figure 2.3 shows a plot of H versus λ for $k = 0.05$. The plot on the left is the region in which H is imaginary (i.e. when $\lambda < \gamma_0$). Note that H has one zero in this region. Since this is the smallest value of λ which satisfies $H(\lambda, k) = 0$, this is the λ_0 given by Theorem 1. Therefore, the associated eigenfunction has no zeros on $(-L, 0)$.

The plot on the right is the region in which H is real (i.e. when $\lambda > \gamma_0$). The x's on the λ axis correspond to $\lambda = \gamma_0$ and $\lambda = \gamma_1$. We see that H has a zero between these two values and the eigenfunction corresponding to this eigenvalue must have one zero in $(-L, 0)$. So this is λ_1 given by Theorem 1. Note that with these values

	$k = 0.05$	$k = 0.20$	$k = 0.70$	$k = 1.20$	$k = 1.35$
σ_0	3.2860×10^{-2}	1.2499×10^{-1}	3.3920×10^{-1}	3.7208×10^{-1}	3.4761×10^{-1}
σ_1	5.9690×10^{-4}	8.7902×10^{-3}	7.1555×10^{-2}	1.0256×10^{-1}	9.1769×10^{-2}
σ_2	1.0464×10^{-4}	1.6506×10^{-3}	1.7766×10^{-2}	3.4771×10^{-2}	3.2629×10^{-2}
σ_3	3.6704×10^{-5}	5.8457×10^{-4}	6.7805×10^{-3}	1.5787×10^{-2}	1.5734×10^{-2}
σ_4	1.7881×10^{-5}	2.8548×10^{-4}	3.3990×10^{-3}	8.6584×10^{-3}	9.0778×10^{-3}
σ_5	1.0430×10^{-5}	1.6667×10^{-4}	2.0071×10^{-3}	5.3685×10^{-3}	5.8527×10^{-3}
σ_6	6.7943×10^{-6}	1.0862×10^{-4}	1.3156×10^{-3}	3.6204×10^{-3}	4.0651×10^{-3}
σ_7	4.7651×10^{-6}	7.6200×10^{-5}	9.2600×10^{-4}	2.5935×10^{-3}	2.9778×10^{-3}
σ_8	3.5222×10^{-6}	5.6332×10^{-5}	6.8597×10^{-4}	1.9435×10^{-3}	2.2700×10^{-3}
σ_9	2.7074×10^{-6}	4.3305×10^{-5}	5.2805×10^{-4}	1.5080×10^{-3}	1.7848×10^{-3}
σ_{10}	2.1451×10^{-6}	3.4312×10^{-5}	4.1880×10^{-4}	1.2028×10^{-3}	1.4384×10^{-3}
σ_{11}	1.7409×10^{-6}	2.7849×10^{-5}	3.4014×10^{-4}	9.8092×10^{-4}	1.1829×10^{-3}
σ_{12}	1.4409×10^{-6}	2.3050×10^{-5}	2.8167×10^{-4}	8.1486×10^{-4}	9.8921×10^{-4}
σ_{13}	1.2121×10^{-6}	1.9391×10^{-5}	2.3705×10^{-4}	6.8742×10^{-4}	8.3906×10^{-4}
σ_{14}	1.0337×10^{-6}	1.6537×10^{-5}	2.0222×10^{-4}	5.8755×10^{-4}	7.2038×10^{-4}

Table 2.1: The fifteen largest values of σ for several different values of k.

of the parameters, $\lambda^*(0.05) < \gamma_n$ for all $n \geq 1$. Therefore, Lemma 2 gives us upper and lower bounds for an infinite sequence of eigenvalues. We claim that this is all of the remaining eigenvalues. To see this, consider the eigenvalue given by Lemma 2 with $n = 1$, that is, $\gamma_1 < \lambda < \gamma_2$. The eigenfunction corresponding to this eigenvalue must have either one or two zeros. So this value must be λ_1 or λ_2. But we already know that $\lambda_1 < \gamma_1$. Therefore, it must be λ_2. Likewise, for any n, the λ given by Lemma 2 must correspond to λ_{n+1}. To show this behavior, we plotted H for larger values of λ in Figure 2.4. The x's denote the values of γ_n. In the plot, we see that H has a zero between each value of γ_n and γ_{n+1} as H continues to oscillate.

The behavior we see for $k = 0.05$ holds for all values of k such that $k < k_0$. In summary, we have

$$\lambda_0 < \gamma_0 < \lambda_1 < \gamma_1 < \lambda_2 < \gamma_2 < \lambda_3 < \gamma_3 < ...$$

In order to illustrate these results, Table 2.2 shows the first fifteen values of γ_i and

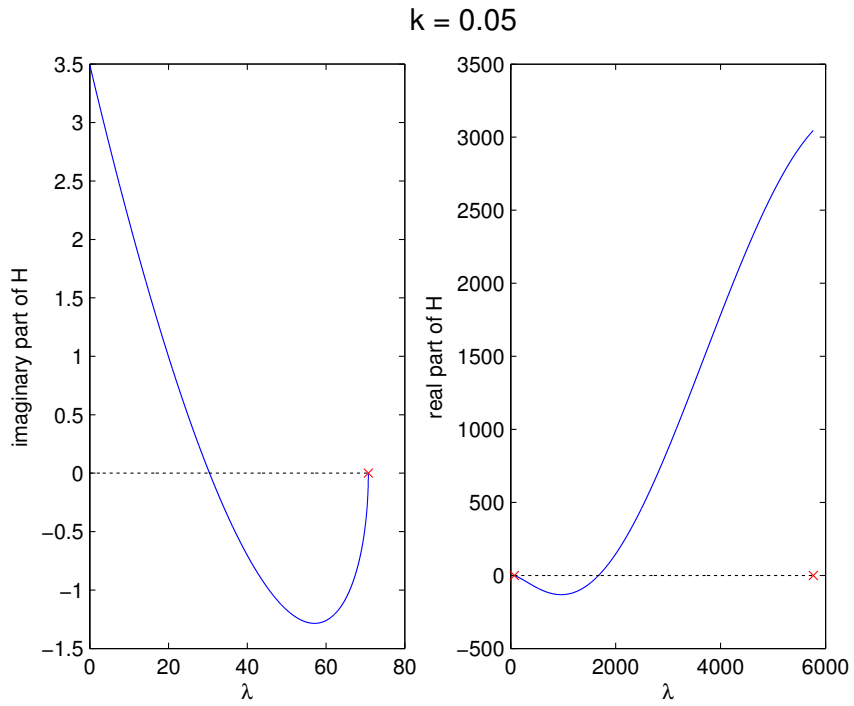

Figure 2.3: Plots of $H(\lambda, k)$ when $k = 0.05$. The left plot shows the range of λ for which $\lambda < \gamma_0$ and the right plot shows the range of λ for which $\lambda > \gamma_0$. The x's denote γ_0 and γ_1.

λ_i. Additionally, we plotted several of the eigenfunctions corresponding to $k = 0.05$ in Figure 2.5.

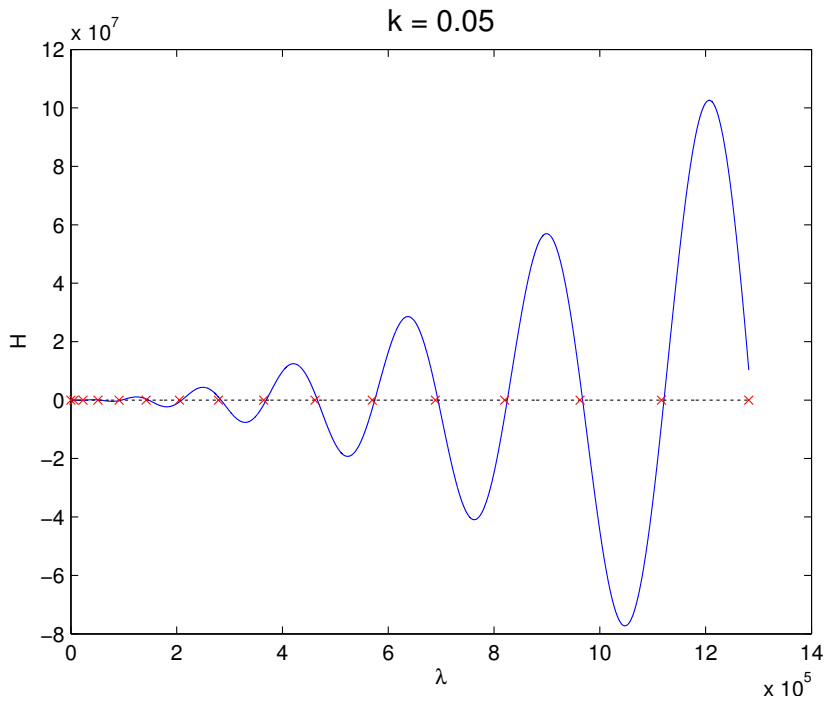

Figure 2.4: A plot of $H(\lambda, k)$ when $k = 0.05$ in the range of λ for which $\lambda > \gamma_0$. The x's denote the values of γ_n.

i	γ_i	λ_i
0	7.0757×10^1	3.0432×10^1
1	5.7663×10^3	1.6753×10^3
2	2.2853×10^4	9.5569×10^3
3	5.1331×10^4	2.7245×10^4
4	9.1199×10^4	5.5925×10^4
5	1.4246×10^5	9.5879×10^4
6	2.0511×10^5	1.4718×10^5
7	2.7915×10^5	2.0986×10^5
8	3.6458×10^5	2.8391×10^5
9	4.6141×10^5	3.6936×10^5
10	5.6962×10^5	4.6619×10^5
11	6.8923×10^5	5.7441×10^5
12	8.2023×10^5	6.9402×10^5
13	9.6262×10^5	8.2502×10^5
14	1.1164×10^6	9.6741×10^5

Table 2.2: The values of γ_i and λ_i for $0 < i < 14$ for $k = 0.05$.

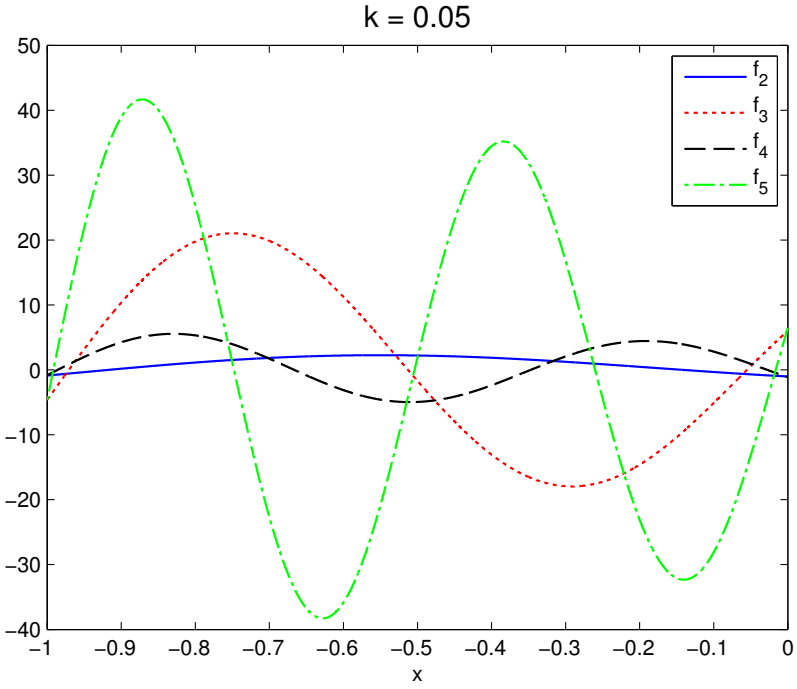

Figure 2.5: A plot of several eigenfunctions when $k = 0.05$.

Next, we investigate the case when $k_0 < k < k_1$. For k in this region, $\lambda^*(k) < \gamma_n$ for all $n \geq 1$. Therefore, there will be an eigenvalue λ such that $\gamma_n < \lambda < \gamma_{n+1}$ for all $n \geq 1$. However, there is no eigenvalue that is less than γ_0. To see this, consider Figure 2.6 in which we plot $H(\lambda, k)$ for $k = 1.2$. The plot on the left shows that H has no zeros in this region. However, H has two zeros in the region between γ_0 and γ_1. These two eigenvalues are λ_0 and λ_1. Therefore, following the argument above, for $n \geq 1$, the eigenvalue between γ_n and γ_{n+1} is λ_{n+1}. So

$$\gamma_0 < \lambda_0 < \lambda_1 < \gamma_1 < \lambda_2 < \gamma_2 < \lambda_3 < \gamma_3 < ...$$

The first fifteen values of γ_i and λ_i when $k = 1.2$ are given in Table 2.3. Several eigenfunctions are plotted in Figure 2.7.

i	γ_i	λ_i
0	1.5630×10^0	2.6876×10^0
1	1.1451×10^1	9.7506×10^0
2	4.1115×10^1	2.8760×10^1
3	9.0556×10^1	6.3341×10^1
4	1.5977×10^2	1.1549×10^2
5	2.4876×10^2	1.8627×10^2
6	3.5753×10^2	2.7621×10^2
7	4.8608×10^2	3.8558×10^2
8	6.3440×10^2	5.1453×10^2
9	8.0250×10^2	6.6313×10^2
10	9.9037×10^2	8.3142×10^2
11	1.1980×10^3	1.0194×10^3
12	1.4254×10^3	1.2272×10^3
13	1.6726×10^3	1.4547×10^3
14	1.9396×10^3	1.7020×10^3

Table 2.3: The values of γ_i and λ_i for $0 < i < 14$ for $k = 1.20$.

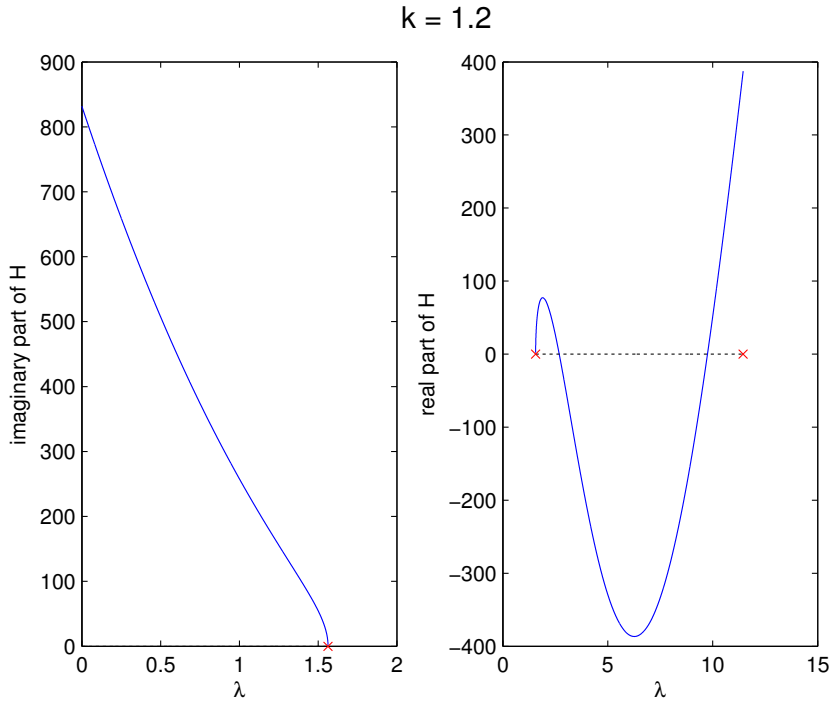

Figure 2.6: Plots of $H(\lambda, k)$ when $k = 1.2$. The left plot shows the range of λ for which $\lambda < \gamma_0$ and the right plot shows the range of λ for which $\lambda > \gamma_0$. The x's denote γ_0 and γ_1.

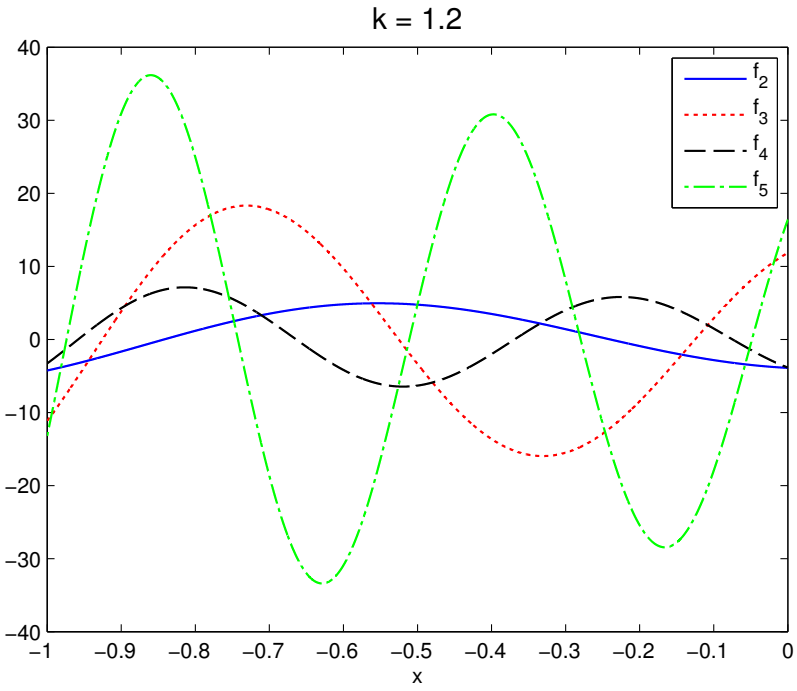

Figure 2.7: A plot of several eigenfunctions when $k = 1.20$.

For values of k such that $k_n < k < k_{n+1}$ for some $n \geq 1$, Lemma 3 tells us that $\gamma_n < \lambda^*(k) < \gamma_{n+1}$. Therefore, there will be exactly one eigenvalue between γ_i and γ_{i+1} except when $i = n$. In this case, we always get two eigenvalues. We see this in Figure 2.8 in which we plotted $H(\lambda, k)$ for $k = 1.35$. Note that this falls in the range $k_1 < k < k_2$. Again, there are no eigenvalues that are less than γ_0. λ_0 is between γ_0 and γ_1. Then there are two eigenvalues between γ_1 and γ_2. So

$$\gamma_0 < \lambda_0 < \gamma_1 < \lambda_1 < \lambda_2 < \gamma_2 < \lambda_3 < \gamma_3 < ...$$

The first fifteen values of γ_i and λ_i for $k = 1.35$ are given in Table 2.4. Several eigenfunctions are plotted in Figure 2.9.

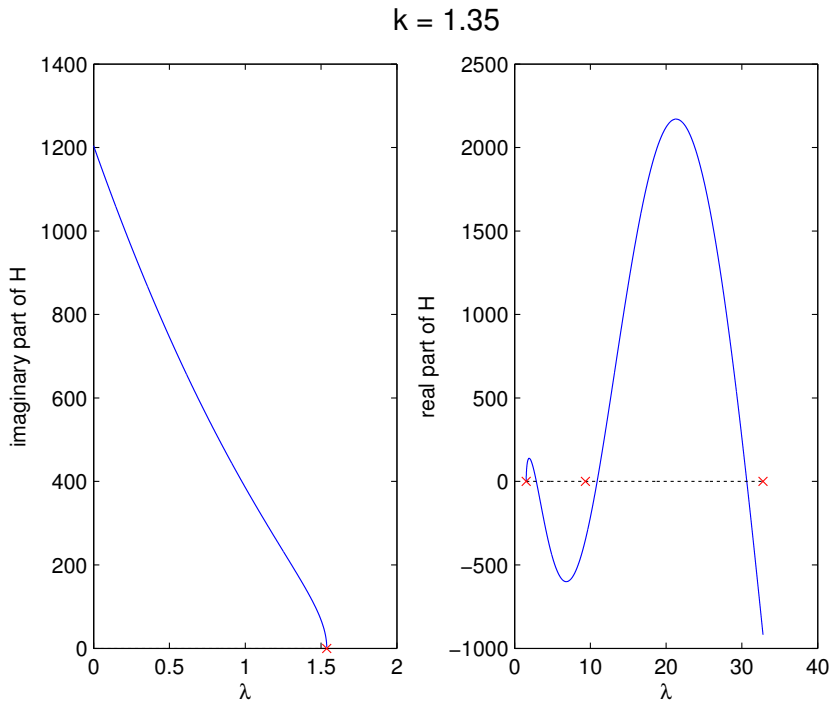

Figure 2.8: Plots of $H(\lambda, k)$ when $k = 1.35$. The left plot shows the range of λ for which $\lambda < \gamma_0$ and the right plot shows the range of λ for which $\lambda > \gamma_0$. The x's denote γ_0 and γ_1.

i	γ_i	λ_i
0	1.5378×10^0	2.8768×10^0
1	9.3506×10^0	1.0897×10^1
2	3.2789×10^1	3.0648×10^1
3	7.1853×10^1	6.3556×10^1
4	1.2654×10^2	1.1016×10^2
5	1.9686×10^2	1.7086×10^2
6	2.8280×10^2	2.4600×10^2
7	3.8437×10^2	3.3582×10^2
8	5.0156×10^2	4.4053×10^2
9	6.3437×10^2	5.6028×10^2
10	7.8282×10^2	6.9521×10^2
11	9.4689×10^2	8.4539×10^2
12	1.1266×10^3	1.0109×10^3
13	1.3219×10^3	1.1918×10^3
14	1.5328×10^3	1.3882×10^3

Table 2.4: The values of γ_i and λ_i for $0 < i < 14$ for $k = 1.35$.

In general, for $n \geq 2$ and $k_n < k < k_{n+1}$

$$\gamma_0 < \lambda_0 < ... < \gamma_{n-1} < \lambda_{n-1} < \gamma_n < \lambda_n < \lambda_{n+1} < \gamma_{n+1} < \lambda_{n+1} < ...$$

As we've seen, for $k > k_1$, the first positive eigenvalue, λ_0 is between γ_0 and γ_1. As k increases, λ_0 gets closer to γ_1. Recall that $\gamma_1 = \frac{4\pi^2+\alpha^2L^2+4k^2L^2}{4k^2L^2U\alpha}$. Therefore, as $k \to \infty$, $\gamma_1 \to \frac{1}{U\alpha}$. Therefore, the growth rate of the most dangerous mode for large wavenumbers approaches $\frac{1}{U\alpha}$. This is seen in Figure 2.10 in which we plot the largest value of $\sigma = \frac{1}{\lambda}$ versus k as well as $\frac{1}{\gamma_1}$ and $U\alpha$.

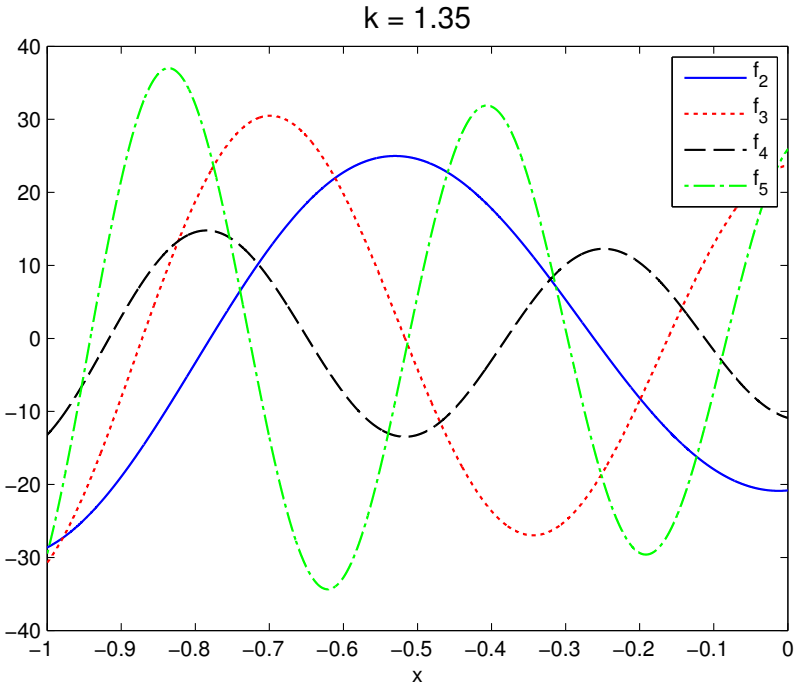

Figure 2.9: A plot of several eigenfunctions when $k = 1.35$.

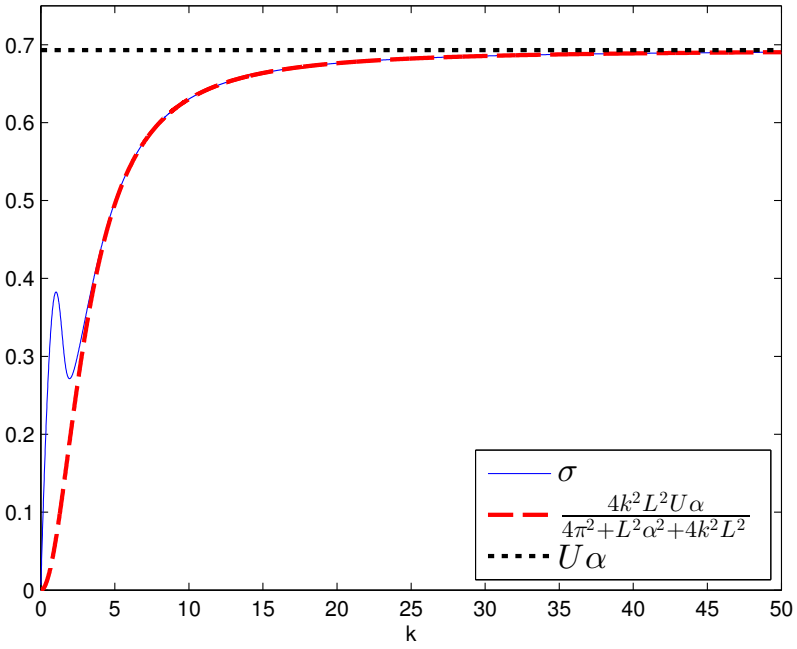

Figure 2.10: For large k, the largest value of σ behaves like $\frac{1}{\gamma_1}$.

2.4.2 Limiting Cases

We now investigate several limiting cases. First, we will look at the case when the viscous gradient in the middle layer vanishes ($\alpha \to 0$, see (2.48)). There are two different physical situations in which this can happen. The first is for the middle layer to maintain a constant, finite length while the viscosities at the endpoints of the middle layer approach each other ($\mu(-L) \to \mu(0)$). In the limit, this amounts to a finite middle layer with constant viscosity. The other physical situation is for the viscosity at each end of the layer to remain the same, but the length of the middle layer to increase to infinity. In this limit, the effects of the two interfaces are decoupled. We investigate both of these cases in section 2.4.2.1.

The other limiting case we investigate is when the length of the middle layer goes to zero. We handle this case in section 2.4.2.2.

2.4.2.1 $\lim_{\alpha \to 0}$ *Case*

We first consider the limit as $\alpha \to 0$. Considering (2.50), $\beta^2 \to -k^2$ as $\alpha \to 0$. Recall that the cutoff value between real and complex values of H is at $\gamma_0 = \frac{\alpha^2+4k^2}{4k^2 U\alpha}$ which goes to ∞ like $\frac{1}{\alpha}$ as $\alpha \to 0$. Therefore, as α vanishes, the infinite sequence of eigenvalues found in the previous section become arbitrarily large. In particular, the values of λ that occur when H is real are bounded below by $\frac{1}{U\alpha}$ (and therefore the corresponding σ values bounded above by $U\alpha$). Now, consider the function $H(\lambda, k)$ as $\alpha \to 0$ in the region $\lambda < \gamma_0$. Note that as $\alpha \to 0$,

$$H_1(\lambda, k) \to \left(\frac{\mu_r k - E_0\lambda}{\mu(0)}\right)\left(\frac{\mu_l k - E_1\lambda}{\mu(-L)}\right) + k^2, \tag{2.66}$$

and H_2 is independent of α. Recall

$$H_2(\lambda,k)=\left\{\frac{\mu_l k-E_1\lambda}{\mu(-L)}+\frac{\mu_r k-E_0\lambda}{\mu(0)}\right\}. \tag{2.67}$$

Using (2.66) and (2.67) in (2.58),

$$\begin{aligned}
H(\lambda,k)\to& i\left\{\left(\frac{\mu_r k-E_0\lambda}{\mu(0)}\right)\left(\frac{\mu_l k-E_1\lambda}{\mu(-L)}\right)+k^2\right\}\sinh(kL)\\
&+ik\left\{\frac{\mu_l k-E_1\lambda}{\mu(-L)}+\frac{\mu_r k-E_0\lambda}{\mu(0)}\right\}\cosh(kL)\\
=&i\left\{\frac{\mu_r k}{\mu(0)}\frac{\mu_l k}{\mu(-L)}-\left(\frac{\mu_r k}{\mu(0)}\frac{E_1}{\mu(-L)}+\frac{\mu_l k}{\mu(-L)}\frac{E_0}{\mu(0)}\right)\lambda+\frac{E_0E_1}{\mu(0)\mu(-L)}\lambda^2+k^2\right\}\sinh(kL)\\
&+i\left\{\left(\frac{\mu_l}{\mu(-L)}+\frac{\mu_r}{\mu(0)}\right)k^2-\left(\frac{E_1k}{\mu(-L)}+\frac{E_0k}{\mu(0)}\right)\lambda\right\}\cosh(kL)\\
=&i\left(\frac{E_0E_1}{\mu(0)\mu(-L)}\sinh(kL)\right)\lambda^2\\
&-i\left\{\left(\frac{\mu_r k}{\mu(0)}\frac{E_1}{\mu(-L)}+\frac{\mu_l k}{\mu(-L)}\frac{E_0}{\mu(0)}\right)\sinh(kL)+\left(\frac{E_1k}{\mu(-L)}+\frac{E_0k}{\mu(0)}\right)\cosh(kL)\right\}\lambda\\
&+ik^2\left\{\left(\frac{\mu_r}{\mu(0)}\frac{\mu_l}{\mu(-L)}+1\right)\sinh(kL)+\left(\frac{\mu_l}{\mu(-L)}+\frac{\mu_r}{\mu(0)}\right)\cosh(kL)\right\}\\
=&i\left(\tilde{c}\lambda^2+\tilde{b}\lambda+\tilde{a}\right),
\end{aligned}$$

where

$$\begin{aligned}
\tilde{c}=&\frac{k^2}{2\mu(0)\mu(-L)}\frac{E_0E_1}{k^2}\left(e^{kL}-e^{-kL}\right),\\
\tilde{b}=&-\frac{k^2}{2\mu(0)\mu(-L)}\left\{\left(\frac{\mu_rE_1}{k}+\frac{\mu_lE_0}{k}\right)\left(e^{kL}-e^{-kL}\right)+\left(\frac{\mu(0)E_1}{k}+\frac{\mu(-L)E_0}{k}\right)\left(e^{kL}+e^{-kL}\right)\right\},\\
\tilde{a}=&\frac{k^2}{2\mu(0)\mu(-L)}\left\{\left[\mu_r\mu_l+\mu(0)\mu(-L)\right]\left(e^{kL}-e^{-kL}\right)+\left[\mu_l\mu(0)+\mu_r\mu(-L)\right]\left(e^{kL}+e^{-kL}\right)\right\}.
\end{aligned}$$

We wish to solve $H(\lambda,k)=0$ which is equivalent to $\frac{2i\mu(0)\mu(-L)\sigma^2H}{k^2}=0$. Therefore, the growth rate σ satisfies $a\sigma^2+b\sigma+c$ where $a=-\frac{2\mu(0)\mu(-L)\tilde{a}}{k^2}$, $b=-\frac{2\mu(0)\mu(-L)\tilde{b}}{k^2}$ and

$c = -\frac{2\mu(0)\mu(-L)\tilde{c}}{k^2}$. After some algebraic manipulation, we get

$$\begin{aligned}
a =& -e^{kL}(\mu_r + \mu(0))(\mu_l + \mu(-L)) + e^{-kL}(\mu_r - \mu(0))(\mu_l - \mu(-L)),\\
b =& \left\{(\mu_r + \mu(0))e^{kL} + (\mu(0) - \mu_r)e^{-kL}\right\}\left(\frac{E_1}{k}\right)\\
&+ \left\{(\mu_l + \mu(-L))e^{kL} + (\mu(-L) - \mu_l)e^{-kL}\right\}\left(\frac{E_0}{k}\right),\\
c =& \frac{E_0 E_1}{k^2}\left(e^{-kL} - e^{kL}\right).
\end{aligned} \tag{2.68}$$

There are two different ways in which $\alpha \to 0$. The first is for $\mu(-L) \to \mu(0)$. In this case, the middle layer is of finite length, but the viscosity of the middle layer is essentially constant. If we denote $\mu \equiv \mu(-L) = \mu(0)$, then a, b, and c correspond to the coefficients found for a constant viscosity middle layer [17]. Therefore, the exponential viscous profile reduces to the constant viscosity case.

The other way in which $\alpha \to 0$ is to preserve the size of the viscous jumps at the interfaces, but let $L \to \infty$. Then

$$\begin{aligned}
c \to& -\frac{E_0}{k}\frac{E_1}{k}e^{kL},\\
b \to& \left[(\mu_r + \mu(0))\frac{E_1}{k} + (\mu_l + \mu(-L))\frac{E_0}{k}\right]e^{kL},\\
a \to& -(\mu_r + \mu(0))(\mu_l + \mu(-L))e^{kL}.
\end{aligned}$$

Then σ is given by $\frac{-b\pm\sqrt{b^2-4ac}}{2a}$. But

$$\begin{aligned}
b^2-4ac=&\left[(\mu_r+\mu(0))\frac{E_1}{k}+(\mu_l+\mu(-L))\frac{E_0}{k}\right]^2 e^{2kL}\\
&-4(\mu_r+\mu(0))(\mu_l+\mu(-L))\frac{E_1}{k}\frac{E_0}{k}e^{2kL}\\
=&(\mu_r+\mu(0))^2\left(\frac{E_1}{k}\right)^2 e^{2kL}+2(\mu_r+\mu(0))(\mu_l+\mu(-L))\frac{E_1}{k}\frac{E_0}{k}e^{2kL}\\
&+(\mu_l+\mu(-L))^2\left(\frac{E_0}{k}\right)^2-4(\mu_r+\mu(0))(\mu_l+\mu(-L))\frac{E_1}{k}\frac{E_0}{k}e^{2kL}\\
=&(\mu_r+\mu(0))^2\left(\frac{E_1}{k}\right)^2 e^{2kL}-2(\mu_r+\mu(0))(\mu_l+\mu(-L))\frac{E_1}{k}\frac{E_0}{k}e^{2kL}\\
&+(\mu_l+\mu(-L))^2\left(\frac{E_0}{k}\right)^2\\
=&\left[(\mu_r+\mu(0))\frac{E_1}{k}-(\mu_l+\mu(-L))\frac{E_0}{k}\right]^2 e^{2kL}.
\end{aligned}$$

Therefore

$$\begin{aligned}
\frac{-b\pm\sqrt{b^2-4ac}}{2a}=&\frac{-\left[(\mu_r+\mu(0))\frac{E_1}{k}+(\mu_l+\mu(-L))\frac{E_0}{k}\right]e^{kL}}{-2(\mu_r+\mu(0))(\mu_l+\mu(-L))e^{kL}}\\
&\pm\frac{\left[(\mu_r+\mu(0))\frac{E_1}{k}-(\mu_l+\mu(-L))\frac{E_0}{k}\right]e^{kL}}{-2(\mu_r+\mu(0))(\mu_l+\mu(-L))e^{kL}}.
\end{aligned}$$

The two solutions are

$$\sigma^+=\frac{-b+\sqrt{b^2-4ac}}{2a}=\frac{-2(\mu_l+\mu(-L))\frac{E_0}{k}}{-2(\mu_r+\mu(0))(\mu_l+\mu(-L))}=\frac{E_0}{k(\mu_r+\mu(0))},$$

and

$$\sigma^-=\frac{-b-\sqrt{b^2-4ac}}{2a}=\frac{-2(\mu_r+\mu(0))\frac{E_1}{k}}{-2(\mu_r+\mu(0))(\mu_l+\mu(-L))}=\frac{E_1}{k(\mu_l+\mu(-L))}.$$

These are the usual Saffman-Taylor growth rates of each interface [64].

2.4.2.2 $\lim_{L\to 0}$ *Case*

Next, we consider the limit as $L \to 0$. Recall that $\alpha = \frac{1}{L}\ln\left(\frac{\mu(0)}{\mu(-L)}\right)$. Therefore, $\alpha \to \infty$ at a rate of $\frac{1}{L}$ as $L \to 0$. Using (2.50), $\beta^2 \to -\frac{\alpha^2}{4}$. Like the previous case, $\gamma_0 \to \infty$ as $L \to 0$, but this time, $\gamma_0 \to \frac{\alpha}{4k^2U}$. Therefore, the values of λ that occur when H is real are bounded below by $\frac{\alpha}{4k^2U}$ (and therefore the corresponding σ values bounded above by $\frac{4k^2U}{\alpha}$). Now, consider the function $H(\lambda, k)$ as $L \to 0$ in the region $\lambda < \gamma_0$. Note that $H_2(\lambda, k)$ is independent of L. We rewrite $H_1(\lambda, k)$ as

$$H_1(\lambda,k) = \left(\frac{\mu_r k - E_0\lambda}{\mu(0)}\right)\left(\frac{\mu_l k - E_1\lambda}{\mu(-L)}\right) + \frac{\alpha}{2}\left(\frac{\mu_r k - E_0\lambda}{\mu(0)} - \frac{\mu_l k - E_1\lambda}{\mu(-L)}\right) - \frac{\alpha^2}{4} - \beta^2.$$

Then as $L \to 0$,

$$H_1(\lambda,k) \to \frac{\alpha}{2}\left(\frac{\mu_r k - E_0\lambda}{\mu(0)} - \frac{\mu_l k - E_1\lambda}{\mu(-L)}\right). \tag{2.69}$$

Therefore, using (2.69) and our estimate for β,

$$\begin{aligned}
H(\lambda,k) =& i\left\{H_1(\lambda,k)\sinh(|\beta|L) + |\beta|H_2(\lambda,k)\cosh(|\beta|L)\right\}\\
\to& i\left\{\frac{\alpha}{2}\left(\frac{\mu_r k - E_0\lambda}{\mu(0)} - \frac{\mu_l k - E_1\lambda}{\mu(-L)}\right)\sinh\left(\frac{\alpha L}{2}\right)\right.\\
&\left.+\frac{\alpha}{2}\left(\frac{\mu_r k - E_0\lambda}{\mu(0)} + \frac{\mu_l k - E_1\lambda}{\mu(-L)}\right)\cosh\left(\frac{\alpha L}{2}\right)\right\}\\
=& \frac{i\alpha}{2}\left\{\left(\frac{\mu_r k - E_0\lambda}{\mu(0)}\right)\left(\cosh\left(\frac{\alpha L}{2}\right) + \sinh\left(\frac{\alpha L}{2}\right)\right)\right.\\
&\left.+\left(\frac{\mu_l k - E_1\lambda}{\mu(-L)}\right)\left(\cosh\left(\frac{\alpha L}{2}\right) - \sinh\left(\frac{\alpha L}{2}\right)\right)\right\}\\
=& \frac{i\alpha}{2}\left\{\left(\frac{\mu_r k - E_0\lambda}{\mu(0)}\right)e^{\frac{\alpha L}{2}} + \left(\frac{\mu_l k - E_1\lambda}{\mu(-L)}\right)e^{-\frac{\alpha L}{2}}\right\}\\
=& \frac{i\alpha}{2}e^{-\frac{\alpha L}{2}}\left\{\left(\frac{\mu_r k - E_0\lambda}{\mu(0)}\right)e^{\alpha L} + \left(\frac{\mu_l k - E_1\lambda}{\mu(-L)}\right)\right\}.
\end{aligned}$$

But $e^{\alpha L} = \frac{\mu(0)}{\mu(-L)}$. Therefore,

$$H(\lambda, k) \to \frac{i\alpha}{2\mu(-L)} e^{-\frac{\alpha L}{2}} \left\{ (\mu_r k - E_0 \lambda) + (\mu_l k - E_1 \lambda) \right\}, \tag{2.70}$$

and $H(\lambda, k) = 0$ if and only if

$$\lambda = \frac{(\mu_r + \mu_l)k}{E_0 + E_1}.$$

Using the definitions of E_0 and E_0, this condition is equivalent to

$$\lambda = \frac{(\mu_r + \mu_l)}{kU(\mu_r - \mu(0) + \mu(-L) - \mu_l) - k^3(T_0 + T_1)}.$$

Then the growth rate is

$$\sigma = \frac{kU(\mu_r - \mu(0) + \mu(-L) - \mu_l) - k^3(T_0 + T_1)}{(\mu_r + \mu_l)}, \tag{2.71}$$

which is the Saffman-Taylor growth rate for a single interface with a viscosity jump equal to the sum of the viscosity jumps at the two interfaces and with interfacial tension equal to the sums of the interfacial tensions of the two interfaces. This implies that even an infinitely small middle layer will be less unstable than the two layer flow.

2.5 Conclusion

We studied the spectrum of a non-standard eigenvalue problem that arises from the linear stability analysis of three-layer Hele-Shaw flows with a variable viscosity middle layer. This problem differs from regular Sturm-Liouville problems because of the presence of the eigenvalue in the boundary conditions. However, we were able to show that there is an infinite set of discrete eigenvalues and that the corresponding

eigenfunctions are complete in a certain Hilbert space. We then applied this theory to the case of an exponential viscous profile. Not only were we able to verify the theoretical results of the previous section, but also provide a sequence of numbers, $\{\gamma_n\}$, that alternate with the eigenvalues of the system. We verified this with numerical computation of the eigenvalues using a pseudo-spectral method. Finally, we investigated several limiting cases. The first is when the viscous profile of the middle layer approaches a constant viscosity, both in the case of a fixed-length middle layer and also as the length of the middle layer goes to infinity. The second limiting case is when the length of the middle layer approaches zero.

3. STABILITY RESULTS WITH DIFFUSION IN THREE-LAYER RECTILINEAR HELE-SHAW AND POROUS MEDIA FLOWS

3.1 Introduction

As in chapter 2, we consider three-layer rectilinear Hele-Shaw flows with a variable viscosity middle layer. However, we now include the effect of diffusion of polymer in the middle layer. We assume that the two exterior fluids are such that the polymer will not permeate through the immiscible interfaces into these layers. This is practical in chemical EOR if the right fluid is oil, the intermediate fluid is a poly-solution (an aqueous phase containing polymer), and the left fluid is a non-aqueous phase liquid (NAPL).

Recall that this scenario has been examined by Daripa and Pasa in [29] and [30]. In Daripa and Pasa [29], the linear stability problem with diffusion of polymer only in the middle layer is first formulated mathematically. Using upper bound estimates, it is found that a disturbance, if unstable, can be stabilized by diffusion. In Daripa and Pasa [30] a constructive method is used to obtain similar upper bounds from analysis of a numerical approximation of the system of second order equations involved.

An alternate version of the numerical scheme proposed in [30] was implemented by Daripa and Ding [23]. They found that the effect of diffusion on stabilization can be dramatic even when the diffusion is very small. However, their method is a finite difference method that is very slow. Additionally, the method suffers from numerical diffusion. Therefore, high resolution calculations are necessary in order to reduce the effect of numerical diffusion, thereby making sure that the drastic stabilization is indeed due to physical diffusion. Since the method is very slow and has limited accuracy, we use an improved numerical method in this chapter to numerically

investigate the effect of diffusion.

The chapter is laid out as follows. In section 3.2, we describe the mathematical model and formulation. In contrast to previous formulations, we use dimensionless variables and consider when viscosity has both linear and exponential dependence on the concentration of polymer. In section 3.3, we improve the proof in [29] that the flow is completely stabilized by large enough diffusion. We also obtain new stabilization results. Numerical results are given in section 3.4 which confirm the drastic stabilization capacity of diffusion which was found in Daripa and Ding [23] with a low order finite difference method. Finally we conclude in section 3.5.

3.2 Preliminaries

The basic preliminaries and mathematical formulation of this problem, which have appeared in earlier works (see [29], [30]), are presented below. Even though this section overlaps to some extent with what has been presented in these two papers, it is necessary to present this formulation here in order to build upon these works. Additionally, the formulation here adds two new components which are not present in the two aforementioned papers: a non-dimensionalization of the problem and the consideration of how viscosity depends on the concentration of polymer.

We consider two-dimensional fluid flows in a three-layer Hele-Shaw cell (see Figure 3.1). In the leftmost layer, $-\infty < x \leq -L$, the fluid has a constant viscosity μ_l. The fluid in this layer can be thought of as some non-aqueous phase liquid (NAPL). The rightmost layer, which may be taken as oil, extends from $x = 0$ up to $x = \infty$ and is characterized by constant viscosity μ_r. The middle layer is of length L and contains a fluid of variable viscosity $\mu(x)$ such that $\mu_l \leq \mu(x) \leq \mu_r$. The fluid in this middle layer is immiscible with the fluids in the other two layers. For the purpose of application to EOR by chemical flooding, this fluid may be taken as a poly-solution

having a concentration profile of polymer. The right interface, separating the middle and the right-most fluid layers, has an interfacial tension T_0, and the left interface, separating the middle and the left-most fluid layers, has an interfacial tension T_1. The fluid upstream at $x = -\infty$ has a velocity $(U, 0)$. The governing equations are the continuity equation, Darcy's law, and the advection-diffusion equation for the concentration of polymer.

$$\nabla \cdot \mathbf{u} = 0, \tag{3.1}$$

$$\nabla\, p = -\frac{\mu}{K}\, \mathbf{u}, \tag{3.2}$$

$$\frac{\partial c}{\partial t} + \mathbf{u} \cdot \nabla c = D \triangle\, c, \tag{3.3}$$

where $\nabla = (\frac{\partial}{\partial x}, \frac{\partial}{\partial y})$, $\triangle$ is the Laplacian in the plane, c is the concentration of polymer in the middle layer, K is the permeability, and D, the diffusion coefficient, is a constant. In a Hele-Shaw cell, $K = b^2/12$ where b is the width of the gap between the plates.

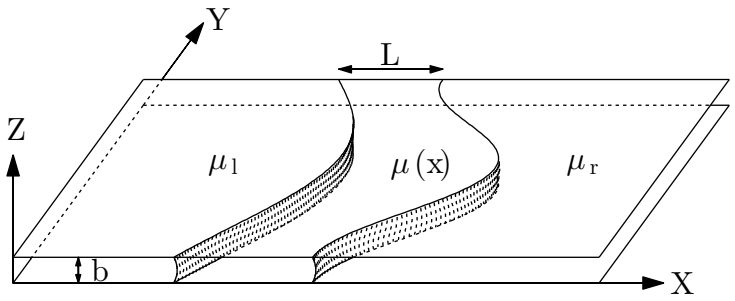

Figure 3.1: Three-layer fluid flow in a Hele-Shaw cell.

The above system (3.1)-(3.3) admits a simple basic solution: all of the fluid moves with speed U in the x direction and the two interfaces are planar (parallel to the

y-axis). In order to have a concentration profile which satisfies equation (3.3) and does not change in time, the concentration profile must be linear. The pressure of the basic solution is obtained by integrating (3.2). In a frame moving with velocity $(U, 0)$, the basic solution is stationary. Below, with slight abuse of notation, the same variable x is used to refer to the $x-$coordinate in the moving frame.

The above equations (3.1) - (3.3) in the moving frame are given by

$$\nabla \cdot \mathbf{u} = 0, \tag{3.4}$$

$$\nabla\, p = -\frac{\mu}{K}\, \mathbf{u} - \frac{\mu}{K}\, U\, \hat{i}, \tag{3.5}$$

$$\frac{\partial c}{\partial t} + \mathbf{u} \cdot \nabla c = D \triangle\, c. \tag{3.6}$$

We scale our variables by the characteristic length L and the characteristic velocity U. Using $\mathbf{u}' := (u', v') = (u/U, v/U) = \mathbf{u}/U$, $x' = x/L$, and $y' = y/L$, equation (3.4) becomes

$$\frac{U}{L} \nabla' \cdot \mathbf{u}' = 0,$$

where $\nabla' = (\frac{\partial}{\partial x'}, \frac{\partial}{\partial y'})$. Therefore,

$$\nabla' \cdot \mathbf{u}' = 0, \tag{3.7}$$

Additionally, we scale our viscosity by the value of an "effective viscosity" of the leading fluid, $\frac{K\mu_r}{L^2}$. Therefore, the characteristic pressure is $U\mu_r/L$. Letting $p' = pL/(U\mu_r)$ and $\mu' = \mu L^2/(K\mu_r)$, equation (3.5) becomes

$$\frac{U\mu_r}{L^2} \nabla'\, p' = -\frac{U\mu_r}{L^2}\, \mu'\, \mathbf{u}' - \frac{U\mu_r}{L^2}\, \mu'\, \hat{i},$$

and therefore

$$\nabla' p' = -\mu' \mathbf{u}' - \mu' \hat{i}. \tag{3.8}$$

Finally, using $\mathbf{u}' = \mathbf{u}/U$, $\nabla' = L \nabla$, $\triangle' = L^2 \triangle$, and $t' = tU/L$, equation (3.6) becomes

$$\frac{U}{L}\frac{\partial c}{\partial t'} + \frac{U}{L}\mathbf{u}' \cdot \nabla' c = \frac{D}{L^2}\triangle' c.$$

Therefore,

$$\frac{\partial c}{\partial t'} + \mathbf{u}' \cdot \nabla' c = \frac{1}{Pe}\triangle' c, \tag{3.9}$$

where $Pe = UL/D$ is the Peclet number.

Next, we consider the interface conditions. Let $x = \eta(y,t)$ be the position of an interface. Then the kinematic interface condition is

$$\frac{\partial \eta}{\partial t} = \mathbf{u} \cdot \hat{n},$$

where $\hat{n}$ is the unit normal vector. The position of the interface in the scaled variables is $x' = \eta'(y',t') = \eta(y,t)/L$. Using this along with $t' = tU/L$ and $\mathbf{u}' = \mathbf{u}/U$,

$$\frac{\partial \eta'}{\partial t'} = \mathbf{u}' \cdot \hat{n}. \tag{3.10}$$

The dynamic interface condition is given by

$$[p] = -T(\nabla \cdot \hat{n}),$$

where $[p]$ is the jump in pressure across the interface and T is the interfacial tension.

Using $p' = pL/(U\mu_r)$ and $\nabla' = L\,\nabla$, this becomes

$$\frac{U\mu_r}{L}[p'] = -\frac{T}{L}(\nabla' \cdot \hat{n}).$$

Therefore,

$$[p'] = -\frac{1}{Ca}\frac{T}{T_0}(\nabla' \cdot \hat{n}), \tag{3.11}$$

where T_0, the interfacial tension of the leading interface, is the characteristic interfacial tension and $Ca = U\mu_r/T_0$ is the capillary number. Collecting equations (3.7) - (3.11) and dropping the primes, we have the dimensionless system

$$\left.\begin{aligned} &\nabla\cdot\mathbf{u} = 0, \\ &\nabla p = -\mu\ \mathbf{u} - \mu\ \hat{i}, \\ &\tfrac{\partial c}{\partial t} + \mathbf{u}\cdot\nabla c = \tfrac{1}{Pe}\triangle c, \\ &\tfrac{\partial \eta}{\partial t} = \mathbf{u}\cdot\hat{n}, \\ &[p] = -\tfrac{1}{Ca}\tfrac{T}{T_0}(\nabla\cdot\hat{n}). \end{aligned}\right\} \tag{3.12}$$

with interfaces at $x = -1$ and $x = 0$.

The basic solution to the above equations is $(u = 0, v = 0, p_0(x), c_0(x))$. The basic pressure, p_0, is obtained by integrating (3.8) and depends only on x. In order to satisfy (3.9), we require that the concentration c_0 is a linear function of x. The viscosity inside the middle layer is a function of concentration. We denote $\mu_0 = \mu(c_0)$. The interfaces remain planar at $x = -1$ and $x = 0$. We perturb this basic solution by $(\widetilde{u}, \widetilde{v}, \widetilde{p}, \widetilde{c})$. Plugging into (3.7) and denoting $\widetilde{\mathbf{u}} = (\widetilde{u}, \widetilde{v})$,

$$\nabla\cdot\widetilde{\mathbf{u}} = 0. \tag{3.13}$$

From the x-coordinate of equation (3.8),

$$\frac{dp_0}{dx} + \frac{\partial \widetilde{p}}{\partial x} = -\mu(c_0 + \widetilde{c})(\widetilde{u} + 1).$$

Within linear approximation, $\mu(c_0 + \widetilde{c}) = \mu_0 + \frac{d\mu}{dc}(c_0)\widetilde{c}$. Using that $\frac{dp_o}{dx} = -\mu_o$,

$$\frac{\partial \widetilde{p}}{\partial x} = -\mu_0 \widetilde{u} - \frac{d\mu}{dc}(c_0)\widetilde{c}\,\widetilde{u} - \frac{d\mu}{dc}(c_0)\widetilde{c}.$$

Again linearizing with respect to the disturbances,

$$\frac{\partial \widetilde{p}}{\partial x} = -\mu_0 \widetilde{u} - \frac{d\mu}{dc}(c_0)\widetilde{c}. \tag{3.14}$$

Using the y-coordinate of equation (3.8),

$$\frac{\partial \widetilde{p}}{\partial y} = -\mu(c_0 + \widetilde{c})\widetilde{v}.$$

We again use $\mu(c_0 + \widetilde{c}) = \mu_0 + \frac{d\mu}{dc}(c_0)\widetilde{c}$ and linearize to get

$$\frac{\partial \widetilde{p}}{\partial y} = -\mu_0 \widetilde{v}. \tag{3.15}$$

Plugging into equation (3.9) gives,

$$\frac{\partial \widetilde{c}}{\partial t} + \frac{dc_0}{dx}\widetilde{u} + \widetilde{\mathbf{u}} \cdot \nabla \widetilde{c} = \frac{1}{Pe} \triangle \widetilde{c}.$$

Linearizing with respect to the disturbances,

$$\frac{\partial \widetilde{c}}{\partial t} + \frac{dc_0}{dx}\widetilde{u} = \frac{1}{Pe} \triangle \widetilde{c}. \tag{3.16}$$

Equations (3.13)-(3.16) govern the disturbances. We use the method of normal modes and express the disturbances as

$$(\widetilde{u}, \widetilde{v}, \widetilde{p}, \widetilde{c}) = (f(x), \psi(x), \phi(x), h(x))\, e^{(i\,k\,y+\sigma t)}. \tag{3.17}$$

Using this ansatz in equations (3.13) and (3.15) gives

$$\psi = \frac{i}{k} f_x, \qquad \phi = -\frac{\mu_0}{k^2} f_x. \tag{3.18}$$

Cross-differentiating equations (3.14) and (3.15) gives

$$\frac{\partial^2 \widetilde{p}}{\partial x \partial y} = \frac{\partial}{\partial y}\left(-\mu_0 \widetilde{u} - \frac{d\mu}{dc}(c_0)\widetilde{c}\right) = -\mu_0 \frac{\partial \widetilde{u}}{\partial y} - \frac{d\mu}{dc}(c_0)\frac{\partial \widetilde{c}}{\partial y},$$

and

$$\frac{\partial^2 \widetilde{p}}{\partial x \partial y} = \frac{\partial}{\partial x}(-\mu_0 \widetilde{v}).$$

Equating these,

$$-\mu_0 \frac{\partial \widetilde{u}}{\partial y} - \frac{d\mu}{dc}(c_0)\frac{\partial \widetilde{c}}{\partial y} = -\frac{\partial}{\partial x}(\mu_0 \widetilde{v}).$$

Using (3.17),

$$-ik\mu_0 f(x) e^{(i\,k\,y+\sigma t)} - ik\frac{d\mu}{dc}(c_0) h(x) e^{(i\,k\,y+\sigma t)} = -\frac{d}{dx}(\mu_0 \psi(x)) e^{(i\,k\,y+\sigma t)}.$$

Using (3.18),

$$-ik\mu_0 f - ik\frac{d\mu}{dc}(c_0) h = -\frac{i}{k}(\mu_0 f_x)_x,$$

and therefore,

$$-(\mu_0 f_x)_x + k^2 \mu_0 f = -k^2 \frac{d\mu}{dc}(c_0) h. \tag{3.19}$$

Next, we use our ansatz (3.17) in (3.16),

$$\sigma h e^{(i\,k\,y+\sigma t)} + \frac{dc_0}{dx} f e^{(i\,k\,y+\sigma t)} = \frac{1}{Pe}\left(h_{xx} - k^2 h\right) e^{(i\,k\,y+\sigma t)},$$

and therefore,

$$h_{xx} - (\sigma Pe + k^2)h = Pe\,\frac{dc_0}{dx} f. \tag{3.20}$$

We now investigate the boundary conditions of the eigenvalue problem given by (3.19) and (3.20). Consider a planar interface at $\eta(y,t) = x_0$ that is perturbed by $\widetilde{\eta}(y,t)$. Plugging this into (3.10) and linearizing, we get

$$\frac{\partial \widetilde{\eta}}{\partial t} = \widetilde{u}(x_0).$$

Using (3.17) and solving the simple differential equation yields

$$\widetilde{\eta} = \frac{f(x_0)}{\sigma} e^{(i\,k\,y+\sigma t)}. \tag{3.21}$$

The linearized form of (3.11) is

$$p^+(x) - p^-(x) = \frac{1}{Ca}\frac{T}{T_0}\widetilde{\eta}_{yy}, \qquad x = x_0 + \widetilde{\eta},$$

where the superscripts '+'; and '−' denote the limits from above and below, respectively. But we can approximate the pressure $p^+(x)$ by

$$\begin{aligned} p^+(x_0+\widetilde{\eta}) &= p_0^+(x_0+\widetilde{\eta}) + \widetilde{p}^{\,+}(x_0+\widetilde{\eta}) \\ &\approx p_0^+(x_0) + \widetilde{\eta}\,\frac{\partial p_0}{\partial x}\bigg|_{x=x_0} + \widetilde{p}^{\,+}(x_0), \end{aligned}$$

and similarly for $p^-(x)$. The basic pressure, p_0, is continuous across the interface.

Also recall that $dp_0/dx = -\mu_0$. Therefore,

$$\widetilde{p}^{\,+}(x_0) - \widetilde{\eta}\mu_0^+(x_0) - \widetilde{p}^{\,-}(x_0) + \widetilde{\eta}\mu_0^-(x_0) = \frac{1}{Ca}\frac{T}{T_0}\widetilde{\eta}_{yy}.$$

Using (3.17) and (3.21),

$$\phi^+(x_0) - \phi^-(x_0) - \left(\mu_0^+(x_0) - \mu_0^-(x_0)\right)\frac{f(x_0)}{\sigma} = -\frac{k^2 T}{\sigma Ca T_0} f(x_0).$$

Using (3.18),

$$\mu_0^-(x_0) f_x^-(x_0) - \mu_0^+(x_0) f_x^+(x_0) = \frac{k^2\left(\mu_0^+(x_0) - \mu_0^-(x_0)\right) - \frac{k^4}{Ca}\frac{T}{T_0}}{\sigma} f(x_0). \tag{3.22}$$

We first investigate this interface condition at $x_0 = -1$. When $x < -1$, $\mu(x) = \mu_l$ and $c \equiv 0$. Therefore, $h \equiv 0$. Equation (3.19) becomes

$$f_{xx} - k^2 f = 0. \tag{3.23}$$

In order to satisfy the far-field boundary condition at $x = -\infty$, f must satisfy

$$f(x) = f(-1)e^{k(x+1)}, \qquad x < -1.$$

Therefore, in equation (3.22), we can use $f_x^-(-1) = kf(-1)$ and $\mu_0^-(-1) = \mu_l$. This gives

$$\mu_0^+(-1) f_x^+(-1) = \left\{ \mu_l\, k - \frac{k^2\left(\mu_0^+(-1) - \mu_l\right) - \frac{k^4}{Ca}\frac{T_1}{T_0}}{\sigma} \right\} f(-1), \tag{3.24}$$

where T_1 is the interfacial tension of the trailing interface. For the interface condition

at $x_0 = 0$, we note that when $x > 0$, the function f again satisfies (3.23). Therefore,

$$f(x) = f(0)e^{-kx}, \qquad x > 0.$$

We use $f_x^+(0) = -kf(0)$ and $\mu_0^+(0) = \mu_r$ in (3.22) to get

$$-\mu_0^-(0)f_x^-(0) = \left\{ \mu_r\, k - \frac{k^2\left(\mu_r - \mu_0^-(0)\right) - \frac{k^4}{Ca}}{\sigma} \right\} f(0). \tag{3.25}$$

Additionally, we require that the concentration of polymer is not perturbed at the interfaces. This amounts to

$$h(-1) = h(0) = 0. \tag{3.26}$$

Collecting the above equations and denoting $\lambda = 1/\sigma$ and $a = (c_0(0) - c_0(-1))$,

$$\left.\begin{aligned} &-\left(\mu f_x\right)_x + k^2\mu f = -k^2\tfrac{d\mu}{dc}(c_0)h, \qquad x \in (-1,0),\\ &h_{xx} - (\sigma Pe + k^2)h = a\, Pe\, f, \qquad x \in (-1,0),\\ &\mu(-1)f_x(-1) = (\mu_l\, k - \lambda E_1)\, f(-1),\\ &-\mu(0)f_x(0) = (\mu_r\, k - \lambda E_0)\, f(0),\\ &h(-1) = h(0) = 0, \end{aligned}\right\} \tag{3.27}$$

where

$$E_0 = k^2\left(\mu_r - \mu(0)\right) - \frac{k^4}{Ca}, \qquad E_1 = k^2\left(\mu(-1) - \mu_l\right) - \frac{k^4}{Ca}\frac{T_1}{T_0}. \tag{3.28}$$

In equation $(3.27)_1$, we have dropped the subscript '0' from μ.

Note: The terms μ_r and μ_l are scaled versions of these variables. From our original scaling, we'll have $\mu_r' = L^2/K$ and $\mu_l' = (\mu_l/\mu_r)(L^2/K)$.

It is often convenient, both numerically and analytically, to eliminate the function

h from the system (3.27) and consider a single equation for the function f. This equation depends on the relationship between the viscosity μ and the concentration of polymer c. We now consider two different cases.

A. $\mu(c)$ is linear

First we consider the case when μ is a linear function of c, which is reasonable to assume for small c. This assumption was made implicitly in [29] and [30], but we make this dependence explicit here. If μ is a linear function of c, then μ is also a linear function of x. Using that $\mu_x = \mu_c c_x$ in equation $(3.27)_1$,

$$-\left(\mu f_x\right)_x + k^2 \mu f = -\frac{k^2 \mu_x}{a} h,$$

where μ_x is a constant. Then

$$h = \frac{a}{k^2 \mu_x}\left(\mu f_{xx} + \mu_x f_x - k^2 \mu f\right). \tag{3.29}$$

Taking two derivatives of this equation,

$$h_x = \frac{a}{k^2 \mu_x}\left(\mu f_{3x} + 2\mu_x f_{xx} - k^2 \mu f_x - k^2 \mu_x f\right),$$

and

$$h_{xx} = \frac{a}{k^2 \mu_x}\left(\mu f_{4x} + 3\mu_x f_{3x} - k^2 \mu f_{xx} - 2k^2 \mu_x f_x\right). \tag{3.30}$$

Plugging (3.29) and (3.30) in equation $(3.27)_2$ and simplifying yields

$$\mu f_{4x} + 3\mu_x f_{3x} - (\sigma Pe + 2k^2)\mu f_{xx} - (\sigma Pe + 3k^2)\mu_x f_x + \left\{(\sigma Pe + k^2)k^2 \mu - Pe\, k^2 \mu_x\right\} f = 0. \tag{3.31}$$

Using $\lambda = 1/\sigma$,

$$Pe\,(\mu f_{xx}+\mu_x f_x-k^2\mu f) = \lambda\Big\{\mu f_{4x}+3\mu_x f_{3x}-2k^2\mu f_{xx}-3k^2\mu_x f_x+\big\{k^4\mu - Pe\,k^2\mu_x\big\}\,f\Big\}. \tag{3.32}$$

Note that in the limit $Pe \to \infty$, this becomes

$$\mu f_{xx} + \mu_x f_x - k^2\mu f = -\lambda k^2 \mu_x f. \tag{3.33}$$

This is the non-dimensional form of the equation derived in the absence of diffusion in [16].

Four boundary conditions are necessary for this fourth-order eigenvalue problem. Two of them come from $(3.27)_3$ and $(3.27)_4$. The other two come from $h(-1) = h(0) = 0$. Combining this with (3.29) and the other two boundary conditions, we get

$$\mu(-1)f_{xx}(-1) = \left\{k^2\mu(-1) - \frac{\mu_x}{\mu(-1)}\,(\mu_l\,k - \lambda E_1)\right\} f(-1), \tag{3.34}$$

$$\mu(0)f_{xx}(0) = \left\{k^2\mu(0) + \frac{\mu_x}{\mu(0)}\,(\mu_r\,k - \lambda E_0)\right\} f(0). \tag{3.35}$$

In summary,

$$\left.\begin{aligned}
&Pe\,(\mu f_{xx} + \mu_x f_x - k^2\mu f)\\
&= \lambda\Big\{\mu f_{4x} + 3\mu_x f_{3x} - 2k^2\mu f_{xx} - 3k^2\mu_x f_x + \{k^4\mu - Pe\,k^2\mu_x\}\,f\Big\}, \quad x \in (-1,0),\\
&\mu(-1)f_x(-1) = (\mu_l\,k - \lambda E_1)\,f(-1),\\
&-\mu(0)f_x(0) = (\mu_r\,k - \lambda E_0)\,f(0),\\
&\mu(-1)f_{xx}(-1) = \Big\{k^2\mu(-1) - \tfrac{\mu_x}{\mu(-1)}\,(\mu_l\,k - \lambda E_1)\Big\}\,f(-1),\\
&\mu(0)f_{xx}(0) = \Big\{k^2\mu(0) + \tfrac{\mu_x}{\mu(0)}\,(\mu_r\,k - \lambda E_0)\Big\}\,f(0).
\end{aligned}\right\} \tag{3.36}$$

B. $\mu(c)$ is exponential

Now, we explore the case when μ depends exponentially on the concentration c, which is a common assumption (see [68]). Let $\mu(c) = \mu(0)e^{Rc}$. Then $d\mu/dc = R\mu$. Plugging this into $(3.27)_1$,

$$-\left(\mu f_x\right)_x + k^2\mu f = -k^2 R\mu h.$$

But $\mu_x = (d\mu/dc)c_x = aR\mu$. Therefore,

$$-f_{xx} - aRf_x + k^2 f = -k^2 Rh. \tag{3.37}$$

Rearranging terms,

$$h = \frac{1}{k^2 R}\left[f_{xx} + aRf_x - k^2 f\right]. \tag{3.38}$$

Taking two derivatives,

$$h_{xx} = \frac{1}{k^2 R}\left[f_{4x} + aRf_{3x} - k^2 f_{xx}\right]. \tag{3.39}$$

Using (3.38) and (3.39) in $(3.27)_2$,

$$f_{4x} + aRf_{3x} - k^2 f_{xx} - (\sigma Pe + k^2)\left(f_{xx} + aRf_x - k^2 f\right) = Pe\, k^2 aRf.$$

Therefore,

$$f_{4x} + aRf_{3x} - (\sigma Pe + 2k^2)f_{xx} - (\sigma Pe + k^2)aRf_x + \left[(\sigma Pe + k^2)k^2 - Pe\, k^2 aR\right] f = 0, \tag{3.40}$$

or

$$Pe\left(f_{xx}+aRf_x-k^2f\right)=\lambda\left\{f_{4x}+aRf_{3x}-2k^2f_{xx}-k^2aRf_x+\left(k^4-Pe\,k^2aR\right)f\right\}. \tag{3.41}$$

In the limit $Pe\to\infty$, this equation reduces to

$$f_{xx}+aRf_x+k^2(\lambda aR-1)f=0. \tag{3.42}$$

This is a dimensionless form of the equation for the case of zero diffusion and μ being an exponential function of x. This was studied in detail in chapter 2.

As in the linear case, we need four boundary conditions for the fourth order equation. Two are given by $(3.27)_3$ and $(3.27)_4$. For the other two, we use $h(-1)=h(0)=0$ with (3.38), which gives

$$f_{xx}(-1)+aRf_x(-1)-k^2f(-1)=0,$$
$$f_{xx}(0)+aRf_x(0)-k^2f(0)=0.$$

Using $(3.27)_3$ and $(3.27)_4$ gives

$$f_{xx}(-1)=\left\{k^2-aR\frac{\mu_l\,k-\lambda E_1}{\mu(-1)}\right\}f(-1), \tag{3.43}$$
$$f_{xx}(0)=\left\{k^2+aR\frac{\mu_r\,k-\lambda E_0}{\mu(0)}\right\}f(0). \tag{3.44}$$

In summary,

$$\left.\begin{aligned}
&Pe\,(f_{xx}+aRf_x-k^2f)\\
&=\lambda\left\{f_{4x}+aRf_{3x}-2k^2f_{xx}-k^2aRf_x+(k^4-Pe\,k^2aR)\,f\right\},\quad x\in(-1,0),\\
&\mu(-1)f_x(-1)=(\mu_l\,k-\lambda E_1)\,f(-1),\\
&-\mu(0)f_x(0)=(\mu_r\,k-\lambda E_0)\,f(0),\\
&f_{xx}(-1)=\left\{k^2-aR\tfrac{\mu_l\,k-\lambda E_1}{\mu(-1)}\right\}f(-1),\\
&f_{xx}(0)=\left\{k^2+aR\tfrac{\mu_r\,k-\lambda E_0}{\mu(0)}\right\}f(0).
\end{aligned}\right\}\tag{3.45}$$

3.3 New Results on Stabilization

In this section, we analytically study the effect of diffusion on the growth rate through the use of upper bounds. The upper bounds have been found in [29] in a dimensional form. We recall the derivation in section 3.3.1 in order to be able to use the intermediate steps in our proofs in the subsequent section. In section 3.3.2, we prove that the maximum growth rate can be made arbitrarily small by choosing an appropriate viscous profile and Peclet number. Similar results have been obtained in [29] under the assumption that certain terms that involve the integral of f and h are independent of the Peclet number. Here, we provide a proof that accounts for the implicit dependence of these parameters on the Peclet number. Finally, in section 3.3.3 we consider the limiting case $Pe = 0$.

3.3.1 Upper Bounds

In order to obtain an upper bound on the growth rate, we use the system (3.27). Multiplying $(3.27)_1$ by f^*, the complex conjugate of f, and integrating from $x=-1$ to $x=0$,

$$-\int_{-1}^{0}(\mu f_x)_x f^*dx+k^2\int_{-1}^{0}\mu|f|^2dx=-k^2\int_{-1}^{0}\mu_c h f^*dx.$$

Using integration by parts on the first term,

$$-\mu f_x f^*\Big|_{-1}^{0} + \int_{-1}^{0} \mu |f_x|^2 dx + k^2 \int_{-1}^{0} \mu |f|^2 dx = -k^2 \int_{-1}^{0} \mu_c h f^* dx.$$

Using the boundary conditions $(3.27)_3$ - $(3.27)_4$,

$$\begin{aligned} &\left(\mu_r k - \frac{E_0}{\sigma}\right)|f(0)|^2 + \left(\mu_l k - \frac{E_1}{\sigma}\right)|f(-1)|^2 + \int_{-1}^{0} \mu |f_x|^2 dx + k^2 \int_{-1}^{0} \mu |f|^2 dx \\ =& -k^2 \int_{-1}^{0} \mu_c h f^* dx. \end{aligned}$$

Multiplying by σ and rearranging,

$$\begin{aligned} &\sigma \left\{ \mu_r k |f(0)|^2 + \mu_l k |f(-1)|^2 + \int_{-1}^{0} \mu |f_x|^2 dx + k^2 \int_{-1}^{0} \mu |f|^2 dx \right\} \\ &- E_0 |f(0)|^2 - E_1 |f(-1)|^2 = -k^2 \sigma \int_{-1}^{0} \mu_c h f^* dx. \end{aligned} \tag{3.46}$$

Next, we multiply $(3.27)_2$ by $\mu_c f^*$ and integrate.

$$\int_{-1}^{0} \mu_c h_{xx} f^* dx - \left(\sigma Pe + k^2\right) \int_{-1}^{0} \mu_c h f^* dx = Pe\, a \int_{-1}^{0} \mu_c |f|^2 dx. \tag{3.47}$$

Multiplying by k^2/Pe and rearranging,

$$-k^2 \sigma \int_{-1}^{0} \mu_c h f^* dx = k^2 a \int_{-1}^{0} \mu_c |f|^2 dx - \frac{k^4}{Pe} \int_{-1}^{0} \mu_c (-h) f^* dx - \frac{k^2}{Pe} \int_{-1}^{0} \mu_c h_{xx} f^* dx. \tag{3.48}$$

Note that the left-hand side of (3.48) is equal to the right-hand side of (3.46). Therefore,

$$\begin{aligned}&\sigma\left\{\mu_r k|f(0)|^2+\mu_l k|f(-1)|^2+\int_{-1}^{0}\mu|f_x|^2dx+k^2\int_{-1}^{0}\mu|f|^2dx\right\}\\&-E_0|f(0)|^2-E_1|f(-1)|^2\\=&k^2a\int_{-1}^{0}\mu_c|f|^2dx-\frac{k^4}{Pe}\int_{-1}^{0}\mu_c(-h)f^*dx-\frac{k^2}{Pe}\int_{-1}^{0}\mu_c h_{xx}f^*dx.\end{aligned}$$

Solving for σ,

$$\sigma=\frac{E_0|f(0)|^2+E_1|f(-1)|^2+k^2a\int_{-1}^{0}\mu_c|f|^2dx}{H}-\frac{k^2}{Pe}\left(\frac{k^2(F_1-iF_2)+G_1+iG_2}{H}\right),\tag{3.49}$$

where

$$\int_{-1}^{0}\mu_c(-h)^*fdx=F_1+iF_2,\qquad\int_{-1}^{0}\mu_c h_{xx}f^*dx=G_1+iG_2,\tag{3.50}$$

$$H=\mu_r k|f(0)|^2+\mu_l k|f(-1)|^2+\int_{-1}^{0}\mu|f_x|^2dx+k^2\int_{-1}^{0}\mu|f|^2dx.\tag{3.51}$$

Taking the real part of (3.49) and denoting $\sigma=\sigma_R+i\sigma_I$,

$$\sigma_R=\frac{E_0|f(0)|^2+E_1|f(-1)|^2+k^2a\int_{-1}^{0}\mu_c|f|^2dx}{H}-\frac{k^2}{Pe}\left(\frac{k^2F_1+G_1}{H}\right).\tag{3.52}$$

A. When μ is a **linear** function of c, we'll have $\mu_c=\mu_x/a$. We use that

$$H\geq\mu_r k|f(0)|^2+\mu_l k|f(-1)|^2+k^2\mu_l\int_{-1}^{0}|f|^2dx.$$

Then, whenever the first term in equation (3.52) is positive,

$$\sigma_R \leq \frac{E_0|f(0)|^2 + E_1|f(-1)|^2 + k^2\mu_x \int_{-1}^{0} |f|^2 dx}{\mu_r k|f(0)|^2 + \mu_l k|f(-1)|^2 + k^2\mu_l \int_{-1}^{0} |f|^2 dx} - \frac{k^2}{Pe}\left(\frac{k^2F_1 + G_1}{H}\right).$$

Using the inequality

$$\frac{A_1 + A_2 + ... + A_n}{B_1 + B_2 + ... + B_n} \leq \max_i \left\{\frac{A_i}{B_i}\right\},$$

we have

$$\sigma_R \leq \max\left\{\frac{E_0}{\mu_r k}, \frac{E_1}{\mu_l k}, \frac{\mu_x}{\mu_l}\right\} - \frac{k^2}{Pe}\left(\frac{k^2F_1 + G_1}{H}\right). \tag{3.53}$$

This is a modal upper bound since it depends on the wavenumber k. However, we can remove the dependence on the wavenumber of the first term by taking the maximum value over all wavenumbers. This gives

$$\begin{aligned}\sigma_R &\leq \max\left\{\max_k\left(\frac{E_0}{\mu_r k}\right), \max_k\left(\frac{E_1}{\mu_l k}\right), \frac{\mu_x}{\mu_l}\right\} - \frac{k^2}{Pe}\left(\frac{k^2F_1 + G_1}{H}\right) \\ &= \max\left\{\frac{2}{\mu_r Ca}\left(Ca\frac{\mu_r - \mu(0)}{3}\right)^{3/2}, \frac{2}{\mu_l Ca}\frac{T_1}{T_0}\left(Ca\frac{T_1}{T_0}\frac{\mu(-1) - \mu_l}{3}\right)^{3/2}, \frac{\mu_x}{\mu_l}\right\} \\ &- \frac{k^2}{Pe}\left(\frac{k^2F_1 + G_1}{H}\right).\end{aligned} \tag{3.54}$$

B. If μ is an **exponential** function of c, then $\mu_c = R\mu$. Using this in (3.52) along with

$$H \geq \mu_r k|f(0)|^2 + \mu_l k|f(-1)|^2 + k^2 \int_{-1}^{0} \mu|f|^2 dx,$$

we get,

$$\sigma_R \leq \frac{E_0|f(0)|^2 + E_1|f(-1)|^2 + k^2 aR \int_{-1}^{0} \mu|f|^2 dx}{\mu_r k|f(0)|^2 + \mu_l k|f(-1)|^2 + k^2 \int_{-1}^{0} \mu|f|^2 dx} - \frac{k^2}{Pe}\left(\frac{k^2F_1 + G_1}{H}\right).$$

Therefore,

$$\sigma_R \leq \max\left\{\frac{E_0}{\mu_r k}, \frac{E_1}{\mu_l k}, aR\right\} - \frac{k^2}{Pe}\left(\frac{k^2 F_1 + G_1}{H}\right), \tag{3.55}$$

and

$$\sigma_R \leq \max\left\{\frac{2}{\mu_r Ca}\left(Ca\frac{\mu_r - \mu(0)}{3}\right)^{3/2}, \frac{2}{\mu_l Ca}\frac{T_1}{T_0}\left(Ca\frac{T_1}{T_0}\frac{\mu(-1) - \mu_l}{3}\right)^{3/2}, aR\right\} - \frac{k^2}{Pe}\left(\frac{k^2 F_1 + G_1}{H}\right). \tag{3.56}$$

3.3.2 Proof of Stabilization with $\mu(c)$ Linear

We now wish to prove that the maximum growth rate can be made arbitrarily small by choosing an appropriate viscous profile and Peclet number. This provides the theoretical basis for our numerical study in section 3.4. For this section, we assume that viscosity is a linear function of concentration.

Lemma 4. *If $\sigma_R > 0$, then $F_1 > 0$ and $G_1 \geq 0$.*

Proof. The proof of this lemma is provided in [29] (see Lemma 1). We multiply $(3.27)_2$ by $\mu_c h^*$ and integrate from $x = -1$ to $x = 0$. Recall that $\mu_c = \mu_x/a$ is a constant. Then

$$\mu_c \int_{-1}^{0} h_{xx} h^* dx - (\sigma Pe + k^2)\mu_c \int_{-1}^{0} |h|^2 dx = a\, Pe\, \mu_c \int_{-1}^{0} f h^* dx.$$

Using integration by parts and the boundary condition $(3.27)_5$,

$$-\mu_c \int_{-1}^{0} |h_x|^2 dx - (\sigma Pe + k^2)\mu_c \int_{-1}^{0} |h|^2 dx = a\, Pe\, \mu_c \int_{-1}^{0} f h^* dx.$$

Using$(3.50)_1$,

$$-\mu_c \int_{-1}^{0} |h_x|^2 dx - (\sigma_R Pe + i\sigma_I Pe + k^2)\mu_c \int_{-1}^{0} |h|^2 dx = -Pe\, a(F_1 + iF_2).$$

The real part of this equation is

$$-\mu_c \int_{-1}^{0} |h_x|^2 dx - (\sigma_R Pe + k^2)\mu_c \int_{-1}^{0} |h|^2 dx = -Pe\, aF_1,$$

and the imaginary part is

$$\sigma_I Pe \mu_c \int_{-1}^{0} |h|^2 dx = Pe\, aF_2,$$

Rearranging, we get

$$(\sigma_R Pe + k^2) = \frac{Pe\, aF_1 - \mu_c \int_{-1}^{0} |h_x|^2 dx}{\mu_c \int_{-1}^{0} |h|^2 dx} \leq \frac{Pe\, aF_1}{\mu_c \int_{-1}^{0} |h|^2 dx} \tag{3.57}$$

$$\sigma_I = \frac{aF_2}{\mu_c \int_{-1}^{0} |h|^2 dx}. \tag{3.58}$$

Equation (3.57) implies that $F_1 > 0$. Next, consider equation (3.47) which can be rewritten as

$$(G_1 + iG_2) + (\sigma_R Pe + i\sigma_I Pe + k^2)(F_1 - iF_2) = Pe\, a\mu_c \int_{-1}^{0} |f|^2 dx.$$

The real part of this equation is

$$G_1 + (\sigma_R Pe + k^2)F_1 + \sigma_I PeF_2) = Pe\, a\mu_c \int_{-1}^{0} |f|^2 dx.$$

We use (3.57) and (3.58) to get

$$G_1 + \frac{Pe\, a}{\mu_c} \frac{F_1^2 + F_2^2}{\int_{-1}^{0} |h|^2 dx} \geq Pe\, a \mu_c \int_{-1}^{0} |f|^2 dx. \tag{3.59}$$

But

$$F_1^2 + F_2^2 = \Big| \int_{-1}^{0} \mu_c (-h)^* f dx \Big|^2 = \mu_c^2 | < f, -h > |^2 \leq \mu_c^2 \int_{-1}^{0} |f|^2 dx \int_{-1}^{0} |h|^2 dx. \tag{3.60}$$

Using (3.60) in (3.59),

$$G + Pe\, a \mu_c \int_{-1}^{0} |f|^2 dx \geq Pe\, a \mu_c \int_{-1}^{0} |f|^2 dx,$$

and therefore $G \geq 0$. □

This lemma, in particular, shows that the last term of our upper bound (3.54) is stabilizing for unstable waves. We now show that the growth rate of any particular wave can be made arbitrarily small by choosing a suitable viscous profile in the middle layer and an appropriate value of Pe.

Lemma 5. *Let μ_r, μ_l, Ca, $\frac{T_1}{T_0}$, and k be fixed and let $\epsilon > 0$. We assume that the viscosity of the intermediate fluid depends linearly on the concentration. Then there exists a concentration profile and value of Pe such that $\sigma_R < \epsilon$.*

Proof. We first establish a new expression for σ_R. Consider equation (3.46). Using the definitions (3.50) and (3.51), this can be rewritten as

$$\sigma H - E_0 |f(0)|^2 - E_1 |f(-1)|^2 = k^2 \sigma (F_1 - i F_2).$$

The real part of this equation, after some algebraic manipulation, is

$$\sigma_R(H - k^2F_1) = E_0|f(0)|^2 + E_1|f(-1)|^2 + k^2\sigma_I F_2, \tag{3.61}$$

and the imaginary part is

$$\sigma_I H = k^2\sigma_I F_1 - k^2\sigma_R F_2.$$

Rearranging, we get

$$\sigma_I = -\frac{\sigma_R k^2 F_2}{H - k^2F_1}. \tag{3.62}$$

Using (3.62) in (3.61),

$$\sigma_R(H - k^2F_1) = E_0|f(0)|^2 + E_1|f(-1)|^2 - \frac{\sigma_R k^4 F_2^2}{H - k^2F_1},$$

and therefore

$$\sigma_R = \frac{E_0|f(0)|^2 + E_1|f(-1)|^2}{H - k^2F_1 + \frac{k^4F_2^2}{H-k^2F_1}} \tag{3.63}$$

We now proceed to prove the lemma. Choose a concentration profile (which is determined by the values $\mu(-1)$ and $\mu(0)$) so that

$$\max_k \frac{E_0}{\mu_r k} < \frac{\epsilon}{3}, \qquad \text{and} \qquad \max_k \frac{E_1}{\mu_l k} < \frac{\epsilon}{3}, \tag{3.64}$$

which can be done by expression (3.54). Next, we consider two cases:

1. First, we consider the case where $k^2F_1 > 2H/3$ for all $Pe > 0$. If $\sigma_R > 0$, we know that $F_1, G_1 \geq 0$. Choose Pe such that $Pe < 2k^2\mu_l/(3\mu_x)$. Then

$$\frac{\mu_x}{\mu_l} - \frac{k^2}{Pe}\left(\frac{k^2F_1 + G_1}{H}\right) < \frac{\mu_x}{\mu_l} - \frac{2k^2}{3Pe} < 0.$$

This, along with the upper bound (3.53) and our choice of $\mu(-1)$ and $\mu(0)$ prove that $\sigma_R < \epsilon/3 < \epsilon$.

2. Otherwise, there is a Peclet number Pe such that $k^2 F_1 < 2H/3$. This implies that $H - k^2 F_1 > H/3 > 0$. Using this fact and equation (3.63), we have that for $\sigma_R > 0$,

$$\begin{aligned}
\sigma_R &< \frac{E_0|f(0)|^2 + E_1|f(-1)|^2}{H - k^2 F_1} \\
&< \frac{E_0|f(0)|^2 + E_1|f(-1)|^2}{H} \frac{H}{H - \frac{2H}{3}} \\
&= 3\frac{E_0|f(0)|^2 + E_1|f(-1)|^2}{H} \\
&\leq 3 \max\left\{ \frac{E_0}{\mu_r k}, \frac{E_1}{\mu_l k} \right\} \\
&< \epsilon
\end{aligned}$$

□

Using this lemma, we may now prove our main theorem.

Theorem 3. *Let μ_r, μ_l, Ca, and $\frac{T_1}{T_0}$ be fixed and let $\epsilon > 0$. We assume that the viscosity of the intermediate fluid depends linearly on the concentration. We also assume that σ_R decreases as Pe decreases. Then there exists a concentration profile and a value of Pe such that $\sigma_R < \epsilon$ for all k.*

Proof. As in Lemma 5 (see (3.64)), choose a concentration profile so that

$$\max_k \frac{E_0}{\mu_r k} < \frac{\epsilon}{3}, \qquad \text{and} \qquad \max_k \frac{E_1}{\mu_l k} < \frac{\epsilon}{3},$$

We now consider two special cases: long waves and short waves.

First, we consider the long wave limit. Consider all wavenumbers k such that $k < \min\{\epsilon\mu_l/6\mu_x, \sqrt{\epsilon\mu_l/6\mu_x}\}$. For convenience, denote $k_1 = \min\{\epsilon\mu_l/6\mu_x, \sqrt{\epsilon\mu_l/6\mu_x}\}$. We claim that for all such wavenumbers, $\sigma_R < \epsilon$ for any value of Pe. Consider (3.52). If $\sigma_R > 0$, we know from Lemma 4 that $F_1, G_1 \geq 0$. Therefore, from (3.52),

$$\sigma_R \leq \frac{E_0|f(0)|^2 + E_1|f(-1)|^2 + k^2 a \int_{-1}^{0} \mu_c |f|^2 dx}{H}.$$

By (3.64), the first two terms are less than $\epsilon/3$. It remains to show that

$$\frac{k^2 \mu_x \int_{-1}^{0} |f|^2 dx}{H} < \frac{\epsilon}{3},$$

where we used that $\mu_x = a\mu_c$. Recall that

$$H = \mu_r k|f(0)|^2 + \mu_l k|f(-1)|^2 + \int_{-1}^{0} \mu |f_x|^2 dx + k^2 \int_{-1}^{0} \mu |f|^2 dx.$$

We derive a simple Poincare inequality:

We start with

$$f(x) = \int_{-1}^{x} f_t dt + f(-1).$$

Therefore,

$$\begin{aligned}
|f(x)|^2 &= \left| \int_{-1}^{x} f_t dt + f(-1) \right|^2 \\
&\leq 2 \left| \int_{-1}^{x} f_t dt \right|^2 + 2|f(-1)|^2 \\
&\leq 2 \left(\int_{-1}^{x} |f_t|^2 dt \right) (x+1) + 2|f(-1)|^2 \\
&\leq 2 \left(\int_{-1}^{0} |f_t|^2 dt \right) + 2|f(-1)|^2.
\end{aligned}$$

Integrating yields

$$\int_{-1}^{0} |f|^2 dx \leq 2\left(\int_{-1}^{0} |f_x|^2 dx\right) + 2|f(-1)|^2.$$

Therefore,

$$\begin{aligned}
\frac{k^2\mu_x \int_{-1}^{0} |f|^2 dx}{H} &\leq \frac{2k^2\mu_x\left(\int_{-1}^{0} |f_x|^2 dx\right) + 2k^2\mu_x|f(-1)|^2}{\mu_l k|f(-1)|^2 + \int_{-1}^{0} \mu|f_x|^2 dx} \\
&\leq \frac{2k^2\mu_x\left(\int_{-1}^{0} |f_x|^2 dx\right) + 2k^2\mu_x|f(-1)|^2}{\mu_l k|f(-1)|^2 + \mu_l \int_{-1}^{0} |f_x|^2 dx} \\
&\leq \max\left\{\frac{2k^2\mu_x}{\mu_l}, \frac{2k^2\mu_x}{\mu_l k}\right\} \\
&< \frac{\epsilon}{3},
\end{aligned}$$

where the last step comes from the fact that $k < \epsilon\mu_l/6\mu_x$ and $k^2 < \epsilon\mu_l/6\mu_x$.

Next we consider short waves. In particular, there will be some wavenumber, which we denote by k_2, such that $E_0, E_1 < 0$ when $k > k_2$. Without loss of generality, we may assume $k_2 > k_1 > 0$. We claim that for $k > k_2$ and $Pe < k_2^2\mu_l/\mu_x$, $\sigma_R < \epsilon$. If $\sigma_R > 0$, then by equation (3.63), it must be that $H - k^2F_1 < 0$. Now consider the upper bound (3.54):

$$\begin{aligned}
\sigma_R \leq \max&\left\{ \frac{2}{\mu_r Ca}\left(Ca\frac{\mu_r - \mu(0)}{3}\right)^{3/2}, \frac{2}{\mu_l Ca}\frac{T_1}{T_0}\left(Ca\frac{T_1}{T_0}\frac{\mu(-1) - \mu_l}{3}\right)^{3/2}, \frac{\mu_x}{\mu_l}\right\} \\
&- \frac{k^2}{Pe}\left(\frac{k^2F_1 + G_1}{H}\right).
\end{aligned}$$

The first two terms of the maximum are less than ϵ by our choice of $\mu(-1)$ and $\mu(0)$.

Since $G_1 \geq 0$ and $H - k^2 F_1 < 0$,

$$\frac{\mu_x}{\mu_l} - \frac{k^2}{Pe}\left(\frac{k^2 F_1 + G_1}{H}\right) < \frac{\mu_x}{\mu_l} - \frac{k^2}{Pe}, \tag{3.65}$$

and this term is negative for $k > k_2$ by our choice of Pe.

It remains to show that all $k \in [k_1, k_2]$ can be stabilized by small enough Pe. By Lemma 5, we know that for each k, there is a Peclet number $Pe(k)$ such that $\sigma_R(k) < \epsilon$. Since σ depends continuously on k, there will be an open interval $I(k)$ such that $\sigma_R(k) < \epsilon$ for all $k \in I(k)$. The set $\{I(k)\}_{k\in[k_1,k_2]}$ is an open cover for the compact set $[k_1, k_2]$ and therefore has a finite subcover $\{I(k_n)\}_{n=1}^{N}$. If $Pe < \min_n Pe(k_n)$, then $\sigma_R < \epsilon$ for all $k \in [k_1, k_2]$. If, in addition, $Pe < k_2^2 \mu_l/\mu_x$, $\sigma_R < \epsilon$ for all k.

□

One thing to note from this proof is that long waves can be stabilized independent of Pe by taking small viscous jumps at the interfaces, while short waves are stabilized by decreasing Pe.

3.3.3 The Case $Pe = 0$

In order to investigate the ability to bound σ_R by any positive constant by increasing diffusion (see Theorem 3), we consider the case $Pe = 0$. Then equation $(3.27)_2$ becomes

$$h_{xx} - k^2 h = 0.$$

This, along with the boundary conditions $h(-1) = h(0) = 0$ implies that $h \equiv 0$. Therefore, equation $(3.27)_1$ becomes

$$-(\mu f_x)_x + k^2 \mu f = 0.$$

If we take the inner product of this expression with f^* and use integration by parts,

$$-\mu f_x f^*|_{-1}^0 + \int_{-1}^0 \mu |f_x|^2 dx + k^2 \int_{-1}^0 \mu |f|^2 dx = 0.$$

Using the boundary conditions $(3.27)_3$ and $(3.27)_4$,

$$\left(\mu_r k - \frac{E_0}{\sigma}\right)|f(0)|^2 + \left(\mu_l k - \frac{E_1}{\sigma}\right)|f(-1)|^2 + \int_{-1}^0 \mu |f_x|^2 dx + k^2 \int_{-1}^0 \mu |f|^2 dx.$$

Solving for σ,

$$\sigma = \frac{E_0|f(0)|^2 + E_1|f(-1)|^2}{\mu_r k|f(0)|^2 + \mu_l k|f(-1)|^2 + \int_{-1}^0 \mu |f_x|^2 dx + k^2 \int_{-1}^0 \mu |f|^2 dx}. \tag{3.66}$$

In particular, σ is real. This leads to the upper bound which holds for all unstable waves

$$\sigma < \max\left\{\frac{E_0}{\mu_r k}, \frac{E_1}{\mu_l k}\right\} \tag{3.67}$$

which is completely independent of the gradient of the viscous profile of the middle layer. This leads to the absolute (over all wavenumbers) upper bound

$$\begin{aligned}\sigma &< \max\left\{\max_k\left(\frac{E_0}{\mu_r k}\right), \max_k\left(\frac{E_1}{\mu_l k}\right)\right\} \\ &= \max\left\{\frac{2}{\mu_r Ca}\left(Ca\frac{\mu_r - \mu(0)}{3}\right)^{3/2}, \frac{2}{\mu_l Ca}\frac{T_1}{T_0}\left(Ca\frac{T_1}{T_0}\frac{\mu(-1) - \mu_l}{3}\right)^{3/2}\right\}.\end{aligned} \tag{3.68}$$

This upper bound can be made arbitrarily small by choosing suitable values of $\mu(-1)$ and $\mu(0)$. Because of the continuous dependence of the equations on the parameter Pe, we can make σ_R as small as desired by using Pe sufficiently small. This supports Theorem 3 above.

3.4 Numerical Results and Discussion

In order to investigate the stabilizing effect of species diffusion in three-layer Hele-Shaw flows, we perform some numerical computations of the eigenvalues. We use a pseudo-spectral Chebyshev method, the details of which can be found in chapter 6. Computations are performed with various values of parameters which can be found in various figure captions below. For certain parameters, their values are kept fixed in all simulations. These are $\mu_l = 0.2$, $\mu_r = 1$, $Ca = 10$, and $T_0 = T_1$. All trends and conclusions included below hold when $\mu(c)$ is both a linear function and an exponential function. Therefore, we only present the case in which the viscosity depends linearly on the concentration profile. The system (3.36) is solved for the eigenvalues λ. The eigenvalues are then inverted to find the growth rate σ. The values of σ computed in this case are complex, but we are interested only in the real part, σ_R, which measures the growth rate of disturbances. Below, all references to growth rate mean the real part σ_R of the growth rate and these are denoted by σ itself, with slight abuse of notation. For example, below $\sigma_{\max}$ in the narrative or figures means the maximum value of σ_R with the maximum taken over all eigenvalues and all wave-numbers.

The maximum growth rate $\sigma_{max}(\mu(x), Pe)$ depends on the viscous profile $\mu(x)$ as well as on the Peclet number Pe. The linear viscous profile is characterized by two parameters, $\mu(0)$ and $\mu(-1)$ (or equivalently a, b if $\mu(x) = a + bx$) with the restriction $\mu(0) \leq \mu_r$ and $\mu_l \leq \mu(-1)$. Keeping these two parameters fixed at values $\mu(-1) = 0.408$ and $\mu(0) = 0.552$, corresponding to the infinite Peclet number optimal profile (see Figure 3.7) having $\sigma_{max} = 0.36039$, σ_{max} is computed for different finite values of Pe. Figure 3.2a shows the plot of σ_{max} versus $1/Pe$ from which we conclude that the effect of the diffusive stabilization is monotonic. However, the decrease in

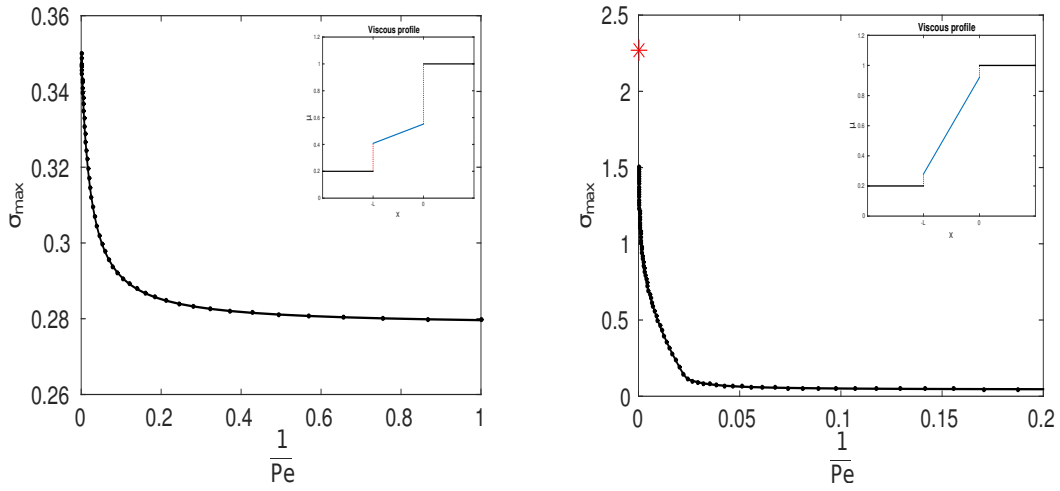

(a) (b)

Figure 3.2: The maximum growth rate σ_{max} versus $1/Pe$ for: (a) $\mu(-1) = 0.408$ and $\mu(0) = 0.552$; and (b) $\mu(-1) = 0.28$ and $\mu(0) = 0.92$. The red '*' marker indicates the value of σ_{max} in the absence of diffusion.

σ_{max} is gradual in this case.

In order to see a more dramatic effect from diffusion, we consider a viscous profile with a larger gradient. Figure 3.2b shows the plot of σ_{max} versus $1/Pe$ for $\mu(-1) = 0.28$ and $\mu(0) = 0.92$. The red '$*$' on the y-axis denotes the value of σ_{max} in the absence of diffusion. Note that the decrease in σ_{max} as the Peclet number decreases is much faster than the previous case. In fact, the flow is almost stable for $Pe < 10$. Unlike the plot in Figure 3.2a, this plot has a point at which the slope of the curve is discontinuous. We will now investigate this point in order to shed light on the physical processes at play. Notice that in this case, the jumps in viscosity at the interfaces are much smaller than the previous case, but the slope of the viscous profile has increased. The first of these phenomena works to stabilize the flow while the second works to destabilize.

To understand the contributions of the instability of the interfaces and the insta-

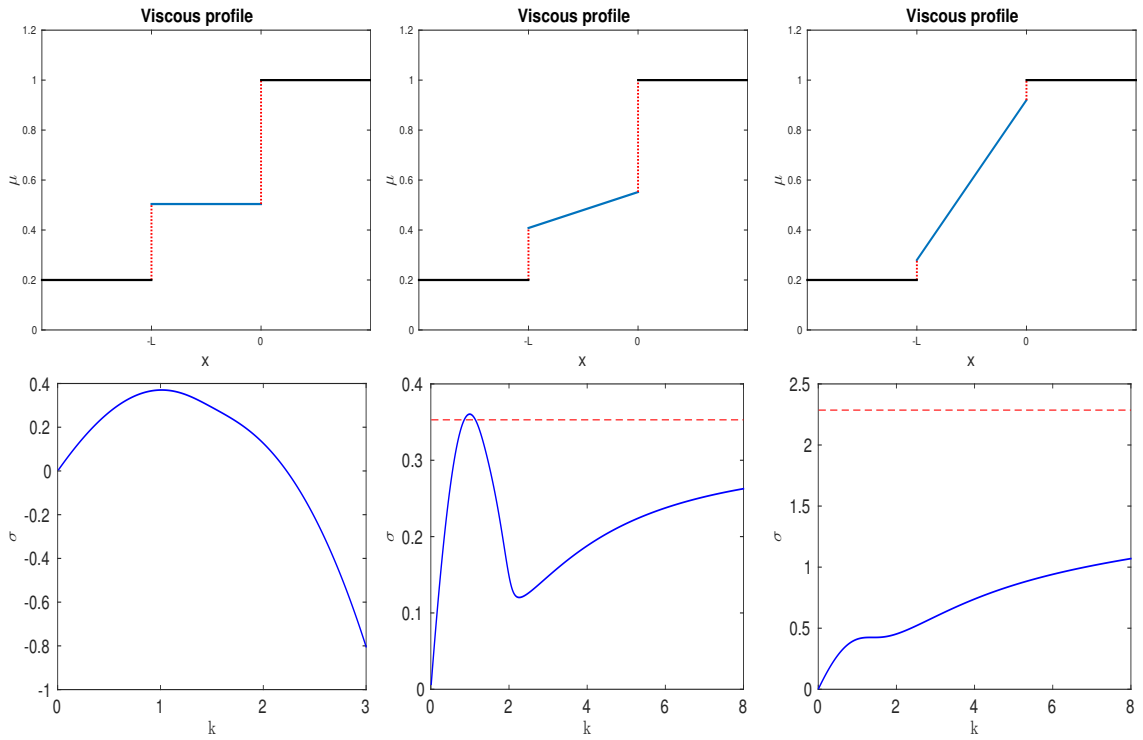

Figure 3.3: The maximum value of the growth rate σ for each wavenumber k is plotted versus k for several different values of $\mu(-1)$ and $\mu(0)$ when $Pe = \infty$. Plot (a) shows $\mu(-1) = \mu(0) = 0.5040$. Plot (b) uses $\mu(-1) = 0.408$ and $\mu(0) = 0.552$. Plot (c) uses $\mu(-1) = 0.28$ and $\mu(0) = 0.92$.

bility of the middle layer itself, we consider three different sets of values for $\mu(-1)$ and $\mu(0)$ when there is no diffusion (i.e. $Pe = \infty$). Figure 3.3 shows plots of the maximum value of σ versus wavenumber k. Plot 3.3a uses the values $\mu(-1) = \mu(0) = 0.5040$. Therefore, the middle layer has a constant viscosity and all of the instability comes from the interfaces. The viscosity jumps destabilize the flow while the interfacial tension completely stabilizes short waves. Plot 3.3b uses $\mu(-1) = 0.408$ and $\mu(0) = 0.552$, which are the values we used for Figure 3.2a. The viscosity jumps are similar to those found in the constant viscosity case, but there is now instability within the middle layer due to the increasing viscosity. As we can see in the plot,

there is still a peak near $k = 1$, but, in contrast to the first plot, the short waves are not stable. In fact, as the wavenumber k increases to infinity, the value of σ asymptotically approaches the dotted red line. The new short wave behavior can be attributed to the middle layer instability. Finally, we consider plot 3.3c, which uses the values $\mu(-1) = 0.28$ and $\mu(0) = 0.92$. These are the values that were used for Figure 3.2b. Like the previous cases, there is a local maximum near $k = 1$ which can be attributed to the instability of the interfaces. However, this is small compared to the short wave instability which comes from the middle layer. Because the viscosity increases more rapidly in the middle layer, the instability due to the middle layer is largest in this case.

When diffusion is added to the system, the growth rate decreases. However, the decrease is more pronounced for short waves, due to the fact that the diffusion affects only the middle layer and not the interfaces. This effect is clearly illustrated by Figures 3.4 and 3.5. Figure 3.4 shows plots of the maximum value of σ versus k when $\mu(-1) = 0.408$ and $\mu(0) = 0.552$ for four different values of Pe. The first plot (top left) shows $Pe = \infty$, which we also saw in Figure 3.3. Notice that the large k limit is approximately equal to the peak near $k = 1$ (which is due to the interfacial instability). This balance is why this is the optimal viscous profile for $Pe = \infty$. The second plot (top right) uses $Pe = 1000$. Note that the peak near $k = 1$ remains and has only been slightly decreased. However, the short waves have now been stabilized by diffusion, adding a second maximum at a larger value of k. This behavior continues for the bottom two plots which correspond to $Pe = 100$ (bottom left) and $Pe = 10$ (bottom right). The stabilization from diffusion is drastic for short waves, but slow for long waves.

This behavior shows why the case where $\mu(-1) = 0.28$ and $\mu(0) = 0.92$ is stabilized much more drastically by diffusion than the previous case. For this viscous

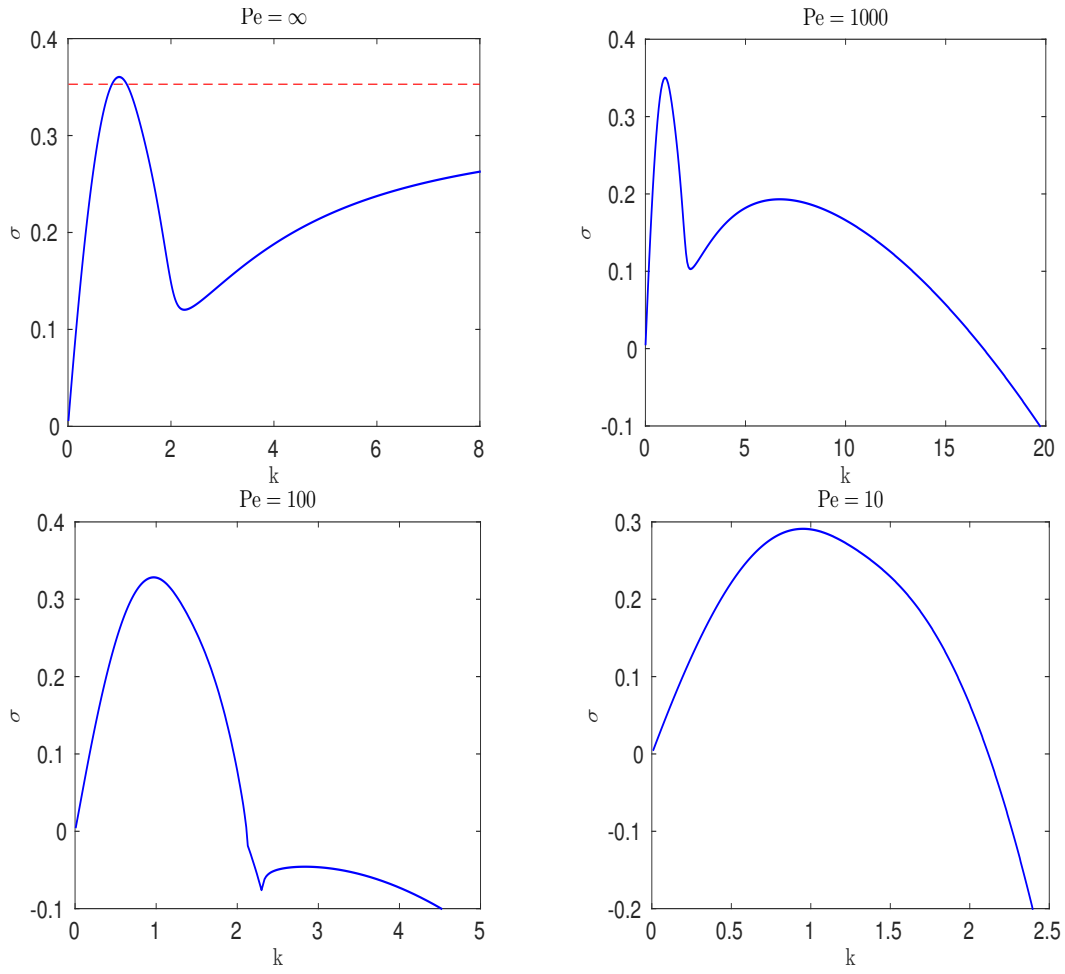

Figure 3.4: The maximum value of the growth rate σ for each wavenumber k is plotted versus k for $\mu(-1) = 0.408$ and $\mu(0) = 0.552$ and for several different values of Pe. Recall $\mu_l = 0.2$ and $\mu_r = 1$.

profile, Figure 3.5 shows plots of the maximum value of σ versus k for the same four values of Pe. Recall that the short wave instability of the middle layer dominates in the absence of diffusion. We see this clearly in the first plot (top left). However, the addition of diffusion, even a small amount, stabilizes short enough waves, as we see in the second plot (top right) when $Pe = 1000$. Here, there is a second local maximum near $k = 12$ and this value is already much smaller than the large k limit for $Pe = \infty$ (given by the dotted line). From the bottom two plots, we see that as

Pe decreases, the short waves become more stabilized until the local maximum that occurs due to the interfacial instability (long waves) overtakes the local maximum due to the middle layer instability (short waves). The last plot (bottom right), which uses $Pe = 10$ shows the case when the interfacial instability dominates. This maximum is much smaller than the one in the last plot of Figure 3.4 because the viscous jumps at the interface are much smaller in this case.

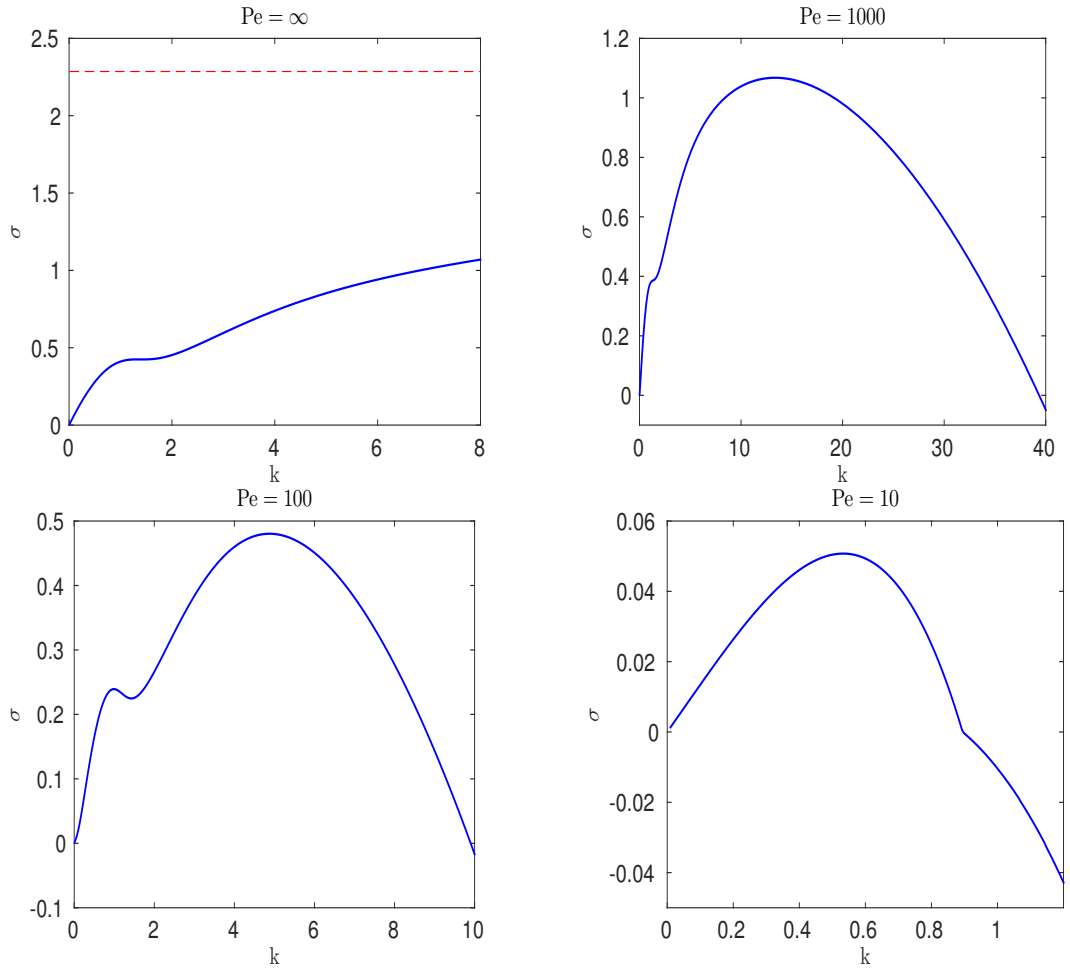

Figure 3.5: The maximum value of the growth rate σ for each wavenumber k is plotted versus k for $\mu(-1) = 0.28$ and $\mu(0) = 0.92$ and for several different values of Pe. Recall $\mu_l = 0.2$ and $\mu_r = 1$.

The last issue to address with regards to this example is the sharp turn in the plot of Figure 3.2b. This turn represents the point at which the diffusion has stabilized the middle layer to the point at which the two local maxima are the same. For the case $\mu(-1) = 0.28$ and $\mu(0) = 0.92$, this occurs when $Pe = 42.7$. We plotted the maximum value of σ versus k for this value of Pe in Figure 3.6.

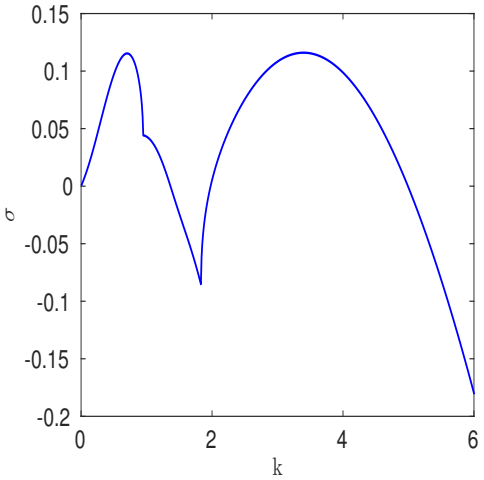

Figure 3.6: The maximum value of the growth rate σ for each wavenumber k is plotted versus k when $\mu(-1) = 0.28$ and $\mu(0) = 0.92$ and $Pe = 42.7$.

The behavior that we have seen shows that diffusion stabilizes flows with highly unstable middle layers more than it stabilizes flows with highly unstable interfaces. Therefore, we expect that for larger diffusion, it would be advantageous to have flows that have a larger viscous gradient in order to minimize the instability of the interfaces. This is what we show next.

For any specific choice of Pe, σ_{max} is computed for all possible values of $\mu(-1)$ and $\mu(0)$, which characterize linear viscous profiles of the middle layer. The square grid mesh in Figure 3.7 shows the maximum growth rate σ_{max} corresponding to $\mu(-1)$

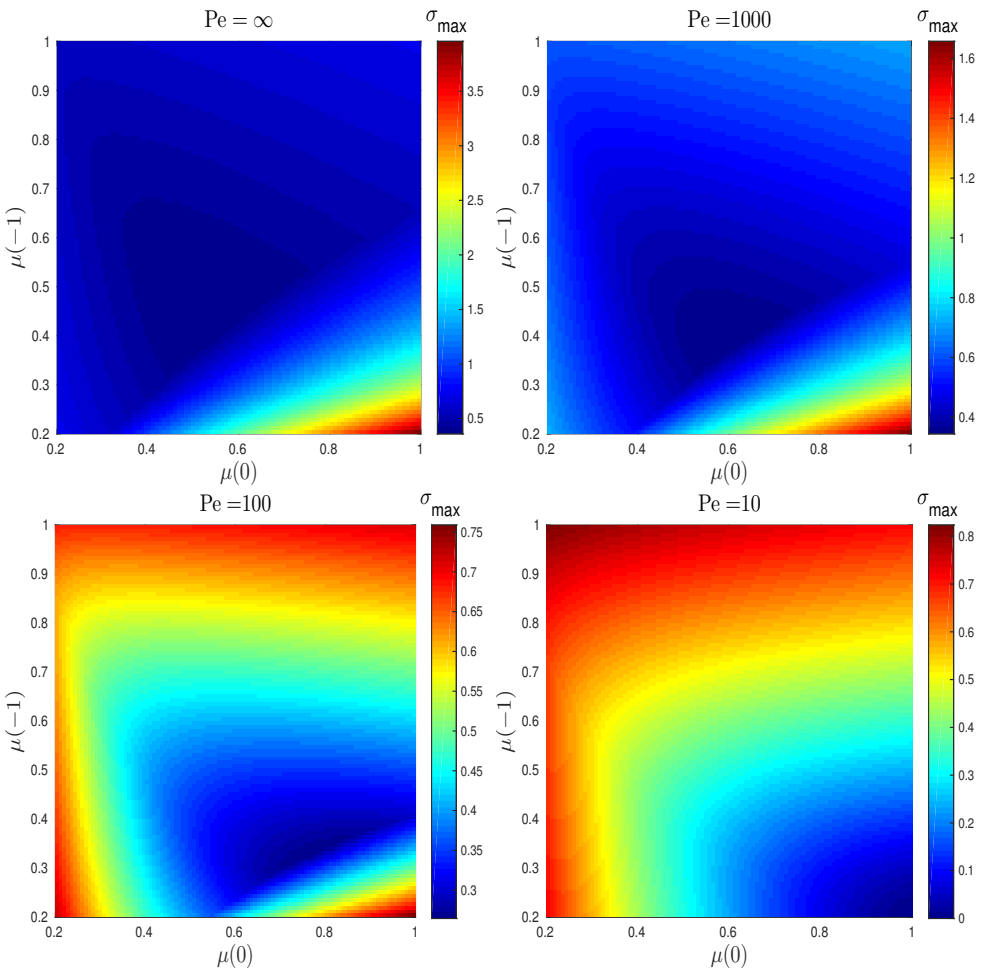

Figure 3.7: The maximum growth rate σ_{max} versus $\mu(-1)$ and $\mu(0)$ for some different Peclet numbers. The other parameter values are $\mu_l = 0.2$, $\mu_r = 1$, $Ca = 10$, and $T_1 = T_0$. This is a color figure.

and $\mu(0)$ for several values of the Peclet number Pe. The value of the maximum growth rate σ_{max} for each cell can be read from the color bar according to the color of the grid cell. The coordinates of each cell give the values $\mu(0)$ and $\mu(-1)$. The plot corresponding to $Pe = \infty$ shows that the optimal viscous profile in this case (recall this is $\mu(-1) = 0.408$ and $\mu(0) = 0.552$) has a relatively small viscous gradient in the middle layer. However, as diffusion increases, the optimal profile has a larger viscous gradient. For $Pe = 10$, the optimal profile has no viscous jump at the interfaces and the flow is almost completely stabilized.

Using data from these simulations, the optimal profile for which the σ_{max} takes its minimum value is found for several values of Pe. Figure 3.8a shows the plot of maximum growth rate σ_{max} against the Peclet number Pe for the optimal profiles. Compare this plot with Figures 3.2a and 3.2b. Notice that choosing the optimal profile for a given value of Pe greatly increases the stabilizing effect of diffusion.

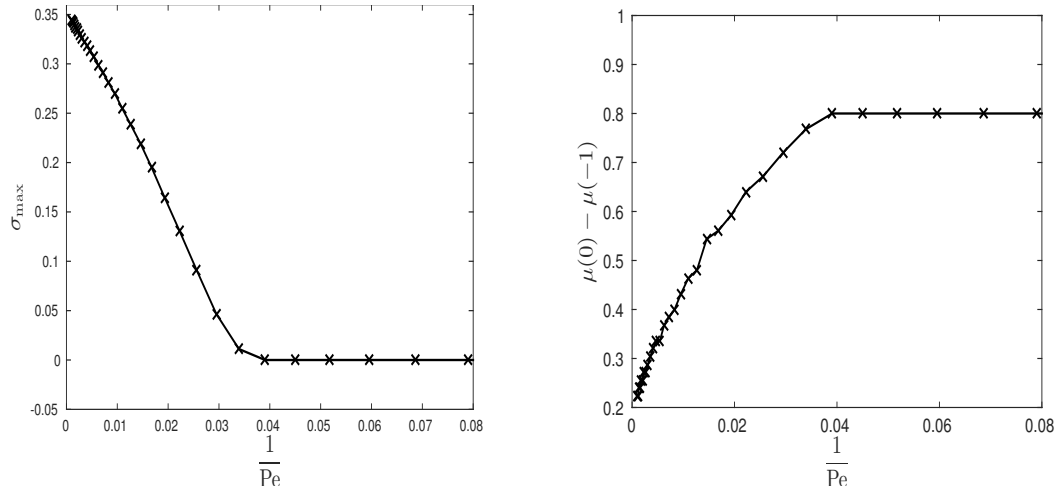

(a) (b)

Figure 3.8: (a) The maximum growth rate σ_{max} versus $1/Pe$ for optimal profiles. (b) The slope $\mu(0) - \mu(-1)$ of the optimal viscous profile versus $1/Pe$. The other parameter values are $\mu_l = 0.2$, $\mu_r = 1$, $Ca = 10$, and $T_1 = T_0$.

As mentioned above, as the diffusion increases, the slope of the optimal viscous profile also increases. To see this dependence, we plot the slope of the optimal viscous profile (given by $\mu(0) - \mu(-1)$) versus $1/Pe$ in Figure 3.8b. Note that this effect is monotonic. Also note that since $\mu(0) < \mu_r = 1$ and $0.2 = \mu_l < \mu(-1)$, the maximum value of the slope is 0.8. When $1/Pe > 0.04$, the optimal viscous profile takes on this value.

In summary, the following useful inferences can be drawn from figures 3.2a, 3.2b 3.7, 3.8a, and 3.8b: (i) decreasing the Peclet number increases the stabilization for the same viscous profile. This may be considered by some as a classic result; (ii) significantly enhanced stabilization can be achieved by a proper choice of viscous profile without changing the Peclet number (compare Fig. 3.2a and Fig. 3.8a); (iii) a very small amount of diffusion can drastically stabilize an otherwise unstable flow provided the viscous profile is carefully chosen. In Fig. 3.8a, we see that $\sigma_{max} \approx 0.05$ when $1/Pe \approx 0.03$ for the optimal viscous profile, an approximate seven-fold decrease from the same for the zero diffusion case resulting in a seven-fold gain in stabilization; (iv) at $1/Pe = 0.04$ (see Fig. 3.8a), $\sigma_{max} \approx 0$ suggesting that the flow is neutrally stable to infinitesimal perturbations with a large enough value of diffusion and corresponding optimal viscous profile.

3.4.1 Large Pe Limit

We now analytically investigate the limit as $Pe \to \infty$. Consider the system (3.27) and let $Pe >> 1$. We can divide equation $(3.27)_2$ by Pe to get

$$\frac{1}{Pe} h_{xx} - (\sigma + \frac{k^2}{Pe}) h = a\, f. \tag{3.69}$$

We now must consider two cases:

1. $k << \sqrt{Pe}$

   When Pe is sufficiently large compared to the wavenumber k, (3.69) reduces to

   $$-\sigma\, h = a\, f.$$

   Note that because of the reduction of order, we can no longer enforce the boundary conditions $h(-1) = h(0) = 0$. We use $h = (-a/\sigma)\, f$ in equation $(3.27)_1$ to get

   $$-\left(\mu f_x\right)_x + k^2 \mu f = \frac{k^2\, \mu_c\, a}{\sigma} f.$$

   Using that $\mu_x = \mu_c\, c_x = \mu_c\, a$, we conclude that

   $$-\left(\mu f_x\right)_x + k^2 \mu f = \frac{k^2\, \mu_x}{\sigma} f,$$

   which is the equation that governs the system in the absence of diffusion (See [28]). Therefore, in the limit $Pe \to \infty$, the growth rate is similar to the zero diffusion case for small wave numbers.

2. $k \approx \sqrt{Pe}$

   For large values of Pe, there will still be waves that are sufficiently short as to have wavenumbers proportional to $\sqrt{Pe}$. When this is the case, (3.69) becomes

   $$-(\sigma + \frac{k^2}{Pe})h = a\, f.$$

   Therefore,

   $$h = -\frac{a}{\sigma + \frac{k^2}{Pe}} f.$$

Using this expression in $(3.27)_1$ yields

$$-\left(\mu f_x\right)_x + k^2 \mu f = \frac{k^2\, \mu_c\, a}{\sigma + \frac{k^2}{Pe}} f.$$

The first term is $\mathcal{O}(1)$ while the last two are $\mathcal{O}(Pe)$. Therefore, we may approximate this by

$$k^2 \mu f = \frac{k^2\, \mu_c\, a}{\sigma + \frac{k^2}{Pe}} f.$$

Canceling terms and again using that $\mu_x = \mu_c\, a$,

$$\mu f = \frac{\mu_x}{\sigma + \frac{k^2}{Pe}} f.$$

Therefore,

$$\left(\mu - \frac{\mu_x}{\sigma + \frac{k^2}{Pe}}\right) f = 0, \qquad x \in (-1, 0). \tag{3.70}$$

When μ depends exponentially on c and c depends linearly on x, $\mu(x)$ will be exponential. Therefore, $\mu_x/\mu = \alpha$ for some constant α. Equation (3.70) becomes

$$\left(1 - \frac{\alpha}{\sigma + \frac{k^2}{Pe}}\right) \mu f = 0, \qquad x \in (-1, 0).$$

This can only be satisfied for all x if

$$\sigma = \alpha - \frac{k^2}{Pe}. \tag{3.71}$$

In order to test the validity of the above analysis we compute the largest values of the growth rate σ for each wavenumber k and compare with the zero diffusion limit and the formula (3.71). A plot of this is shown in Figure 3.9. The solid blue line represents the the growth rate for $Pe = 10,000$. The dashed black line is the growth

rate for the zero diffusion case. The dotted red line represents the values of σ given by equation (3.71). Note that in this case, $\sqrt{Pe} = 100$. We see good agreement between the zero diffusion case and $Pe = 10,000$ for small k. Additionally, for large enough k the growth rate for $Pe = 10,000$ matches the function $\alpha - k^2/Pe$. This agrees with our analysis above.

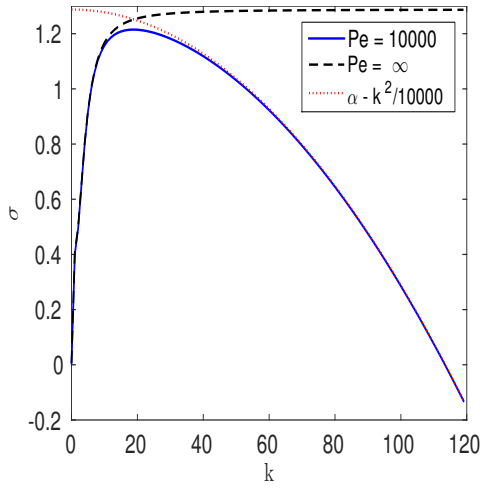

Figure 3.9: The maximum value of the growth rate is plotted versus the wavenumber k for $Pe = 10,000$ as a solid blue line. The zero diffusion growth rate is given by the dashed black line and the curve given by equation (3.71) is the dotted red line. The other parameter values are $\mu(-1) = 0.2349$, $\mu(0) = 0.8513$, $\mu_l = 0.2$, $\mu_r = 1$, $Ca = 10$, and $T_1 = T_0$.

3.5 Conclusion

In Daripa and Pasa [29], this problem was studied theoretically. There, using a weak formulation, upper bounds on the growth rate of individual disturbances and on the maximum growth rate over all disturbances were obtained. From these upper bounds, it was conjectured that the flow can be stabilized by strong enough diffusion of species. In Daripa and Pasa [30], a numerical approach to solve the problem

(3.27) using a finite difference scheme was presented and analyzed. An upper bound on the growth rate was derived from numerical analysis of the discrete system. This approach also supports the diffusive slowdown of instabilities. To-date, no numerical simulation has been performed on this problem to investigate the singular effect of diffusion in this problem. Such a study has been undertaken here.

In this chapter, we have studied the effect of the diffusion of polymer on the hydrodynamic instability of immiscible three-layer Hele-Shaw flows. We started by formulating the problem in terms of the dimensionless Peclet and Capillary numbers. In both previous papers on the topic, there was the implicit assumption that the viscosity depends linearly on the concentration of polymer. We make this assumption explicit in our derivation of the linear stability equations, and we also derive the equations in the case that the viscosity depends exponentially on concentration. In both cases, the linear stability analysis gives a non-self-adjoint fourth-order eigenvalue problem with the eigenvalue appearing linearly in the boundary conditions. This is in contrast to the zero diffusion case in which we obtain a self-adjoint second-order eigenvalue problem. Therefore, diffusion acts as a singular perturbation. The eigenvalues can be complex and their real parts correspond to the growth rates of various waves.

For convenience, we reestablish the upper bounds of Daripa and Pasa [29] in terms of the dimensionless quantities. We then extend the proof from this paper that the growth rate can be made arbitrarily small by increasing the diffusion coefficient. In this proof, we see that small jumps at the interfaces can bound the growth rate of long waves regardless of the Peclet number, while decreasing the Peclet number can bound the growth rate of short waves.

We then use a pseudo-spectral method to numerically compute the eigenvalues. This method is found to be preferable to the previously proposed finite difference

methods. Our numerical results confirm the theoretical prediction that the diffusion has a drastic stabilizing effect on short waves and that the viscous jumps dominate the instability of long waves. We also find that using the optimal viscous profile for each Peclet number can substantially decrease the instability of the system. Using this technique, the maximum growth rate can be made very small, even for modest values of the Peclet number.

The results of this study suggest ways to modify the conventional polymer flooding process to make it work more efficiently in controlling instabilities. We recall that in our treatment in this chapter, polymer does not diffuse across the two interfaces. As justified before, this is physically sound if the fluid displacing the poly-solution is an NAPL in which polymer cannot diffuse. Conventional flooding uses water to displace the poly-solution. This causes the polymer to diffuse from the poly-solution to the water, diluting the polymer concentration continuously in time which has a significant negative effect. This negative effect can be completely arrested if there is a way to manipulate the properties of the interface between the water and poly-solution so that polymer does not diffuse through the interface. One simple way to do this would be to displace the poly-solution with an NAPL or any other fluid in which polymer cannot diffuse for a very short period to create a buffer between the water and poly-solution. Such a buffer is likely to have a very negligible effect on the drastic stabilization capacity of the diffusion in the poly-solution only.

The Peclet number and the viscous profile of the middle layer are the primary controls in our numerical studies above. In practice, the Peclet number depends on the type of polymer used and the viscous profile depends on the way the polymer concentration in the poly-solution is adjusted as it is injected in the well. The later can be adjusted to create any desired viscous profile over an injection period.

Finally, we summarize some of our results below.

(i) The maximum growth rate is a monotonically increasing function of Peclet number.

(ii) We can significantly enhance stabilization by a proper choice of the viscous profile without changing the Peclet number.

(iii) A small amount diffusion can significantly stabilize an otherwise unstable flow but can more drastically stabilize such an unstable flow provided the viscous profile is carefully chosen.

(iv) The optimal linear viscous profile, i.e. the one whose maximum growth rate is the least among all possible linear profiles, depends on the Peclet number.

(v) The smaller the value of the Peclet number, the steeper the optimal viscous profile.

(vi) A theorem was proven, analogous to the one in Daripa and Pasa [29], that shows that the growth rate can be arbitrarily small by proper choice of the viscous profile and Peclet number.

(vii) Numerical evidence supports this theorem.

4. STABILITY RESULTS FOR MULTI-LAYER RADIAL HELE-SHAW AND POROUS MEDIA FLOWS PART I: CONSTANT VISCOSITY*

4.1 Introduction

In this chapter, we study the linear stability of multi-layer radial Hele-Shaw flows in which all fluids have constant viscosity. Similar work has been done for rectilinear flows (see [16]), but no previous studies have examined multi-layer radial flows in which several or all of the interfaces can be unstable. The chapter is laid out as follows. In section 4.2, we formulate the linear stability problem for two-layer radial flows because the linearized stability equations, including the ones at the interface, will be the building block for setting up the stability problem for multi-layer radial flows in section 4.3. In section 4.3.1, we first develop the eigenvalue problem for 3-layer radial flows from linear stability analysis and then analyze this problem for the dispersion relation and upper bounds on the growth rate. The treatment in this section becomes the building block for the stability analysis of the multi-layer case with an arbitrary number of layers which is presented in section 4.3.2. In section 4.3.2, we derive upper bounds on the growth rate for multi-layer radial flows. Section 4.3.3 discusses some special cases. In particular, we show how the previously obtained result on the upper bound on the growth rate for the rectilinear geometry (see [16]) can be recovered from the results obtained in this paper for the multi-layer radial geometry. In section 4.4, we show using the upper bounds on the growth rate for multi-layer radial flows that an otherwise unstable two-layer radial flow can be significantly stabilized by the addition of many layers of fluid with small

*The findings of this chapter have been adapted and reprinted with permission from "Stability results for multi-layer radial Hele-Shaw and porous media flows" by C. Gin and P. Daripa, 2015. *Phys. Fluids,* **27**, 012101, Copyright 2015 AIP Publishing LLC.

positive jumps in viscosity. Numerical results are presented in section 4.5. Finally, we conclude in section 4.6.

4.2 Preliminaries

We start by deriving the equations for two-layer Hele-Shaw flows. Although this is done in numerous other works [8, 53, 60] with the use of the potential function, we follow an approach that does not use the potential function. That is because our approach can be easily adapted to study flows with variable viscosity fluids which do not have a potential function. This is of considerable interest to EOR and is covered in chapter 5.

We consider a Hele-Shaw flow in which two incompressible, immiscible fluids are present. The less viscous fluid is injected into the center of the cell, displacing the more viscous fluid. We denote the viscosity of the less viscous inner fluid by μ_i and the viscosity of the more viscous outer fluid by μ_o (Figure 4.1).

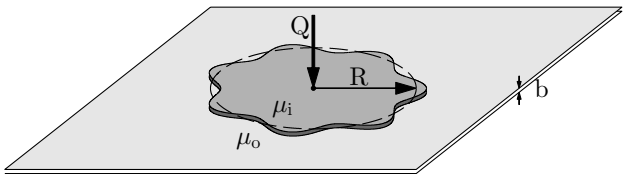

Figure 4.1: Radial flow in a Hele-Shaw cell

By averaging across the gap, we may consider a two-dimensional flow domain in polar coordinates, $\Omega := (r, \theta) = \mathbb{R}^2$. The fluid flow is governed by the following equations

$$\nabla \cdot \mathbf{u} = 0, \quad \nabla\, p = -\mu\, \mathbf{u}. \tag{4.1}$$

The first equation $(4.1)_1$ is the continuity equation for incompressible flow, and the

second equation $(4.1)_2$ is Darcy's law [15]. We start with the fluids separated by a circular interface with radius R_0. Fluid is then injected into the cell at the origin at a constant injection rate, Q. This set-up is shown in Figure 4.2.

The equations admit a simple basic solution in which all of the fluid moves outward radially with velocity $\mathbf{u}^b := \left(u_r^b, u_\theta^b\right) = (Q/2\pi r, 0)$. The interface remains circular and its radius is given by $R(t) = \sqrt{Qt/\pi + R_0^2}$. The pressure, $p_b = p_b(r)$, may be obtained by integrating equation $(4.1)_2$. We perturb the basic solution $\left(u_r^b, u_\theta^b, p_b\right)$

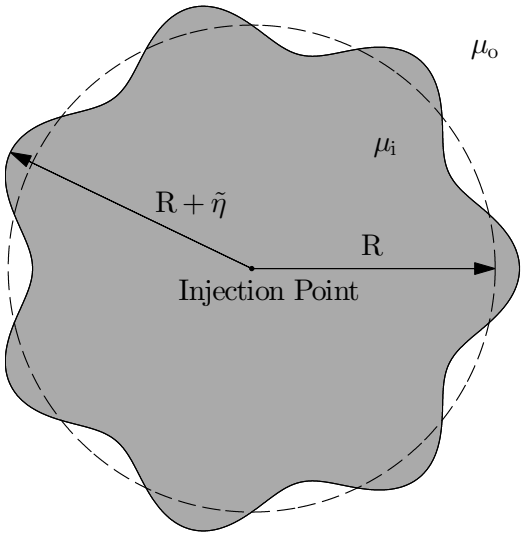

Figure 4.2: Two-Layer radial Hele-Shaw flow.

by $(\tilde{u_r}, \tilde{u_\theta}, \tilde{p})$ where the disturbances are assumed to be small. We plug these into equations (4.1) and only keep terms that are linear with respect to the disturbances. Since equations (4.1) are, in fact, linear, the disturbances satisfy the same equations. Therefore,

$$\frac{\partial \tilde{u_r}}{\partial r} + \frac{\tilde{u_r}}{r} + \frac{1}{r}\frac{\partial \tilde{u_\theta}}{\partial \theta} = 0, \quad \frac{\partial \tilde{p}}{\partial r} = -\mu \tilde{u_r}, \quad \frac{1}{r}\frac{\partial \tilde{p}}{\partial \theta} = -\mu \tilde{u_\theta}. \tag{4.2}$$

We investigate the growth of these disturbances by the method of normal modes.

Since the basic solution is time dependent, due to the time dependence of the position of the interface, the growth rate is also time dependent. We consider the following ansatz for the disturbances

$$(\tilde{u_r}, \tilde{u_\theta}, \tilde{p}) = (f(r), \tau(r), \psi(r))e^{in\theta+\int_0^t \sigma(s)ds}, \tag{4.3}$$

where n denotes the wave number of the disturbance. Plugging this ansatz into equations $(4.2)_1$ and $(4.2)_3$ gives

$$\tau(r) = \frac{i}{n}(f(r) + rf'(r)), \qquad \psi(r) = -\frac{r\mu}{n^2}(f(r) + rf'(r)). \tag{4.4}$$

We then cross-differentiate the pressure equation, $(4.2)_2$ and $(4.2)_3$. Taking $\frac{\partial}{\partial\theta}$ of $(4.2)_2$ and $\frac{\partial}{\partial r}$ of $(4.2)_3$ yields

$$\frac{\partial^2\tilde{p}}{\partial r\partial\theta} = -\mu\frac{\partial\tilde{u_r}}{\partial\theta}, \qquad \frac{\partial^2\tilde{p}}{\partial\theta\partial r} = \frac{1}{r}\frac{\partial\tilde{p}}{\partial\theta} - r\mu\frac{\partial\tilde{u_\theta}}{\partial r}.$$

Setting these equal gives

$$-\mu\frac{\partial\tilde{u_r}}{\partial\theta} = \frac{1}{r}\frac{\partial\tilde{p}}{\partial\theta} - r\mu\frac{\partial\tilde{u_\theta}}{\partial r}. \tag{4.5}$$

We use the ansatz (4.3) in equation (4.5) and get

$$-i\,\mu\,nf(r)e^{in\theta+\int_0^t \sigma(s)ds} = \frac{in}{r}\psi(r)e^{in\theta+\int_0^t \sigma(s)ds} - r\mu\tau'(r)e^{in\theta+\int_0^t \sigma(s)ds}. \tag{4.6}$$

Using (4.4) in (4.6), we get

$$-\mu inf(r) = -\mu\frac{i}{n}(f(r) + rf'(r)) - r\mu\frac{i}{n}(2f'(r) + rf''(r)).$$

With some algebraic manipulation, we get the following ordinary differential equation

for $f(r)$:

$$r^2 f''(r) + 3rf'(r) + \left(1 - n^2\right) f(r) = 0. \tag{4.7}$$

It is often convenient to use an equivalent form of this equation. By multiplying by r, we get

$$r^3 f''(r) + 3r^2 f'(r) + \left(1 - n^2\right) rf(r) = 0,$$

which implies that

$$\left(r^3 f'(r)\right)' - \left(n^2 - 1\right) rf(r) = 0. \tag{4.8}$$

The solution must also satisfy linearized kinematic and dynamic interface conditions. Let $\tilde{\eta}(\theta, t)$ be the disturbance of the interface. Then the position of the interface is given by $\eta(\theta, t) = R(t) + \tilde{\eta}$. The linearized kinematic condition is given by

$$\frac{\partial \tilde{\eta}}{\partial t} = \tilde{u_r}(R) - \tilde{\eta} \frac{Q}{2\pi R^2}. \tag{4.9}$$

where $\tilde{u_r}$ is continuous at $r = R$. Consistent with the ansatz (4.3), we assume $\tilde{\eta} = \tilde{\eta}_0 \, e^{in\theta + \int_0^t \sigma(s) ds}$ for some constant $\tilde{\eta}_0$. We use this in (4.9) along with the ansatz $(4.3)_1$ for $\tilde{u_r}$ and get

$$\tilde{\eta}(\theta, t) = \frac{f(R)}{\sigma + \frac{Q}{2\pi R^2}} e^{in\theta + \int_0^t \sigma(s) ds}. \tag{4.10}$$

Next, we consider the linearized dynamic interface condition

$$p^+(\eta) - p^-(\eta) = -T \left(\frac{1}{R} - \frac{\tilde{\eta}}{R^2} - \frac{1}{R^2} \frac{\partial^2 \tilde{\eta}}{\partial \theta^2} \right),$$

where T is the interfacial tension and the "+" and "-" superscripts denote the right and left limit values, respectively. The values of the pressure are given within linear

approximation by

$$p^+(\eta) = p_b^+(R) + \tilde{p}^+(R) + \tilde{\eta}\frac{\partial p_b^+}{\partial r}(R), \qquad p^-(\eta) = p_b^-(R) + \tilde{p}^-(R) + \tilde{\eta}\frac{\partial p_b^-}{\partial r}(R).$$

The pressure of the basic solution satisfies $p_b^+(R) - p_b^-(R) = -T/R$. Additionally, since the pressure of the basic solution satisfies equation $(4.1)_2$ with $u_r = Q/(2\pi r)$, we have that $\frac{\partial p_b^+}{\partial r} = -Q\mu^+/(2\pi r)$ and $\frac{\partial p_b^-}{\partial r} = -Q\mu^-/(2\pi r)$. Therefore,

$$\left\{\tilde{p}^+(R) - \tilde{\eta}\frac{Q\mu^+}{2\pi R}\right\} - \left\{\tilde{p}^-(R) - \tilde{\eta}\frac{Q\mu^-}{2\pi R}\right\} = T\frac{\tilde{\eta} + \frac{\partial^2\tilde{\eta}}{\partial\theta^2}}{R^2} \tag{4.11}$$

Plugging the ansatz into this interface condition, we get

$$\begin{aligned}&\left\{\psi^+(R) - \frac{f(R)}{\sigma + \frac{Q}{2\pi R^2}}\frac{Q\mu^+}{2\pi R}\right\} - \left\{\psi^-(R) - \frac{f(R)}{\sigma + \frac{Q}{2\pi R^2}}\frac{Q\mu^-}{2\pi R}\right\}\\ &= \frac{T}{R^2}\left\{\frac{f(R)}{\sigma + \frac{Q}{2\pi R^2}} + \frac{\partial^2}{\partial\theta^2}\left(\frac{f(R)}{\sigma + \frac{Q}{2\pi R^2}}\right)\right\}.\end{aligned}$$

Using (4.4), the equation becomes

$$\begin{aligned}&\left\{-\frac{R\mu^+(R)}{n^2}(f(R) + R(f^+)'(R)) - \frac{f(R)}{\sigma + \frac{Q}{2\pi R^2}}\frac{Q\mu^+}{2\pi R}\right\}\\ &- \left\{-\frac{R\mu^-(R)}{n^2}(f(R) + R(f^-)'(R)) - \frac{f(R)}{\sigma + \frac{Q}{2\pi R^2}}\frac{Q\mu^-}{2\pi R}\right\} = \frac{T}{R^2}\frac{1-n^2}{\sigma + \frac{Q}{2\pi R^2}}f(R).\end{aligned}$$

Multiplying by $\left(\sigma + \frac{Q}{2\pi R^2}\right) Rn^2$ and rearranging gives

$$\begin{aligned}&\left(\sigma + \frac{Q}{2\pi R^2}\right) R^3\{\mu^-(f^-)'(R) - \mu^+(f^+)'(R)\}\\ &= \left\{\left(\sigma + \frac{Q}{2\pi R^2}\right) R^2(\mu^+ - \mu^-) + \frac{Qn^2}{2\pi}(\mu^+ - \mu^-) - T\frac{n^4 - n^2}{R}\right\} f(R).\end{aligned} \tag{4.12}$$

The eigenvalue problem is given by the equations (4.7) and (4.12). We seek solutions of the form $f(r) = Cr^m$ where C and m are constants. Plugging this into (4.7) yields

$$(m^2 + 2m + 1 - n^2)r^m = 0, \quad n \geq 1.$$

In order for this to hold for all r, we need that

$$m^2 + 2m + 1 - n^2 = 0.$$

The solutions to this quadratic equation are $m = n - 1$ and $m = -n - 1$. Therefore, solutions are of the form

$$f(r) = Ar^{n-1} + Br^{-(n+1)}. \tag{4.13}$$

Since equation (4.7) holds in the regions $r < R$ and $r > R$, in general we have

$$f(r) = \begin{cases} A_1 r^{n-1} + B_1 r^{-(n+1)}, & r < R \\ A_2 r^{n-1} + B_2 r^{-(n+1)}, & r > R. \end{cases}$$

We require that $f(r) \to$ finite as $r \to 0$ and $f(r) \to 0$ as $r \to \infty$. Therefore, $A_2 = 0$ and $B_1 = 0$, and

$$f(R) = A_1 R^{n-1} = B_2 R^{-(n+1)}.$$

Using these equalities, we get

$$f(r) = \begin{cases} f(R)\left(\frac{r}{R}\right)^{n-1}, & r < R \\ f(R)\left(\frac{R}{r}\right)^{n+1}, & r > R. \end{cases}$$

By differentiating these equations, we get

$$(f^-)'(r) = \frac{f(R)}{R}(n-1)\left(\frac{r}{R}\right)^{n-2}, \qquad (f^+)'(r) = -\frac{f(R)}{R}(n+1)\left(\frac{R}{r}\right)^{n+2}.$$

We plug these into (4.12) and use that $\mu^- = \mu_i$ and $\mu^+ = \mu_o$ to get

$$\begin{aligned}&\left(\sigma + \frac{Q}{2\pi R^2}\right) R^3 \left\{\mu_i \frac{f(R)}{R}(n-1) + \mu_o \frac{f(R)}{R}(n+1)\right\} \\ &= \left\{\left(\sigma + \frac{Q}{2\pi R^2}\right) R^2(\mu_o - \mu_i) + \frac{Qn^2}{2\pi}(\mu_o - \mu_i) - T\frac{n^4 - n^2}{R}\right\} f(R).\end{aligned}$$

Solving this equation for σ gives the classical result for the growth rate of the interfacial disturbance of the two-layer radial Hele-Shaw problem [60]:

$$\sigma = \frac{Qn}{2\pi R^2}\frac{\mu_o - \mu_i}{\mu_o + \mu_i} - \frac{Q}{2\pi R^2} - \frac{T}{\mu_o + \mu_i}\frac{n\,(n^2-1)}{R^3} \tag{4.14}$$

Several facts are obvious from this formula: (i) short waves are stable for any non-zero value of T, as expected; (ii) very long waves on the circular interface of any radius are stable when $T = 0$; (iii) there are very long waves with wave number below a critical value for which the circular interface of very small radius is stable for finite values of T. This is due to the high curvature of the interface when the stabilization effect of interfacial tension overcomes the destabilization effect of mobility jump across the interface; These effects (ii) and (iii) are different from that in rectilinear flow; (iv) the most dangerous wave number, $n = n_m$, is easily found and is given by $n_m = \sqrt{QR(\mu_o - \mu_i)/(6\pi T) + 1/3}$. The most dangerous wavenumber n_m is a monotonically decreasing function of interfacial tension T. The corresponding maximum growth rate, σ_M, can easily be found from (4.14) with $n = n_m$.

Finally, (v) there exists an optimal value of $T = T_o$ which minimizes σ_M. This value is given by $T_o = QR(\mu_o - \mu_i)/4\pi$ and easily follows from taking the derivative

of (4.14) with $n = n_m$ with respect to T and setting it to zero. However, this minimization of σ_M is performed over all positive values of n. The only physically relevant values of the wavenumber n are positive integers. It can be seen from equation (4.14) that for any $n > 1$, σ decreases monotonically as T increases. It can be checked from the formula for n_m in item (iv) above that $n_m = 1$ when $T = T_o$. Also, $\sigma(n)$ is a decreasing function of n for all $n > n_m$. Therefore, when $T \geq T_o$, $n = 1$ will be the most unstable wave and hence from (4.14), $\min \sigma_M = -(Q\mu_i)/(\pi R^2(\mu_o + \mu_i))$. This means that the flow is actually stable since $\sigma_M < 0$ when $T > T_o$ regardless of the radius of the circular interface. This leads to a possibly new and important observation. A circular interface of any radius R moving outward at any velocity displacing a fluid of viscosity μ_o is stable if interfacial tension $T = QR(\mu_o - \mu_i)/4\pi$ where Q is the volumetric injection rate of the displacing fluid having viscosity μ_i.

4.3 Linear Stability Analysis for Multi-layer Radial Flows

4.3.1 Three-layer Flows

We now wish to extend the results of the previous section to flows that contain three layers of fluid (Figure 4.3). Each fluid region is initially separated from the neighboring fluid regions by a circular interface. The least viscous fluid, with viscosity μ_i, is injected into the Hele-Shaw cell with constant injection rate Q. The most viscous fluid, with viscosity μ_o, is the outermost fluid. The intermediate fluid has viscosity μ_1 where $\mu_i < \mu_1 < \mu_o$. The basic solution consists of all fluid moving outward radially with velocity $\mathbf{u}^b = (Q/2\pi r, 0)$. The interfaces remain circular with R_0 denoting the radius of the inner interface and R_1 denoting the radius of the outer interface. These radii are given by $R_0(t) = \sqrt{Qt/\pi + R_0^2(0)}$ and $R_1(t) = \sqrt{Qt/\pi + R_1^2(0)}$. The pressure is obtained by integrating equation $(4.1)_2$.

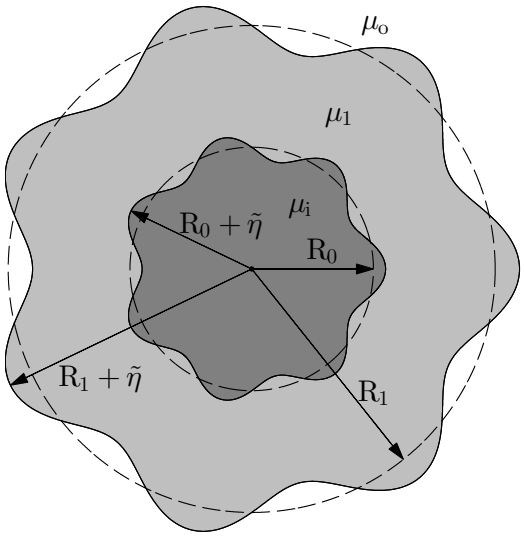

Figure 4.3: Three-layer flow

Equation (4.8) holds within each layer of fluid. Therefore, the solution, $f(r)$, is of the form

$$f(r) = \begin{cases} A_1 r^{n-1} + B_1 r^{-(n+1)}, & r < R_0 \\ A_2 r^{n-1} + B_2 r^{-(n+1)}, & R_0 < r < R_1 \\ A_3 r^{n-1} + B_3 r^{-(n+1)}, & r > R_1. \end{cases}$$

In order to ensure that the disturbances go to zero as $r \to \infty$ and to avoid a singularity at $r = 0$, we require that $B_1 = 0$ and $A_3 = 0$. Therefore,

$$(f^-)'(R_0) = (n-1)A_1 R_0^{n-2} = \frac{(n-1)f(R_0)}{R_0}, \tag{4.15}$$

and

$$(f^+)'(R_1) = -(n+1)B_3 R_1^{-(n+2)} = -\frac{(n+1)f(R_1)}{R_1}. \tag{4.16}$$

Using the interface condition (4.12) at the inner interface, we get

$$\begin{aligned}&\left(\sigma+\frac{Q}{2\pi R_0^2}\right)R_0^3\{\mu_i(f^-)'(R_0)-\mu_1(f^+)'(R_0)\}\\&=\left\{\left(\sigma+\frac{Q}{2\pi R_0^2}\right)R_0^2(\mu_1-\mu_i)+\frac{Qn^2}{2\pi}(\mu_1-\mu_i)-T_0\frac{n^4-n^2}{R_0}\right\}f(R_0),\end{aligned}\tag{4.17}$$

where T_0 denotes the interfacial tension at the inner interface. Using (4.15) in (4.17) and rearranging terms, we get

$$\left(\sigma+\frac{Q}{2\pi R_0^2}\right)\mu_1R_0^3(f^+)'(R_0)=-\left[E_0+\frac{Q\mu_1}{2\pi}-\sigma R_0^2(n\mu_i-\mu_1)\right]f(R_0),\tag{4.18}$$

where

$$E_0=\frac{Qn^2}{2\pi}(\mu_1-\mu_i)-\frac{Qn}{2\pi}\mu_i-T_0\frac{n^4-n^2}{R_0}.\tag{4.19}$$

For the outer interface, the interface condition will be

$$\begin{aligned}&\left(\sigma+\frac{Q}{2\pi R_1^2}\right)R_1^3\{\mu_1(f^-)'(R_1)-\mu_o(f^+)'(R_1)\}\\&=\left\{\left(\sigma+\frac{Q}{2\pi R_1^2}\right)R_1^2(\mu_o-\mu_1)+\frac{Qn^2}{2\pi}(\mu_o-\mu_1)-T_1\frac{n^4-n^2}{R_1}\right\}f(R_1),\end{aligned}\tag{4.20}$$

where T_1 denotes the interfacial tension at the outer interface. Using (4.16) in (4.20) and rearranging terms, we get

$$\left(\sigma+\frac{Q}{2\pi R_1^2}\right)\mu_1R_1^3(f^-)'(R_1)=\left[E_1-\frac{Q\mu_1}{2\pi}-\sigma R_1^2(\mu_1+n\mu_o)\right]f(R_1),\tag{4.21}$$

where

$$E_1=\frac{Qn^2}{2\pi}(\mu_o-\mu_1)-\frac{Qn}{2\pi}\mu_o-T_1\frac{n^4-n^2}{R_1},\tag{4.22}$$

4.3.1.1 Dispersion relation

Recall that the form of $f(r)$ in the region $R_0 < r < R_1$ is $f(r) = A_2 r^{n-1} + B_2 r^{-(n+1)}$. Plugging this form into (4.18) and simplifying yields

$$\left[E_0 + \frac{Qn}{2\pi}\mu_1 + \sigma R_0^2 n(\mu_1 - \mu_i)\right] R_0^n A_2 + \left[E_0 - \frac{Qn}{2\pi}\mu_1 - \sigma R_0^2 n(\mu_1 + \mu_i)\right] R_0^{-n} B_2 = 0. \tag{4.23}$$

Likewise, we use (4.21) to find that

$$\left[E_1 - \frac{Qn}{2\pi}\mu_1 - \sigma R_1^2 n(\mu_o + \mu_1)\right] R_1^n A_2 + \left[E_1 + \frac{Qn}{2\pi}\mu_1 - \sigma R_1^2 n(\mu_o - \mu_1)\right] R_1^{-n} B_2 = 0. \tag{4.24}$$

We may consider this as a matrix equation of the form $\mathbf{Ax} = \mathbf{0}$ where $\mathbf{x} = (A_2, B_2)$. In order for this system to have a nontrivial solution, the matrix must be singular. That is, we need $det(\mathbf{A}) = 0$. This condition, computed from (4.23) and (4.24), gives a quadratic equation for σ which is given by

$$a\sigma^2 + b\sigma + c = 0 \tag{4.25}$$

where

$$\begin{aligned}
a =& -(\mu_1 - \mu_i)(\mu_o - \mu_1)\left(\frac{R_0}{R_1}\right)^n - (\mu_1 + \mu_i)(\mu_o + \mu_1)\left(\frac{R_1}{R_0}\right)^n, \\
b =& \left\{(\mu_1 - \mu_i)\left(\frac{E_1}{nR_1^2} + \frac{Q\mu_1}{2\pi R_1^2}\right) - (\mu_o - \mu_1)\left(\frac{E_0}{nR_0^2} + \frac{Q\mu_1}{2\pi R_0^2}\right)\right\}\left(\frac{R_0}{R_1}\right)^n \\
&+ \left\{(\mu_1 + \mu_i)\left(\frac{E_1}{nR_1^2} - \frac{Q\mu_1}{2\pi R_1^2}\right) + (\mu_o + \mu_1)\left(\frac{E_0}{nR_0^2} - \frac{Q\mu_1}{2\pi R_0^2}\right)\right\}\left(\frac{R_1}{R_0}\right)^n, \\
c =& \left(\frac{E_0}{nR_0^2} + \frac{Q\mu_1}{2\pi R_0^2}\right)\left(\frac{E_1}{nR_1^2} + \frac{Q\mu_1}{2\pi R_1^2}\right)\left(\frac{R_0}{R_1}\right)^n \\
&- \left(\frac{E_0}{nR_0^2} - \frac{Q\mu_1}{2\pi R_0^2}\right)\left(\frac{E_1}{nR_1^2} - \frac{Q\mu_1}{2\pi R_1^2}\right)\left(\frac{R_1}{R_0}\right)^n.
\end{aligned}$$

Therefore, σ is given by the expression

$$\sigma^{\pm} = \frac{-b \pm \sqrt{b^2 - 4ac}}{2a} \tag{4.26}$$

Here, there are two values of the growth rate, σ^+ and σ^-, which corresponds to the number of interfaces in the flow. However, it should be stressed that these values do not correspond to the stability of the individual interfaces, but instead characterize the stability of the system as a whole.

A typical plot of the the real part of σ, denoted σ_R, versus the wavenumber n is given in Figure 4.4. Here we used the values $R_0 = 20$, $R_1 = 30$, $\mu_i = 2$, $\mu_1 = 5$, $\mu_o = 10$, $Q = 10$, $T_0 = 1$, and $T_1 = 1$. In this case, σ is real for all n. Note that both modes are stable for short waves due to interfacial tension. Also, the wave with wavenumber $n = 1$ is stable. It can be shown that when $n = 1$, $a, b, c < 0$ for any values of the parameters. Therefore, the wave whose wavelength is the entire circumference of the interface is always stable. This stands in stark contrast to rectilinear flow in which long waves are unstable. Therefore, we can conclude that the curvature has the effect of stabilizing long waves. We also note that there are exactly two values of n for which $\sigma_R^+ = 0$. We refer to the greater of these values as the maximum neutral wavenumber and the lesser of these as the minimum neutral wavenumber. The difference between these values is the unstable bandwidth.

Note that it is possible for σ to be complex. The imaginary part of sigma corresponds to the phase speed of the wave. Consider, for example, the values $R_0 = 9$, $R_1 = 11$, $\mu_i = 2$, $\mu_1 = 8$, $\mu_o = 10$, $Q = 1$, $T_0 = 1$, and $T_1 = 1$. Then, for a range of wavenumbers, σ is complex. In particular, for $n = 3$ we get $\sigma = -.0019 \pm .0002i$. Figure 4.5 shows σ_R versus the wavenumber n. σ is complex when the two curves coincide. This is a unique feature of multi-layer radial flows because σ is always real

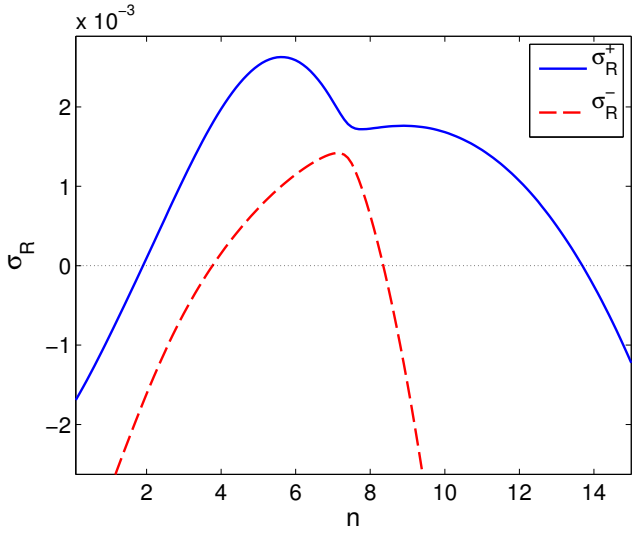

Figure 4.4: Plot of the real part of the growth rate σ_R versus the wavenumber n for $R_0 = 20$, $R_1 = 30$, $\mu_i = 2$, $\mu_1 = 6$, $\mu_o = 10$, $Q = 10$, $T_0 = 1$, and $T_1 = 1$.

for both two-layer radial flow and multi-layer rectilinear flow. Notice that in our example, the complex σ has a negative real part. Therefore, this complex growth rate corresponds to a stable wave. We believe this to be the only case in which σ is complex.

We now consider this solution in some limiting cases. First, consider the thick-layer limit when $R_1 >> R_0$. In this case, the terms that are multiplied by $(R_1/R_0)^n$ dominate those that are multiplied by $(R_0/R_1)^n$. Therefore,

$$a \to -(\mu_1 + \mu_i)(\mu_o + \mu_1)\left(\frac{R_1}{R_0}\right)^n \tag{4.27}$$

$$b \to \left\{(\mu_1 + \mu_i)\left(\frac{E_1}{nR_1^2} - \frac{Q\mu_1}{2\pi R_1^2}\right) + (\mu_o + \mu_1)\left(\frac{E_0}{nR_0^2} - \frac{Q\mu_1}{2\pi R_0^2}\right)\right\}\left(\frac{R_1}{R_0}\right)^n \tag{4.28}$$

$$c \to -\left(\frac{E_0}{nR_0^2} - \frac{Q\mu_1}{2\pi R_0^2}\right)\left(\frac{E_1}{nR_1^2} - \frac{Q\mu_1}{2\pi R_1^2}\right)\left(\frac{R_1}{R_0}\right)^n. \tag{4.29}$$

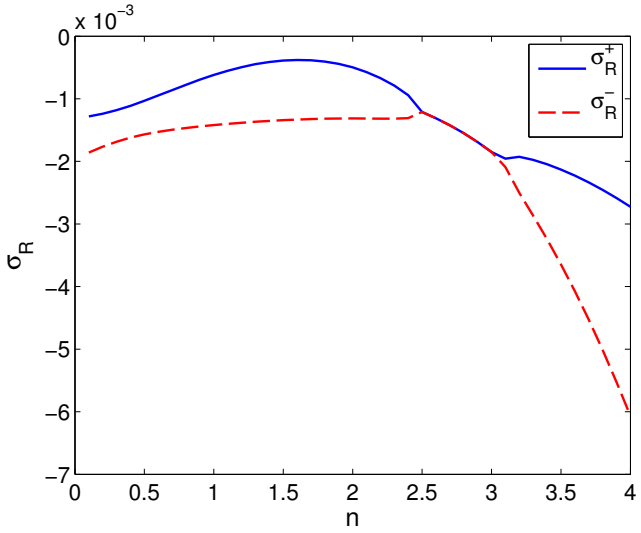

Figure 4.5: Plot of the real part of the growth rate σ_R versus the wavenumber n for $R_0 = 9$, $R_1 = 11$, $\mu_i = 2$, $\mu_1 = 8$, $\mu_o = 10$, $Q = 1$, $T_0 = 1$, and $T_1 = 1$.

Using (4.27) - (4.29),

$$\begin{aligned} b^2 - 4ac \to & \left[(\mu_1+\mu_i)\left(\frac{E_1}{nR_1^2} - \frac{Q\mu_1}{2\pi R_1^2}\right)\right]^2 \left(\frac{R_1}{R_0}\right)^{2n} \\ & + 2(\mu_1+\mu_i)(\mu_o+\mu_1)\left(\frac{E_1}{nR_1^2} - \frac{Q\mu_1}{2\pi R_1^2}\right)\left(\frac{E_0}{nR_0^2} - \frac{Q\mu_1}{2\pi R_0^2}\right)\left(\frac{R_1}{R_0}\right)^{2n} \\ & + \left[(\mu_o+\mu_1)\left(\frac{E_0}{nR_0^2} - \frac{Q\mu_1}{2\pi R_0^2}\right)\right]^2 \left(\frac{R_1}{R_0}\right)^{2n} \\ & - 4(\mu_1+\mu_i)(\mu_o+\mu_1)\left(\frac{E_1}{nR_1^2} - \frac{Q\mu_1}{2\pi R_1^2}\right)\left(\frac{E_0}{nR_0^2} - \frac{Q\mu_1}{2\pi R_0^2}\right)\left(\frac{R_1}{R_0}\right)^{2n} \\ = & \left\{(\mu_1+\mu_i)\left(\frac{E_1}{nR_1^2} - \frac{Q\mu_1}{2\pi R_1^2}\right) - (\mu_o+\mu_1)\left(\frac{E_0}{nR_0^2} - \frac{Q\mu_1}{2\pi R_0^2}\right)\right\}^2 \left(\frac{R_1}{R_0}\right)^{2n}. \end{aligned}$$

We denote $\sigma^+ = (-b + \sqrt{b^2-4ac})/(2a)$ and $\sigma^- = (-b - \sqrt{b^2-4ac})/(2a)$. Then

$$\sigma^+ = \frac{-2(\mu_o+\mu_1)\left(\frac{E_0}{nR_0^2} - \frac{Q\mu_1}{2\pi R_0^2}\right)\left(\frac{R_1}{R_0}\right)^n}{-2(\mu_1+\mu_i)(\mu_o+\mu_1)\left(\frac{R_1}{R_0}\right)^n} = \frac{\frac{E_0}{nR_0^2} - \frac{Q\mu_1}{2\pi R_0^2}}{\mu_1+\mu_i}.$$

Plugging in the expression (4.19) for E_0, we get

$$\sigma^+ = \frac{Qn}{2\pi R_0^2}\frac{\mu_1 - \mu_i}{\mu_1 + \mu_i} - \frac{Q}{2\pi R_0^2} - \frac{T_0}{\mu_1 + \mu_i}\frac{n\left(n^2-1\right)}{R_0^3}. \tag{4.30}$$

Likewise, we can calculate σ^-,

$$\sigma^- = \frac{-2(\mu_1+\mu_i)\left(\frac{E_1}{nR_1^2} - \frac{Q\mu_1}{2\pi R_1^2}\right)\left(\frac{R_1}{R_0}\right)^n}{-2(\mu_1+\mu_i)(\mu_o+\mu_1)\left(\frac{R_1}{R_0}\right)^n} = \frac{\frac{E_1}{nR_1^2} - \frac{Q\mu_1}{2\pi R_1^2}}{\mu_o+\mu_1}.$$

Plugging in the expression (4.22) for E_1, we get

$$\sigma^- = \frac{Qn}{2\pi R_1^2}\frac{\mu_o - \mu_1}{\mu_o + \mu_1} - \frac{Q}{2\pi R_1^2} - \frac{T_1}{\mu_o + \mu_1}\frac{n\left(n^2-1\right)}{R_1^3}. \tag{4.31}$$

Note that σ^+ is the two-layer growth rate at the inner interface and σ^- is the two-layer growth rate at the outer interface. This is what we expect since the interfaces do not interact in the thick-layer limit.

Next we consider the thin-layer limit. Fix R and consider the limit as $R_0, R_1 \to R$. Then, in particular, $(R_0/R_1)^n, (R_1/R_0)^n \to 1$ for all n. In addition,

$$E_0 \to \frac{Qn^2}{2\pi}(\mu_1 - \mu_i) - \frac{Qn}{2\pi}\mu_i - T_0\frac{n^4-n^2}{R}, \tag{4.32}$$

$$E_1 \to \frac{Qn^2}{2\pi}(\mu_o - \mu_1) - \frac{Qn}{2\pi}\mu_o - T_1\frac{n^4-n^2}{R}, \tag{4.33}$$

and

$$
\begin{aligned}
a &\to -(\mu_1-\mu_i)(\mu_o-\mu_1)-(\mu_1+\mu_i)(\mu_o+\mu_1)\\
b &\to \left\{(\mu_1-\mu_i)\left(\frac{E_1}{nR^2}+\frac{Q\mu_1}{2\pi R^2}\right)-(\mu_o-\mu_1)\left(\frac{E_0}{nR^2}+\frac{Q\mu_1}{2\pi R^2}\right)\right\},\\
&+\left\{(\mu_1+\mu_i)\left(\frac{E_1}{nR^2}-\frac{Q\mu_1}{2\pi R^2}\right)+(\mu_o+\mu_1)\left(\frac{E_0}{nR^2}-\frac{Q\mu_1}{2\pi R^2}\right)\right\},\\
c &\to \left(\frac{E_0}{nR^2}+\frac{Q\mu_1}{2\pi R^2}\right)\left(\frac{E_1}{nR^2}+\frac{Q\mu_1}{2\pi R^2}\right)-\left(\frac{E_0}{nR^2}-\frac{Q\mu_1}{2\pi R^2}\right)\left(\frac{E_1}{nR^2}-\frac{Q\mu_1}{2\pi R^2}\right).
\end{aligned}
$$

Simplifying, we get

$$a \to -2\mu_1(\mu_o+\mu_i), \tag{4.34}$$

$$b \to 2\mu_1\left(\frac{E_0}{nR^2}+\frac{E_1}{nR^2}-\frac{Q}{2\pi R^2}(\mu_o+\mu_i)\right), \tag{4.35}$$

$$c = 2\mu_1\frac{Q}{2\pi R^2}\left(\frac{E_0}{nR^2}+\frac{E_1}{nR^2}\right). \tag{4.36}$$

Using (4.34) - (4.36)

$$
\begin{aligned}
b^2-4ac \to & 4\mu_1^2\left(\frac{E_0}{nR^2}+\frac{E_1}{nR^2}\right)^2-8\mu_1^2\left(\frac{E_0}{nR^2}+\frac{E_1}{nR^2}\right)\left(\frac{Q}{2\pi R^2}(\mu_o+\mu_i)\right)\\
&+4\mu_1^2\left(\frac{Q}{2\pi R^2}(\mu_o+\mu_i)\right)^2+16\mu_1^2\left(\frac{E_0}{nR^2}+\frac{E_1}{nR^2}\right)\left(\frac{Q}{2\pi R^2}(\mu_o+\mu_i)\right)\\
=&\left\{2\mu_1\left(\frac{E_0}{nR^2}+\frac{E_1}{nR^2}+\frac{Q}{2\pi R^2}(\mu_o+\mu_i)\right)\right\}^2.
\end{aligned}
$$

Then

$$\sigma^+ = \frac{4\mu_1\left\{\frac{Q}{2\pi R^2}(\mu_o+\mu_i)\right\}}{-4\mu_1(\mu_o+\mu_i)} = -\frac{Q}{2\pi R^2}, \tag{4.37}$$

which is independent of n and stable, and

$$\sigma^- = \frac{-4\mu_1\left\{\frac{E_0}{nR^2}+\frac{E_1}{nR^2}\right\}}{-4\mu_1(\mu_o+\mu_i)} = \frac{E_0+E_1}{nR^2(\mu_o+\mu_i)}.$$

Using (4.32) and (4.33), we get

$$\sigma^{-} = \frac{Qn}{2\pi R^2}\frac{\mu_o - \mu_i}{\mu_o + \mu_i} - \frac{Q}{2\pi R^2} - \frac{T_0 + T_1}{\mu_o + \mu_i}\frac{n\left(n^2-1\right)}{R^3}. \tag{4.38}$$

This expression is the growth rate of a single interface at R separating fluids with the viscosities of the outer and inner fluids and with its interfacial tension equal to the sum of the interfacial tensions of our two interfaces.

4.3.1.2 Upper bounds on the growth rate

To obtain upper bounds on σ_R we take the Ordinary Differential Equation (4.8), multiply by $\left(\sigma + Q/(2\pi r^2)\right)\mu_1 f^*(r)$, and integrate from R_0 to R_1. Then

$$\begin{aligned}&\int_{R_0}^{R_1}\left(r^3 f'(r)\right)' f^*(r)\left(\sigma\mu_1 + \frac{Q\mu_1}{2\pi r^2}\right)dr \\ &-\left(n^2-1\right)\int_{R_0}^{R_1} r|f(r)|^2\left(\sigma\mu_1 + \frac{Q\mu_1}{2\pi r^2}\right)dr = 0.\end{aligned}$$

Using integration by parts on the first term and using the interface conditions (4.18) and (4.21), we get

$$\begin{aligned}&\left[E_1 - \frac{Q\mu_1}{2\pi} - \sigma R_1^2(\mu_1 + n\mu_o)\right]|f(R_1)|^2 + \left[E_0 + \frac{Q\mu_1}{2\pi} - \sigma R_0^2(n\mu_i - \mu_1)\right]|f(R_0)|^2 \\ &-\sigma\mu_1\left\{\int_{R_0}^{R_1} r^3|f'(r)|^2 dr + \left(n^2-1\right)\int_{R_0}^{R_1} r|f(r)|^2 dr\right\} \\ &-\frac{Q\mu_1}{2\pi}\left\{\int_{R_0}^{R_1} r|f'(r)|^2 dr + \left(n^2-1\right)\int_{R_0}^{R_1}\frac{|f(r)|^2}{r}dr\right\} + \frac{Q\mu_1}{2\pi}\int_{R_0}^{R_1} 2f'(r)f^*(r)dr = 0.\end{aligned} \tag{4.39}$$

But note that

$$\left(|f(r)|^2\right)' = \left(f(r)f^*(r)\right)' = f'(r)f^*(r) + f(r)(f^*(r))'. \tag{4.40}$$

Therefore

$$\begin{aligned}\int_{R_0}^{R_1} 2f'(r)f^*(r)dr &= \int_{R_0}^{R_1} f'(r)f^*(r) + f'(r)f^*(r)dr \\ &= \int_{R_0}^{R_1} \left(|f(r)|^2\right)' + f'(r)f^*(r) - f(r)(f^*(r))'dr \\ &= |f(R_1)|^2 - |f(R_0)|^2 + \int_{R_0}^{R_1} f'(r)f^*(r) - f(r)(f^*(r))'dr.\end{aligned}$$

Using this expression in (4.39) gives

$$\begin{aligned}&\left[E_1 - \sigma R_1^2(\mu_1 + n\mu_o)\right]|f(R_1)|^2 + \left[E_0 - \sigma R_0^2(n\mu_i - \mu_1)\right]|f(R_0)|^2 \\ &- \sigma\mu_1\left\{\int_{R_0}^{R_1} r^3|f'(r)|^2dr + \left(n^2-1\right)\int_{R_0}^{R_1} r|f(r)|^2dr\right\} \\ &- \frac{Q\mu_1}{2\pi}\left\{\int_{R_0}^{R_1} r|f'(r)|^2dr + \left(n^2-1\right)\int_{R_0}^{R_1}\frac{|f(r)|^2}{r}dr\right\} \\ &+ \frac{Q\mu_1}{2\pi}\int_{R_0}^{R_1} f'(r)f^*(r) - f(r)(f^*(r))'dr = 0.\end{aligned}$$

Solving for σ gives the expression

$$\sigma = \frac{E_0|f(R_0)|^2 + E_1|f(R_1)|^2 + \frac{Q\mu_1}{2\pi}I_0 - \frac{Q\mu_1}{2\pi}I_1}{R_0^2(n\mu_i - \mu_1)|f(R_0)|^2 + R_1^2(\mu_1 + n\mu_o)|f(R_1)|^2 + \mu_1 I_2}. \tag{4.41}$$

where

$$I_0 = \int_{R_0}^{R_1} f'(r)f^*(r) - f(r)(f^*(r))'dr, \tag{4.42}$$

$$I_1 = \int_{R_0}^{R_1}\left(r|f'(r)|^2 + \left(n^2-1\right)\frac{|f(r)|^2}{r}\right)dr, \tag{4.43}$$

$$I_2 = \int_{R_0}^{R_1}\left(r^3|f'(r)|^2 + \left(n^2-1\right)r|f(r)|^2\right)dr. \tag{4.44}$$

Note that I_1 and I_2 are both real and positive for a non-zero $f(r)$. Also note that the integrand of I_0 is the difference of complex conjugates and is thus purely imaginary. Let σ_R denote the real part of σ and σ_i denote the imaginary part. Then

$$\sigma_R = \frac{E_0|f(R_0)|^2 + E_1|f(R_1)|^2 - \frac{Q\mu_1}{2\pi} I_1}{R_0^2(n\mu_i - \mu_1)|f(R_0)|^2 + R_1^2(\mu_1 + n\mu_o)|f(R_1)|^2 + \mu_1 I_2}, \tag{4.45}$$

and

$$i\sigma_i = \frac{\frac{Q\mu_1}{2\pi} I_0}{R_0^2(n\mu_i - \mu_1)|f(R_0)|^2 + R_1^2(\mu_1 + n\mu_o)|f(R_1)|^2 + \mu_1 I_2}. \tag{4.46}$$

We wish to bound σ_R. We do this by invoking the following lemma.

Lemma 6. *Let $f(r)$ solve the differential equation* (4.8) *and I_2 be defined by* (4.44). *Then*

$$I_2 > n\, g(R_0, R_1)\Big(\lambda_1 R_0^2|f(R_0)|^2 + \lambda_2 R_1^2|f(R_1)|^2\Big) + R_0^2|f(R_0)|^2 - R_1^2|f(R_1)|^2, \tag{4.47}$$

where

$$g(r,s) = \frac{\left(\frac{s}{r}\right)^n - \left(\frac{r}{s}\right)^n}{\left(\frac{s}{r}\right)^n + \left(\frac{r}{s}\right)^n}, \tag{4.48}$$

for any $\lambda_1, \lambda_2 > 0$ such that $\lambda_1 + \lambda_2 \leq 1$.

Proof. If $f(r)$ solves (4.8), then

$$\left(r^3 f'(r)\right)' = \left(n^2 - 1\right) r f(r).$$

Using the product rule,

$$\left(r^3 f'(r) f^*(r)\right)' = r^3|f'(r)|^2 + \left(r^3 f'(r)\right)' f^*(r) = r^3|f'(r)|^2 + \left(n^2 - 1\right) r|f(r)|^2.$$

Therefore,

$$I_2 = \int_{R_0}^{R_1} \left(r^3 f'(r) f^*(r)\right)' dr = R_1^3 f'(R_1) f^*(R_1) - R_0^3 f'(R_0) f^*(R_0). \tag{4.49}$$

Solutions to (4.8) can be written in the form

$$f(r) = C_1 \left(\frac{r}{R_0}\right)^{-n-1} + C_2 \left(\frac{r}{R_1}\right)^{n-1}.$$

Therefore,

$$f(R_0) = C_1 + C_2 \left(\frac{R_0}{R_1}\right)^{n-1},$$
$$f(R_1) = C_1 \left(\frac{R_0}{R_1}\right)^{n+1} + C_2.$$

We can solve this system of equations to find C_1 and C_2. We find that

$$C_1 = \frac{f(R_1)\left(\frac{R_0}{R_1}\right)^{n-1} - f(R_0)}{\left(\frac{R_0}{R_1}\right)^{2n} - 1},$$

and

$$C_2 = \frac{f(R_0)\left(\frac{R_0}{R_1}\right)^{n+1} - f(R_1)}{\left(\frac{R_0}{R_1}\right)^{2n} - 1}.$$

Therefore,

$$f(r) = \frac{\left[f(R_1)\left(\frac{R_0}{R_1}\right)^{n-1} - f(R_0)\right]\left(\frac{r}{R_0}\right)^{-n-1} + \left[f(R_0)\left(\frac{R_0}{R_1}\right)^{n+1} - f(R_1)\right]\left(\frac{r}{R_1}\right)^{n-1}}{\left(\frac{R_0}{R_1}\right)^{2n} - 1}.$$

Taking a derivative, we get that

$$f'(r) = \frac{-\left[f(R_1)\left(\frac{R_0}{R_1}\right)^{n-1} - f(R_0)\right](n+1)\frac{r^{-n-2}}{R_0^{-n-1}}}{\left(\frac{R_0}{R_1}\right)^{2n} - 1} + \frac{\left[f(R_0)\left(\frac{R_0}{R_1}\right)^{n+1} - f(R_1)\right](n-1)\frac{r^{n-2}}{R_1^{n-1}}}{\left(\frac{R_0}{R_1}\right)^{2n} - 1}.$$

Therefore,

$$f'(R_0) = \frac{n}{R_0}\frac{f(R_0)\left[\left(\frac{R_0}{R_1}\right)^{2n} + 1\right] - 2f(R_1)\left(\frac{R_0}{R_1}\right)^{n-1}}{\left(\frac{R_0}{R_1}\right)^{2n} - 1} - \frac{f(R_0)}{R_0},$$

and

$$f'(R_1) = -\frac{n}{R_1}\frac{f(R_1)\left[\left(\frac{R_0}{R_1}\right)^{2n} + 1\right] - 2f(R_0)\left(\frac{R_0}{R_1}\right)^{n+1}}{\left(\frac{R_0}{R_1}\right)^{2n} - 1} - \frac{f(R_1)}{R_1}.$$

Using these expressions for $f'(R_0)$, and $f'(R_1)$ in equation (4.49), we get

$$\begin{aligned} I_2 =& \frac{-nR_1^2\left\{|f(R_1)|^2\left[\left(\frac{R_0}{R_1}\right)^{2n} + 1\right] - 2f(R_0)f^*(R_1)\left(\frac{R_0}{R_1}\right)^{n+1}\right\}}{\left(\frac{R_0}{R_1}\right)^{2n} - 1} \\ &+ \frac{-nR_0^2\left\{|f(R_0)|^2\left[\left(\frac{R_0}{R_1}\right)^{2n} + 1\right] - 2f^*(R_0)f(R_1)\left(\frac{R_0}{R_1}\right)^{n-1}\right\}}{\left(\frac{R_0}{R_1}\right)^{2n} - 1} \\ &+ R_0^2|f(R_0)|^2 - R_1^2|f(R_1)|^2. \end{aligned}$$

Through some algebraic manipulation, this becomes

$$I_2 = \frac{n(R_1^2|f(R_1)|^2 + R_0^2|f(R_0)|^2)}{g(R_0,R_1)} - \frac{2nR_0R_1[f^*(R_0)f(R_1) + f(R_0)f^*(R_1)]}{\left(\frac{R_1}{R_0}\right)^n - \left(\frac{R_0}{R_1}\right)^n}$$
$$+ R_0^2|f(R_0)|^2 - R_1^2|f(R_1)|^2,$$

where $g(\cdot,\cdot)$ has been defined in (4.48). But

$$f^*(R_0)f(R_1) + f(R_0)f^*(R_1) = 2Re(f(R_0)f^*(R_1)) \leq 2|f(R_0)||f(R_1)|.$$

Therefore,

$$I_2 > \frac{n(R_1^2|f(R_1)|^2 + R_0^2|f(R_0)|^2)}{g(R_0,R_1)} - \frac{4nR_0R_1|f(R_0)||f(R_1)|}{\left(\frac{R_1}{R_0}\right)^n - \left(\frac{R_0}{R_1}\right)^n} + R_0^2|f(R_0)|^2 - R_1^2|f(R_1)|^2.$$

Let $b = \ln\left(\left(\frac{R_1}{R_0}\right)^n\right)$, $\zeta = R_0|f(R_0)|$, and $\chi = R_1|f(R_1)|$. Then

$$I_2 > n\,F(\zeta,\chi) + \zeta^2 - \chi^2, \tag{4.50}$$

where

$$F(\zeta,\chi) = \frac{1}{\sinh(b)}\left\{\zeta^2\cosh(b) - 2\zeta\chi + \chi^2\cosh(b)\right\}.$$

We recall the following procedure from Daripa [16].

$$\begin{aligned} F(\zeta,\chi) &= \frac{1}{\sinh(b)\cosh(b)}\left\{\zeta^2\cosh^2(b) - 2\zeta\chi\cosh(b) + \chi^2\cosh^2(b)\right\} \\ &= \frac{1}{\sinh(b)\cosh(b)}\left\{\zeta^2\cosh^2(b) - 2\zeta\chi\cosh(b) + \chi^2 + \chi^2\sinh^2(b)\right\} \\ &= \frac{1}{\sinh(b)\cosh(b)}\left\{(\zeta\cosh(b) - \chi)^2 + \chi^2\sinh^2(b)\right\} \\ &\geq \frac{1}{\sinh(b)\cosh(b)}\left\{\chi^2\sinh^2(b)\right\} \\ &= \tanh(b)\chi^2. \end{aligned}$$

Note that since $F(\zeta,\chi)$ is symmetric, we also have that

$$F(\zeta,\chi) \geq \tanh(b)\zeta^2.$$

Therefore, we can take convex combinations of $\tanh(b)\chi^2$ and $\tanh(b)\zeta^2$ and get that for any $\lambda_1, \lambda_2 > 0$ such that $\lambda_1 + \lambda_2 = 1$,

$$F(\zeta,\chi) \geq \tanh(b)(\lambda_1\zeta^2 + \lambda_2\chi^2).$$

Since $b > 0$, all terms are positive and this result also holds for any $\lambda_1 + \lambda_2 \leq 1$. Inserting this equality in (4.50), we obtain

$$I_2 > n\tanh(b)\left(\lambda_1\zeta^2 + \lambda_2\chi^2\right) + \zeta^2 - \chi^2.$$

By reinserting our values for b, ζ, and χ, we obtain Lemma 6. □

We now use the result of Lemma 6 in our expression (4.45). If $\sigma_R > 0$,

$$\sigma_R < \frac{E_0|f(R_0)|^2 + E_1|f(R_1)|^2 - \frac{Q\mu_1}{2\pi} I_1}{nR_0^2\left(\mu_i + \mu_1\lambda_1 g(R_0,R_1)\right)|f(R_0)|^2 + nR_1^2\left(\mu_o + \mu_1\lambda_2 g(R_0,R_1)\right)|f(R_1)|^2},$$

Since the denominator is now positive, we may also ignore the negative term in the numerator. Therefore,

$$\sigma_R < \frac{E_0|f(R_0)|^2 + E_1|f(R_1)|^2}{nR_0^2\left(\mu_i + \mu_1\lambda_1 g(R_0,R_1)\right)|f(R_0)|^2 + nR_1^2\left(\mu_o + \mu_1\lambda_2 g(R_0,R_1)\right)|f(R_1)|^2}.$$

We consider four cases:

1. If $E_0 < 0$ and $E_1 < 0$, then $\sigma_R < 0$.

2. If $E_0 < 0$ and $E_1 > 0$, then we can neglect the negative term $E_0|f(R_0)|^2$ in the numerator and the corresponding positive term in the denominator to get

$$\sigma_R < \frac{E_1}{nR_1^2\left(\mu_o + \mu_1\lambda_2 g(R_0,R_1)\right)}.$$

3. If $E_0 > 0$ and $E_1 < 0$, we neglect the negative term $E_1|f(R_1)|^2$ in the numerator and the corresponding positive term in the denominator to get

$$\sigma_R < \frac{E_0}{nR_0^2\left(\mu_i + \mu_1\lambda_1 g(R_0,R_1)\right)}.$$

4. If $E_0 > 0$ and $E_1 > 0$, then all terms are positive. We use the following inequality which holds for any N if $A_i > 0$, $B_i > 0$, and $X_i > 0$ for all $i = 1, ..., N$. Then

$$\frac{\sum_{i=1}^{N} A_i X_i}{\sum_{i=1}^{N} B_i X_i} \leq \max_i \left\{\frac{A_i}{B_i}\right\}.$$

By using this inequality with $N = 2$, we get

$$\sigma_R < \max\left(\frac{E_0}{nR_0^2\left(\mu_i + \mu_1\lambda_1 g(R_0, R_1)\right)}, \frac{E_1}{nR_1^2\left(\mu_o + \mu_1\lambda_2 g(R_0, R_1)\right)}\right). \tag{4.51}$$

Clearly, the upper bound (4.51) holds for the second and third cases above. Therefore, it holds for all unstable modes.

We now see the results for several different combinations of λ_1 and λ_2. First, consider $\lambda_1 = \lambda_2 = 0$. Note that this minimizes the denominator and thus gives the worst possible upper bound among all choices of $\lambda_i's$. This choice yields the upper bound

$$\sigma_R < \max\left(\frac{E_0}{nR_0^2\mu_i}, \frac{E_1}{nR_1^2\mu_o}\right). \tag{4.52}$$

We can find an upper bound for all waves by finding the maximum of these functions over all values of the wavenumber n. To find the wavenumber that maximizes each, we take a derivative.

$$\begin{aligned}\frac{d}{dn}\left\{\frac{E_0}{nR_0^2\mu_i}\right\} &= \frac{d}{dn}\left\{\frac{Qn}{2\pi R_0^2}\left(\frac{\mu_1 - \mu_i}{\mu_i}\right) - \frac{Q}{2\pi R_0^2} - T_0\frac{n^3 - n}{R_0^3}\frac{1}{\mu_i}\right\} \\ &= \frac{Q}{2\pi R_0^2}\left(\frac{\mu_1 - \mu_i}{\mu_i}\right) - T_0\frac{3n^2 - 1}{R_0^3}\frac{1}{\mu_i}.\end{aligned}$$

Setting this equation equal to zero and solving for n, we obtain the wave number that maximizes the first term in our upper bound. We call this value n_0. Then

$$n_0 = \sqrt{\frac{QR_0}{6\pi T_0}(\mu_1 - \mu_i) + \frac{1}{3}}. \tag{4.53}$$

Likewise, we can find the wavenumber, n_1, that maximizes the second term of our upper bound. A similar calculation shows

$$n_1 = \sqrt{\frac{QR_1}{6\pi T_1}(\mu_o - \mu_1) + \frac{1}{3}}. \tag{4.54}$$

Therefore, we have an absolute upper bound σ_R^u such that $\sigma_R(n) < \sigma_R^u$ for any value of n. The absolute upper bound is given by

$$\sigma_R^u = \max\left\{\left[\frac{Qn_0}{2\pi R_0^2}\left(\frac{\mu_1-\mu_i}{\mu_i}\right) - \frac{Q}{2\pi R_0^2} - T_0\frac{n_0^3-n_0}{R_0^3}\frac{1}{\mu_i}\right],\right.$$
$$\left.\left[\frac{Qn_1}{2\pi R_1^2}\left(\frac{\mu_o-\mu_1}{\mu_o}\right) - \frac{Q}{2\pi R_1^2} - T_1\frac{n_1^3-n_1}{R_1^3}\frac{1}{\mu_o}\right]\right\}. \tag{4.55}$$

Compare these values to the value of n_m in the case of two-layer flow (see section 4.2). Note that n_0 and n_1 correspond to the values of n_m for flows with only the inner and outer interface, respectively. We find that the absolute upper bound is minimized by the choice of interfacial tensions

$$T_0 = \frac{QR_0(\mu_1-\mu_i)}{4\pi}, \qquad T_1 = \frac{QR_1(\mu_o-\mu_1)}{4\pi}. \tag{4.56}$$

As in the two-layer case, these values of T_0 and T_1 are the values of interfacial tension that correspond to $n_0 = n_1 = 1$. Therefore, all flows with values of T_0 and T_1 that are greater than the expressions given in (4.56) will have $n = 1$ as their most unstable wave and the absolute upper bound will become

$$\sigma_R^u = \max\left\{\left[\frac{Q}{2\pi R_0^2}\left(\frac{\mu_1-2\mu_i}{\mu_i}\right)\right], \left[\frac{Q}{2\pi R_1^2}\left(\frac{-\mu_1}{\mu_o}\right)\right]\right\}, \tag{4.57}$$

which is independent of T_0 and T_1 and negative whenever $\mu_1 < 2\mu_i$.

For improved estimates, we can choose nonzero values for λ_i. Of particular interest is $\lambda_1 = 1$ and $\lambda_2 = 0$, which minimizes the term corresponding to the inner interface. This gives the upper bound

$$\sigma_R < \max\left(\frac{E_0}{nR_0^2\left(\mu_i + \mu_1 g(R_0,R_1)\right)}, \frac{E_1}{nR_1^2\mu_o}\right). \tag{4.58}$$

Conversely, we can consider $\lambda_1 = 0$ and $\lambda_2 = 1$ which minimizes the term corresponding to the outer interface and get

$$\sigma_R < \max\left(\frac{E_0}{nR_0^2\mu_i}, \frac{E_1}{nR_1^2\left(\mu_o + \mu_1 g(R_0, R_1)\right)}\right). \tag{4.59}$$

Note that both σ^+ and σ^- given by (4.26) will satisfy these upper bounds.

4.3.2 Multi-layer Flows

We now consider the case of an arbitrary number of fluid layers (see Figure 4.6). Let there be N intermediate layers of fluid - and thus $N+2$ total layers of fluid - with $N+1$ interfaces at $R_0 < R_1 < ... < R_{N-1} < R_N$. The respective interfacial tensions are $T_0, ..., T_N$. As before, the fluid in the inner region has viscosity μ_i and the fluid in the outer region has viscosity μ_o. For j = 1,...N, the fluid in the annulus $R_{j-1} < r < R_j$ has viscosity μ_j. We assume that $\mu_i < \mu_1 < \mu_2 < ... < \mu_N < \mu_o$.

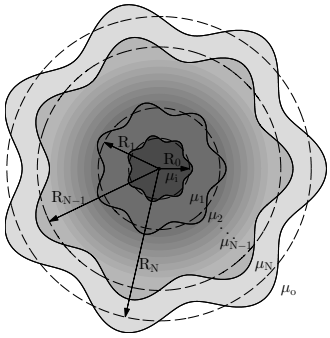

Figure 4.6: N-layer flow

Equation (4.8) holds within each layer of fluid. Therefore, the solution, $f(r)$, is

of the form

$$f(r) = \begin{cases} A_0 r^{n-1} + B_0 r^{-(n+1)}, & r < R_0 \\ A_j r^{n-1} + B_j r^{-(n+1)}, & R_{j-1} < r < R_j, \quad 1 \le j \le N \\ A_{N+1} r^{n-1} + B_{N+1} r^{-(n+1)}, & r > R_N. \end{cases} \tag{4.60}$$

According to equation (4.12), the interface conditions at $r = R_j$ are given by

$$\begin{aligned} &\left(\sigma + \frac{Q}{2\pi R_j^2}\right) R_j^3 \{\mu^-(f^-)'(R_j) - \mu^+(f^+)'(R_j)\} \\ &= \left\{ \left(\sigma + \frac{Q}{2\pi R_j^2}\right) R_j^2(\mu^+ - \mu^-) + \frac{Qn^2}{2\pi}(\mu^+ - \mu^-) - T_j \frac{n^4 - n^2}{R_j} \right\} f(R_j). \end{aligned} \tag{4.61}$$

As in the three-layer problem, we require that $B_0 = 0$ and $A_{N+1} = 0$ so that the disturbances go to zero as $r \to \infty$, and there is no singularity at $r = 0$. Using (4.60) in (4.61) leads to the following expressions for the interface conditions on the inner and outermost interfaces

$$\left(\sigma + \frac{Q}{2\pi R_0^2}\right) \mu_1 R_0^3 (f^+)'(R_0) = -\left[E_0 + \frac{Q\mu_1}{2\pi} - \sigma R_0^2(n\mu_i - \mu_1)\right] f(R_0), \tag{4.62}$$

$$\left(\sigma + \frac{Q}{2\pi R_N^2}\right) \mu_N R_N^3 (f^-)'(R_N) = \left[E_N - \frac{Q\mu_N}{2\pi} - \sigma R_N^2(\mu_N + n\mu_o)\right] f(R_N), \tag{4.63}$$

where

$$E_0 = \frac{Qn^2}{2\pi}(\mu_1 - \mu_i) - \frac{Qn}{2\pi}\mu_i - T_0 \frac{n^4 - n^2}{R_0}, \quad E_N = \frac{Qn^2}{2\pi}(\mu_o - \mu_N) - \frac{Qn}{2\pi}\mu_o - T_N \frac{n^4 - n^2}{R_N}.$$

For the intermediate interfaces, we have for $j = 1, ..., N-1$

$$\begin{aligned}&\left(\sigma + \frac{Q}{2\pi R_j^2}\right) R_j^3(\mu_j(f^-)'(R_j) - \mu_{j+1}(f^+)'(R_j)) \\ &= \left[E_j + \frac{Q}{2\pi}(\mu_{j+1} - \mu_j) + \sigma R_j^2(\mu_{j+1} - \mu_j)\right] f(R_j),\end{aligned} \tag{4.64}$$

where

$$E_j = \frac{Qn^2}{2\pi}(\mu_{j+1} - \mu_j) - T_j \frac{n^4 - n^2}{R_j}.$$

Note that there are $(2N + 2)$ constants to be determined in equation (4.60). The function $f(r)$ must be continuous across each of the $N + 1$ interfaces. This leaves $N + 1$ free constants. The set of $N + 1$ interface conditions gives a system of the form $\mathbf{Ax} = 0$ where $\mathbf{x}$ is a vector of length $N + 1$ and $\mathbf{A}$ is a square matrix. For this equation to have nontrivial solutions, we need $det(\mathbf{A}) = 0$. Since the interface conditions are linear in σ, this results in an $N+1$ degree polynomial for σ. Therefore, there are at most $N + 1$ distinct values of σ for each wave number n.

We now return to equation (4.8) which holds in each layer of fluid. For any $1 \le j \le N$

$$\left(r^3 f'(r)\right)' - \left(n^2 - 1\right) r f(r) = 0, \quad R_{j-1} < r < R_j.$$

We multiply by $\left(\sigma + Q/(2\pi r^2)\right) \mu_j f^*(r)$ and integrate from R_{j-1} to R_j to get

$$\int_{R_{j-1}}^{R_j} \left(\left(r^3 f'(r)\right)' f^*(r) - \left(n^2 - 1\right) r |f(r)|^2\right) \left(\sigma\mu_j + \frac{Q\mu_j}{2\pi r^2}\right) dr = 0.$$

We again use integration by parts on the first term. Then,

$$\begin{aligned}&\left(\sigma + \frac{Q}{2\pi r^2}\right) r^3 \mu_j f'(r) f(r)\Big|_{R_{j-1}}^{R_j} - \mu_j \int_{R_{j-1}}^{R_j} r^3 |f'(r)|^2 \left(\sigma + \frac{Q}{2\pi r^2}\right) dr \\ &+\mu_j \int_{R_{j-1}}^{R_j} r^3 f'(r) f(r) \frac{Q}{\pi r^3} dr - \left(n^2 - 1\right) \int_{R_{j-1}}^{R_j} r |f(r)|^2 \left(\sigma + \frac{Q}{2\pi r^2}\right) dr = 0.\end{aligned}$$

Since this holds for each $1 \leq j \leq N$, we may sum this expression over all values of j. Using the interface conditions in this sum, we get

$$\begin{aligned}
&\left[E_0 + \frac{Q\mu_1}{2\pi} - \sigma R_0^2(\mu_1 - n\mu_i)\right] |f(R_0)|^2 \\
&+ \sum_{j=1}^{N-1} \left[E_j + \frac{Q}{2\pi}(\mu_{j+1} - \mu_j) + \sigma R_j^2(\mu_{j+1} - \mu_j)\right] |f(R_j)|^2 \\
&+ \left[E_N - \frac{Q\mu_N}{2\pi} - \sigma R_N^2(\mu_N + n\mu_o)\right] |f(R_N)|^2 \\
&- \sum_{j=1}^{N} \left\{\mu_j \int_{R_{j-1}}^{R_j} r^3 |f'(r)|^2 \left(\sigma + \frac{Q}{2\pi r^2}\right) dr\right\} + \frac{Q}{2\pi} \sum_{j=1}^{N} \left\{\mu_j \int_{R_{j-1}}^{R_j} 2f'(r)f^*(r)dr\right\} \\
&- \sum_{j=1}^{N} \left\{\left(n^2 - 1\right) \int_{R_{j-1}}^{R_j} r|f(r)|^2 \left(\sigma + \frac{Q}{2\pi r^2}\right) dr\right\} = 0.
\end{aligned}$$

As in the three-layer case, we use that

$$\int_{R_{j-1}}^{R_j} 2f'(r)f^*(r)dr = |f(R_j)|^2 - |f(R_{j-1})|^2 + \int_{R_{j-1}}^{R_j} f'(r)f^*(r) - f(r)(f^*(r))'dr.$$

Therefore

$$\begin{aligned}
&\left[E_0 - \sigma R_0^2(\mu_1 - n\mu_i)\right] |f(R_0)|^2 + \sum_{j=1}^{N-1} \left[E_j + \sigma R_j^2(\mu_{j+1} - \mu_j)\right] |f(R_j)|^2 \\
&+ \left[E_N - \sigma R_N^2(\mu_N + n\mu_o)\right] |f(R_N)|^2 - \sum_{j=1}^{N} \left\{\mu_j \int_{R_{j-1}}^{R_j} r^3 |f'(r)|^2 \left(\sigma + \frac{Q}{2\pi r^2}\right) dr\right\} \\
&+ \frac{Q}{2\pi} \sum_{j=1}^{N} \left\{\mu_j \int_{R_{j-1}}^{R_j} f'(r)f^*(r) - f(r)(f^*(r))'dr\right\} \\
&- \sum_{j=1}^{N} \left\{\left(n^2 - 1\right) \int_{R_{j-1}}^{R_j} r|f(r)|^2 \left(\sigma + \frac{Q}{2\pi r^2}\right) dr\right\} = 0.
\end{aligned}$$

Solving for σ gives the expression

$$\sigma = \frac{\sum_{j=0}^{N} E_j |f(R_j)|^2 + \frac{Q}{2\pi} J_0 - \frac{Q}{2\pi} J_1}{\sum_{j=0}^{N} F_j |f(R_j)|^2 + J_2}, \tag{4.65}$$

where $F_0 = R_0^2(n\mu_i - \mu_1)$, $F_j = R_j^2(\mu_j - \mu_{j+1})$ for $1 \leq j \leq N-1$, $F_N = R_N^2(\mu_N + n\mu_o)$, and

$$\begin{aligned}
J_0 &= \sum_{j=1}^{N} \left\{ \mu_j \int_{R_{j-1}}^{R_j} f'(r) f^*(r) - f(r)(f^*(r))' dr \right\}, \\
J_1 &= \sum_{j=1}^{N} \left\{ \mu_j \int_{R_{j-1}}^{R_j} \left(r|f'(r)|^2 + \left(n^2 - 1\right) \frac{|f(r)|^2}{r} \right) dr \right\}, \\
J_2 &= \sum_{j=1}^{N} \left\{ \mu_j \int_{R_{j-1}}^{R_j} \left(r^3 |f'(r)|^2 + \left(n^2 - 1\right) r |f(r)|^2 \right) dr \right\}.
\end{aligned}$$

Again, J_0 is the difference of complex conjugates and is therefore purely imaginary. Therefore,

$$\sigma_R = \frac{\sum_{j=0}^{N} E_j |f(R_j)|^2 - \frac{Q}{2\pi} J_1}{\sum_{j=0}^{N} F_j |f(R_j)|^2 + J_2}. \tag{4.66}$$

Lemma 6 implies that for any $j = 1, ..., N$,

$$\begin{aligned}
&\int_{R_{j-1}}^{R_j} \left(r^3 |f'(r)|^2 + (n^2 - 1) r |f(r)|^2 \right) dr \geq \\
&n\, g(R_{j-1}, R_j) \left(\lambda_{j,1} R_{j-1}^2 |f(R_{j-1})|^2 + \lambda_{j,2} R_j^2 |f(R_j)|^2 \right) + R_{j-1}^2 |f(R_{j-1})|^2 - R_j^2 |f(R_j)|^2,
\end{aligned}$$

for any $\lambda_{j,1}, \lambda_{j,2} \geq 0$ such that $\lambda_{j,1} + \lambda_{j,2} \leq 1$, where $g(\cdot, \cdot)$ has been defined in (4.48).

Therefore,

$$
\begin{aligned}
J_2 \geq & \left(\lambda_{1,1}\mu_1\, n\, g(R_0,R_1)R_0^2 + \mu_1 R_0^2\right)|f(R_0)|^2 \\
& + \sum_{j=1}^{N-1} R_j^2\left(\lambda_{j,2}\mu_j\, n\, g(R_{j-1},R_j) + \lambda_{j+1,1}\mu_{j+1}\, n\, g(R_j,R_{j+1}) + (\mu_{j+1}-\mu_j)\right)|f(R_j)|^2 \\
& + \left(\lambda_{N,2}\mu_N\, n\, g(R_{N-1},R_N)R_N^2 - \mu_N R_N^2\right)|f(R_N)|^2.
\end{aligned}
$$

Using this expression in place of J_2 and ignoring the negative integral term in the numerator, we get

$$\sigma_R < \frac{\sum_{j=0}^{N} E_j |f(R_j)|^2}{\sum_{j=0}^{N} n R_j^2 G_j |f(R_j)|^2}, \tag{4.67}$$

where

$$
\begin{aligned}
G_0 &= \lambda_{1,1}\mu_1 g(R_0,R_1) + \mu_i, \\
G_j &= \lambda_{j,2}\mu_j g(R_{j-1},R_j) + \lambda_{j+1,1}\mu_{j+1} g(R_j,R_{j+1}), \qquad 1 \leq j \leq N-1 \\
G_N &= \lambda_{N,2}\mu_N g(R_{N-1},R_N) + \mu_o
\end{aligned}
$$

for any choice of $\lambda_{j,k}$'s such that $\lambda_{j_1} + \lambda_{j_2} \leq 1$ for all j. In particular this means that for all unstable modes,

$$\sigma_R < \max_{0\leq j\leq N}\left(\frac{E_j}{nR_j^2 G_j}\right). \tag{4.68}$$

Note that when $N = 1$, this corresponds with the three-layer upper bound, (4.51), where $\lambda_1 = \lambda_{1,1}$ and $\lambda_2 = \lambda_{N,2}$.

4.3.3 Special Cases

In this section, we show how to construct appropriate limits in order to recover well-known results for rectilinear flows and a special case for radial flows. This analysis in turn establishes a connection between instabilities in radial and rectilinear

geometries.

4.3.3.1 Connection to rectilinear flow

The curvature of the interface is an important physical aspect of this radial flow configuration. However, as more fluid is injected into the cell, the curvatures of the interfaces decrease. In particular, as the radius of a circular interface goes to infinity, the curvature goes to zero. Additionally, since an interface at R_j moves with velocity $Q/(2\pi R_j)$, the inner interfaces moves faster than the outer interfaces. Therefore, if interfaces are located at R_j and R_k, then the ratio R_j/R_k approaches 1 as more fluid is pumped into the cell.

In light of this information, we investigate the zero curvature limit. Let $R_j \to \infty$ for $0 \leq j \leq N$ such that $R_j/R_k \to 1$ for all $0 \leq j, k \leq N$ and also $Q, n \to \infty$ such that $Q/(2\pi R_0)$ and n/R_0 are constants. We denote these constants by U and k, respectively. Note in particular that since $R_0/R_j \to 1$ for all j, $Q/(2\pi R_j) \to U$ and $n/R_j \to k$. The equation (4.8) is rewritten as

$$f''(r) + \frac{3}{r} f'(r) + \frac{1 - n^2}{r^2} f(r) = 0.$$

In any of the intermediate layers, we'll have $R_0 < r < R_N$. Therefore, $r \to \infty$ such that $n/r \to k$. Taking this limit, we are left with

$$f''(r) - k^2 f(r) = 0. \tag{4.69}$$

Now consider the boundary condition (4.12) at $R = R_j$ and divide by R_j^3. Then

$$\left(\sigma + \frac{Q}{2\pi R_j^2}\right)\left\{\mu^-(f^-)'(R_j) - \mu^+(f^+)'(R_j)\right\}$$
$$= \left\{\left(\frac{\sigma}{R_j} + \frac{Q}{2\pi R_j^3}\right)(\mu^+ - \mu^-) + \frac{Qn^2}{2\pi R_j^3}(\mu^+ - \mu^-) - T_j\frac{n^4 - n^2}{R_j^4}\right\} f(R_j).$$

Taking the prescribed limits gives

$$\sigma\left\{\mu^-(f^-)'(R_j) - \mu^+(f^+)'(R_j)\right\} = \left\{Uk^2(\mu^+ - \mu^-) - T_jk^4\right\} f(R_j).$$

Therefore

$$\mu^-(f^-)'(R_j)f(R_j) - \mu^+(f^+)'(R_j)f(R_j) = \frac{Uk^2(\mu^+ - \mu^-) - T_jk^4}{\sigma}|f(R_j)|^2. \quad (4.70)$$

Equations (4.69) and (4.70) agree with the equations derived by Daripa [16] for rectilinear flow in a Hele-Shaw cell.

Next, consider a three-layer radial flow. Recall that σ is the solution to a quadratic equation $a\sigma^2 + b\sigma + c = 0$ given by (4.25). We now require that $R_0/R_1 = exp(-L/R_0)$ for some constant L. This ensures that $R_0/R_1 \to 1$ as $R_0, R_1 \to \infty$. Then $(R_0/R_1)^n = exp(-nL/R_0) = exp(-kL)$. Using this limit along with the previously imposed limits, we get

$$a = e^{-kL}(\mu - \mu_i)(\mu - \mu_o) - e^{kL}(\mu + \mu_i)(\mu_o + \mu),$$
$$b = \left[e^{kL}(\mu + \mu_i) + e^{-kL}(\mu - \mu_i)\right]\xi - \left[e^{kL}(\mu_o + \mu) + e^{-kL}(\mu - \mu_o)\right]\tau,$$
$$c = \tau\xi(e^{kL} - e^{-kL}),$$

where $\tau = -\left[Uk(\mu - \mu_i) - T_0k^3\right]$ and $\xi = \left[Uk(\mu_o - \mu) - T_1k^3\right]$. This agrees with the exact solution found for rectilinear flow by Daripa [17].

4.3.3.2 Stable inner interface

Recall from equation (4.10) that the amplitude of the disturbance of an interface at $r = R$ at any time t is given by

$$\frac{f(R)}{\sigma + \frac{Q}{2\pi R^2}} e^{\int_0^t \sigma(s)ds}.$$

Therefore, imposing the condition $f(R) = 0$ gives a completely stable interface. Consider three-layer flow in which the inner interface is stable. This is a reasonable assumption if $\mu_i >> \mu_1$. The new eigenvalue problem is defined by

$$\begin{cases} \left(r^3 f'(r)\right)' - \left(n^2 - 1\right) r f(r) = 0, \quad R_0 \le r \le R_1 \\ f(R_0) = 0, \\ \left(\sigma + \frac{Q}{2\pi R_1^2}\right) \mu_1 R_1^3 (f^-)'(R_1) = \left[E_1 - \frac{Q\mu_1}{2\pi} - \sigma R_1^2(\mu_1 + n\mu_o)\right] f(R_1). \end{cases} \tag{4.71}$$

A solution that satisfies the interface condition at $r = R_0$ must take the form

$$f(r) = \frac{C}{R_0^n} r^{n-1} - C R_0^n r^{-(n+1)},$$

for some constant C. Then

$$\begin{aligned} f(R_1) &= \frac{C}{R_1}\left(\frac{R_1}{R_0}\right)^n - \frac{C}{R_1}\left(\frac{R_0}{R_1}\right)^n, \\ f'(R_1) &= \frac{C(n-1)}{R_1^2}\left(\frac{R_1}{R_0}\right)^n + \frac{C(n+1)}{R_1^2}\left(\frac{R_0}{R_1}\right)^n. \end{aligned}$$

Plugging these into the interface condition $(4.71)_3$, we get

$$\left(\sigma + \frac{Q}{2\pi R_1^2}\right)\mu_1 R_1 \left\{(n-1)\left(\frac{R_1}{R_0}\right)^n + (n+1)\left(\frac{R_0}{R_1}\right)^n\right\}$$
$$= \left[\frac{E_1}{R_1} - \frac{Q\mu_1}{2\pi R_1} - \sigma R_1(\mu_1 + n\mu_o)\right]\left\{\left(\frac{R_1}{R_0}\right)^n - \left(\frac{R_0}{R_1}\right)^n\right\},$$

where E_1 is given by (4.22). Note that

$$\frac{E_1}{R_1} - \frac{Q\mu_1}{2\pi R_1} - \sigma R_1(\mu_1 + n\mu_o)$$
$$= \left(\frac{Qn^2}{2\pi R_1}(\mu_o - \mu_i) - T_1\frac{n^4 - n^2}{R_1^2}\right) - \left(\sigma + \frac{Q}{2\pi R_1^2}\right)(\mu_1 + n\mu_o)R_1.$$

Then

$$\left(\sigma + \frac{Q}{2\pi R_1^2}\right)\mu_1 R_1 \left\{(n-1)\left(\frac{R_1}{R_0}\right)^n + (n+1)\left(\frac{R_0}{R_1}\right)^n\right\}$$
$$= \left(\frac{Qn^2}{2\pi R_1}(\mu_o - \mu_i) - T_1\frac{n^4 - n^2}{R_1^2}\right)\left\{\left(\frac{R_1}{R_0}\right)^n - \left(\frac{R_0}{R_1}\right)^n\right\}$$
$$- \left(\sigma + \frac{Q}{2\pi R_1^2}\right)(\mu_1 + n\mu_o)R_1\left\{\left(\frac{R_1}{R_0}\right)^n - \left(\frac{R_0}{R_1}\right)^n\right\}.$$

Solving for σ gives

$$\sigma = -\frac{Q}{2\pi R_1^2} + \frac{\frac{Qn}{2\pi R_1^2}(\mu_o - \mu_i) - T_1\frac{n^3 - n}{R_1^3}}{\mu_1\frac{\left(\frac{R_1}{R_0}\right)^n + \left(\frac{R_0}{R_1}\right)^n}{\left(\frac{R_1}{R_0}\right)^n - \left(\frac{R_0}{R_1}\right)^n} + \mu_o},$$

which agrees with the result obtained by Cardoso and Woods [8].

4.4 Stabilization

We will show that the flow may be stabilized by the addition of many layers of fluid with small positive jumps in viscosity. First, we consider the upper bound

(4.67) with $\lambda_{j,k} = 0$ for all j and k. Then $G_j = 0$ for $1 \leq j \leq N-1$ and

$$\sigma_R < \frac{\sum_{j=0}^{N} E_j |f(R_j)|^2}{nR_0^2\mu_i|f(R_j)|^2 + nR_N^2\mu_o|f(R_j)|^2}$$

We now use the following fact: If $E_j < 0$ for $1 \leq j \leq N-1$, then

$$\begin{aligned}\sigma_R &< \max\left\{\frac{E_0}{nR_0^2\mu_i}, \frac{E_N}{nR_N^2\mu_o}\right\} \\ &= \max\left\{\left(\frac{Qn}{2\pi R_0^2}\left(\frac{\mu_1-\mu_i}{\mu_i}\right) - \frac{Q}{2\pi R_0^2} - T_0\frac{n^3-n}{R_0^3}\frac{1}{\mu_i}\right), \right. \\ &\qquad \left.\left(\frac{Qn}{2\pi R_N^2}\left(\frac{\mu_o-\mu_N}{\mu_o}\right) - \frac{Q}{2\pi R_N^2} - T_N\frac{n^3-n}{R_N^3}\frac{1}{\mu_o}\right)\right\}.\end{aligned}$$

Let μ be any value such that $\mu_1 \leq \mu \leq \mu_N$. Then since $\mu_1 - \mu_i \leq \mu - \mu_i$ and $\mu_o - \mu_N \leq \mu_o - \mu$,

$$\begin{aligned}&\max\left\{\left(\frac{Qn}{2\pi R_0^2}\left(\frac{\mu_1-\mu_i}{\mu_i}\right) - \frac{Q}{2\pi R_0^2} - T_0\frac{n^3-n}{R_0^3}\frac{1}{\mu_i}\right), \right. \\ &\qquad \left.\left(\frac{Qn}{2\pi R_N^2}\left(\frac{\mu_o-\mu_N}{\mu_o}\right) - \frac{Q}{2\pi R_N^2} - T_N\frac{n^3-n}{R_N^3}\frac{1}{\mu_o}\right)\right\} \\ &< \max\left\{\left(\frac{Qn}{2\pi R_0^2}\left(\frac{\mu-\mu_i}{\mu_i}\right) - \frac{Q}{2\pi R_0^2} - T_0\frac{n^3-n}{R_0^3}\frac{1}{\mu_i}\right), \right. \\ &\qquad \left.\left(\frac{Qn}{2\pi R_N^2}\left(\frac{\mu_o-\mu}{\mu_o}\right) - \frac{Q}{2\pi R_N^2} - T_N\frac{n^3-n}{R_N^3}\frac{1}{\mu_o}\right)\right\}\end{aligned}$$

which is the three-layer upper bound when the intermediate layer viscosity is μ. Therefore, this is an improvement over the three-layer upper bound if $E_j < 0$ for $1 \leq j \leq N-1$. We consider these terms. Recall that

$$E_j = \frac{Qn^2}{2\pi}(\mu_{j+1} - \mu_j) - T_j\frac{n^4-n^2}{R_j}.$$

We investigate the zeros of this function. The only nonzero values of n for which $E_j = 0$ occur when

$$\frac{Q}{2\pi}(\mu_{j+1} - \mu_j) - T_j \frac{n^2 - 1}{R_j} = 0.$$

The positive value of n that satisfies this, which we will denote n_j, is given by

$$n_j = \sqrt{\frac{QR_j}{2\pi T_j}(\mu_{j+1} - \mu_j) + 1}.$$

By observing that E_j is negative for large enough n, we can deduce that $E_j < 0$ for all $n > n_j$. Note that $E_j > 0$ for $n = 1$ whenever $\mu_{j+1} - \mu_j > 0$. However, by choosing sufficiently small jumps in viscosity at the intermediate interfaces, we can ensure that $E_j < 0$ for all $n \geq 2$. In particular, this will be true when $n_j < 2$. This is satisfied when

$$(\mu_{j+1} - \mu_j) < \frac{6\pi T_j}{QR_j}. \tag{4.72}$$

Note that this expression does not depend on the thickness of the layer. Therefore, we can include many thin layers, each with a small jump in viscosity. To see this, consider the situation in which the innermost interface is at R_0 and the outermost interface is at R_N (where the value of N is yet to be determined). We fix some values for μ_1 and μ_N. We assume that the minimum value of interfacial tension between any two layers of fluid is given by some number $T = \min T_j$. Then, let N be the unique integer such that

$$(N-2) < \frac{(\mu_N - \mu_1)QR_N}{6\pi T} \leq (N-1). \tag{4.73}$$

Then we let

$$R_j = R_0 + \left(\frac{R_N - R_0}{N}\right) j, \quad 1 \leq j \leq N-1, \tag{4.74}$$

$$\mu_{j+1} = \mu_j + \frac{6\pi T}{QR_N}, \quad 1 \leq j \leq N-2. \tag{4.75}$$

Since, $6\pi T/(QR_N) < 6\pi T_j/(QR_j)$ for all $1 \leq j \leq N-1$, it is clear that (4.75) ensures that $(\mu_{j+1} - \mu_j) < 6\pi T_j/(QR_j)$ for $1 \leq j \leq N-2$. It remains to show that this holds for the interface between the fluids of viscosity μ_{N-1} and μ_N. Note that (4.75) can be rewritten as $\mu_{j+1} = \mu_1 + 6\pi T j/(QR_N)$. Therefore, $\mu_{N-1} = \mu_1 + (N-2)6\pi T/(QR_N)$. Using this equality and (4.73), we get

$$\begin{aligned}
\mu_N - \mu_{N-1} &= \mu_N - \left(\mu_1 + (N-2)\frac{6\pi T}{QR_N}\right) \\
&= (\mu_N - \mu_1) - (N-2)\frac{6\pi T}{QR_N} \\
&> (\mu_N - \mu_1) - \left(\frac{(\mu_N - \mu_1)QR_N}{6\pi T}\right)\frac{6\pi T}{QR_N} \\
&= 0
\end{aligned}$$

and likewise

$$\begin{aligned}
\mu_N - \mu_{N-1} &= \mu_N - \left(\mu_1 + (N-2)\frac{6\pi T}{QR_N}\right) \\
&= (\mu_N - \mu_1) - (N-2)\frac{6\pi T}{QR_N} \\
&= (\mu_N - \mu_1) - (N-1)\frac{6\pi T}{QR_N} + \frac{6\pi T}{QR_N} \\
&< (\mu_N - \mu_1) - \left(\frac{(\mu_N - \mu_1)QR_N}{6\pi T}\right)\frac{6\pi T}{QR_N} + \frac{6\pi T}{QR_N} \\
&= \frac{6\pi T}{QR_N}.
\end{aligned}$$

Therefore, (4.72) holds for all $1 \leq j \leq N-1$, and this system will have the property that $E_j < 0$ for all $n \geq 2$. Since this can be done for arbitrary values of μ_1 and μ_N, we may choose these values to be such that the destabilizing terms $(Qn/2\pi R_0^2)\left((\mu_1 - \mu_i)/\mu_i\right)$ and $(Qn/2\pi R_N^2)\left((\mu_o - \mu_N)/\mu_o\right)$ in our upper bounds are arbitrarily small.

As an example of this procedure, consider the values $Q = 10$, $\mu_i = 2$, $\mu_o = 10$, $R_0 = 20$ and $R_N = 30$. We choose fluids for the innermost and outermost intermediate layers so that $\mu_1 = 2.05$, $\mu_N = 9.96$, and $T_0 = T_N = 1$. With these choices, the terms E_0 and E_N will be negative for all $n \geq 1$. If all other fluids can be chosen so that $T_j \geq 1$ for all j, then, according to equation (4.73), $N = 127$. Using 128 evenly spaced interfaces with radii given by (4.74) and fluid viscosity jumps of $\pi/50 \approx 0.063$, $E_j < 0$ for all $1 \leq j \leq N-1$ and $n \geq 2$.

4.5 Numerical Results

We now use the dispersion relation that we found in section 4.3.1.1 to numerically investigate the effect of different parameters on the growth rate in three-layer flow.

4.5.1 Validation of the Upper Bounds

First, we wish to validate the upper bound (4.51). In Figure 4.7, we plot the same dispersion curves as in Figure 4.4, labeled σ_R^+ and σ_R^-, but include the upper bound using several different values of λ_1 and λ_2. The parameter values are $R_0 = 20$, $R_1 = 30$, $\mu_i = 2$, $\mu_1 = 5$, $\mu_o = 10$, $Q = 10$, $T_0 = 1$, and $T_1 = 1$. The first upper bound we plot uses the values $\lambda_1 = \lambda_2 = 0$. This upper bound is given in equation (4.52). Recall that this is the worst upper bound. We can see that the upper bound is, in fact, an upper bound because it is greater than both σ_R^+ and σ_R^- everywhere inside the unstable band. Recall that equation (4.51) consists of two terms, one corresponding to each interface. The discontinuity in the slope of the upper bound

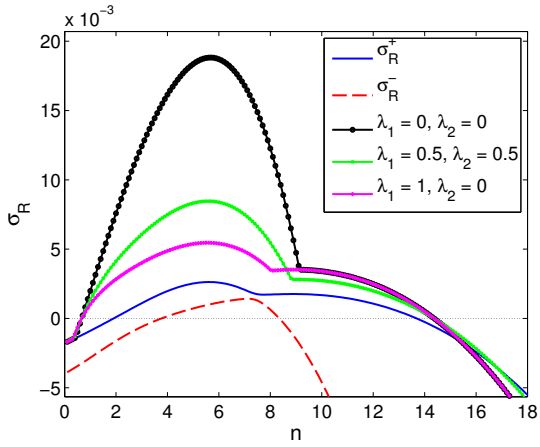

Figure 4.7: Plots of exact dispersion relations and the upper bounds (see equation (4.51)) of the growth rate for several different values of λ_1 and λ_2. The parameter values are $R_0 = 20$, $R_1 = 30$, $\mu_i = 2$, $\mu_1 = 5$, $\mu_o = 10$, $Q = 10$, $T_0 = 1$, and $T_1 = 1$.

corresponds to the point where the term corresponding to the inner interface is equal to the term corresponding to the outer interface. We call this wavenumber n^*. When $n < n^*$, the term corresponding to one of the interfaces is larger, and when $n > n^*$, the term corresponding to the other interface is larger. Therefore, in essence, one region corresponds to wave numbers where the inner interface is more unstable and the other region corresponds to wave numbers where the outer interface is more unstable. Note that qualitatively, σ_R^+ has a similar shape to the upper bound. We also plotted the upper bound that comes from the values $\lambda_1 = \lambda_2 = 1/2$. This gives equal stabilization to the inner and outer interface. Note that this upper bound is an improvement over the previous upper bound, but has a similar shape. For the particular values of the parameters chosen here, the term corresponding to the inner interface is greater for $n < n^*$. Since this is the region where the growth rate is largest, and, in fact, contains most of the unstable band, we optimize the upper bound by minimizing this term. Therefore, the maximal upper bound is given when $\lambda_1 = 1$ and $\lambda_2 = 0$. Clearly this upper bound is better than the previous two choices

of the λ's for the most unstable wavenumbers.

4.5.2 The Effect of the Middle Layer Viscosity

Recall that we use n_m to denote the wavenumber of the most dangerous wave and σ_M to denote its growth rate. We now investigate the behavior of σ_M under changes in the viscosity of the middle layer, μ_1. We allow μ_1 to vary between μ_i and μ_o, which are 2 and 10 respectively. Here, we use the values $R_0 = 20$ and $R_1 = 22$ so that there will be sufficient interaction between the interfaces, and we use $Q = 10$. Figures 4.8a and 4.8a show the results. Figure 4.8a uses the value $T_1 = 1$ and has curves corresponding to $T_0 = 1, 2, ..., 5$. Figure 4.8b uses $T_0 = 1$ and T_1 varies between 1 and 5. For each set of values T_0 and T_1, there is a value of μ_1 within this range that minimizes σ_M. We would expect this because values near μ_i result in a large destabilizing jump in viscosity at the outer interface and values near μ_o result in a large destabilizing jump in viscosity at the inner interface. As T_0 increases in comparison to T_1, the value of μ_1 that minimizes σ_M increases because the stabilizing effect of interfacial tension on the inner interface counteracts the destabilizing effect of a larger viscous jump. Similarly, as T_1 increases in comparison to T_0, the value of μ_1 that minimizes σ_M decreases.

In Figure 4.9a, we plot the values of the maximum neutral wave number, minimum neutral wave number, and n_m versus μ_1 for the values $T_0 = T_1 = 1$ (which corresponds to the solid line in Figures 4.8a and 4.8a). The unstable band consists of those wavenumbers between the maximum and minimum neutral waves. Note first that there is a value of μ_1 that minimizes n_m. This value, seen as the minimum point of the middle curve in Figure 4.9a, is relatively close to the value that minimizes σ_M. However, there is a different value of μ_1 that minimizes the unstable bandwidth. To see this, we plot the unstable bandwidth versus μ_1 in Figure 4.9b.

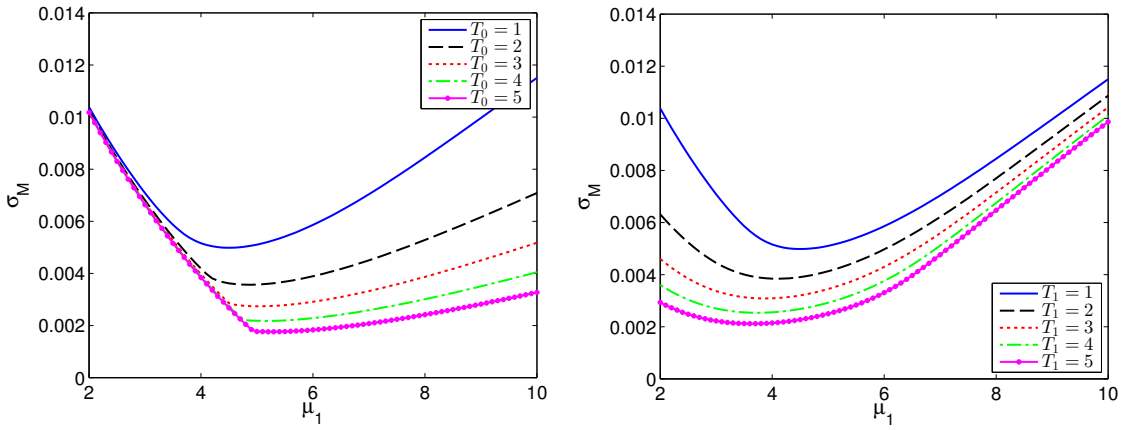

(a) (b)

Figure 4.8: A plot of the maximum value of the growth rate (see equation (4.26)) versus the viscosity of the intermediate layer, μ_1. In plot (a), T_1 is held constant at $T_1 = 1$ while T_0 varies. In plot (b), T_0 is held constant at $T_0 = 1$ while T_1 varies. The other parameter values are $R_0 = 20$, $R_1 = 22$, $\mu_i = 2$, $\mu_o = 10$, and $Q = 10$.

4.5.3 The Effect of Interfacial Tension

Next, we investigate the effect of the interfacial tension on σ_M. We use the same interfacial tension at each interface and denote $T = T_0 = T_1$. We also use the values $R_0 = 20$, $R_1 = 30$, $\mu_i = 2$, $\mu_1 = 3$, $\mu_o = 10$, and $Q = 10$. Figure 4.10 shows the results. Note that the values that minimize the three layer upper bounds as given in (4.56) are $T_0 = 15.9155$ and $T_1 = 167.1127$. Therefore, we know from (4.57) and our choice of μ_1 that when $T > 167.1127$, $\sigma_M < 0$. We see from Figure 4.10 that, in fact, $\sigma_M < 0$ for much smaller values of T. Also, σ_M decreases much more rapidly for small values of T and appears to approach a fixed value in the large T limit. This agrees with our analysis of the two-layer case in Section 4.2 which shows that for large T, $n = 1$ is the most dangerous wavenumber and the value of the growth rate at $n = 1$ is independent of T.

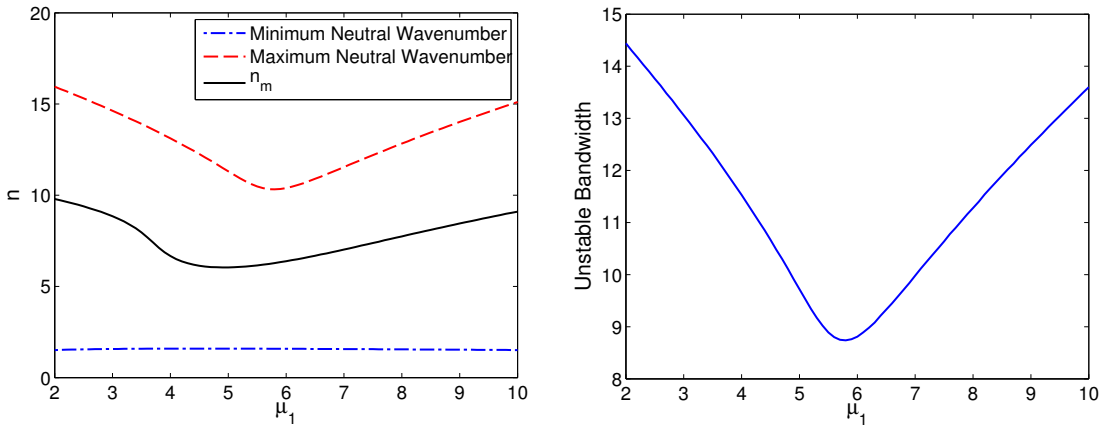

(a) (b)

Figure 4.9: (a) Plot of the neutral wavenumbers and most dangerous wavenumber, n_m, versus the viscosity of the intermediate layer, μ_1. (b) A plot of the unstable bandwidth versus μ_1. Both plots use $R_0 = 20$, $R_1 = 22$, $\mu_i = 2$, $\mu_o = 10$, $Q = 10$, $T_0 = 1$ and $T_1 = 1$.

4.5.4 The Effect of the Curvature of the Interfaces

We now investigate the stability of the system for different values of the curvature of the interfaces. To elucidate the results for three-layer flows, we begin by investigating the effect of curvature in two-layer radial flows. Recall the expression for the growth rate, (4.14). Also, recall that $n_m = \sqrt{QR(\mu_o - \mu_i)/(6\pi T) + 1/3}$. Therefore, as $R \to 0$, the wave corresponding to $n = 1$ is the most dangerous wave. The growth of this wave is given by $\sigma_M = -(Q\mu_i)/(\pi R^2(\mu_o + \mu_i))$. In the limit as $R \to 0$, σ_M decreases without bound like $-1/R^2$. Therefore, the flow is stable as the curvature of the interface increases to infinity. To investigate the limit as $R \to \infty$, we use (4.14) with $n = n_m$. Since n_m is proportional to $\sqrt{R}$, this expression goes to zero as $R \to \infty$ at the rate $R^{-\frac{3}{2}}$. Therefore, σ_M goes to zero as the curvature of the interface goes to zero. Physically, this results from the fact that the velocity of the interface goes to zero as $R \to \infty$. However, between these two limiting cases, the dependence

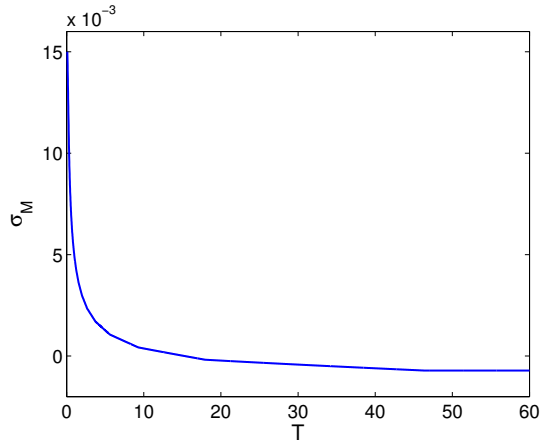

Figure 4.10: A plot of the maximum growth rate versus interfacial tension for $R_0 = 20$, $R_1 = 30$, $\mu_i = 2$, $\mu_1 = 3$, $\mu_o = 10$, and $Q = 10$.

of σ_M on the curvature is not monotonic. Figure 4.11 shows σ_M versus the curvature of the interface using the values $\mu_i = 2$, $\mu_o = 10$, $Q = 10$, and $T = 1$. We see that for large values of the curvature, the flow is stable. For small values of the curvature, the flow is unstable, but there is a finite value of curvature for which the flow is most unstable. We can also see the effect of the curvature on the unstable band and

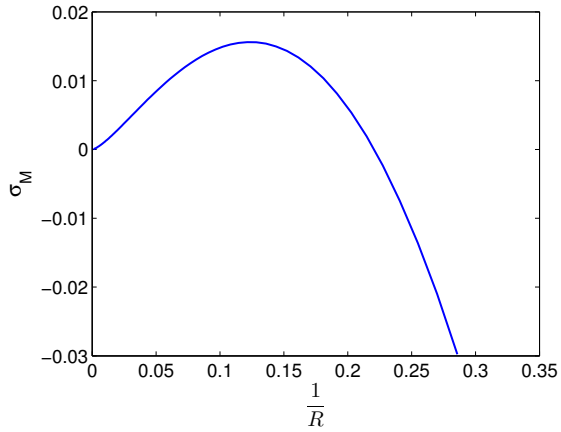

Figure 4.11: A plot of the maximum growth rate versus the curvature of the interface for two-layer flow. The parameter values are $\mu_i = 2$, $\mu_o = 10$, $Q = 10$, and $T = 1$.

n_m. Figure 4.12a shows the values of the two neutral wavenumbers and n_m versus R. As predicted by the expression for n_m above, we see that as the interface moves outward and the curvature decreases, n_m increases. Additionally, this is true for the maximum neutral wavenumber. This, combined with the fact that the minimum neutral wavenumber remains relatively fixed as R increases, means that the decrease in curvature results in an increase in the unstable bandwidth. To investigate the exact rate of this increase in n_m and the unstable bandwidth, we plot n_m and maximum neutral wavenumber against $\sqrt{R}$ in Figure 4.12b. Note that after an initial period, the growth of each of these values is linear. Therefore, when the interfaces are far from the origin, the unstable bandwidth and n_m increase proportional to $\sqrt{R}$.

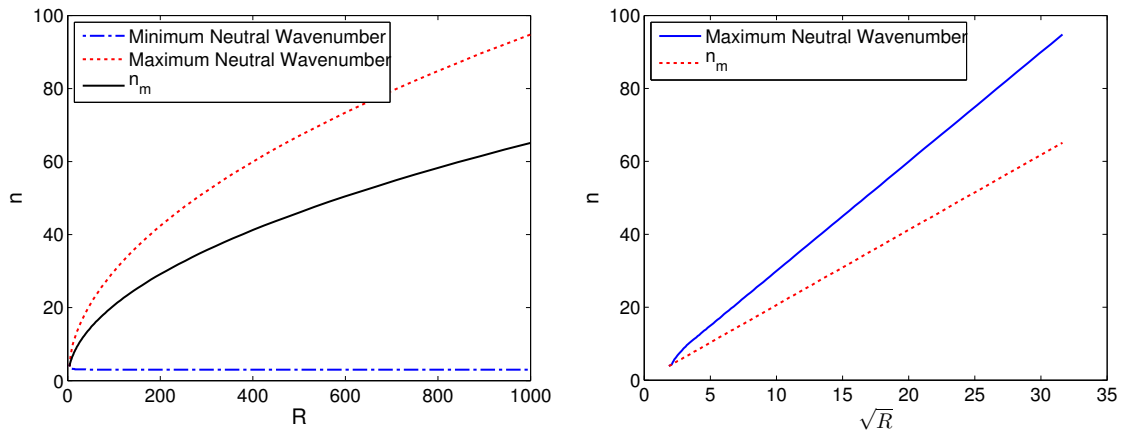

(a) (b)

Figure 4.12: (a) Plot of the neutral wavenumbers and most dangerous wavenumber, n_m, versus the radius of the interface for two-layer flow. (b) Plot of the maximum neutral wavenumber and most dangerous wavenumber, n_m, versus $\sqrt{R}$. The parameter values are $\mu_i = 2$, $\mu_o = 10$, $Q = 10$, and $T = 1$.

Next, we consider three-layer flow. We adjust the curvature of the inner interface

while preserving the area of the fluid region between the interfaces. This is consistent with the basic solution whose stability we are investigating. Therefore, as the curvature of the inner interface decreases, so does the curvature of the outer interface. For Figures 4.13 - 4.14b, we fix the area of the middle layer at 300π. We use viscosity $\mu_1 = 6$ for the middle layer and interfacial tension $T_0 = T_1 = 1$. As the interfaces move farther away from the origin, there are several factors at play. First, the curvature of each interface is reduced. Also, the distance between the interfaces decreases, resulting in greater interaction between the interfaces. Figure 4.13 shows σ_M versus the curvature of the inner interface. We see similar behavior to the two-layer case. As the curvature goes to zero, σ_M approaches zero. There is some finite value of curvature for which the flow is most unstable. When the curvature is large, the flow is stable. The primary difference occurs for large values of curvature. Recall that in the two-layer case, σ_M behaves like $-1/R^2$ in the large curvature limit. However, the curve in Figure 4.13 decays much more slowly for large values of curvature. This is due to the fact that the outer interface's curvature does not increase without bound. Therefore, it adds to the instability of the system as a whole. We also plot the neutral wavenumbers as well as n_m versus the position of the inner interface. This plot is in Figure 4.14a. As in two-layer flow, n_m and the maximum neutral wavenumber increase with R_0, while the minimum neutral wavenumber remains relatively constant. Figure 4.14b shows that as R_0 becomes large, the unstable bandwidth and n_m increase proportional to $\sqrt{R_0}$.

4.6 Conclusion

In this chapter, we investigate the instability of multi-layer radial Hele-Shaw flows in which each layer of fluid has a constant viscosity. We obtain the following key results.

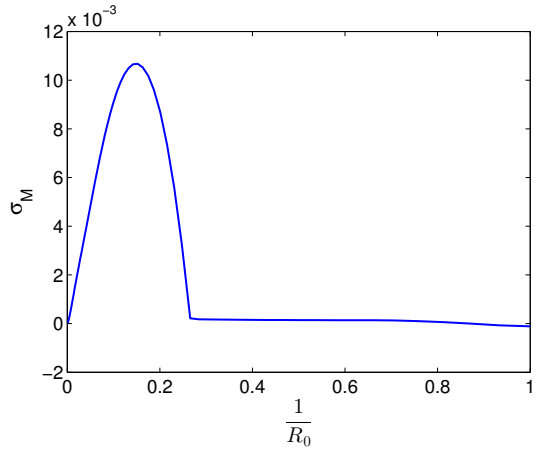

Figure 4.13: A plot of the maximum growth rate versus the curvature of the inner interface for three-layer flow. The parameter values are $\mu_i = 2$, $\mu_1 = 6$, $\mu_o = 10$, $Q = 10$, $T_0 = 1$ and $T_1 = 1$.

1. We provide a new formulation (see section 4.2) of the eigenvalue problem for two-layer radial Hele-Shaw flows. While previous formulations [8, 53, 60], which only treat restricted cases, make use of the potential function, the current formulation does not. The advantage of this approach is that it can be extended to flows with variable viscosity fluids, which is the subject of the next chapter. Our formulation is able to reproduce the results previously found with the potential function approach.

2. We perform linear stability analysis of the multi-layer radial flows and obtain the associated eigenvalue problem. We perform analysis on this eigenvalue problem and obtain some results, some of which are summarized below.

3. We give an exact expression for the growth rate, σ, for three-layer flows (see equation (4.26)). Unlike two-layer radial flow (see section 4.2) and multi-layer rectilinear flow (see [16]), σ can be complex for three-layer radial flow. We also investigate (see section 4.3.1) the thin-layer and thick-layer limit solutions. In

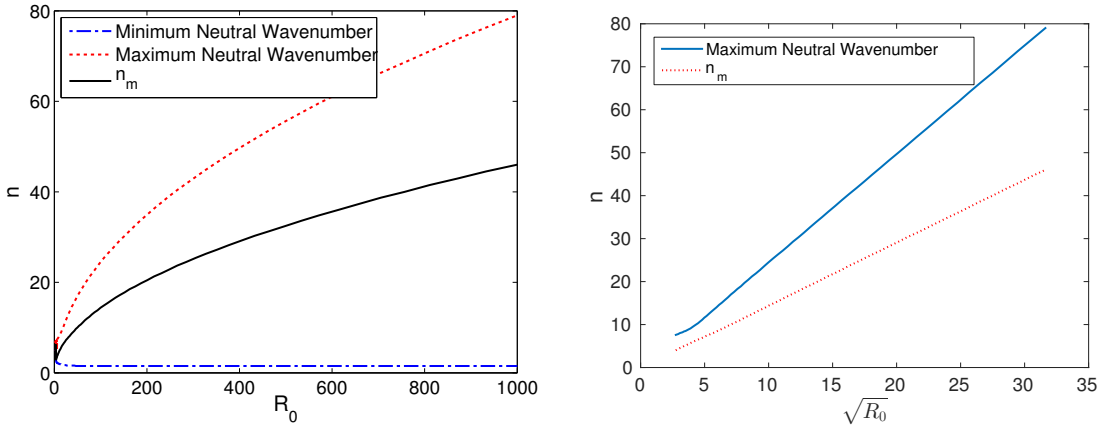

(a) (b)

Figure 4.14: (a) Plot of the neutral wavenumbers and most dangerous wavenumber, n_m, versus the radius of the inner interface for three-layer flow. (b) Plot of the maximum neutral wavenumber and most dangerous wavenumber, n_m, versus $\sqrt{R_0}$. The parameter values are $\mu_i = 2$, $\mu_1 = 6$, $\mu_o = 10$, $Q = 10$, $T_0 = 1$, and $T_1 = 1$.

the thick-layer limit, the two values of σ are simply the two-layer growth rates of each interface. When the width of the middle layer is small, the unstable growth rate coincides with the two-layer growth rate that comes from the innermost and outermost fluid, with interfacial tension that is the sum of the interfacial tensions of the two interfaces.

4. Upper bounds are found for the real part of σ, denoted by σ_R, of the three-layer flow (see equation (4.51)). The upper bounds depend on two parameters, λ_1 and λ_2. When both are zero, we are able to find exact expressions for the wavenumbers that maximize the terms in the upper bound. These wavenumbers are the same as that of the most dangerous wave for each of the two individual interfaces in the two-layer setting. The use of these wavenumbers allow us to find an absolute upper bound on σ_R. Additionally, we give values of interfacial tension (see equation (4.56)) that minimize the upper bounds and

can completely stabilize the flow. Their formulas coincide with the value of T_o in the two-layer setting (see section 4.2).

5. We extend the three-layer upper bounds to flows with an arbitrary number of fluid layers (see equation (4.68)). Using this upper bound, we are able to show that the use of many thin layers of fluid with sufficiently small positive jumps in viscosity (in the direction of the basic velocity) at the interfaces improves upon the upper bound for the three-layer case. This indicates that it is likely that the addition of many layers of fluid with slowly varying viscosities is a good strategy for stabilization of the flow.

6. We reproduce several old results as limiting cases of the expression for σ. In particular, we obtain the growth rate of rectilinear Hele-Shaw flows found by Daripa [16, 17]. We also show the result of Cardoso and Woods [8] by assuming that the inner interface is stable.

7. We numerically investigate the theoretical results for three-layer flows. We are able to validate the upper bounds and investigate the significance of the parameters λ_1 and λ_2. We also show that there are values of the middle layer viscosity that minimize both the instability of the most dangerous wave and the unstable bandwidth. We show that the flow is completely stable for large enough values of interfacial tension.

8. We investigate the effect of curvature on the system. It is well known that rectilinear flow is always unstable when less viscous fluids are driving more viscous fluids [16, 17]. This does not hold for radial flow in which the basic flow has curvature. We show that for large values of curvature, the flow is stable. The effect of curvature on the system is found to be non-monotonic, as

there is a finite value of curvature that maximizes the instability of the flow. As the interfaces move far away from the origin and the curvature goes to zero, σ_M goes to zero because the velocity of the interface goes to zero. This is consistent with two-layer flows as evident by equation (4.14).

5. STABILITY RESULTS FOR MULTI-LAYER RADIAL HELE-SHAW AND POROUS MEDIA FLOWS PART II: VARIABLE VISCOSITY

5.1 Introduction

We now turn our attention to three-layer radial Hele-Shaw flows in which the intermediate layer has variable viscosity. No previous stability analysis has been done for such flows. This work provides a significant step forward toward a more realistic model of chemical EOR flows near an injection or production well. The stability of variable viscosity fluids in rectilinear flows has been studied extensively (see [16, 20, 21, 24, 27, 28, 30, 41]). However, there are challenges for radial flow that are not present for rectilinear flow due to the time-dependence of the basic solution: namely, (i) the curvatures of the interfaces decrease with time; (ii) the thickness of the intermediate layer shrinks with time; and (iii) the viscous profile changes with time. In this chapter, we seek to overcome these challenges to provide a framework with which to study variable viscosity radial flows.

The following is an outline for this chapter. In section 5.2, we give a change of variables that allows us to formulate the eigenvalue problem which governs the growth rate of disturbances of the flow. In section 5.3, we use our newly found eigenvalue problem to investigate the simplified problem of constant viscosity fluid layers. In section 5.4, we calculate upper bounds for the growth rate which depend simply on the parameters of the problem. In section 5.5, we characterize the eigenvalues and eigenfunctions of the system. In section 5.6, we provide some numerical calculations of the growth rate. Finally, we conclude in section 5.7.

5.2 Derivation of the Stability Equations

We consider a radial Hele-Shaw flow consisting of three regions of incompressible, immiscible fluid. By averaging across the gap, we may consider a two-dimensional flow domain in polar coordinates, $\Omega := (r, \theta) = \mathbb{R}^2$. The least viscous fluid with constant viscosity μ_i is injected into the center of the cell at a constant injection rate, Q. The most viscous fluid, with constant viscosity μ_o, is the outermost fluid. The intermediate fluid has a smooth, axisymmetric viscous profile $\mu(r)$ where $\mu_i < \mu(r) < \mu_o$. The fluid flow is governed by the following equations

$$\nabla \cdot \mathbf{u} = 0, \qquad \nabla\, p = -\mu\, \mathbf{u}, \qquad \frac{\partial \mu}{\partial t} + \mathbf{u} \cdot \nabla \mu = 0, \qquad \text{for } r \neq 0. \tag{5.1}$$

The first equation $(5.1)_1$ is the continuity equation for incompressible flow, the second equation $(5.1)_2$ is Darcy's law [15], and the third equation $(5.1)_3$ is an advection equation for viscosity. We start with our fluids separated by circular interfaces with radii $R_1(0)$ and $R_2(0)$, where $R_1(t)$ and $R_2(t)$ are the positions of the interfaces at time t. This set-up is shown in Figure 5.1.

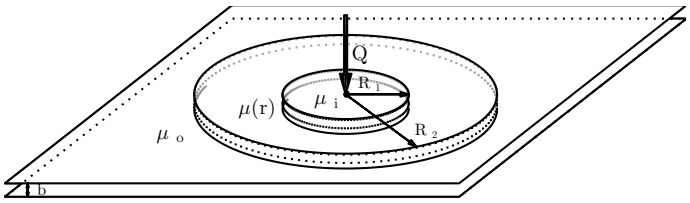

Figure 5.1: The basic solution for three-layer flow

The equations admit a simple basic solution in which all of the fluid moves outward radially with velocity $\mathbf{u} := (u_r, u_\theta) = (Q/(2\pi r), 0)$. The interfaces re-

main circular and their radii are given by $R_1(t) = \sqrt{Qt/\pi + R_1(0)^2}$ and $R_2(t) = \sqrt{Qt/\pi + R_2(0)^2}$. The pressure, $p_b = p_b(r)$, may be obtained by integrating equation $(5.1)_2$.

We define the quantity $R_0(t) = \sqrt{Qt/\pi}$. Note that for $i = 1, 2$,

$$R_i^2(t) = R_i^2(0) + R_0^2(t), \tag{5.2}$$

and therefore

$$R_i^2(0) = R_i^2(t) - R_0^2(t). \tag{5.3}$$

We define the following coordinate transformation:

$$\zeta = \frac{r^2 - R_0^2(t)}{R_2^2(t) - R_0^2(t)} = \frac{r^2 - R_0^2(t)}{R_2^2(0)}, \tag{5.4}$$

$$\alpha = \theta, \tag{5.5}$$

$$\tau = t. \tag{5.6}$$

Note that

$$\frac{dR_i(t)}{dt} = \frac{Q}{2\pi R_i(t)}. \tag{5.7}$$

For an arbitrary function $f(t, r, \theta)$,

$$\begin{aligned} \frac{\partial f}{\partial t} &= \frac{\partial f}{\partial \tau}\frac{\partial \tau}{\partial t} + \frac{\partial f}{\partial \zeta}\frac{\partial \zeta}{\partial t} + \frac{\partial f}{\partial \alpha}\frac{\partial \alpha}{\partial t} \\ &= \frac{\partial f}{\partial \tau} + \frac{\partial f}{\partial \zeta}\left(-\frac{2R_0(t)}{R_2^2(0)}\frac{dR_0(t)}{dt}\right) \\ &= \frac{\partial f}{\partial \tau} - \frac{Q}{\pi R_2^2(0)}\frac{\partial f}{\partial \zeta}. \end{aligned} \tag{5.8}$$

Likewise,

$$\begin{aligned}\frac{\partial f}{\partial r} &= \frac{\partial f}{\partial \tau}\frac{\partial \tau}{\partial r} + \frac{\partial f}{\partial \zeta}\frac{\partial \zeta}{\partial r} + \frac{\partial f}{\partial \alpha}\frac{\partial \alpha}{\partial r} \\ &= \frac{2r}{R_2^2(0)}\frac{\partial f}{\partial \zeta},\end{aligned} \tag{5.9}$$

and

$$\begin{aligned}\frac{\partial f}{\partial \theta} &= \frac{\partial f}{\partial \tau}\frac{\partial \tau}{\partial \theta} + \frac{\partial f}{\partial \zeta}\frac{\partial \zeta}{\partial \theta} + \frac{\partial f}{\partial \alpha}\frac{\partial \alpha}{\partial \theta} \\ &= \frac{\partial f}{\partial \alpha}.\end{aligned} \tag{5.10}$$

Therefore,

$$\begin{aligned}u_r = \frac{d}{dt}(r) &= \frac{d}{dt}\left(\sqrt{\zeta R_2^2(0) + R_0^2(t)}\right) \\ &= \left(\frac{1}{2\sqrt{\zeta R_2^2(0) + R_0^2(t)}}\right)\left(\frac{d\zeta}{dt}R_2^2(0) + \frac{dR_0^2(t)}{dt}\right) \\ &= \frac{1}{2r}\left(\frac{d\zeta}{d\tau}R_2^2(0) + \frac{Q}{\pi}\right) \\ &= \frac{R_2^2(0)}{2r}u_\zeta + \frac{Q}{2\pi r}.\end{aligned} \tag{5.11}$$

Also

$$\frac{u_\theta}{r} = \frac{d\theta}{dt} = \frac{\partial \theta}{\partial \tau}\frac{\partial \tau}{\partial t} + \frac{\partial \theta}{\partial \zeta}\frac{\partial \zeta}{\partial t} + \frac{\partial \theta}{\partial \alpha}\frac{\partial \alpha}{\partial t} = \frac{\partial \theta}{\partial \tau} = \frac{\partial \alpha}{\partial \tau},$$

and

$$\frac{u_\alpha}{\zeta} = \frac{d\alpha}{d\tau} = \frac{\partial \alpha}{\partial t}\frac{\partial t}{\partial \tau} + \frac{\partial \alpha}{\partial r}\frac{\partial r}{\partial \tau} + \frac{\partial \alpha}{\partial \theta}\frac{\partial \theta}{\partial \tau} = \frac{\partial \alpha}{\partial t} = \frac{\partial \alpha}{\partial \tau}.$$

Therefore,

$$\frac{u_\theta}{r} = \frac{u_\alpha}{\zeta}. \tag{5.12}$$

Now, we use (5.4) - (5.12) to investigate the nature of the governing system of equations (5.1) in the new coordinate system. In polar coordinates, $(5.1)_1$ is

$$\frac{\partial u_r}{\partial r} + \frac{u_r}{r} + \frac{1}{r}\frac{\partial u_\theta}{\partial \theta} = 0.$$

Using (5.10), (5.11), and (5.12),

$$\frac{\partial}{\partial r}\left(\frac{R_2^2(0)}{2r}u_\zeta + \frac{Q}{2\pi r}\right) + \frac{1}{r}\left(\frac{R_2^2(0)}{2r}u_\zeta + \frac{Q}{2\pi r}\right) + \frac{\partial}{\partial \alpha}\left(\frac{u_\alpha}{\zeta}\right) = 0.$$

Therefore,

$$-\frac{R_2^2(0)}{2r^2}u_\zeta + \frac{R_2^2(0)}{2r}\frac{\partial u_\zeta}{\partial r} - \frac{Q}{2\pi r^2} + \frac{R_2^2(0)}{2r^2}u_\zeta + \frac{Q}{2\pi r^2} + \frac{1}{\zeta}\frac{\partial u_\alpha}{\partial \alpha} = 0.$$

Canceling terms and using (5.9),

$$\frac{\partial u_\zeta}{\partial \zeta} + \frac{1}{\zeta}\frac{\partial u_\alpha}{\partial \alpha} = 0. \tag{5.13}$$

The r-coordinate of equation $(5.1)_2$ is

$$\frac{\partial p}{\partial r} = -\mu u_r.$$

Using (5.9) and (5.11),

$$\frac{2r}{R_2^2(0)}\frac{\partial p}{\partial \zeta} = -\mu\left(\frac{R_2^2(0)}{2r}u_\zeta + \frac{Q}{2\pi r}\right).$$

With some algebraic manipulation and using that $r^2 = \zeta R_2^2(0) + R_0^2(\tau)$,

$$\frac{\partial p}{\partial \zeta} = -\frac{R_2^4(0)}{4(\zeta R_2^2(0) + R_0^2(\tau))}\mu u_\zeta - \frac{QR_2^2(0)}{4\pi(\zeta R_2^2(0) + R_0^2(\tau))}\mu. \tag{5.14}$$

The θ-coordinate of equation $(5.1)_2$ is

$$\frac{1}{r}\frac{\partial p}{\partial \theta} = -\mu u_\theta.$$

Using (5.10) and (5.12),

$$\frac{1}{r}\frac{\partial p}{\partial \alpha} = -\mu\left(\frac{r}{\zeta}u_\alpha\right).$$

Therefore,

$$\frac{\partial p}{\partial \alpha} = -\frac{\zeta R_2^2(0) + R_0^2(\tau)}{\zeta}\mu u_\alpha. \tag{5.15}$$

Finally, equation $(5.1)_3$ is

$$\frac{\partial \mu}{\partial t} + u_r\frac{\partial \mu}{\partial r} + \frac{u_\theta}{r}\frac{\partial \mu}{\partial \theta} = 0.$$

Using (5.8) - (5.12),

$$\frac{\partial \mu}{\partial \tau} - \frac{Q}{\pi R_2^2(0)}\frac{\partial \mu}{\partial \zeta} + \left(\frac{R_2^2(0)}{2r}u_\zeta + \frac{Q}{2\pi r}\right)\left(\frac{2r}{R_2^2(0)}\frac{\partial \mu}{\partial \zeta}\right) + \frac{u_\alpha}{\zeta}\frac{\partial \mu}{\partial \alpha} = 0,$$

which simplifies to

$$\frac{\partial \mu}{\partial \tau} + u_\zeta\frac{\partial \mu}{\partial \zeta} + \frac{u_\alpha}{\zeta}\frac{\partial \mu}{\partial \alpha} = 0. \tag{5.16}$$

Combining equations (5.13) - (5.16), we get the transformed system

$$\left.\begin{array}{l} \frac{\partial u_\zeta}{\partial \zeta} + \frac{1}{\zeta}\frac{\partial u_\alpha}{\partial \alpha} = 0 \\ \frac{\partial p}{\partial \zeta} = -\frac{R_2^4(0)}{4(\zeta R_2^2(0)+R_0^2(\tau))}\mu u_\zeta - \frac{QR_2^2(0)}{4\pi(\zeta R_2^2(0)+R_0^2(\tau))}\mu \\ \frac{\partial p}{\partial \alpha} = -\frac{\zeta R_2^2(0)+R_0^2(\tau)}{\zeta}\mu u_\alpha \\ \frac{\partial \mu}{\partial \tau} + u_\zeta\frac{\partial \mu}{\partial \zeta} + \frac{u_\alpha}{\zeta}\frac{\partial \mu}{\partial \alpha} = 0. \end{array}\right\} \tag{5.17}$$

Using (5.11) and (5.12), the basic solution in these coordinates is $(u_\zeta, u_\alpha) = (0, 0)$

with the interfaces stationary at $\zeta = R_1^2(0)/R_2^2(0)$ and $\zeta = 1$. The pressure can be obtained by integrating $(5.17)_2$. By equation $(5.17)_4$, $\mu = \mu(\zeta)$ is now independent of time.

We perturb this steady basic solution $(u_\zeta = 0, u_\alpha = 0, p_b, \mu)$ by $(\tilde{u_\zeta}, \tilde{u_\alpha}, \tilde{p}, \tilde{\mu})$ where the disturbances are assumed to be small. Plugging this into $(5.17)_1$, we get

$$\frac{\partial \tilde{u_\zeta}}{\partial \zeta} + \frac{1}{\zeta}\frac{\partial \tilde{u_\alpha}}{\partial \alpha} = 0. \tag{5.18}$$

Plugging into $(5.17)_2$ gives

$$\frac{\partial p}{\partial \zeta} + \frac{\partial \tilde{p}}{\partial \zeta} = -\frac{R_2^4(0)}{4(\zeta R_2^2(0) + R_0^2(\tau))}(\mu + \tilde{\mu})\tilde{u_\zeta} - \frac{QR_2^2(0)}{4\pi(\zeta R_2^2(0) + R_0^2(\tau))}(\mu + \tilde{\mu}),$$

and therefore,

$$\frac{\partial \tilde{p}}{\partial \zeta} = -\frac{R_2^4(0)}{4(\zeta R_2^2(0) + R_0^2(\tau))}(\mu\tilde{u_\zeta} + \tilde{\mu}\tilde{u_\zeta}) - \frac{QR_2^2(0)}{4\pi(\zeta R_2^2(0) + R_0^2(\tau))}\tilde{\mu}.$$

Linearizing with respect to the disturbances yields

$$\frac{\partial \tilde{p}}{\partial \zeta} = -\frac{R_2^4(0)}{4(\zeta R_2^2(0) + R_0^2(\tau))}\mu\tilde{u_\zeta} - \frac{QR_2^2(0)}{4\pi(\zeta R_2^2(0) + R_0^2(\tau))}\tilde{\mu}. \tag{5.19}$$

Plugging into $(5.17)_3$ gives

$$\frac{\partial \tilde{p}}{\partial \alpha} = -\frac{\zeta R_2^2(0) + R_0^2(\tau)}{\zeta}(\mu + \tilde{\mu})\tilde{u_\alpha},$$

and the linearized equation is

$$\frac{\partial \tilde{p}}{\partial \alpha} = -\frac{\zeta R_2^2(0) + R_0^2(\tau)}{\zeta}\mu\tilde{u_\alpha}. \tag{5.20}$$

Plugging into $(5.17)_4$ gives

$$\frac{\partial \tilde{\mu}}{\partial \tau} + \tilde{u_\zeta}\left(\frac{\partial \mu}{\partial \zeta} + \frac{\partial \tilde{\mu}}{\partial \zeta}\right) + \frac{\tilde{u_\alpha}}{\zeta}\frac{\partial \tilde{\mu}}{\partial \alpha} = 0,$$

and the linearized equation is

$$\frac{\partial \tilde{\mu}}{\partial \tau} + \tilde{u_\zeta}\frac{\partial \mu}{\partial \zeta} = 0. \tag{5.21}$$

We use the method of normal modes and take the disturbances to be of the form

$$(\tilde{u_\zeta}, \tilde{u_\alpha}, \tilde{p}, \tilde{\mu}) = \big(f(\zeta), \tau(\zeta), \psi(\zeta), \phi(\zeta)\big)e^{in\alpha+\sigma\tau}. \tag{5.22}$$

Plugging this ansatz into equation (5.18), we get

$$f'(\zeta)e^{in\alpha+\sigma\tau} + \frac{in}{\zeta}\tau(\zeta)e^{in\alpha+\sigma\tau} = 0.$$

Therefore,

$$\tau(\zeta) = \frac{i}{n}\zeta f'(\zeta). \tag{5.23}$$

Using the ansatz in equation (5.20) yields

$$in\psi(\zeta)e^{in\alpha+\sigma\tau} = -\frac{\zeta R_2^2(0) + R_0^2(\tau)}{\zeta}\mu\tau(\zeta)e^{in\alpha+\sigma\tau}.$$

Replacing τ by (5.23) and solving for ψ,

$$\psi(\zeta) = -\frac{\mu}{n^2}\left(\zeta R_2^2(0) + R_0^2(\tau)\right) f'(\zeta). \tag{5.24}$$

Using the ansatz in equation (5.21) gives

$$\sigma\phi(\zeta)e^{in\alpha+\sigma\tau} + \frac{d\mu}{d\zeta}f(\zeta)e^{in\alpha+\sigma\tau} = 0.$$

Solving for ϕ,

$$\phi(\zeta) = -\frac{1}{\sigma}\frac{d\mu}{d\zeta}f(\zeta). \tag{5.25}$$

We now cross-differentiate equations (5.19) and (5.20). Equation (5.19) gives

$$\begin{aligned}\frac{\partial^2\tilde{p}}{\partial\zeta\partial\alpha} &= \frac{\partial}{\partial\alpha}\left\{-\frac{R_2^4(0)}{4(\zeta R_2^2(0)+R_0^2(\tau))}\mu\tilde{u_\zeta} - \frac{QR_2^2(0)}{4\pi(\zeta R_2^2(0)+R_0^2(\tau))}\tilde{\mu}\right\} \\ &= -\frac{R_2^4(0)}{4(\zeta R_2^2(0)+R_0^2(\tau))}\mu\frac{\partial\tilde{u_\zeta}}{\partial\alpha} - \frac{QR_2^2(0)}{4\pi(\zeta R_2^2(0)+R_0^2(\tau))}\frac{\partial\tilde{\mu}}{\partial\alpha}.\end{aligned} \tag{5.26}$$

Equation (5.20) gives

$$\begin{aligned}\frac{\partial^2\tilde{p}}{\partial\zeta\partial\alpha} &= \frac{\partial}{\partial\zeta}\left\{-\frac{\zeta R_2^2(0)+R_0^2(\tau)}{\zeta}\mu\tilde{u_\alpha}\right\} \\ &= \frac{\partial}{\partial\zeta}\left(-\frac{\zeta R_2^2(0)+R_0^2(\tau)}{\zeta}\right)\mu\tilde{u_\alpha} - \frac{\zeta R_2^2(0)+R_0^2(\tau)}{\zeta}\left(\frac{d\mu}{d\zeta}\tilde{u_\alpha} + \mu\frac{d\tilde{u_\alpha}}{d\zeta}\right) \\ &= -\frac{R_2^2(0)}{\zeta}\mu\tilde{u_\alpha} + \frac{\zeta R_2^2(0)+R_0^2(\tau)}{\zeta^2}\mu\tilde{u_\alpha} - \frac{\zeta R_2^2(0)+R_0^2(\tau)}{\zeta}\left(\frac{d\mu}{d\zeta}\tilde{u_\alpha} + \mu\frac{d\tilde{u_\alpha}}{d\zeta}\right).\end{aligned} \tag{5.27}$$

Therefore, by (5.26) and (5.27),

$$\begin{aligned}&-\frac{R_2^4(0)}{4(\zeta R_2^2(0)+R_0^2(\tau))}\mu\frac{\partial\tilde{u_\zeta}}{\partial\alpha} - \frac{QR_2^2(0)}{4\pi(\zeta R_2^2(0)+R_0^2(\tau))}\frac{\partial\tilde{\mu}}{\partial\alpha} \\ =&-\frac{R_2^2(0)}{\zeta}\mu\tilde{u_\alpha} + \frac{\zeta R_2^2(0)+R_0^2(\tau)}{\zeta}\left(\frac{\mu}{\zeta}\tilde{u_\alpha} - \frac{d\mu}{d\zeta}\tilde{u_\alpha} - \mu\frac{d\tilde{u_\alpha}}{d\zeta}\right).\end{aligned}$$

Using the ansatz (5.22),

$$\begin{aligned}
&-\frac{i\,R_2^4(0)}{4(\zeta R_2^2(0)+R_0^2(\tau))}\mu n f(\zeta)-\frac{i\,QR_2^2(0)}{4\pi(\zeta R_2^2(0)+R_0^2(\tau))}n\phi(\zeta)\\
=&-\frac{R_2^2(0)}{\zeta}\mu\tau(\zeta)+\frac{\zeta R_2^2(0)+R_0^2(\tau)}{\zeta}\left(\frac{\mu}{\zeta}\tau(\zeta)-\frac{d\mu}{d\zeta}\tau(\zeta)-\mu\tau'(\zeta)\right).
\end{aligned}$$

We can use (5.23) and (5.25) to replace $\tau(\zeta)$ and $\phi(\zeta)$ in this equation. In addition, by (5.23),

$$\tau'(\zeta)=\frac{i}{n}\zeta f''(\zeta)+\frac{i}{n}f'(\zeta).$$

Therefore,

$$\begin{aligned}
&-\frac{i\,R_2^4(0)}{4(\zeta R_2^2(0)+R_0^2(\tau))}\mu n f(\zeta)+\frac{1}{\sigma}\frac{d\mu}{d\zeta}\frac{i\,QR_2^2(0)}{4\pi(\zeta R_2^2(0)+R_0^2(\tau))}nf(\zeta)\\
=&-\frac{R_2^2(0)}{\zeta}\mu\frac{i}{n}\zeta f'(\zeta)\\
&+\frac{\zeta R_2^2(0)+R_0^2(\tau)}{\zeta}\left(\frac{\mu}{\zeta}\frac{i}{n}\zeta f'(\zeta)-\frac{d\mu}{d\zeta}\frac{i}{n}\zeta f'(\zeta)-\mu\frac{i}{n}\zeta f''(\zeta)-\mu\frac{i}{n}f'(\zeta)\right),
\end{aligned}$$

or

$$\begin{aligned}
&-\frac{R_2^4(0)}{4(\zeta R_2^2(0)+R_0^2(\tau))}\mu n^2 f(\zeta)+\frac{1}{\sigma}\frac{d\mu}{d\zeta}\frac{QR_2^2(0)}{4\pi(\zeta R_2^2(0)+R_0^2(\tau))}n^2f(\zeta)\\
=&-R_2^2(0)\mu f'(\zeta)-\left(\zeta R_2^2(0)+R_0^2(\tau)\right)\left(\frac{d\mu}{d\zeta}f'(\zeta)+\mu f''(\zeta)\right).
\end{aligned}$$

Rearranging terms, we have

$$\begin{aligned}
&\left(\zeta R_2^2(0)+R_0^2(\tau)\right)\mu f''(\zeta)+\left(\zeta R_2^2(0)+R_0^2(\tau)\right)\frac{d\mu}{d\zeta}f'(\zeta)+R_2^2(0)\mu f'(\zeta)\\
&-\frac{n^2R_2^4(0)}{4(\zeta R_2^2(0)+R_0^2(\tau))}\mu f(\zeta)+\frac{1}{\sigma}\frac{d\mu}{d\zeta}\frac{Qn^2R_2^2(0)}{4\pi(\zeta R_2^2(0)+R_0^2(\tau))}f(\zeta)=0,
\end{aligned}\tag{5.28}$$

or

$$\Big(\left(\zeta R_2^2(0) + R_0^2(\tau)\right) \mu f'(\zeta) \Big)' - \left(\frac{n^2 R_2^4(0)}{4(\zeta R_2^2(0) + R_0^2(\tau))} \right) \left(\mu - \frac{2}{\sigma} \frac{d\mu}{d\zeta} \frac{Q}{2\pi R_2^2(0)} \right) f(\zeta) = 0. \tag{5.29}$$

This defines the eigenvalue problem for the growth rate, σ. In the innermost and outermost layers, the viscosity is constant. In these regions, equation (5.29) becomes

$$\Big(\left(\zeta R_2^2(0) + R_0^2(\tau)\right) f'(\zeta) \Big)' - \left(\frac{n^2 R_2^4(0)}{4(\zeta R_2^2(0) + R_0^2(\tau))} \right) f(\zeta) = 0. \tag{5.30}$$

We seek solutions of the form $f(\zeta) = C \left(\sqrt{\zeta R_2^2(0) + R_0^2(\tau)} \right)^m$. Then

$$\begin{aligned} f'(\zeta) &= Cm \left(\sqrt{\zeta R_2^2(0) + R_0^2(\tau)} \right)^{m-1} \left(\frac{R_2^2(0)}{2\sqrt{\zeta R_2^2(0) + R_0^2(\tau)}} \right) \\ &= \frac{CmR_2^2(0)}{2} \left(\sqrt{\zeta R_2^2(0) + R_0^2(\tau)} \right)^{m-2}. \end{aligned}$$

Therefore

$$\left(\zeta R_2^2(0) + R_0^2(\tau)\right) f'(\zeta) = \frac{CmR_2^2(0)}{2} \left(\sqrt{\zeta R_2^2(0) + R_0^2(\tau)} \right)^m = \frac{mR_2^2(0)}{2} f(\zeta),$$

and using this equality,

$$\begin{aligned} \Big(\left(\zeta R_2^2(0) + R_0^2(\tau)\right) f'(\zeta) \Big)' &= \frac{mR_2^2(0)}{2} f'(\zeta) \\ &= \frac{m^2 R_4^2(0)}{4} C \left(\sqrt{\zeta R_2^2(0) + R_0^2(\tau)} \right)^{m-2} \\ &= \frac{m^2 R_4^2(0)}{4(\zeta R_2^2(0) + R_0^2(\tau))} f(\zeta). \end{aligned}$$

This satisfies (5.30) when $m^2 = n^2$ or $m = \pm n$. So the general solution of (5.30) is

$$f(\zeta) = C_1 \left(\zeta R_2^2(0) + R_0^2(\tau)\right)^{\frac{n}{2}} + C_2 \left(\zeta R_2^2(0) + R_0^2(\tau)\right)^{-\frac{n}{2}} \tag{5.31}$$

5.2.1 Interface Conditions

We now derive the interface conditions. In the original coordinates, we have two interface conditions: kinematic and dynamic. For an interface located at $r = \eta(\theta, t)$, the kinematic condition is given by

$$\frac{D\eta}{Dt} = u_r(r), \qquad r = \eta(\theta, t)$$

where D/Dt is the material derivative. Using the coordinate transformation (5.4), the interface in the new coordinates is located at $\zeta = \gamma(\alpha, \tau)$ where

$$\gamma = \frac{\eta^2 - R_0^2(t)}{R_2^2(0)},$$

or

$$\eta = \sqrt{\gamma R_2^2(0) + R_0^2(t)}.$$

Using (5.8),

$$\begin{aligned}
\frac{\partial \eta}{\partial t} &= \frac{\partial}{\partial \tau}\sqrt{\gamma R_2^2(0) + R_0^2(\tau)} \\
&= \frac{1}{2\sqrt{\gamma R_2^2(0) + R_0^2(\tau)}} \left(R_2^2(0)\frac{\partial \gamma}{\partial \tau} + \frac{\partial R_0^2}{\partial \tau} \right) \\
&= \frac{1}{2\sqrt{\gamma R_2^2(0) + R_0^2(\tau)}} \left(R_2^2(0)\frac{\partial \gamma}{\partial \tau} + \frac{Q}{\pi} \right).
\end{aligned}$$

Using (5.10),

$$\begin{aligned}\frac{\partial \eta}{\partial \theta} &= \frac{\partial}{\partial \alpha}\sqrt{\gamma R_2^2(0) + R_0^2(\tau)} \\ &= \frac{R_2^2(0)}{2\sqrt{\gamma R_2^2(0) + R_0^2(\tau)}}\frac{\partial \gamma}{\partial \alpha}.\end{aligned} \tag{5.32}$$

Also recall (5.11) and (5.12). Then the kinematic condition in the new coordinates is

$$\begin{aligned}&\frac{1}{2\sqrt{\gamma R_2^2(0) + R_0^2(\tau)}}\left(R_2^2(0)\frac{\partial \gamma}{\partial \tau} + \frac{Q}{\pi}\right) + \frac{u_\alpha}{\zeta}\frac{1}{2\sqrt{\gamma R_2^2(0) + R_0^2(\tau)}}\left(R_2^2(0)\frac{\partial \gamma}{\partial \alpha}\right) \\ =&\frac{R_2^2(0)}{2\sqrt{\gamma R_2^2(0) + R_0^2(\tau)}}u_\zeta + \frac{Q}{2\pi\sqrt{\gamma R_2^2(0) + R_0^2(\tau)}}.\end{aligned}$$

Simplifying,

$$\frac{D\gamma}{D\tau} = u_\zeta(\zeta), \qquad \zeta = \gamma(\alpha, \tau). \tag{5.33}$$

In the original coordinate system, the dynamic boundary condition is given by

$$p^+(r) - p^-(r) = -T\nabla \cdot \hat{n}, \qquad r = \eta(\theta, t)$$

where the superscripts "+" and "-" denote the limits from above and below, respectively, T denotes the interfacial tension between the fluids, and $\hat{n}$ denotes the unit normal vector. For the interface given by $r = \eta(\theta, t)$,

$$\hat{n} = \frac{(1, -\frac{1}{r}\frac{\partial \eta}{\partial \theta})}{\sqrt{1 + \left(\frac{1}{r}\frac{\partial \eta}{\partial \theta}\right)^2}} \tag{5.34}$$

Therefore,

$$\nabla \cdot \hat{n} = \frac{1}{r}\frac{\partial}{\partial r}\left(\frac{r}{\sqrt{1+\left(\frac{1}{r}\frac{\partial \eta}{\partial \theta}\right)^2}}\right) + \frac{1}{r}\frac{\partial}{\partial \theta}\left(-\frac{\frac{1}{r}\frac{\partial \eta}{\partial \theta}}{\sqrt{1+\left(\frac{1}{r}\frac{\partial \eta}{\partial \theta}\right)^2}}\right)$$
$$= \frac{1}{r}\left\{\frac{1}{\sqrt{1+\left(\frac{1}{r}\frac{\partial \eta}{\partial \theta}\right)^2}} + \frac{\frac{1}{r^2}\left(\frac{\partial \eta}{\partial \theta}\right)^2}{\left(1+\left(\frac{1}{r}\frac{\partial \eta}{\partial \theta}\right)^2\right)^{\frac{3}{2}}} - \frac{\frac{1}{r}\frac{\partial^2 \eta}{\partial \theta^2}}{\sqrt{1+\left(\frac{1}{r}\frac{\partial \eta}{\partial \theta}\right)^2}} + \frac{\frac{1}{r^2}\left(\frac{\partial \eta}{\partial \theta}\right)^2\frac{\partial^2 \eta}{\partial \theta^2}}{\left(1+\left(\frac{1}{r}\frac{\partial \eta}{\partial \theta}\right)^2\right)^{\frac{3}{2}}}\right\} \tag{5.35}$$

Taking a derivative of equation (5.32),

$$\frac{\partial^2 \eta}{\partial \theta^2} = \frac{\partial}{\partial \alpha}\left(\frac{R_2^2(0)}{2\sqrt{\gamma R_2^2(0)+R_0^2(\tau)}}\frac{\partial \gamma}{\partial \alpha}\right)$$
$$= \frac{R_2^2(0)}{2\sqrt{\gamma R_2^2(0)+R_0^2(\tau)}}\frac{\partial^2 \gamma}{\partial \alpha^2} - \frac{R_2^2(0)}{4(\gamma R_2^4(0)+R_0^2(\tau))^{3/2}}\left(\frac{\partial \gamma}{\partial \alpha}\right)^2. \tag{5.36}$$

Using (5.36) and (5.32) in (5.35),

$$\nabla \cdot \hat{n} = \frac{1}{\sqrt{\zeta R_2^2(0)+R_0^2(\tau)}}\left\{\frac{1}{\sqrt{1+\left(\frac{1}{\sqrt{\zeta R_2^2(0)+R_0^2(\tau)}}\frac{R_2^2(0)}{2\sqrt{\gamma R_2^2(0)+R_0^2(\tau)}}\frac{\partial \gamma}{\partial \alpha}\right)^2}}\right.$$
$$+\frac{\frac{1}{\zeta R_2^2(0)+R_0^2(\tau)}\left(\frac{R_2^2(0)}{2\sqrt{\gamma R_2^2(0)+R_0^2(\tau)}}\frac{\partial \gamma}{\partial \alpha}\right)^2}{\left(1+\left(\frac{1}{\sqrt{\zeta R_2^2(0)+R_0^2(\tau)}}\frac{R_2^2(0)}{2\sqrt{\gamma R_2^2(0)+R_0^2(\tau)}}\frac{\partial \gamma}{\partial \alpha}\right)^2\right)^{\frac{3}{2}}}$$
$$-\frac{\frac{1}{\sqrt{\zeta R_2^2(0)+R_0^2(\tau)}}\left(\frac{R_2^2(0)}{2\sqrt{\gamma R_2^2(0)+R_0^2(\tau)}}\frac{\partial^2 \gamma}{\partial \alpha^2} - \frac{R_2^2(0)}{4(\gamma R_2^4(0)+R_0^2(\tau))^{3/2}}\left(\frac{\partial \gamma}{\partial \alpha}\right)^2\right)}{\sqrt{1+\left(\frac{1}{\sqrt{\zeta R_2^2(0)+R_0^2(\tau)}}\frac{R_2^2(0)}{2\sqrt{\gamma R_2^2(0)+R_0^2(\tau)}}\frac{\partial \gamma}{\partial \alpha}\right)^2}}$$
$$\left.+\frac{\frac{1}{\zeta R_2^2(0)+R_0^2(\tau)}\left(\frac{R_2^2(0)}{2\sqrt{\gamma R_2^2(0)+R_0^2(\tau)}}\frac{\partial \gamma}{\partial \alpha}\right)^2\left(\frac{R_2^2(0)}{2\sqrt{\gamma R_2^2(0)+R_0^2(\tau)}}\frac{\partial^2 \gamma}{\partial \alpha^2} - \frac{R_2^2(0)}{4(\gamma R_2^4(0)+R_0^2(\tau))^{3/2}}\left(\frac{\partial \gamma}{\partial \alpha}\right)^2\right)}{\left(1+\left(\frac{1}{\sqrt{\zeta R_2^2(0)+R_0^2(\tau)}}\frac{R_2^2(0)}{2\sqrt{\gamma R_2^2(0)+R_0^2(\tau)}}\frac{\partial \gamma}{\partial \alpha}\right)^2\right)^{\frac{3}{2}}}\right\}. \tag{5.37}$$

Therefore, in the new coordinate system, the dynamic boundary condition is given by

$$p^+(\zeta) - p^-(\zeta) = -T\nabla \cdot \hat{n}, \qquad \zeta = \gamma(\alpha, \tau), \tag{5.38}$$

with $\nabla \cdot \hat{n}$ given by (5.37).

The basic solution has two circular interfaces. Let one of these interfaces be located at $r = R_*$ at time t. Then in the new coordinates, the interface is circular and located at $\zeta = \zeta_* := (R_*^2(\tau) - R_0^2(\tau))/R_2^2(0)$. We perturb this interface by some small quantity $\tilde{\gamma}(\alpha, \tau)$. Then $\gamma = \zeta_* + \tilde{\gamma}$, and

$$\frac{\partial \gamma}{\partial \tau} = \frac{\partial \tilde{\gamma}}{\partial \tau}, \qquad \frac{\partial \gamma}{\partial \alpha} = \frac{\partial \tilde{\gamma}}{\partial \alpha}.$$

Using these facts in equation (5.33),

$$\frac{\partial \tilde{\gamma}}{\partial \tau} + \frac{\tilde{u_\alpha}}{\zeta}\frac{\partial \tilde{\gamma}}{\partial \alpha} = \tilde{u_\zeta}(\zeta), \qquad \zeta = \zeta_* + \tilde{\gamma}(\alpha, \tau).$$

Up to linear approximation, this is

$$\frac{\partial \tilde{\gamma}}{\partial \tau} = \tilde{u_\zeta}(\zeta), \qquad \zeta = \zeta_*, \tag{5.39}$$

which is our linearized kinematic condition. For the dynamic boundary condition, we expand the pressure terms into Taylor series about $\zeta = \zeta_*$. Then

$$\begin{aligned} p^+(\zeta) &= p^+(\zeta_*) + \tilde{\gamma}\frac{\partial p^+}{\partial \zeta}(\zeta_*) + O(\tilde{\gamma}^2) \\ &= p_b^+(\zeta_*) + \tilde{p}^+(\zeta_*) + \tilde{\gamma}\frac{\partial p_b^+}{\partial \zeta}(\zeta_*) + \tilde{\gamma}\frac{\partial \tilde{p}^+}{\partial \zeta}(\zeta_*) + O(\tilde{\gamma}^2), \end{aligned}$$

where p_b is the pressure of the basic solution. After linearization,

$$p^+(\zeta) = p_b^+(\zeta_*) + \tilde{p}^+(\zeta_*) + \tilde{\gamma}\frac{\partial p_b^+}{\partial \zeta}(\zeta_*), \tag{5.40}$$

and similarly

$$p^-(\zeta) = p_b^-(\zeta_*) + \tilde{p}^-(\zeta_*) + \tilde{\gamma}\frac{\partial p_b^-}{\partial \zeta}(\zeta_*). \tag{5.41}$$

Plugging the basic solution into (5.38),

$$p_b^+(\zeta) - p_b^-(\zeta) = -\frac{T}{\sqrt{\zeta_* R_2^2(0) + R_0^2(\tau)}} = -\frac{T}{R_*(\tau)}. \tag{5.42}$$

Using $\gamma = \zeta_* + \tilde{\gamma}$ in (5.37) and linearizing about $\zeta = \zeta_*$,

$$\nabla \cdot \hat{n} = \left(\frac{1}{\sqrt{\zeta_* R_2^2(0) + R_0^2(\tau)}} - \tilde{\gamma}\frac{R_2^2(0)}{2(\zeta_* R_2^2(0) + R_0^2(\tau))^{3/2}}\right) \times \tag{5.43}$$

$$\left(1 - \frac{R_2^2(0)}{2(\zeta_* R_2^2(0) + R_0^2(\tau))}\frac{\partial^2 \tilde{\gamma}}{\partial \alpha^2}\right)$$

$$\approx \frac{1}{R_*(\tau)} - \tilde{\gamma}\frac{R_2^2(0)}{2R_*^3(\tau)} - \frac{R_2^2(0)}{2R_*^3(\tau)}\frac{\partial^2 \tilde{\gamma}}{\partial \alpha^2}. \tag{5.44}$$

Using equations (5.40) - (5.44) in (5.38),

$$\tilde{p}^+(\zeta_*) - \tilde{p}^-(\zeta_*) + \tilde{\gamma}\frac{\partial p_b^+}{\partial \zeta}(\zeta_*) - \tilde{\gamma}\frac{\partial p_b^-}{\partial \zeta}(\zeta_*) - \frac{T}{R_*(\tau)} = -\frac{T}{R_*(\tau)} + \tilde{\gamma}\frac{TR_2^2(0)}{2R_*^3(\tau)} + \frac{TR_2^2(0)}{2R_*^3(\tau)}\frac{\partial^2 \tilde{\gamma}}{\partial \alpha^2}.$$

Using the basic solution in $(5.17)_2$,

$$\frac{\partial p_b^+}{\partial \zeta}(\zeta_*) = -\frac{QR_2^2(0)}{4\pi R_*^2(\tau)}\mu^+(\zeta_*), \qquad \frac{\partial p_b^-}{\partial \zeta}(\zeta_*) = -\frac{QR_2^2(0)}{4\pi R_*^2(\tau)}\mu^-(\zeta_*).$$

Therefore,

$$\tilde{p}^+(\zeta_*) - \tilde{p}^-(\zeta_*) - \tilde{\gamma}\frac{QR_2^2(0)}{4\pi R_*^2(\tau)}\Big(\mu^+(\zeta_*) - \mu^-(\zeta_*)\Big) = T\frac{R_2^2(0)}{2R_*^3(\tau)}\left(\tilde{\gamma} + \frac{\partial^2\tilde{\gamma}}{\partial\alpha^2}\right).$$

Multiplying by $2R_*^2(\tau)/R_2^2(0)$, we arrive at the linearized dynamic boundary condition

$$\frac{2R_*^2(\tau)}{R_2^2(0)}\Big(\tilde{p}^+(\zeta_*) - \tilde{p}^-(\zeta_*)\Big) - \tilde{\gamma}\frac{Q}{2\pi}\Big(\mu^+(\zeta_*) - \mu^-(\zeta_*)\Big) = T\left(\frac{\tilde{\gamma} + \frac{\partial^2\tilde{\gamma}}{\partial\alpha^2}}{R_*(\tau)}\right). \tag{5.45}$$

Using the ansatz (5.22) in (5.39),

$$\frac{\partial\tilde{\gamma}}{\partial\tau} = f(\zeta_*)e^{in\alpha+\sigma\tau},$$

and therefore,

$$\tilde{\gamma} = \frac{f(\zeta_*)}{\sigma}e^{in\alpha+\sigma\tau}. \tag{5.46}$$

Using (5.22) and (5.24),

$$\begin{aligned}\tilde{p}^+(\zeta_*) &= -\frac{\mu^+(\zeta_*)}{n^2}\Big(\zeta_* R_2^2(0) + R_0^2(\tau)\Big)(f^+)'(\zeta_*)e^{in\alpha+\sigma\tau} \\ &= -\frac{R_*^2(\tau)}{n^2}\mu^+(\zeta_*)(f^+)'(\zeta_*)e^{in\alpha+\sigma\tau}.\end{aligned} \tag{5.47}$$

Likewise,

$$\tilde{p}^-(\zeta_*) = -\frac{R_*^2(\tau)}{n^2}\mu^-(\zeta_*)(f^-)'(\zeta_*)e^{in\alpha+\sigma\tau}. \tag{5.48}$$

Using (5.46) - (5.48) in (5.45),

$$\begin{aligned}&\frac{2R_*^4(\tau)}{n^2R_2^2(0)}\left(-\mu^+(\zeta_*)(f^+)'(\zeta_*)+\mu^-(\zeta_*)(f^-)'(\zeta_*)\right)-\frac{Q}{2\pi}\Big(\mu^+(\zeta_*)-\mu^-(\zeta_*)\Big)\frac{f(\zeta_*)}{\sigma}\\ =&T\left(\frac{1-n^2}{R_*(\tau)}\right)\frac{f(\zeta_*)}{\sigma}.\end{aligned}$$

With some algebraic manipulation,

$$\begin{aligned}&\frac{2R_*^4(\tau)}{R_2^2(0)}\Big(-\mu^+(\zeta_*)(f^+)'(\zeta_*)+\mu^-(\zeta_*)(f^-)'(\zeta_*)\Big)\\ =&\left(\frac{Qn^2}{2\pi}\Big(\mu^+(\zeta_*)-\mu^-(\zeta_*)\Big)-T\frac{n^4-n^2}{R_*(\tau)}\right)\frac{f(\zeta_*)}{\sigma}.\end{aligned}\tag{5.49}$$

This is the boundary condition at each interface for the eigenvalue problem (5.29). We may now evaluate this condition at each of the two interfaces. For the inner interface, $\zeta_* = R_1^2(0)/R_2^2(0)$. We denote this value by ζ_1. Also, $R_* = R_1$ and $\mu^-(\zeta_1) = \mu_i$. We denote the interfacial tension by T_1. Then (5.49) becomes

$$\begin{aligned}&\frac{2R_1^4(\tau)}{R_2^2(0)}\Big(-\mu^+(\zeta_1)(f^+)'(\zeta_1)+\mu_i(f^-)'(\zeta_1)\Big)\\ =&\left(\frac{Qn^2}{2\pi}\Big(\mu^+(\zeta_1)-\mu_i\Big)-T_1\frac{n^4-n^2}{R_1(\tau)}\right)\frac{f(\zeta_1)}{\sigma}.\end{aligned}\tag{5.50}$$

When $\zeta < \zeta_1$, the viscosity is constant. Recall that the general form of $f(\zeta)$ in this region is given by (5.31). When $\tau = 0$, in order to avoid a singularity when $\zeta \to 0$, f must be of the form

$$f(\zeta) = C_1(\zeta R_2^2(0) + R_0^2(\tau))^{\frac{n}{2}}.$$

We assume this also to be true for $\tau > 0$. Then

$$f'(\zeta) = C_1\frac{n}{2}(\zeta R_2^2(0) + R_0^2(\tau))^{\frac{n}{2}-1}R_2^2(0) = \frac{nR_2^2(0)}{2(\zeta R_2^2(0) + R_0^2(\tau))}f(\zeta),$$

and therefore,

$$(f^-)'(\zeta_1) = \frac{nR_2^2(0)}{2R_1^2(\tau)} f(\zeta_1). \tag{5.51}$$

Using (5.51) in (5.50),

$$\begin{aligned} &- \frac{2R_1^4(\tau)}{R_2^2(0)}\mu^+(\zeta_1)(f^+)'(\zeta_1) + nR_1^2(\tau)\mu_i f(\zeta_1) \\ &= \left(\frac{Qn^2}{2\pi}\Big(\mu^+(\zeta_1) - \mu_i\Big) - T_1\frac{n^4 - n^2}{R_1(\tau)}\right)\frac{f(\zeta_1)}{\sigma}. \end{aligned}$$

Therefore,

$$\frac{2R_1^4(\tau)}{R_2^2(0)}\mu^+(\zeta_1)(f^+)'(\zeta_1) = \left(nR_1^2(\tau)\mu_i - \frac{E_1}{\sigma}\right) f(\zeta_1), \tag{5.52}$$

where

$$E_1 = \frac{Qn^2}{2\pi}\Big(\mu^+(\zeta_1) - \mu_i\Big) - T_1\frac{n^4 - n^2}{R_1(\tau)}. \tag{5.53}$$

For the outer interface, $\zeta_* = 1$, $R_* = R_2$, and $\mu^+(1) = \mu_o$. We denote the interfacial tension by T_2. Then

$$\frac{2R_2^4(\tau)}{R_2^2(0)}\Big(- \mu_o(f^+)'(1) + \mu^-(1)(f^-)'(1)\Big) = \left(\frac{Qn^2}{2\pi}\Big(\mu_o - \mu^-(1)\Big) - T_2\frac{n^4 - n^2}{R_2(\tau)}\right)\frac{f(1)}{\sigma}. \tag{5.54}$$

When $\zeta > 1$, the viscosity is constant. In order for the disturbances to decay as $\zeta \to \infty$, f must be of the form

$$f(\zeta) = C_2(\zeta R_2^2(0) + R_0^2(\tau))^{-\frac{n}{2}}.$$

Then

$$f'(\zeta) = -\frac{nR_2^2(0)}{2(\zeta R_2^2(0) + R_0^2(\tau))} f(\zeta),$$

and therefore,

$$(f^+)'(1) = -\frac{nR_2^2(0)}{2R_2^2(\tau)} f(1). \tag{5.55}$$

Using (5.55) in (5.54),

$$\frac{2R_2^4(\tau)}{R_2^2(0)}\mu^-(1)(f^-)'(1) + nR_2^2(\tau)\mu_o f(1) = \left(\frac{Qn^2}{2\pi}\Big(\mu_o - \mu^-(1)\Big) - T_2\frac{n^4-n^2}{R_2(\tau)}\right)\frac{f(1)}{\sigma}.$$

Therefore,

$$-\frac{2R_2^4(\tau)}{R_2^2(0)}\mu^-(1)(f^-)'(1) = \left(nR_2^2(\tau)\mu_o - \frac{E_2}{\sigma}\right) f(1), \tag{5.56}$$

where

$$E_2 = \frac{Qn^2}{2\pi}\Big(\mu_o - \mu^-(1)\Big) - T_2\frac{n^4-n^2}{R_2(\tau)}. \tag{5.57}$$

The eigenvalue problem which governs the growth of the disturbances is given by the system (5.29), (5.52), and (5.56) which we recall here

$$\left.\begin{array}{l} \Big(\left(\zeta R_2^2(0) + R_0^2(\tau)\right)\mu f'(\zeta)\Big)' - \left(\frac{n^2R_2^4(0)}{4(\zeta R_2^2(0)+R_0^2(\tau))}\right)\left(\mu - \frac{2}{\sigma}\frac{d\mu}{d\zeta}\frac{Q}{2\pi R_2^2(0)}\right) f(\zeta) = 0, \\ \frac{2R_1^4(\tau)}{R_2^2(0)}\mu(\zeta_1)f'(\zeta_1) = \left(nR_1^2(\tau)\mu_i - \frac{E_1}{\sigma}\right) f(\zeta_1), \\ -\frac{2R_2^4(\tau)}{R_2^2(0)}\mu(1)f'(1) = \left(nR_2^2(\tau)\mu_o - \frac{E_2}{\sigma}\right) f(1), \end{array}\right\}$$

where we have dropped the superscripts "+" and "-".

5.3 Constant Viscosity Fluids

We now investigate the case where all fluids have constant viscosity. We begin by considering two-layer flows.

5.3.1 Two-layer Flow

When there are only two fluids (i.e. one interface located at $r = R(t)$), the above analysis holds with the coordinate transformation

$$\zeta = \frac{r^2 - R_0^2(t)}{R^2(0)}.$$

In the new coordinates, the basic solution has the interface fixed at $\zeta = 1$. Let μ_i denote the viscosity of the inner fluid and μ_o denote the viscosity of the outer fluid. The interface condition (5.49) still holds in this case. Also, similar to our derivation of the boundary conditions above,

$$f(\zeta) = C_1\Big(\zeta R^2(0) + R_0^2(\tau)\Big)^{\frac{n}{2}}, \qquad \zeta < 1,$$

and

$$f(\zeta) = C_2\Big(\zeta R^2(0) + R_0^2(\tau)\Big)^{-\frac{n}{2}}, \qquad \zeta > 1.$$

Therefore,

$$(f^-)'(1) = \frac{nR^2(0)}{2R^2(\tau)} f(1), \tag{5.58}$$

and

$$(f^+)'(1) = -\frac{nR^2(0)}{2R^2(\tau)} f(1). \tag{5.59}$$

Plugging (5.58) and (5.59) into (5.49),

$$nR^2(\tau)\Big(\mu_o + \mu_i\Big) f(1) = \left(\frac{Qn^2}{2\pi}\Big(\mu_o - \mu_i\Big) - T\frac{n^4 - n^2}{R(\tau)}\right)\frac{f(1)}{\sigma}.$$

Therefore,

$$\sigma = \frac{Qn}{2\pi R^2(\tau)}\frac{\mu_o - \mu_i}{\mu_i + \mu_o} - \frac{T}{\mu_i + \mu_o}\frac{n^3 - n}{R^3(\tau)}. \tag{5.60}$$

This gives the growth rate of the disturbance of the interface in the new coordinate system. This problem can be solved in the original (physical) coordinate system, and the result is a classic one [60]. We recall this result, which has been reproduced using our current notation in [40]. If we let $\sigma(r)$ denote the growth rate of the interface in the original coordinate system, then

$$\sigma(r) = \frac{Qn}{2\pi R^2(\tau)} \frac{\mu_o - \mu_i}{\mu_i + \mu_o} - \frac{T}{\mu_i + \mu_o} \frac{n^3 - n}{R^3(\tau)} - \frac{Q}{2\pi R^2(\tau)}. \tag{5.61}$$

Using $\sigma(\zeta)$ to denote the growth rate in the new coordinate system and comparing (5.60) and (5.61),

$$\sigma(r) = \sigma(\zeta) - \frac{Q}{2\pi R^2(\tau)}. \tag{5.62}$$

5.3.2 Three-layer Flow

We now return to three-layer flow, but consider the case in which the intermediate layer also has constant viscosity, μ. Then equation (5.29) becomes

$$\Big(\left(\zeta R_2^2(0) + R_0^2(\tau)\right) f'(\zeta) \Big)' - \frac{n^2 R_2^4(0)}{4(\zeta R_2^2(0) + R_0^2(\tau))} f(\zeta) = 0,$$

which, as mentioned above, has solutions of the form

$$f(\zeta) = C_1 \Big(\zeta R^2(0) + R_0^2(\tau) \Big)^{\frac{n}{2}} + C_2 \Big(\zeta R^2(0) + R_0^2(\tau) \Big)^{-\frac{n}{2}}. \tag{5.63}$$

Therefore,

$$f(\zeta_1) = C_1 R_1^n(\tau) + C_2 R_1^{-n}(\tau), \qquad f(1) = C_1 R_2^n(\tau) + C_2 R_2^{-n}(\tau). \tag{5.64}$$

Taking a derivative of (5.63),

$$\begin{aligned} f'(\zeta) =& C_1 \frac{nR_2^2(0)}{2(\zeta R_2^2(0) + R_0^2(\tau))} \left(\zeta R_2^2(0) + R_0^2(\tau)\right)^{\frac{n}{2}} \\ & - C_2 \frac{nR_2^2(0)}{2(\zeta R_2^2(0) + R_0^2(\tau))} \left(\zeta R_2^2(0) + R_0^2(\tau)\right)^{-\frac{n}{2}} \\ =& \frac{nR_2^2(0)}{2(\zeta R_2^2(0) + R_0^2(\tau))} \left\{ C_1 \left(\zeta R_2^2(0) + R_0^2(\tau)\right)^{\frac{n}{2}} - C_2 \left(\zeta R_2^2(0) + R_0^2(\tau)\right)^{-\frac{n}{2}} \right\}. \end{aligned}$$

Therefore,

$$f'(\zeta_1) = \frac{nR_2^2(0)}{2R_1^2(\tau)} \Big(C_1 R_1^n(\tau) - C_2 R_1^{-n}(\tau) \Big), \tag{5.65}$$

and

$$f'(1) = \frac{nR_2^2(0)}{2R_2^2(\tau)} \Big(C_1 R_2^n(\tau) - C_2 R_2^{-n}(\tau) \Big). \tag{5.66}$$

Plugging $(5.64)_1$ and (5.65) into the boundary condition (5.52),

$$nR_1^2(\tau)\mu \Big(C_1 R_1^n(\tau) - C_2 R_1^{-n}(\tau) \Big) = \left(nR_1^2(\tau)\mu_i - \frac{E_1}{\sigma} \right) \left(C_1 R_1^n(\tau) + C_2 R_1^{-n}(\tau) \right).$$

Therefore,

$$\Big(\sigma n R_1^2(\tau)(\mu - \mu_i) + E_1 \Big) R_1^n(\tau) C_1 + \Big(-\sigma n R_1^2(\tau)(\mu + \mu_i) + E_1 \Big) R_1^{-n}(\tau) C_2 = 0. \tag{5.67}$$

Plugging $(5.64)_2$ and (5.66) into the boundary condition (5.56),

$$-nR_2^2(\tau)\mu \Big(C_1 R_2^n(\tau) - C_2 R_2^{-n}(\tau) \Big) = \left(nR_2^2(\tau)\mu_o - \frac{E_2}{\sigma} \right) \left(C_1 R_2^n(\tau) + C_2 R_2^{-n}(\tau) \right).$$

Therefore,

$$\Big(-\sigma n R_2^2(\tau)(\mu_o + \mu) + E_2 \Big) R_2^n(\tau) C_1 + \Big(-\sigma n R_2^2(\tau)(\mu_o - \mu) + E_2 \Big) R_2^{-n}(\tau) C_2 = 0. \tag{5.68}$$

Together, equations (5.67) and (5.68) give a matrix equation of the form $\mathbf{Ax} = \mathbf{0}$ which has a nontrivial solution if and only if $\det(\mathbf{A}) = 0$. This condition is quadratic in σ, and therefore has two solutions.

5.4 Upper Bounds

To derive an upper bound on the growth rate, we take an inner product of (5.29) with f.

$$\int_{\zeta_1}^{1} \Big(\left(\zeta R_2^2(0) + R_0^2(\tau)\right) \mu(\zeta) f'(\zeta) \Big)' f^*(\zeta) d\zeta - \frac{n^2 R_2^4(0)}{4} \int_{\zeta_1}^{1} \frac{\mu(\zeta)}{\zeta R_2^2(0) + R_0^2(\tau)} |f(\zeta)|^2 d\zeta$$
$$+ \frac{n^2 R_2^2(0)}{2\sigma} \frac{Q}{2\pi} \int_{\zeta_1}^{1} \frac{\mu'(\zeta)}{\zeta R_2^2(0) + R_0^2(\tau)} |f(\zeta)|^2 d\zeta = 0.$$

Using integration by parts on the first term,

$$\left(\zeta R_2^2(0) + R_0^2(\tau)\right) \mu(\zeta) f'(\zeta) f^*(\zeta) \Big|_{\zeta_1}^{1} - \int_{\zeta_1}^{1} \left(\zeta R_2^2(0) + R_0^2(\tau)\right) \mu(\zeta) |f'(\zeta)|^2 d\zeta$$
$$- \frac{n^2 R_2^4(0)}{4} \int_{\zeta_1}^{1} \frac{\mu(\zeta)}{\zeta R_2^2(0) + R_0^2(\tau)} |f(\zeta)|^2 d\zeta$$
$$+ \frac{n^2 R_2^2(0)}{2\sigma} \frac{Q}{2\pi} \int_{\zeta_1}^{1} \frac{\mu'(\zeta)}{\zeta R_2^2(0) + R_0^2(\tau)} |f(\zeta)|^2 d\zeta = 0.$$

Using the boundary conditions (5.52) and (5.56),

$$\left(\zeta R_2^2(0) + R_0^2(\tau)\right) \mu(\zeta) f'(\zeta) f^*(\zeta) \Big|_{\zeta_1}^{1}$$
$$= R_2^2(\tau) \mu(1) f'(1) f^*(1) - R_1^2(\tau) \mu(\zeta_1) f'(\zeta_1) f^*(\zeta_1)$$
$$= - \frac{R_2^2(0)}{2R_2^2(\tau)} \left(n R_2^2(\tau) \mu_o - \frac{E_2}{\sigma} \right) |f(1)|^2 - \frac{R_2^2(0)}{2R_1^2(\tau)} \left(n R_1^2(\tau) \mu_i - \frac{E_1}{\sigma} \right) |f(\zeta_1)|^2.$$

Therefore,

$$
\begin{aligned}
&- \frac{R_2^2(0)}{2R_2^2(\tau)}\left(nR_2^2(\tau)\mu_o - \frac{E_2}{\sigma}\right)|f(1)|^2 - \frac{R_2^2(0)}{2R_1^2(\tau)}\left(nR_1^2(\tau)\mu_i - \frac{E_1}{\sigma}\right)|f(\zeta_1)|^2 \\
&- \int_{\zeta_1}^1 \left(\zeta R_2^2(0) + R_0^2(\tau)\right)\mu(\zeta)|f'(\zeta)|^2 d\zeta \\
&- \frac{n^2 R_2^4(0)}{4}\int_{\zeta_1}^1 \frac{\mu(\zeta)}{\zeta R_2^2(0) + R_0^2(\tau)}|f(\zeta)|^2 d\zeta \\
&+ \frac{n^2 R_2^2(0)}{2\sigma}\frac{Q}{2\pi}\int_{\zeta_1}^1 \frac{\mu'(\zeta)}{\zeta R_2^2(0) + R_0^2(\tau)}|f(\zeta)|^2 d\zeta = 0.
\end{aligned}
$$

With some algebraic manipulation,

$$
\begin{aligned}
&n\mu_o|f(1)|^2 + n\mu_i|f(\zeta_1)|^2 + \frac{2}{R_2^2(0)}\int_{\zeta_1}^1 \left(\zeta R_2^2(0) + R_0^2(\tau)\right)\mu(\zeta)|f'(\zeta)|^2 d\zeta \\
&+ \frac{n^2 R_2^2(0)}{2}\int_{\zeta_1}^1 \frac{\mu(\zeta)}{\zeta R_2^2(0) + R_0^2(\tau)}|f(\zeta)|^2 d\zeta \\
&= \frac{1}{\sigma}\left(\frac{E_2}{R_2^2(\tau)}|f(1)|^2 + \frac{E_1}{R_1^2(\tau)}|f(\zeta_1)|^2 + \frac{Qn^2}{2\pi}\int_{\zeta_1}^1 \frac{\mu'(\zeta)}{\zeta R_2^2(0) + R_0^2(\tau)}|f(\zeta)|^2 d\zeta\right),
\end{aligned}
$$

and therefore,

$$
\sigma = \frac{\frac{E_1}{R_1^2(\tau)}|f(\zeta_1)|^2 + \frac{E_2}{R_2^2(\tau)}|f(1)|^2 + \frac{Qn^2}{2\pi}I_1}{n\mu_i|f(\zeta_1)|^2 + n\mu_o|f(1)|^2 + \frac{2}{R_2^2(0)}I_2 + \frac{n^2 R_2^2(0)}{2}I_3}, \tag{5.69}
$$

where

$$
I_1 = \int_{\zeta_1}^1 \frac{\mu'(\zeta)}{\zeta R_2^2(0) + R_0^2(\tau)}|f(\zeta)|^2 d\zeta, \tag{5.70}
$$

$$
I_2 = \int_{\zeta_1}^1 \left(\zeta R_2^2(0) + R_0^2(\tau)\right)\mu(\zeta)|f'(\zeta)|^2 d\zeta, \tag{5.71}
$$

$$
I_3 = \int_{\zeta_1}^1 \frac{\mu(\zeta)}{\zeta R_2^2(0) + R_0^2(\tau)}|f(\zeta)|^2 d\zeta. \tag{5.72}
$$

Note that all terms in (5.69) are real. Therefore, σ **is real for all wavenumbers.**

When $\sigma > 0$, we may ignore the positive term containing I_2 in the denominator and get

$$\sigma < \frac{\frac{E_1}{R_1^2(\tau)}|f(\zeta_1)|^2 + \frac{E_2}{R_2^2(\tau)}|f(1)|^2 + \frac{Qn^2}{2\pi}I_1}{n\mu_i|f(\zeta_1)|^2 + n\mu_o|f(1)|^2 + \frac{n^2R_2^2(0)}{2}I_3},$$

We use the following inequality

$$\frac{\sum_{i=1}^{N} A_i X_i}{\sum_{i=1}^{N} B_i X_i} \leq \max_i \left\{ \frac{A_i}{B_i} \right\}.$$

which holds for any N if $A_i > 0$, $B_i > 0$, and $X_i > 0$ for all $i = 1, ..., N$. By using this inequality with $N = 3$, we get

$$\sigma < \max \left\{ \frac{E_1}{nR_1^2(\tau)\mu_i}, \frac{E_2}{nR_2^2(\tau)\mu_o}, \frac{Q}{\pi R_2^2(0)} \frac{I_1}{I_3} \right\}.$$

But

$$\frac{I_1}{I_3} = \frac{\int_{\zeta_1}^1 \frac{\mu'(\zeta)}{\zeta R_2^2(0)+R_0^2(\tau)}|f(\zeta)|^2 d\zeta}{\int_{\zeta_1}^1 \frac{\mu(\zeta)}{\zeta R_2^2(0)+R_0^2(\tau)}|f(\zeta)|^2 d\zeta} < \frac{\sup_{\zeta\in(\zeta_1,1)} \mu'(\zeta) \int_{\zeta_1}^1 \frac{1}{\zeta R_2^2(0)+R_0^2(\tau)}|f(\zeta)|^2 d\zeta}{\inf_{\zeta\in(\zeta_1,1)} \mu(\zeta) \int_{\zeta_1}^1 \frac{1}{\zeta R_2^2(0)+R_0^2(\tau)}|f(\zeta)|^2 d\zeta}$$
$$< \frac{\sup_{\zeta\in(\zeta_1,1)} \mu'(\zeta)}{\mu_i}.$$

Therefore,

$$\sigma < \max \left\{ \frac{E_1}{nR_1^2(\tau)\mu_i}, \frac{E_2}{nR_2^2(\tau)\mu_o}, \frac{Q}{\pi R_2^2(0)} \frac{1}{\mu_i} \sup_{\zeta\in(\zeta_1,1)} \mu'(\zeta) \right\}. \tag{5.73}$$

Using the definitions of E_1 and E_2 given by (5.53) and (5.57),

$$\sigma < \max\left\{ \frac{Qn}{2\pi R_1^2(\tau)}\left(\frac{\mu(\zeta_1)-\mu_i}{\mu_i}\right) - \frac{T_1}{\mu_i}\frac{n^3-n}{R_1^3(\tau)}, \right. \\ \left. \frac{Qn}{2\pi R_2^2(\tau)}\left(\frac{\mu_o-\mu(1)}{\mu_o}\right) - \frac{T_2}{\mu_o}\frac{n^3-n}{R_2^3(\tau)}, \frac{Q}{\pi R_2^2(0)}\frac{1}{\mu_i}\sup_{\zeta\in(\zeta_1,1)}\mu'(\zeta)\right\}, \tag{5.74}$$

which is the modal upper bound for a wave with wavenumber n. We can find an absolute upper bound for all wavenumbers by taking the maximum of the first two terms over all values of n. By taking the derivative and setting it equal to zero, we find that the first term reaches a maximum at

$$n = \sqrt{\frac{QR_1(\tau)}{6\pi T_1}(\mu(\zeta_1)-\mu_i)+\frac{1}{3}},$$

and the second term reaches a maximum at

$$n = \sqrt{\frac{QR_2(\tau)}{6\pi T_2}(\mu_o-\mu(1))+\frac{1}{3}}.$$

By plugging these into (5.74) and simplifying, we get the following absolute upper bound

$$\sigma < \max\left\{ \frac{2T_1}{\mu_i R_1^3(\tau)}\left(\frac{QR_1(\tau)}{6\pi T_1}(\mu(\zeta_1)-\mu_i)+\frac{1}{3}\right)^{\frac{3}{2}}, \right. \\ \left. \frac{2T_2}{\mu_o R_2^3(\tau)}\left(\frac{QR_2(\tau)}{6\pi T_2}(\mu_o-\mu(1))+\frac{1}{3}\right)^{\frac{3}{2}}, \frac{Q}{\pi R_2^2(0)}\frac{1}{\mu_i}\sup_{\zeta\in(\zeta_1,1)}\mu'(\zeta)\right\}. \tag{5.75}$$

5.5 Characterization of the Eigenvalues and Eigenfunctions

Recall that the eigenvalue problem is

$$\left.\begin{array}{l} \Big(\left(\zeta R_2^2(0) + R_0^2(\tau)\right) \mu f'(\zeta) \Big)' - \left(\frac{n^2 R_2^4(0)}{4(\zeta R_2^2(0) + R_0^2(\tau))} \right) \left(\mu - \frac{2}{\sigma} \frac{d\mu}{d\zeta} \frac{Q}{2\pi R_2^2(0)} \right) f(\zeta) = 0, \\ \frac{2R_1^4(\tau)}{R_2^2(0)} \mu(\zeta_1) f'(\zeta_1) = \left(n R_1^2(\tau) \mu_i - \frac{E_1}{\sigma} \right) f(\zeta_1), \\ -\frac{2R_2^4(\tau)}{R_2^2(0)} \mu(1) f'(1) = \left(n R_2^2(\tau) \mu_o - \frac{E_2}{\sigma} \right) f(1). \end{array}\right\}$$

Using $\lambda = 1/\sigma$ and rearranging terms,

$$\left.\begin{array}{l} \Big(\left(\zeta R_2^2(0) + R_0^2(\tau)\right) \mu f'(\zeta) \Big)' - \left(\frac{n^2 R_2^4(0)}{4(\zeta R_2^2(0) + R_0^2(\tau))} \mu - \frac{Q n^2 R_2^2(0)}{4\pi(\zeta R_2^2(0) + R_0^2(\tau))} \mu' \lambda \right) f(\zeta) = 0, \\ \left(n R_1^2(\tau) \mu_i - \lambda E_1 \right) f(\zeta_1) - \frac{2R_1^4(\tau)}{R_2^2(0)} \mu(\zeta_1) f'(\zeta_1) = 0, \\ \left(n R_2^2(\tau) \mu_o - \lambda E_2 \right) f(1) + \frac{2R_2^4(\tau)}{R_2^2(0)} \mu(1) f'(1) = 0. \end{array}\right\} \tag{5.76}$$

Note that E_1 and E_2 are positive for small values of n and negative for large values of n (see equations (5.53) and (5.57)). From the upper bound (5.73), we can see that as long as the viscous gradient $\mu'(\zeta)$ is not too large, the maximum value of σ will occur when E_1 and E_2 are positive. For this range of wavenumbers, we have the following characterization of the eigenvalues and eigenfunctions.

Theorem 4. *Let E_1, E_2, Q, n, μ_i, $\mu_o > 0$. Let $\mu(\zeta)$ be a positive, strictly increasing function in $C^1([\zeta_1, 1])$. Then the eigenvalue problem* (5.76) *has a countably infinite number of real eigenvalues that can be ordered*

$$0 < \lambda_0 < \lambda_1 < \lambda_2 < ...$$

with the property that for the corresponding eigenfunctions, $\{f_i\}_{i=0}^{\infty}$, f_i has exactly i zeros in the interval $(\zeta_1, 1)$. Additionally, the eigenfunctions are continuous with a continuous derivative.

Proof. The fact that there are a countably infinite number of real eigenvalues that can be

ordered and corresponding eigenfunctions with the prescribed number of zeros is proven by Ince [47, p. 232-233] in Theorem I and Theorem II using

$$
\begin{aligned}
&a = \zeta_1, \qquad b = 1, \qquad K(x,\lambda) = \left(xR_2^2(0) + R_0^2(\tau)\right)\mu(x),\\
&G(x,\lambda) = \frac{n^2 R_2^4(0)}{4(xR_2^2(0)+R_0^2(\tau))}\mu(x) - \frac{Qn^2R_2^2(0)}{4\pi(xR_2^2(0)+R_0^2(\tau))}\mu'(x)\lambda,\\
&\alpha = \frac{2R_1^4(\tau)}{R_2^2(0)}\mu(\zeta_1), \qquad \alpha' = nR_1^2(\tau)\mu_i - \lambda E_1,\\
&\beta = \frac{2R_2^4(\tau)}{R_2^2(0)}\mu(1), \qquad \beta' = nR_2^2(\tau)\mu_o - \lambda E_2.
\end{aligned}
$$

The regularity of the eigenfunctions comes from the existence theorem of Ince [47, p. 73]. We saw from equation (5.69) that σ is real for all n, and a closer look at each term in (5.69) shows that if $E_1, E_2 > 0$ and $\mu(\zeta), \mu'(\zeta) > 0$, then all terms are positive and $\sigma > 0$. □

5.5.1 Self-Adjointness and Expansion Theorem

We now rewrite equation (5.76) as

$$
\left.
\begin{aligned}
&-\Big(\left(\zeta R_2^2(0) + R_0^2(\tau)\right)\mu f'(\zeta)\Big)' + \left(\tfrac{n^2R_2^4(0)}{4(\zeta R_2^2(0)+R_0^2(\tau))}\right)\mu f(\zeta) = \tfrac{Qn^2R_2^2(0)}{4\pi(\zeta R_2^2(0)+R_0^2(\tau))}\mu'\lambda f(\zeta),\\
&-\left(-\tfrac{nR_1^2(\tau)\mu_i}{E_1}f(\zeta_1) + \tfrac{2R_1^4(\tau)}{R_2^2(0)E_1}\mu(\zeta_1)f'(\zeta_1)\right) = \lambda f(\zeta_1),\\
&-\left(-\tfrac{nR_2^2(\tau)\mu_o}{E_2}f(1) - \tfrac{2R_2^4(\tau)}{R_2^2(0)E_2}\mu(1)f'(1)\right) = \lambda f(1).
\end{aligned}
\right\} \tag{5.77}
$$

This is of the form

$$
\left.
\begin{aligned}
&Tf := \tfrac{1}{r}\left\{-\left(pf'\right)' + qf\right\} = \lambda f, && \zeta_1 < \zeta < 1,\\
&-\left(\beta_{11}f(\zeta_1) - \beta_{12}f'(\zeta_1)\right) = \lambda\left(\alpha_{11}f(\zeta_1) - \alpha_{12}f'(\zeta_1)\right),\\
&-\left(\beta_{21}f(1) - \beta_{22}f'(1)\right) = \lambda\left(\alpha_{21}f(1) - \alpha_{22}f'(1)\right),
\end{aligned}
\right\} \tag{5.78}
$$

where

$$
\begin{aligned}
&p(\zeta) = \left(\zeta R_2^2(0) + R_0^2(\tau)\right)\mu(\zeta),\\
&q(\zeta) = \tfrac{n^2 R_2^4(0)\mu(\zeta)}{4(\zeta R_2^2(0)+R_0^2(\tau))},\\
&r(\zeta) = \tfrac{Qn^2 R_2^2(0)\mu'(\zeta)}{4\pi(\zeta R_2^2(0)+R_0^2(\tau))},\\
&\beta_{11} = -\tfrac{nR_1^2(\tau)\mu_i}{E_1}, \qquad \beta_{12} = -\tfrac{2R_1^4(\tau)}{R_2^2(0)E_1}\mu(\zeta_1),\\
&\alpha_{11} = 1, \qquad \alpha_{12} = 0,\\
&\beta_{21} = -\tfrac{nR_2^2(\tau)\mu_o}{E_2}, \qquad \beta_{22} = \tfrac{2R_2^4(\tau)}{R_2^2(0)E_2}\mu(1),\\
&\alpha_{21} = 1, \qquad \alpha_{22} = 0.
\end{aligned}
\tag{5.79}
$$

Given the same assumptions as in Theorem 4, we have the following theorem from a paper by Walter [75].

Theorem 5. *Let E_1, E_2, Q, n, μ_i, $\mu_o > 0$. Let $\mu(\zeta)$ be a positive, strictly increasing function in $C^1([\zeta_1, 1])$. Let $p(\zeta)$, $q(\zeta)$, and $r(\zeta)$ be defined by* (5.79)*. Let*

$$
L_r^2(\zeta_1, 1) = \left\{ f(\zeta) \middle| \int_{\zeta_1}^1 |f(\zeta)|^2 r(\zeta) d\zeta < \infty \right\},
$$

and define the operator T on $L_r^2(\zeta_1, 1)$ by

$$
Tf := \frac{1}{r}\left\{ -(pf')' + qf \right\}.
$$

Define the measure:

$$
\nu(M) := \begin{cases} \frac{R_2^2(0)E_1}{2R_1^2(\tau)}, & \text{for } M = \{\zeta_1\} \\ \int_M r(\zeta) d\zeta, & \text{for } M \subset (\zeta_1, 1) \\ \frac{R_2^2(0)E_2}{2R_2^2(\tau)}, & \text{for } M = \{1\}. \end{cases}
\tag{5.80}
$$

We consider the Hilbert space $H := L^2([\zeta_1, 1]; \nu)$. Consider the operator A with

domain

$$D(A) = \{f \in H | f, f' \text{ absolutely continuous in } (\zeta_1, 1), Tf \in L^2_r(\zeta_1, 1)\}, \tag{5.81}$$

and defined by

$$(Af)(\zeta) = \begin{cases} \lim_{\zeta\to\zeta_1} \left(\frac{nR_1^2(\tau)\mu_i}{E_1} f(\zeta) - \frac{2R_1^4(\tau)}{R_2^2(0)E_1}\mu(\zeta_1)f'(\zeta) \right), & \text{if } \zeta = \{\zeta_1\} \\ (Tf)(\zeta), & \text{if } \zeta \in (\zeta_1, 1) \\ \lim_{\zeta\to 1} \left(\frac{nR_2^2(\tau)\mu_o}{E_2} f(\zeta) + \frac{2R_2^4(\tau)}{R_2^2(0)E_2}\mu(1)f'(\zeta) \right), & \text{if } \zeta = \{1\}. \end{cases} \tag{5.82}$$

Then (f, λ) *satisfies* (5.77) *if and only if* $Af = \lambda f$. *A is a self-adjoint operator on* H *and for any* $u \in H$,

$$u = \sum_{k=0}^{\infty} f_k \int_{\zeta_1}^{1} u(\zeta) f_k(\zeta) d\mu,$$

where the f_k *are the eigenfunctions of* A.

Sketch of proof :

The statement and proof of this theorem are given in Walter [75]. However, for the ease of the reader, we give a brief sketch here. Define

$$\begin{aligned} (f)_{\alpha_1} &= \lim_{\zeta\to\zeta_1} (\alpha_{11} f(\zeta) - \alpha_{12} f'(\zeta)), \qquad (f)_{\beta_1} = \lim_{\zeta\to\zeta_1} (\beta_{11} f(\zeta) - \beta_{12} f'(\zeta)), \\ (f)_{\alpha_2} &= \lim_{\zeta\to 1} (\alpha_{21} f(\zeta) - \alpha_{22} f'(\zeta)), \qquad (f)_{\beta_2} = \lim_{\zeta\to 1} (\beta_{21} f(\zeta) - \beta_{22} f'(\zeta)). \end{aligned} \tag{5.83}$$

Then our eigenvalue problem is

$$\left.\begin{aligned} &\tfrac{1}{r}\left\{-(pf')' + qf\right\} = \lambda f, \qquad \zeta_1 < \zeta < 1, \\ &-(f)_{\beta_1} = \lambda (f)_{\alpha_1}, \\ &-(f)_{\beta_2} = \lambda (f)_{\alpha_2}. \end{aligned}\right\} \tag{5.84}$$

Let

$$L_r^2(\zeta_1, 1) = \left\{ f(\zeta) \Big| \int_{\zeta_1}^1 |f(\zeta)|^2 r(\zeta) d\zeta < \infty \right\},$$

and $(\cdot, \cdot)_r$ denote its inner product. Then for $f, g \in C^2([\zeta_1, 1])$

$$\begin{aligned}
(Tf, g)_r =& \int_{\zeta_1}^1 \frac{1}{r} \left\{ -(pf')' + qf \right\} g^* r d\zeta \\
=& -\int_{\zeta_1}^1 (pf')' g^* + \int_{\zeta_1}^1 qfg^* d\zeta \\
=& -pf'g^* \Big|_{\zeta_1}^1 + \int_{\zeta_1}^1 pf'(g^*)' d\zeta + \int_{\zeta_1}^1 qfg^* d\zeta \\
=& -pf'g^* \Big|_{\zeta_1}^1 + pf(g^*)' \Big|_{\zeta_1}^1 - \int_{\zeta_1}^1 (p(g^*)')' f d\zeta + \int_{\zeta_1}^1 qfg^* d\zeta \\
=& (f, Tg)_r - \Big\{ p(1)[f'(1)g^*(1) - f(1)(g^*)'(1)] \\
& + p(\zeta_1)[f(\zeta_1)(g^*)'(\zeta_1) - f'(\zeta_1)g^*(\zeta_1)] \Big\}. \qquad (5.85)
\end{aligned}$$

But also for any $f, g \in C^2([\zeta_1, 1])$,

$$\begin{aligned}
(f)_{\alpha_1}(g^*)_{\beta_1} - (f)_{\beta_1}(g^*)_{\alpha_1} =& (\alpha_{11} f(\zeta_1) - \alpha_{12} f'(\zeta_1))(\beta_{11} g^*(\zeta_1) - \beta_{12}(g^*)'(\zeta_1)) \\
& - (\beta_{11} f(\zeta_1) - \beta_{12} f'(\zeta_1))(\alpha_{11} g^*(\zeta_1) - \alpha_{12}(g^*)'(\zeta_1)) \\
=& \alpha_{11}\beta_{11} f(\zeta_1) g^*(\zeta_1) - \alpha_{11}\beta_{12} f(\zeta_1)(g^*)'(\zeta_1) \\
& - \alpha_{12}\beta_{11} f'(\zeta_1) g^*(\zeta_1) + \alpha_{12}\beta_{12} f'(\zeta_1)(g^*)'(\zeta_1) \\
& - \alpha_{11}\beta_{11} f(\zeta_1) g^*(\zeta_1) + \alpha_{11}\beta_{12} f'(\zeta_1) g^*(\zeta_1) \\
& + \alpha_{12}\beta_{11} f(\zeta_1)(g^*)'(\zeta_1) - \alpha_{12}\beta_{12} f'(\zeta_1)(g^*)'(\zeta_1) \\
=& (\alpha_{12}\beta_{11} - \alpha_{11}\beta_{12})[f(\zeta_1)(g^*)'(\zeta_1) - f'(\zeta_1) g^*(\zeta_1)].
\end{aligned}$$

If we define $\delta_1 = \alpha_{12}\beta_{11} - \alpha_{11}\beta_{12}$, then

$$f(\zeta_1)(g^*)'(\zeta_1) - f'(\zeta_1)g^*(\zeta_1) = \frac{1}{\delta_1}\left[(f)_{\alpha_1}(g^*)_{\beta_1} - (f)_{\beta_1}(g^*)_{\alpha_1}\right]. \tag{5.86}$$

Following the same procedure, we get

$$f'(1)g^*(1) - f(1)(g^*)'(1) = \frac{1}{\delta_2}\left[(f)_{\alpha_2}(g^*)_{\beta_2} - (f)_{\beta_2}(g^*)_{\alpha_2}\right]. \tag{5.87}$$

where $\delta_2 = \alpha_{21}\beta_{22} - \alpha_{22}\beta_{21}$. Therefore, from (5.85) - (5.87)

$$\begin{aligned}&(Tf, g)_r \\ =&(f, Tg)_r - \left\{\frac{p(1)}{\delta_2}\left[(f)_{\alpha_2}(g^*)_{\beta_2} - (f)_{\beta_2}(g^*)_{\alpha_2}\right] + \frac{p(\zeta_1)}{\delta_1}\left[(f)_{\alpha_1}(g^*)_{\beta_1} - (f)_{\beta_1}(g^*)_{\alpha_1}\right]\right\},\end{aligned}$$

and

$$\begin{aligned}(Tf, g)_r - \frac{p(\zeta_1)}{\delta_1}(f)_{\beta_1}(g^*)_{\alpha_1} - \frac{p(1)}{\delta_2}(f)_{\beta_2}(g^*)_{\alpha_2} \\ =(f, Tg)_r - \frac{p(\zeta_1)}{\delta_1}(f)_{\alpha_1}(g^*)_{\beta_1} - \frac{p(1)}{\delta_2}(f)_{\alpha_2}(g^*)_{\beta_2}.\end{aligned} \tag{5.88}$$

We define the measure

$$\nu(M) := \begin{cases} \frac{p(\zeta_1)}{\delta_1}, & \text{for } M = \{\zeta_1\} \\ \int_M r d\zeta, & \text{for } M \subset (\zeta_1, 1) \\ \frac{p(1)}{\delta_2}, & \text{for } M = \{1\}. \end{cases} \tag{5.89}$$

We consider the Hilbert space $H := L^2([\zeta_1, 1]; \nu)$. Consider the operator A with domain

$$D(A) = \{f \in H | f, f' \text{ absolutely continuous in } (\zeta_1, 1), Tf \in L^2_r(\zeta_1, 1)\}, \tag{5.90}$$

and defined by

$$(Af)(\zeta) = \begin{cases} -(f)_{\beta_1}, & \text{if } \zeta = \{\zeta_1\} \\ (Tf)(\zeta), & \text{if } \zeta \in (\zeta_1, 1) \\ -(f)_{\beta_2}, & \text{if } \zeta = \{1\}. \end{cases} \tag{5.91}$$

Then (5.84) is given by $Af = \lambda f$. By (5.88), $[Af, g] = [f, Ag]$ where $[\cdot, \cdot]$ is the inner product in H.

5.5.2 Notes on the Assumptions

The above theorem holds assuming

$$p \in C^1([\zeta_1, 1]), \qquad q \in C^0([\zeta_1, 1]), \qquad r \in C^0([\zeta_1, 1]),$$

and $p(\zeta) > 0, r(\zeta) > 0$ for $\zeta \in [\zeta_1, 1]$. This is satisfied if

$$\mu(\zeta) \in C^1([\zeta_1, 1]), \qquad \mu'(\zeta) > 0. \tag{5.92}$$

Also, we need $\delta_i > 0$. But

$$\delta_1 = \alpha_{12}\beta_{11} - \alpha_{11}\beta_{12} = -\beta_{12} = \frac{2R_1^4(\tau)}{R_2^2(0)E_1}\mu(\zeta_1),$$

and

$$\delta_2 = \alpha_{21}\beta_{22} - \alpha_{22}\beta_{21} = \beta_{22} = \frac{2R_2^4(\tau)}{R_2^2(0)E_2}\mu(1)$$

Therefore, it holds when $E_1, E_2 > 0$, or

$$n < \min\left\{ \sqrt{\frac{QR_1(\tau)}{2\pi T_1}(\mu(\zeta_1) - \mu_i) + 1}, \sqrt{\frac{QR_2(\tau)}{2\pi T_2}(\mu_o - \mu(1)) + 1} \right\}. \tag{5.93}$$

5.5.3 Upper Bound from New Formulation

We now seek to derive some upper bounds from this new self-adjoint formulation of the problem. We find that this upper bound agrees with the one found previously in section 5.4. To begin, note that

$$\begin{aligned}
[Af, f] &= (Tf, f)_r - \frac{p(\zeta_1)}{\delta_1}(f)_{\beta_1}(f^*)_{\alpha_1} - \frac{p(1)}{\delta_2}(f)_{\beta_2}(f^*)_{\alpha_2} \\
&= \int_{\zeta_1}^1 \frac{1}{r}\left\{-(pf')' + qf\right\} f^* r d\zeta + \lambda\left(\frac{p(\zeta_1)}{\delta_1}|(f)_{\alpha_1}|^2 + \frac{p(1)}{\delta_2}|(f)_{\alpha_2}|^2\right) \\
&= -\int_{\zeta_1}^1 (pf')' f^* d\zeta + \int_{\zeta_1}^1 q|f|^2 d\zeta + \lambda\left(\frac{p(\zeta_1)}{\delta_1}|f(\zeta_1)|^2 + \frac{p(1)}{\delta_2}|f(1)|^2\right) \\
&= -pf'f^*\Big|_{\zeta_1}^1 + \int_{\zeta_1}^1 p|f'|^2 d\zeta + \int_{\zeta_1}^1 q|f|^2 d\zeta + \lambda\left(\frac{p(\zeta_1)}{\delta_1}|f(\zeta_1)|^2 + \frac{p(1)}{\delta_2}|f(1)|^2\right).
\end{aligned} \tag{5.94}$$

On the other hand,

$$[Af, f] = \lambda[f, f] = \lambda\left(\int_{\zeta_1}^1 |f|^2 r d\zeta + \frac{p(\zeta_1)}{\delta_1}|f(\zeta_1)|^2 + \frac{p(1)}{\delta_2}|f(1)|^2\right). \tag{5.95}$$

Combining (5.94) and (5.95), we get

$$-pf'f^*\Big|_{\zeta_1}^1 + \int_{\zeta_1}^1 p|f'|^2 d\zeta + \int_{\zeta_1}^1 q|f|^2 d\zeta = \lambda\int_{\zeta_1}^1 |f|^2 r d\zeta.$$

We now consider each of these terms. By the boundary conditions of (5.76),

$$\begin{aligned}
-pf'f^*\Big|_{\zeta_1}^1 =& -\left(\zeta R_2^2(0)+R_0^2(\tau)\right)\mu(\zeta)f'(\zeta)f^*(\zeta)\Big|_{\zeta_1}^1 \\
=& -R_2^2(\tau)\mu(1)f'(1)f^*(1)+R_1^2(\tau)\mu(\zeta_1)f'(\zeta_1)f^*(\zeta_1) \\
=& \frac{R_2^2(0)}{2R_2^2(\tau)}\left(nR_2^2(\tau)\mu_o-\lambda E_2\right)|f(1)|^2+\frac{R_2^2(0)}{2R_1^2(\tau)}\left(nR_1^2(\tau)\mu_i-\lambda E_1\right)|f(\zeta_1)|^2 \\
=& -\lambda\frac{R_2^2(0)}{2}\left\{\frac{E_1}{R_1^2(\tau)}|f(\zeta_1)|^2+\frac{E_2}{R_2^2(\tau)}|f(1)|^2\right\} \\
& +\frac{R_2^2(0)}{2}\left(n\mu_i|f(\zeta_1)|^2+n\mu_o|f(1)|^2\right).
\end{aligned}$$

Using (5.79) and (5.71),

$$\int_{\zeta_1}^1 p|f'|^2d\zeta=\int_{\zeta_1}^1\left(\zeta R_2^2(0)+R_0^2(\tau)\right)\mu(\zeta)|f'(\zeta)|^2d\zeta=I_2.$$

Likewise, using (5.79) and (5.72),

$$\int_{\zeta_1}^1 q|f|^2d\zeta=\int_{\zeta_1}^1\frac{n^2R_2^4(0)\mu(\zeta)}{4(\zeta R_2^2(0)+R_0^2(\tau))}|f(\zeta)|^2d\zeta=\frac{n^2R_2^4(0)}{4}I_3,$$

and using (5.70),

$$\int_{\zeta_1}^1|f|^2rd\zeta=\int_{\zeta_1}^1\frac{Qn^2R_2^2(0)\mu'(\zeta)}{4\pi(\zeta R_2^2(0)+R_0^2(\tau))}|f(\zeta)|^2d\zeta=\frac{Qn^2R_2^2(0)}{4\pi}I_1.$$

Combining these equalities,

$$\begin{aligned}
&-\lambda\frac{R_2^2(0)}{2}\left\{\frac{E_1}{R_1^2(\tau)}|f(\zeta_1)|^2+\frac{E_2}{R_2^2(\tau)}|f(1)|^2\right\}+\frac{R_2^2(0)}{2}\left(n\mu_i|f(\zeta_1)|^2+n\mu_o|f(1)|^2\right) \\
&+I_2+\frac{n^2R_2^4(0)}{4}I_3=\lambda\frac{Qn^2R_2^2(0)}{4\pi}I_1.
\end{aligned}$$

Multiplying by $2/R_2^2(0)$ and rearranging terms,

$$\lambda\left\{\frac{E_1}{R_1^2(\tau)}|f(\zeta_1)|^2+\frac{E_2}{R_2^2(\tau)}|f(1)|^2+\frac{Qn^2}{2\pi}I_1\right\}$$
$$=n\mu_i|f(\zeta_1)|^2+n\mu_o|f(1)|^2+\frac{2}{R_2^2(0)}I_2+\frac{n^2R_2^2(0)}{2}I_3.$$

Therefore,

$$\lambda=\frac{n\mu_i|f(\zeta_1)|^2+n\mu_o|f(1)|^2+\frac{2}{R_2^2(0)}I_2+\frac{n^2R_2^2(0)}{2}I_3}{\frac{E_1}{R_1^2(\tau)}|f(\zeta_1)|^2+\frac{E_2}{R_2^2(\tau)}|f(1)|^2+\frac{Qn^2}{2\pi}I_1}. \tag{5.96}$$

Considering that $\sigma=1/\lambda$, this agrees with (5.69) and will produce the same upper bounds.

5.6 Numerical Results

We now turn to some numerical results to investigate the behavior of the growth rate. We calculate the eigenvalues of (5.76) to find the values of λ and then invert those values to find σ. To calculate the eigenvalues, we use a pseudo-spectral Chebyshev method, the details of which can be found in chapter 6. We use the notation σ_{max} to denote the maximum growth rate, where the maximum is taken over all wavenumbers and all eigenvalues for each wavenumber. For consistency, we often use the same parameter values throughout our results. Unless otherwise stated, $\mu_i=2$, $\mu_o=10$, $T_0=T_1=1$, and $Q=10$.

5.6.1 Compare Two Growth Rates

First, we use some numerical results to get insight into the relationship between the growth rate of disturbances in our transformed coordinate system (which comes from (5.28)) and the growth rate of disturbances in the physical coordinate system.

Recall from (5.62) that for two-layer Hele-Shaw flow,

$$\sigma(r) = \sigma(\zeta) - \frac{Q}{2\pi R^2(\tau)}.$$

where $\sigma(\zeta)$ is the growth rate in the transformed coordinates and $\sigma(r)$ is the growth rate in the physical coordinates. We now wish to compare the two different growth rates for three-layer flows with constant viscosity. Recall from section 5.3.2 that $\sigma(\zeta)$ solves a quadratic equation. We use, consistent with chapter 4, the notation $\sigma^+(\zeta)$ and $\sigma^-(\zeta)$ to denote the two solutions, where $\sigma^+(\zeta) > \sigma^-(\zeta)$. From chapter 4, we know that $\sigma(r)$ also has two values for three-layer flow, which we denote by $\sigma^+(r)$ and $\sigma^-(r)$. The question becomes, how do $\sigma^+(\zeta)$ and $\sigma^-(\zeta)$ relate to $\sigma^+(r)$ and $\sigma^-(r)$?

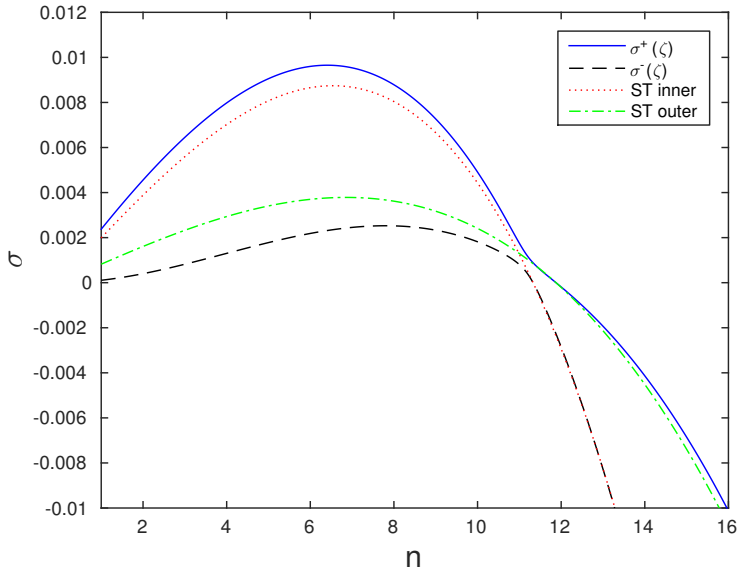

Figure 5.2: A plot of the two modes, σ^+ and σ^-, for three-layer constant viscosity radial Hele-Shaw flow, and the individual Saffman-Taylor growth rates of each interface.

For two-layer flows, the difference between the growth rates is $Q/(2\pi R^2)$ where R is the radius of the interface. Now, there are two interfaces with radii R_1 and R_2. Therefore, intuition may suggest that the difference will be either $Q/(2\pi R_1^2)$ or $Q/(2\pi R_2^2)$. In a sense, both of these are correct. To understand why, we first consider the relationship between $\sigma^+(\zeta)$ and $\sigma^-(\zeta)$ and the individual Saffman-Taylor growth rates of each interface (given by equation (5.60)). Figure 5.2 shows a plot of $\sigma^+(\zeta)$ and $\sigma^-(\zeta)$ as well as the individual Saffman-Taylor growth rates when $R_1 = 20$, $R_2 = 22$ and the viscosity of the intermediate layer is $\mu = 6$. Notice that $\sigma^+(\zeta)$ follows the shape of the interface whose Saffman-Taylor growth rate is larger. In this case, that is the inner interface for small n and the outer interface for large n. Conversely, $\sigma^-(\zeta)$ follows the shape of the interface whose Saffman-Taylor growth rate is smaller. Therefore, in the region where n is small, we can identify $\sigma^+(\zeta)$ with the inner interface and $\sigma^-(\zeta)$ with the outer interface. For large n, we can identify $\sigma^+(\zeta)$ with the outer interface and $\sigma^-(\zeta)$ with the inner interface.

In light of this comparison, we conclude that $\sigma^+(r) \approx \sigma^+(\zeta) - Q/(2\pi R_1^2)$ and $\sigma^-(r) \approx \sigma^-(\zeta) - Q/(2\pi R_2^2)$ for small n. Likewise, $\sigma^+(r) \approx \sigma^+(\zeta) - Q/(2\pi R_2^2)$ and $\sigma^-(r) \approx \sigma^-(\zeta) - Q/(2\pi R_1^2)$ for large n. These conclusions are justified by our numerical results in Figure 5.3.

5.6.2 Constant Viscosity Limit

Now that we understand the constant viscosity growth rate, we investigate the limit as a non-constant viscous profile approaches a constant viscous profile. For simplicity, we consider the case in which $\mu(r)$ is a linear function at time $t = 0$. Additionally, we take $R_1 = 20$ and $R_2 = 30$. For each of the viscous profiles considered, $\mu(R_1) = 5$. The dispersion relations for three different linear viscous profiles as well as a constant viscous profile $\mu \equiv 5$ are plotted in Figure 5.4a, where the value

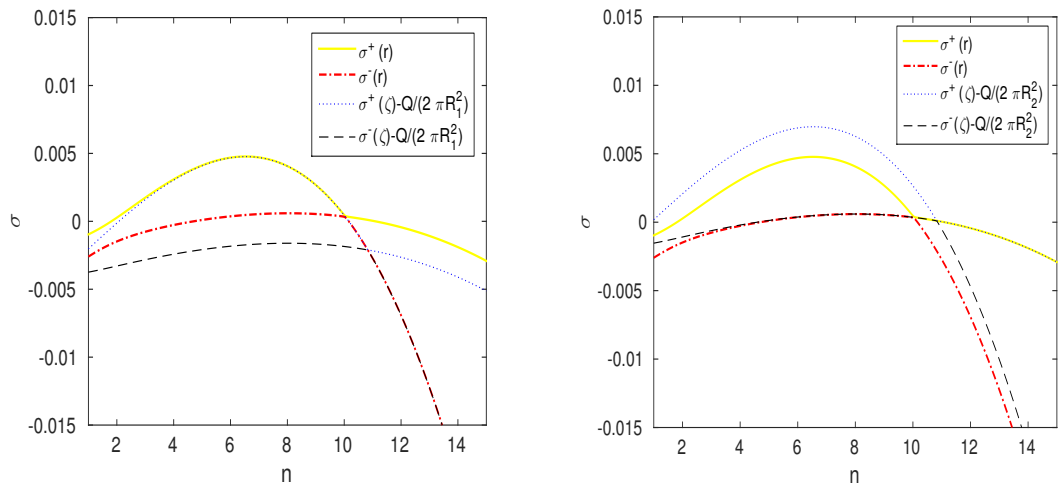

(a) (b)

Figure 5.3: Plots of the three-layer constant viscosity growth rates in the physical coordinate system ($\sigma^{\pm}(r)$) and the growth rates in the transformed coordinates minus the term (a) $Q/2\pi R_1^2$ and (b) $Q/2\pi R_1^2$.

of σ plotted is the maximum value over all eigenvalues. The corresponding viscous profiles are plotted in 5.4b.

We see from these figures that as $\mu(R_2)$ decreases to 5 (and hence a constant viscous profile), the curves approach the constant viscosity limit for small values of n. However, for large n, the growth rate is negative for the constant viscosity middle layer because interfacial tension stabilizes the disturbance of the interfaces. But for any variable viscous profile with positive gradient, the unstable intermediate layer causes the short waves to become unstable. Therefore, as the variable viscous profiles approach the constant viscous profile, $\sigma \to 0$ for large n.

5.6.3 Decay of σ Over Time

The main difference between radial and rectilinear flow is that the radial flow solution is time dependent. Hence, the growth rate is time dependent for radial flow. Therefore, it is important to study how σ changes with time. It is not immediately

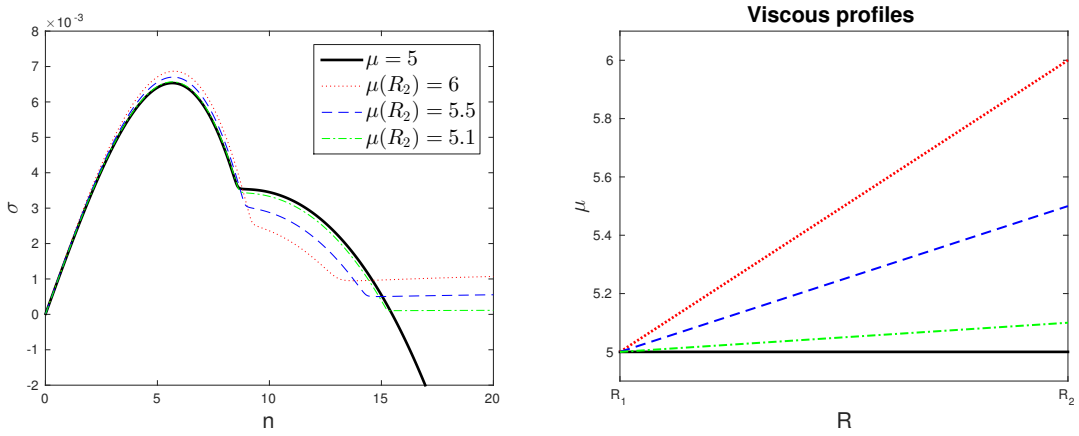

(a) (b)

Figure 5.4: (a) The dispersion relations for several different linear viscous profiles. (b) Plots of the viscous profiles of the intermediate layer as functions of r. The inner fluid has viscosity $\mu_l = 2$ and the outer fluid has viscosity $\mu_r = 10$.

clear intuitively what to expect. As time increases and the radii of the interfaces increase, several factors are at play. First, the curvatures of the interfaces decrease, which works to destabilize the flow. Second, the interfaces move more slowly, which works to stabilize the flow. These factors result in a non-monotonic change in the growth rate for constant viscosity radial flows in the physical coordinates, $\sigma(r)$ (see section 4.5.4). For variable viscosity flows, another important factor is that the length of the intermediate layer $(R_2 - R_1)$ decreases, causing the viscous gradient to increase. This also works to destabilize the flow.

However, the growth rate in the transformed coordinates behaves differently. We can see it analytically for two- layer constant viscosity flows. Recall that the growth rate is given by

$$\sigma = \frac{Qn}{2\pi R^2}\frac{\mu_o - \mu_i}{\mu_i + \mu_o} - \frac{T}{\mu_i + \mu_o}\frac{n^3 - n}{R^3}.$$

By taking a derivative with respect to n and setting equal to zero, we get that the

most dangerous wave is given by

$$n_{max} = \sqrt{\frac{QR}{6\pi T}(\mu_o - \mu_i) + \frac{1}{3}}, \tag{5.97}$$

and the growth rate of this wave is

$$\begin{aligned}\sigma_{max} =& \frac{Q}{2\pi R^2}\sqrt{\frac{QR}{6\pi T}(\mu_o - \mu_i) + \frac{1}{3}}\left(\frac{\mu_o - \mu_i}{\mu_i + \mu_o}\right) \\ &- \frac{T}{\mu_i + \mu_o}\sqrt{\frac{QR}{6\pi T}(\mu_o - \mu_i) + \frac{1}{3}}\left(\frac{QR}{6\pi T}(\mu_o - \mu_i) - \frac{2}{3}\right)\frac{1}{R^3}.\end{aligned} \tag{5.98}$$

We can take a derivative of this expression with respect to R. After simplifying,

$$\frac{\partial \sigma_{max}}{\partial R} = -\frac{T\left(\frac{Q}{\pi T}(\mu_o - \mu_i)R + 2\right)\left(\frac{Q}{\pi T}(\mu_o - \mu_i)R + 4\right)}{12R^4(\mu_i + \mu_o)n_{max}}, \tag{5.99}$$

and this expression will be negative for all $R > 0$ if $\mu_o > \mu_i$. Therefore, σ_{max} is a strictly decreasing function of R in the transformed coordinates. The upper bound (5.73) gives us reason to believe that the same is true for three-layer variable viscosity flows. For convenience, we recall this upper bound below:

$$\sigma < \max\left\{\frac{E_1}{nR_1^2(\tau)\mu_i}, \frac{E_2}{nR_2^2(\tau)\mu_o}, \frac{Q}{\pi R_2^2(0)}\frac{1}{\mu_i}\sup_{\zeta\in(\zeta_1,1)}\mu'(\zeta)\right\},$$

where

$$E_1 = \frac{Qn^2}{2\pi}\Big(\mu(\zeta_1) - \mu_i\Big) - T_1\frac{n^4 - n^2}{R_1(\tau)}, \tag{5.100}$$

and

$$E_2 = \frac{Qn^2}{2\pi}\Big(\mu_o - \mu(1)\Big) - T_2\frac{n^4 - n^2}{R_2(\tau)}. \tag{5.101}$$

Note that the first two terms of the upper bound are of the same form as the two-layer growth rate (4.14) . Therefore, by an identical analysis to that done above, the

first two terms are decreasing functions of R_1 and R_2, respectively. The last term in the upper bound is independent of the radii (and therefore time). So the upper bound is a decreasing function of time. Numerical results verify that the maximum growth rate of three-layer variable viscosity flows is a decreasing function of time. As an example, we plotted the dispersion relation at several different times for a flow with $\mu(R_1) = 5$, $\mu(R_2) = 6$, $R_1(0) = 20$ and $R_2(0) = 30$ with an initially linear viscous profile. This is shown in Figure 5.5. Notice that as R_1 increases, and thus time increases, the maximum value of σ decreases.

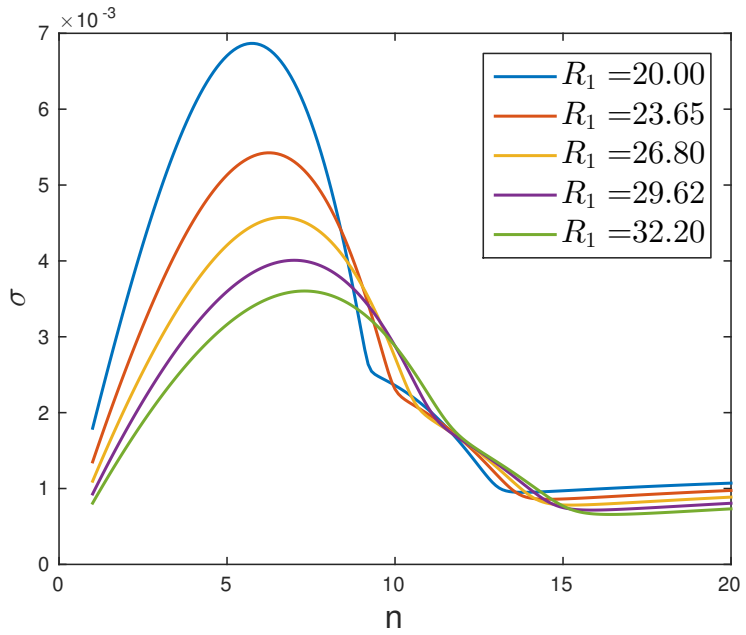

Figure 5.5: Dispersion relations for several different times, represented by the position of the inner radius, R_1. The flow begins with a linear viscous profile at time $t = 0$ and $R_1(0) = 20$.

We also plotted the value of σ_{max} verses the value of the inner radius R_1 as well as the most dangerous wavenumber n_{max} versus R_1. You can find these in Figures 5.6a

and 5.6b, respectively. Note that σ_{max} is a decreasing function of R_1. However, when R_1 reaches a value of approximately 68, σ_{max} is almost constant. For all times after this point, σ no longer attains an absolute maximum value. Instead, σ approaches its supremum as $n \to \infty$. This is illustrated by Figure 5.6b in which the value of n_{max} goes to infinity when R_1 reaches this point. We have previously demonstrated for rectilinear flow that the short wave (large n) behavior is governed by the instability of the intermediate layer, which is represented by the last term of the upper bound. Therefore, σ_{max} decreases with time for early times when the interfacial instability dominates, and then remains constant for later times when the intermediate layer instability dominates. As an example of this long-time behavior, we have plotted

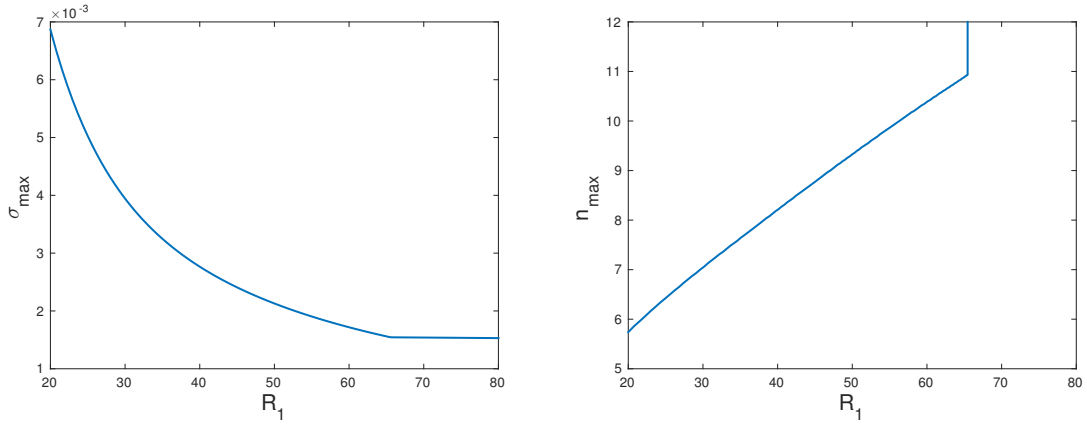

(a) (b)

Figure 5.6: (a) A plot of the maximum growth rate σ_{max} versus the position of the inner interface R_1. (b) A plot of the most dangerous wavenumber n_{max} versus the position of the inner interface R_1. The vertical line represents the point at which $n_max = \infty$.

the dispersion relation for a later time ($R_1 = 121$) in Figure 5.7. Note that the short waves are the most unstable.

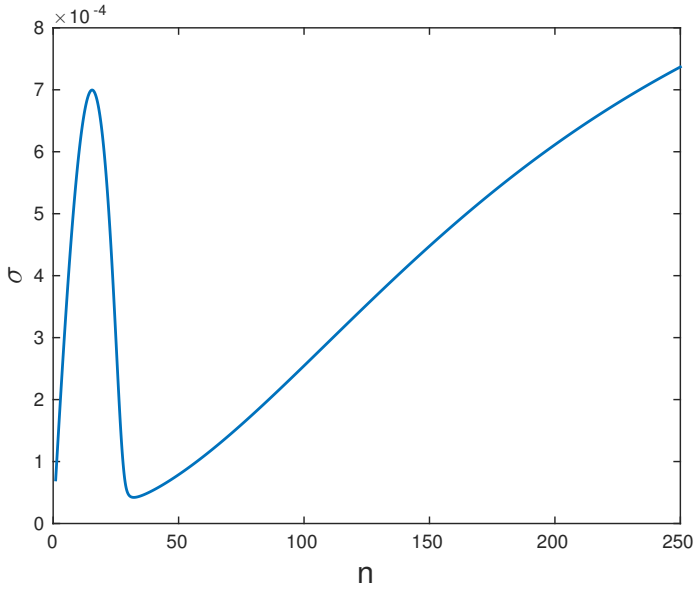

Figure 5.7: The dispersion relation when $R_1 = 121$. The flow begins with a linear viscous profile at time $t = 0$ and $R_1(0) = 20$.

5.6.4 Optimal Viscous Profiles

Next, we seek to minimize the value of σ_{max} by choosing an optimal viscous profile. First, we will consider the optimal profile at time $t = 0$. Then, we will investigate whether this profile remains optimal for later times. To start, we consider only viscous profiles that are initially linear with respect to r. Such profiles are uniquely determined by the values at the endpoints, $\mu(R_1)$ and $\mu(R_2)$. As done above, we use $\mu_i = 2$ and $\mu_o = 10$ as the viscosities of the inner and outer fluids, respectively. We allow $\mu(R_1)$ and $\mu(R_2)$ to vary between these two values and seek the profile which minimizes σ_{max}. Figure 5.8 shows a plot of σ_{max} for each of these viscous profiles. It uses the values $R_1(0) = 20$ and $R_2(0) = 30$. Note that all points on the diagonal $\mu(R_1) = \mu(R_2)$ are constant viscosity intermediate layers. Clearly the profile which minimizes σ_{max} is off the diagonal and therefore non-constant. In fact, the optimal viscous profile is $\mu(R_1) = 3.415$ and $\mu(R_2) = 5.088$ and has a maximum growth rate

of $\sigma_{max} = 3.888 \times 10^{-3}$. Among all constant viscous profiles, the optimal choice is $\mu \equiv 4.173$ which has a maximum growth rate of $\sigma_{max} = 4.962 \times 10^{-3}$. To compare the growth rates of these two profiles, we plotted the dispersion relations in Figure 5.9a. The viscous profiles are plotted in 5.9b. It is important to note, however, that even though the optimal variable viscosity profile has a smaller value of σ_{max}, it is unstable for short waves while the constant viscosity profile is stable for short waves.

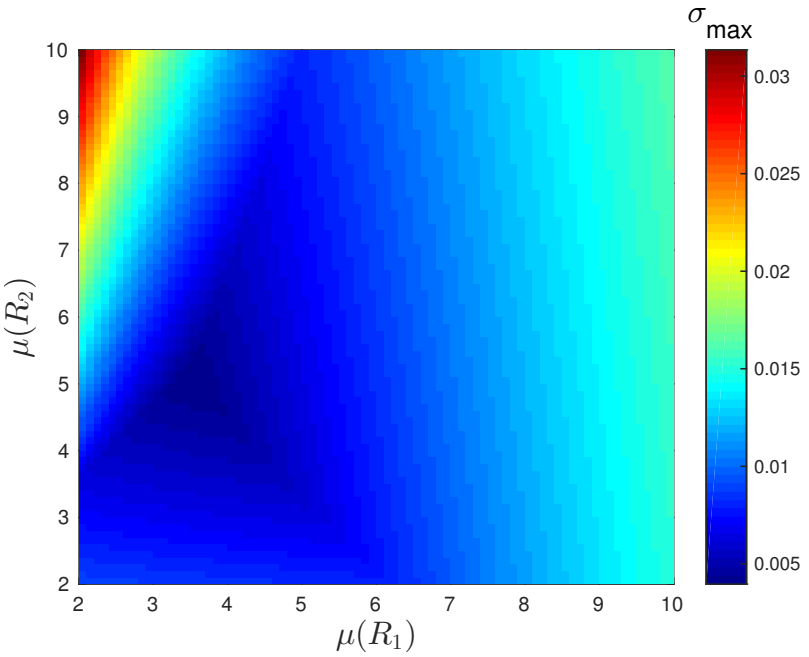

Figure 5.8: A plot of σ_{max} for different linear viscous profiles, which are determined by the values $\mu(R_1)$ and $\mu(R_2)$. The color bar on the right shows the scales for σ_{max}.

Similar optimization procedures were done for several other types of viscous profiles. Recall that for rectilinear flows, an exponential viscous profile was found to be optimal. However, among all viscous profiles which are exponential in r, the optimal profile has $\mu(R_1) = 3.636$ and $\mu(R_2) = 4.907$ and a maximum growth rate

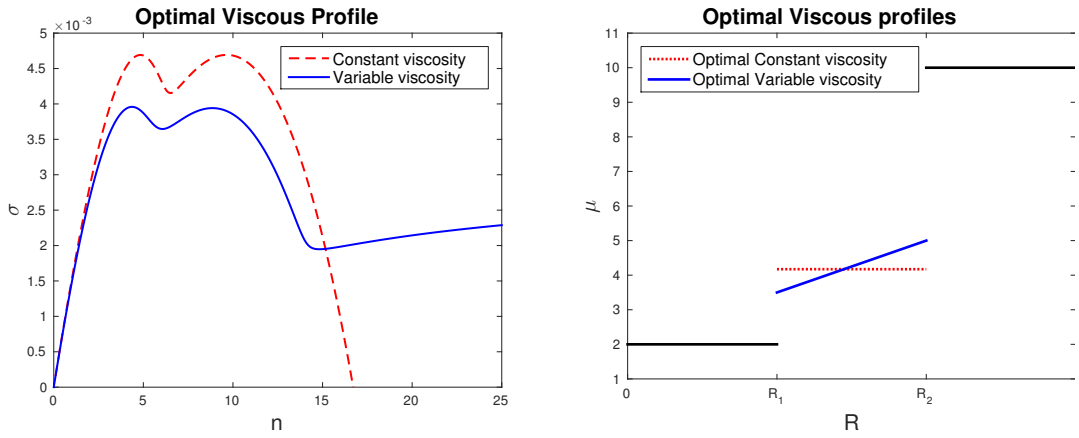

(a) (b)

Figure 5.9: (a) Plots of the dispersion relations for the optimal linear viscous profile and the optimal constant viscous profile. (b) Plots of the corresponding viscous profiles.

of $\sigma_{max} = 4.425 \times 10^{-3}$. This is more unstable than the optimal linear viscous profile. Among all viscous profiles which are logarithmic with respect to r, the optimal profile has $\mu(R_1) = 3.619$ and $\mu(R_2) = 4.684$ and a maximum growth rate of $\sigma_{max} = 4.144 \times 10^{-3}$.

Because the growth rate is not in the physical coordinates (with r as the radial variable) but in the transformed coordinates (with ζ as the radial variable), it may be wise to choose the viscous profile with respect to the ζ variable. This makes sense since the nature of the viscous profile will not change in these coordinates. Numerical evidence backs up this idea. Among all viscous profiles which are linear with respect to ζ, the optimal one has $\mu(\zeta_1) = 3.330$ and $\mu(1) = 5.320$ (which corresponds to $\mu(R_1) = 3.330$ and $\mu(R_2) = 5.320$) and a maximum growth rate of $\sigma_{max} = 3.798 \times 10^{-3}$. Among all profiles which are exponential in ζ, the optimal one is $\mu(\zeta_1) = 3.224$ and $\mu(R_2) = 5.774$ with a maximum growth rate of $\sigma_{max} = 3.712 \times 10^{-3}$. Therefore, among all the profiles we have mentioned, this is the best.

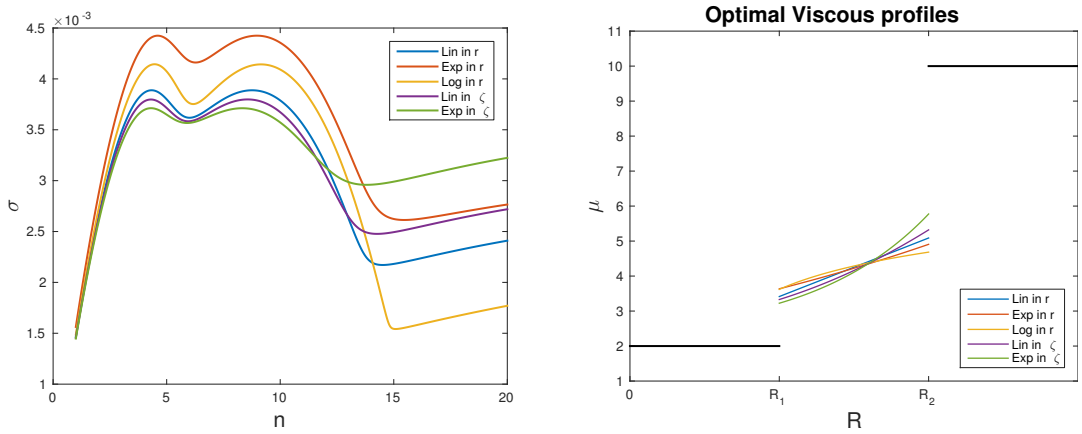

(a) (b)

Figure 5.10: (a) Plot of the dispersion relations for the optimal viscous profiles which are (i) linear with respect to r, (ii) exponential with respect to r, (iii) logarithmic with respect to r, (iv) linear with respect to ζ, and (v) exponential with respect to ζ. (b) Plot of the corresponding viscous profiles.

In Figure 5.10a, we plotted the dispersion curves for each of the optimal viscous profiles mentioned above. Figure 5.10b shows the corresponding viscous profiles plotted as functions of r. Two things are worth mentioning. First, note that the steeper the optimal viscous profile, the lower the value of σ_{max}. Second, it is not clear from the figure, but in the limit as $n \to \infty$ for each of these viscous profiles, σ approaches σ_{max}. However, σ_{max} is also the value of the local maxima shown in the plot of the dispersion curves. Therefore, these viscous profiles are optimal because they strike the perfect balance between instability of the interfaces and instability of the intermediate layer.

Next, we investigate whether these optimal viscous profiles at time $t = 0$ are still optimal at later times. Recall from section 5.6.3 that σ_{max} decreases with time when the interfacial instabilities dominate, but remain constant when the instability of the intermediate layer dominates. For the optimal viscous profiles given above, the instability of the intermediate layer (given by the large n behavior) is already

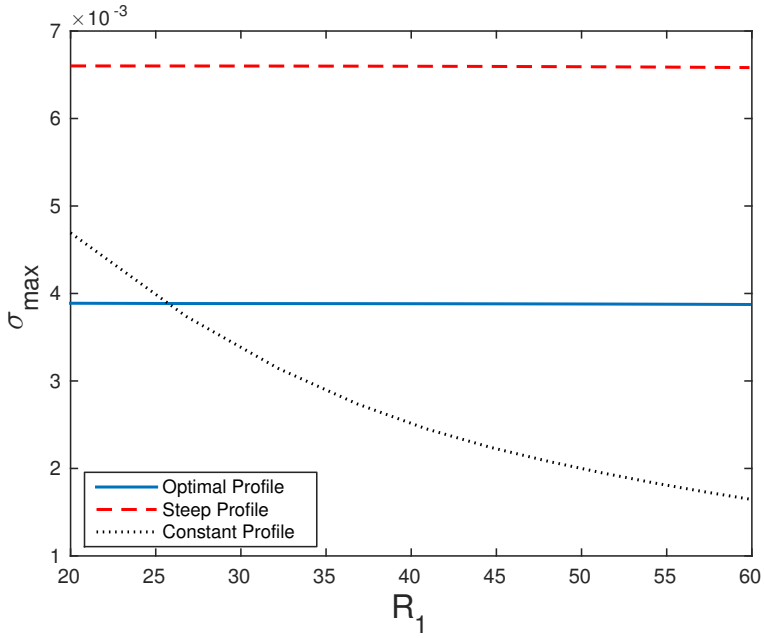

Figure 5.11: Plot of the maximum value of the growth rate, σ_{max}, versus the inner radius $R_1(t)$ for three different viscous profiles. The solid blue line corresponds to an initially linear viscous profile with $\mu(R_1) = 3.415$ and $\mu(R_2) = 5.088$. The dashed red line corresponds to an initially linear viscous profile with $\mu(R_1) = 3$ and $\mu(R_2) = 5.5$. The dotted black line corresponds to a constant viscous profile with $\mu(R_1) = \mu(R_2) = 4.173$.

as strong as the interfacial instability. Therefore, σ_{max} remains constant with time. This is also true for any viscous profile which is steeper than the optimal profile. However, any viscous profile that is less steep than the optimal viscous profile will have a period in which σ_{max} decreases. In particular, this will be true of a constant viscosity intermediate layer. To demonstrate this, we plotted the value of σ_{max} versus R_1 (which increases with time) for three different viscous profiles in Figure 5.11. The solid blue line represents the value of σ_{max} for the optimal viscous profile which is initially linear in r. The red dashed line gives the value of σ_{max} for an initially linear profile which is steeper than the optimal viscous profile. The black dotted line gives the value of σ_{max} for the optimal (at time $t = 0$) constant viscous profile. Notice

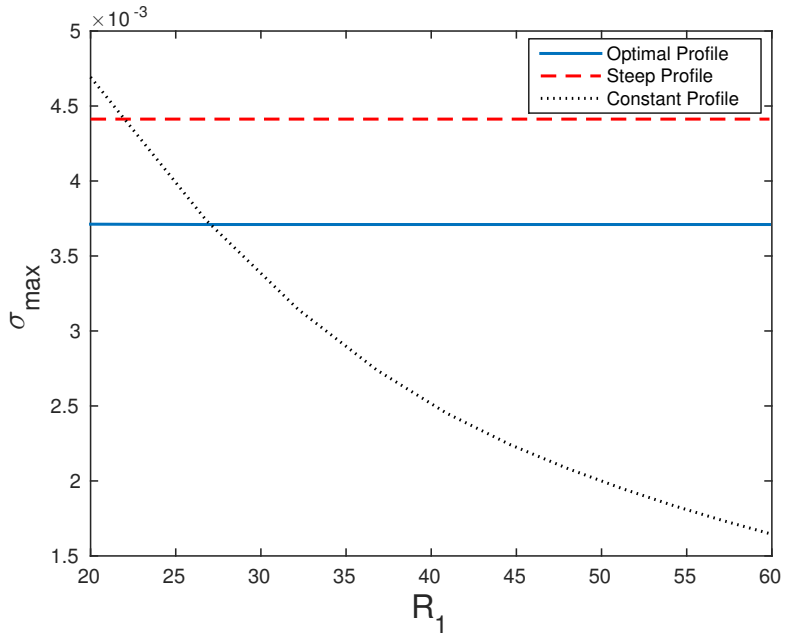

Figure 5.12: Plot of the maximum value of the growth rate, σ_{max}, versus the inner radius $R_1(t)$ for three different viscous profiles. The solid blue line corresponds to an exponential (in ζ) viscous profile with $\mu(R_1) = 3.224$ and $\mu(R_2) = 5.774$. The dashed red line corresponds to an exponential viscous profile with $\mu(R_1) = 3$ and $\mu(R_2) = 6$. The dotted black line corresponds to a constant viscous profile with $\mu(R_1) = \mu(R_2) = 4.173$.

that the optimal linear profile chosen at $t = 0$ is only less unstable than the constant viscous profile for a short time. This same behavior also holds for viscous profiles which are exponential with respect to ζ, which, if you recall, is the optimal choice of the profiles we considered. This is shown in Figure 5.12.

In light of this information, a recommended strategy is to use an initial viscous profile with a small viscous gradient. Although this will sacrifice some stability during early times, the flow will be more stable than the initially optimal viscous profile at later times. In Figure 5.13, we plotted σ_{max} versus R_1 for a variable viscous profile with small gradient and for the optimal constant viscous profile. For the variable viscous profile, we used a profile which is exponential in the transformed coordinates

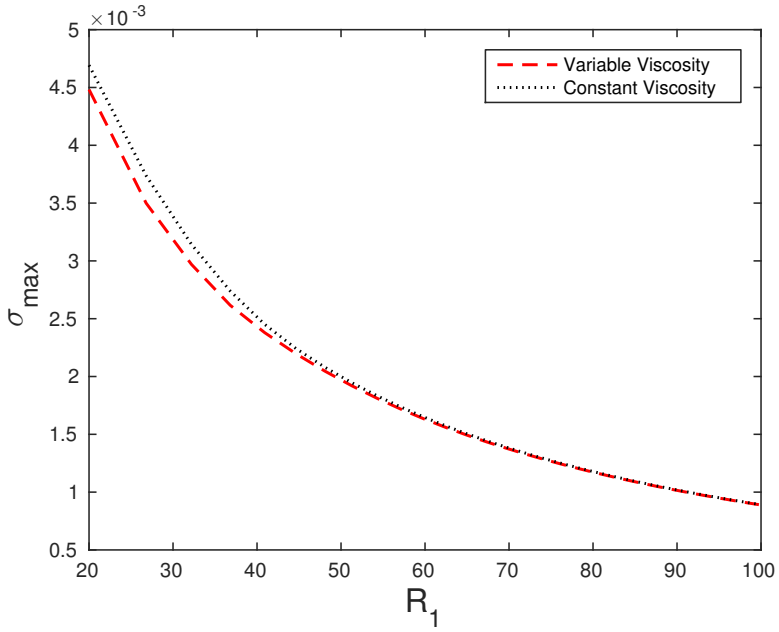

Figure 5.13: Plot of the maximum value of the growth rate, σ_{max}, versus the inner radius $R_1(t)$ for two different viscous profiles. The dashed red line corresponds to an exponential viscous profile (in ζ) with $\mu(R_1) = 4$ and $\mu(R_2) = 4.5$. The dotted black line corresponds to a constant viscous profile with $\mu(R_1) = \mu(R_2) = 4.173$.

with $\mu(\zeta_1) = 4$ and $\mu(1) = 4.5$. Recall that the optimal constant viscous profile is $\mu = 4.173$. For early times, the variable viscous profile is more stable than the constant viscous profile. However, as opposed to our use of the optimal viscous profile in Figure 5.12, this time the value of σ_{max} at later times is comparable for the variable and constant viscous profiles.

5.7 Conclusion

In this chapter, we have studied the stability of three-layer variable viscosity radial Hele-Shaw flows. The eigenvalue problem for this type of flow has not previously been formulated or studied. Therefore, this formulation can be a springboard into many future studies of multi-layer Hele-Shaw flows in the radial geometry. Below, we summarize the main contributions of this chapter.

1. First, we derive the eigenvalue problem that governs the growth rate of three-layer variable viscosity radial Hele-Shaw flows (see section 5.2). In order to use the classical method of normal modes, we first prescribe an appropriate change of variables in order to fix the basic solution.

2. We use our formulation to consider the limiting case in which all fluids have constant viscosity. For two-layer flow (see section 5.3.1), we can obtain an exact expression for the growth rate and compare this with the well-known Saffman-Taylor growth rate in the original, physical coordinate system. We also find an exact expression for the growth rate of three-layer constant viscosity flows (see section 5.3.2).

3. In section 5.4, we find an upper bound on the growth rate by using variational techniques. The growth rate depends on three terms - one corresponding to each interface and one to the intermediate layer. This upper bound is analogous to the one given for rectilinear flows in [28] and can be useful in devising optimal injection policies for chemical EOR.

4. In section 5.5, we provide a characterization of the eigenvalues and eigenfunctions of the eigenvalue problem (5.76) for a set of wavenumbers inside the unstable band. As we found in chapter 2 for rectilinear flows, when the viscosity of the intermediate layer is an increasing function, there are a countably infinite number of positive eigenvalues with a limit point at infinity. We can also characterize the oscillatory nature of the eigenfunctions. Then, by defining a Hilbert space that depends on a new measure, we see that the eigenvalue problem is self-adjoint and that the eigenfunctions are complete in this Hilbert space.

5. Finally, in section 5.6, we numerically investigate the growth rate. We first provide a basis for comparison between the growth rate in the new coordinate system and the growth rate in the original coordinate system. We then validate that the constant viscosity case is a limit of variable viscosity flows. We show that the maximum growth rate is a decreasing function of time. Finally, we investigate optimal viscous profiles at time $t = 0$ and find that at later times, profiles which are initially less steep become more stable. We use this information to suggest a method of using variable viscous profiles to provide enhanced stability over constant viscous profiles.

6. NUMERICAL METHODS

The numerical results in chapters 2, 3, and 5 require us to approximate the eigenvalues of variable viscosity Hele-Shaw flows. In [27] and [21], finite difference methods are used to solve the eigenvalue problem for three-layer variable viscosity rectilinear flows. In [30] and an unpublished work by Daripa and Ding [23], two different finite difference methods are proposed for solving the problem with diffusion of polymer in the middle layer. Here, we instead use a pseudo-spectral method in which we expand the eigenfunctions into Chebyshev polynomials. This method was found to be preferable to the finite difference methods, both in its computational speed and its convergence rates. Methods of this type are common for solving all types of differential equations, and it is well-known that for smooth solutions, exponential convergence can be achieved. Below, we describe the general method for solving an eigenvalue problem with the pseudo-spectral Chebyshev method. We then look more closely at the particulars addressed in each of our three chapters which make use of the method.

6.1 Pseudo-Spectral Chebyshev Method

In order to numerically compute the eigenvalues, we use a pseudo-spectral method. Here, we describe the general aspects of the method. For a more detailed treatment and proofs of convergence rates, see [5, 71].

Let $T_n(y)$ denote the n^{th} Chebyshev polynomial, which can be defined in terms of trigonometric functions as

$$T_n(y) = \cos(n \cos^{-1}(y)), \qquad y \in [-1, 1]. \tag{6.1}$$

Alternatively, they may be defined by the recurrence relation

$$T_0 = 1, \qquad T_1 = y, \qquad T_n = 2yT_{n-1} - T_{n-2}. \tag{6.2}$$

The Chebyshev polynomials satisfy the orthogonality condition

$$\int_{-1}^{1} \frac{T_n(y)T_m(y)}{\sqrt{1-y^2}} dy = C_n \delta_{nm}, \tag{6.3}$$

where $C_0 = \pi$ and $C_n = \frac{\pi}{2}$ for $n \neq 0$. Additionally, the Chebyshev polynomials form a complete set with respect to this weight function. That is, if $w(y) = \frac{1}{\sqrt{1-y^2}}$, then $\{T_n\}_{n=0}^{\infty}$ is complete in the space

$$L_w^2([-1,1]) = \left\{ f(y) \middle| \int_{-1}^{1} \frac{f^2(y)}{\sqrt{1-y^2}} dy < \infty \right\}.$$

Therefore, for any $f \in L_w^2([-1,1])$, we may expand f as

$$f(y) = \sum_{n=0}^{\infty} a_n T_n(y), \qquad a_n = \frac{1}{\sqrt{C_n}} \int_{-1}^{1} \frac{f(y)T_n(y)}{\sqrt{1-y^2}} dy. \tag{6.4}$$

In order to use this expansion to solve our eigenvalue problem, we approximate the solution as the finite sum of the first N Chebyshev polynomials

$$f(y) \approx \sum_{n=0}^{N} a_n T_n(y). \tag{6.5}$$

In order to optimize the rate of convergence, we evaluate these at the extremal values of the Chebyshev polynomials (the Gauss-Chebyshev-Lobatto points), which are given by

$$y_j = \cos\left(\frac{j\pi}{N}\right), \qquad j = 0, ..., N. \tag{6.6}$$

Using these points, $T_n(y_j) = \cos\left(\frac{nj\pi}{N}\right)$. In order to solve an eigenvalue problem, we also need an expansion for the derivatives of f. We write the k^{th} derivative of f as

$$f^{(k)}(y) = \sum_{n=0}^{N} a_n T_n^{(k)}(y). \tag{6.7}$$

Using the change of variables $y = cos(\theta)$ and (6.1), we get $T_n(y) = \cos(n\theta)$. Therefore

$$T_n'(y) = -n\sin(n\theta)\frac{d\theta}{dy} = \frac{n\sin(n\theta)}{\sin(\theta)}. \tag{6.8}$$

Using (6.8),

$$\begin{aligned}
T_n'(y) &= \frac{n\sin(n\theta)}{\sin(\theta)} \\
&= \frac{n\sin((n-2)\theta + 2\theta)}{\sin(\theta)} \\
&= \frac{n}{\sin(\theta)}\{\sin((n-2)\theta)\cos(2\theta) + \cos((n-2)\theta)\sin(2\theta)\} \\
&= \frac{n}{\sin(\theta)}\{\sin((n-2)\theta)(1-2\sin^2(\theta)) + 2\cos((n-2)\theta)\sin(\theta)\cos(\theta)\} \\
&= 2n\{\cos((n-2)\theta)\cos(\theta) - \sin((n-2)\theta)\sin(\theta))\} + \frac{n\sin((n-2)\theta)}{\sin(\theta)} \\
&= 2n\cos((n-2)\theta + \theta) + \left(\frac{n}{n-2}\right)T_{n-2}'(y) \\
&= 2n\cos((n-1)\theta) + \left(\frac{n}{n-2}\right)T_{n-2}'(y) \\
&= 2nT_{n-1}(y) + \left(\frac{n}{n-2}\right)T_{n-2}'(y).
\end{aligned}$$

In general, for $k \geq 1$,the k^{th} derivative satisfies the recurrence relation

$$T_0^{(k)}(y) = 0, \qquad T_1^{(k)}(y) = T_0^{(k-1)}(y), \qquad T_n^{(k)}(y) = 2nT_{n-1}^{(k-1)}(y) + \left(\frac{n}{n-2}\right)T_{n-2}^{(k)}(y). \tag{6.9}$$

We may use this relation to build differentiation matrices in the following way. Let $\mathbf{a} = \{a_0, ..., a_N\}^T$ where the a_i's are the coefficients from (6.5). Let $\mathbf{D_0}$ be an $(N+1) \times (N+1)$ matrix such that the entry in row i and column j is given by

$$(\mathbf{D_0})_{i,j} = T_{j-1}(y_{i-1}). \tag{6.10}$$

Then $\mathbf{D_0 a} = \mathbf{f}$ where $\mathbf{f} = \{f(y_0), f(y_1), ..., f(y_N)\}^T$. We denote the k^{th} differentiation matrix by $\mathbf{D_k}$. Using (6.9), we can recursively build $\mathbf{D_k}$ from $\mathbf{D_{k-1}}$ using

$$(\mathbf{D_k})_{i,j} = T^{(k)}_{j-1}(y_{i-1}) = \begin{cases} 0, & j = 1, \\ (\mathbf{D_{k-1}})_{i,j-1}, & j = 2, \\ 2(j-1)(\mathbf{D_{k-1}})_{i,j-1} + \left(\frac{j-1}{j-3}\right)(\mathbf{D_k})_{i,j-2}, & 3 \leq j \leq N+1. \end{cases} \tag{6.11}$$

Then, for any $k \geq 0$, $\mathbf{D_k a} = \mathbf{f_k}$ where $\mathbf{f_k} = \{f^{(k)}(y_0), f^{(k)}(y_1), ..., f^{(k)}(y_N)\}^T$. For an explicit example of a MATLAB program that builds these matrices, see Schmid and Henningson [65, p. 491-492]. With these differentiation matrices, we can write a differential eigenvalue problem as a matrix equation and solve for the eigenvalues using any standard solver.

6.2 Variable Viscosity Rectilinear Flow

We now show how to use the Chebyshev method to solve the eigenvalue problem (2.5), which holds for three-layer variable viscosity rectilinear flows with no diffusion. Recall equation $(2.5)_1$:

$$(\mu f')' - (k^2\mu - k^2 U \mu' \lambda) f = 0, \quad -L < x < 0.$$

Note that the Gauss-Chebyshev-Lobatto points are in the interval $[-1,1]$. We map these points to the interval $[-L,0]$ using the affine map $x = \frac{L}{2}(y-1)$. Therefore, our collocation points are $x_i = \frac{L}{2}(y_i - 1)$. Additionally, since $\frac{d}{dx} = \frac{2}{L}\frac{d}{dy}$, we let $\mathbf{D_k^x} = \left(\frac{2}{L}\right)^k \mathbf{D_k}$. Note that $(2.5)_1$ can be rewritten as

$$-\mu(x)f''(x) - \mu'(x)f'(x) + k^2\mu(x)f(x) = \lambda k^2 U\mu'(x)f(x). \tag{6.12}$$

We require that this equation hold at each collocation point, x_i, which gives a system of $N+1$ equations. Let $\mathbf{V}$ and $\mathbf{V}'$ be the matrices defined by

$$(\mathbf{V})_{i,j} = \begin{cases} \mu(x_{i-1}), & j = i, \\ 0, & \text{otherwise} \end{cases}, \qquad (\mathbf{V}')_{i,j} = \begin{cases} \mu'(x_{i-1}), & j = i, \\ 0, & \text{otherwise} \end{cases}. \tag{6.13}$$

Then the i^{th} entry of the vector $\mathbf{V}\mathbf{D_k^x}\mathbf{a}$ is $\mu(x_{i-1})f^{(k)}(x_{i-1})$ and likewise for $\mathbf{V}'\mathbf{D_k^x}\mathbf{a}$. Therefore, the condition that (6.12) holds for each x_i is given by the matrix equation

$$-\mathbf{V}\mathbf{D_2^x}\mathbf{a} - \mathbf{V}'\mathbf{D_1^x}\mathbf{a} + k^2\mathbf{V}\mathbf{D_0^x}\mathbf{a} = \lambda k^2 U\mathbf{V}'\mathbf{D_0^x}\mathbf{a}. \tag{6.14}$$

Let $\mathbf{A} = -\mathbf{V}\mathbf{D_2^x} - \mathbf{V}'\mathbf{D_1^x} + k^2\mathbf{V}\mathbf{D_0^x}$ and $\mathbf{B} = k^2 U\mathbf{V}'\mathbf{D_0^x}$. Then we have the generalized eigenvalue problem $\mathbf{A}\mathbf{a} = \lambda\mathbf{B}\mathbf{a}$. However, we must enforce the boundary conditions by amending the first and last rows of $\mathbf{A}$ and $\mathbf{B}$, which correspond to $x_0 = 0$ and $x_N = -L$, respectively. The boundary conditions $(2.5)_2$ and $(2.5)_3$ can be rewritten as

$$\begin{aligned} &\mu(0)f'(0) + \mu_r k f(0) = E_0\lambda f(0), \\ &\mu(-L)f'(-L) - \mu_l k f(-L) = -E_1\lambda f(-L). \end{aligned}$$

Therefore, the first and last rows of $\mathbf{A}$ and $\mathbf{B}$ are

$$(\mathbf{A})_{1,j} = \mu(0)(\mathbf{D_1^x})_{1,j} + \mu_r k(\mathbf{D_0^x})_{1,j}, \qquad (\mathbf{B})_{1,j} = E_0(\mathbf{D_0^x})_{1,j},$$
$$(\mathbf{A})_{N+1,j} = \mu(-L)(\mathbf{D_1^x})_{N+1,j} - \mu_l k(\mathbf{D_0^x})_{N+1,j}, \qquad (\mathbf{B})_{N+1,j} = -E_1(\mathbf{D_0^x})_{N+1,j}.$$

We solve the generalized eigenvalue problem using MATLAB's "eig" command.

6.2.1 Finding the Eigenfunctions

Once the eigenvalues are known, we can compute the eigenfunctions from the general form (2.51):

$$f(x) = e^{-\frac{\alpha x}{2}}(A\cos(\beta x) + B\sin(\beta x)).$$

Plugging in $x = 0$ yields $f(0) = A$. So

$$f(x) = e^{-\frac{\alpha x}{2}}(f(0)\cos(\beta x) + B\sin(\beta x)).$$

We then plug in $x = -L$.

$$f(-L) = e^{\frac{\alpha L}{2}}(f(0)\cos(-\beta L) + B\sin(-\beta L)).$$

Solving for B, we get

$$B = \frac{f(0)\cos(\beta L) - f(-L)e^{-\frac{\alpha L}{2}}}{\sin(\beta L)}.$$

Therefore,

$$f(x) = e^{-\frac{\alpha x}{2}}\left(f(0)\cos(\beta x) + \frac{f(0)\cos(\beta L) - f(-L)e^{-\frac{\alpha L}{2}}}{\sin(\beta L)}\sin(\beta x)\right), \qquad (6.15)$$

and

$$f'(x) = -\frac{\alpha}{2} f(x) + \beta e^{-\frac{\alpha x}{2}} \left(-f(0)\sin(\beta x) + \frac{f(0)\cos(\beta L) - f(-L)e^{-\frac{\alpha L}{2}}}{\sin(\beta L)} \cos(\beta x) \right). \tag{6.16}$$

Therefore,

$$\begin{aligned} f'(0) &= -\frac{\alpha}{2} f(0) + \beta \left(\frac{f(0)\cos(\beta L) - f(-L)e^{-\frac{\alpha L}{2}}}{\sin(\beta L)} \right) \\ &= \left(-\frac{\alpha}{2} + \beta \frac{\cos(\beta L)}{\sin(\beta L)} \right) f(0) - \beta \frac{e^{-\frac{\alpha L}{2}}}{\sin(\beta L)} f(-L). \end{aligned} \tag{6.17}$$

Plugging this into the boundary condition $(2.5)_3$,

$$-\left(-\frac{\alpha}{2} + \beta \frac{\cos(\beta L)}{\sin(\beta L)} \right) f(0) + \beta \frac{e^{-\frac{\alpha L}{2}}}{\sin(\beta L)} f(-L) = \left(\frac{\mu_r k - E_0 \lambda}{\mu(0)} \right) f(0).$$

After some algebraic manipulation,

$$\frac{e^{-\frac{\alpha L}{2}}}{\sin(\beta L)} f(-L) = \left(\frac{\mu_r k - E_0 \lambda}{\mu(0)\beta} - \frac{\alpha}{2\beta} + \frac{\cos(\beta L)}{\sin(\beta L)} \right) f(0). \tag{6.18}$$

Using (6.18) in (6.15),

$$\begin{aligned} f(x) =& e^{-\frac{\alpha x}{2}} \left(f(0)\cos(\beta x) + \frac{f(0)\cos(\beta L) - f(-L)e^{-\frac{\alpha L}{2}}}{\sin(\beta L)} \sin(\beta x) \right) \\ =& e^{-\frac{\alpha x}{2}} \left(f(0)\cos(\beta x) + f(0)\frac{\cos(\beta L)}{\sin(\beta L)} \sin(\beta x) - \frac{e^{-\frac{\alpha L}{2}}}{\sin(\beta L)} f(-L)\sin(\beta x) \right) \\ =& e^{-\frac{\alpha x}{2}} \left(f(0)\cos(\beta x) + f(0)\frac{\cos(\beta L)}{\sin(\beta L)} \sin(\beta x) \right) \\ & - e^{-\frac{\alpha x}{2}} \left(\frac{\mu_r k - E_0 \lambda}{\mu(0)\beta} - \frac{\alpha}{2\beta} + \frac{\cos(\beta L)}{\sin(\beta L)} \right) f(0)\sin(\beta x), \end{aligned}$$

and

$$f(x) = f(0)e^{-\frac{\alpha x}{2}} \left(\cos(\beta x) + \left(\frac{\alpha}{2} - \frac{\mu_r k - E_0 \lambda}{\mu(0)} \right) \frac{\sin(\beta x)}{\beta} \right). \tag{6.19}$$

This gives the eigenfunction up to an arbitrary constant, $f(0)$. We choose this constant so that

$$\int_{-L}^{0} f(x)dx = 1. \tag{6.20}$$

Therefore,

$$f(0) \int_{-L}^{0} e^{-\frac{\alpha x}{2}} \left(\cos(\beta x) + \left(\frac{\alpha}{2} - \frac{\mu_r k - E_0 \lambda}{\mu(0)} \right) \frac{\sin(\beta x)}{\beta} \right) dx = 1.$$

We use that

$$\int_{-L}^{0} e^{-\frac{\alpha x}{2}} \cos(\beta x)dx = \frac{-\frac{\alpha}{2} + e^{\frac{\alpha L}{2}} (\frac{\alpha}{2} \cos(\beta L) + \beta \sin(\beta L))}{\frac{\alpha^2}{4} + \beta^2},$$

and

$$\int_{-L}^{0} e^{-\frac{\alpha x}{2}} \sin(\beta x)dx = \frac{-\beta + e^{\frac{\alpha L}{2}} (\beta \cos(\beta L) - \frac{\alpha}{2} \sin(\beta L))}{\frac{\alpha^2}{4} + \beta^2}.$$

Then,

$$\begin{aligned}
\frac{1}{f(0)} =& \int_{-L}^{0} e^{-\frac{\alpha x}{2}} \cos(\beta x)dx + \frac{1}{\beta}\left(\frac{\alpha}{2} - \frac{\mu_r k - E_0\lambda}{\mu(0)}\right)\int_{-L}^{0} e^{-\frac{\alpha x}{2}} \sin(\beta x)dx \\
=& \frac{-\frac{\alpha}{2} + e^{\frac{\alpha L}{2}}(\frac{\alpha}{2}\cos(\beta L) + \beta\sin(\beta L))}{\frac{\alpha^2}{4}+\beta^2} \\
&+ \frac{1}{\beta}\left(\frac{\alpha}{2} - \frac{\mu_r k - E_0\lambda}{\mu(0)}\right)\frac{-\beta + e^{\frac{\alpha L}{2}}(\beta\cos(\beta L) - \frac{\alpha}{2}\sin(\beta L))}{\frac{\alpha^2}{4}+\beta^2} \\
=& \frac{-\frac{\alpha}{2} + e^{\frac{\alpha L}{2}}(\frac{\alpha}{2}\cos(\beta L) + \beta\sin(\beta L))}{\frac{\alpha^2}{4}+\beta^2} + \frac{-\frac{\alpha}{2} + e^{\frac{\alpha L}{2}}(\frac{\alpha}{2}\cos(\beta L) - \frac{\alpha^2}{4\beta}\sin(\beta L))}{\frac{\alpha^2}{4}+\beta^2} \\
&+ \left(\frac{\mu_r k - E_0\lambda}{\mu(0)}\right)\frac{1 + e^{\frac{\alpha L}{2}}(-\cos(\beta L) + \frac{\alpha}{2\beta}\sin(\beta L))}{\frac{\alpha^2}{4}+\beta^2} \\
=& \frac{-\alpha + e^{\frac{\alpha L}{2}}\left(\alpha\cos(\beta L) + \left(\beta^2 - \frac{\alpha^2}{4}\right)\frac{\sin(\beta L)}{\beta}\right)}{\frac{\alpha^2}{4}+\beta^2} \\
&+ \frac{\left(\frac{\mu_r k - E_0\lambda}{\mu(0)}\right)\left(1 + e^{\frac{\alpha L}{2}}\left(\frac{\alpha}{2}\frac{\sin(\beta L)}{\beta} - \cos(\beta L)\right)\right)}{\frac{\alpha^2}{4}+\beta^2}.
\end{aligned}$$

Therefore,

$$f(0) = \frac{\frac{\alpha^2}{4}+\beta^2}{-\alpha + e^{\frac{\alpha L}{2}}\left(\alpha\cos(\beta L) + \left(\beta^2 - \frac{\alpha^2}{4}\right)\frac{\sin(\beta L)}{\beta}\right) + \left(\frac{\mu_r k - E_0\lambda}{\mu(0)}\right)\left(1 + e^{\frac{\alpha L}{2}}\left(\frac{\alpha}{2}\frac{\sin(\beta L)}{\beta} - \cos(\beta L)\right)\right)}. \tag{6.21}$$

Plugging (6.21) into (6.19) gives the normalized eigenfunction. Note that λ appears explicitly in the expression for the eigenfunctions in addition to the fact that β depends on λ. When we have obtained the eigenvalues $\{\lambda_i\}$, we get $f_i(x)$ by plugging λ_i into (6.21) and (6.19).

6.3 Variable Viscosity Rectilinear Flows with Diffusion

We now use the Chebyshev method to solve the eigenvalue problem (3.36), which holds for three-layer variable viscosity rectilinear Hele-Shaw flows with diffusion of polymer in the middle layer and in which the viscosity depends linearly on the

concentration of polymer. This method is easily adaptable to the system (3.45) in which viscosity depends exponentially on the concentration of polymer. Recall equation $(3.36)_1$:

$$\begin{aligned} &Pe\,(\mu f_{xx} + \mu_x f_x - k^2 \mu f) \\ =&\lambda\Big\{\mu f_{4x} + 3\mu_x f_{3x} - 2k^2 \mu f_{xx} - 3k^2 \mu_x f_x + \left\{k^4 \mu - k^2 \mu_x\, Pe\right\} f\Big\}, \quad x \in (-1, 0) \end{aligned}$$

As in the previous example, we map the interval $[-1, 1]$ to the interval $[-1, 0]$ using the affine map $x = \frac{1}{2}(y - 1)$. Therefore, our collocation points are $x_i = \frac{1}{2}(y_i - 1)$. Additionally, since $\frac{d}{dx} = 2\frac{d}{dy}$, we let $\mathbf{D_k^x} = 2^k \mathbf{D_k}$. We require that equation $(3.36)_1$ hold at each collocation point, x_i, which gives a system of $N + 1$ equations. Let $\mathbf{V}$ and $\mathbf{V}'$ be the matrices defined (6.13). Then the condition that $(3.36)_1$ holds for each x_i is given by the matrix equation

$$\begin{aligned} &Pe\left(\mathbf{V D_2^x a} + \mathbf{V' D_1^x a} - k^2 \mathbf{V D_0^x a}\right) \\ =&\lambda\left(\mathbf{V D_4^x a} + 3\mathbf{V' D_3^x a} - 2k^2 \mathbf{V D_2^x a} - 3k^2 \mathbf{V' D_1^x a} + (k^2 \mathbf{V} - k^2 \mathbf{V'}\, Pe)\mathbf{D_0^x a}\right). \end{aligned} \tag{6.22}$$

Let $\mathbf{A} = Pe\,(\mathbf{V D_2^x} + \mathbf{V' D_1^x} - k^2 \mathbf{V D_0^x})$ and $\mathbf{B} = \mathbf{V D_4^x} + 3\mathbf{V' D_3^x} - 2k^2 \mathbf{V D_2^x} - 3k^2 \mathbf{V' D_1^x} + (k^2 \mathbf{V} - k^2 \mathbf{V'}\, Pe)\mathbf{D_0^x}$. Then we have the generalized eigenvalue problem $\mathbf{Aa} = \lambda \mathbf{Ba}$. However, we must also enforce the boundary conditions. As in Schmid and Henningson [65, p. 489], we use the first, second, second to last, and last rows of our matrices

to do it. The boundary conditions of (3.36) can be rewritten as

$$\begin{aligned}
&\mu(0)f_x(0) + \mu_r\, kf(0) = \lambda E_0 f(0),\\
&-\mu(0)f_{xx}(0) + \left(k^2\mu(0) + \frac{\mu_x}{\mu(0)}\mu_r\, k\right) f(0) = \lambda\frac{\mu_x}{\mu(0)}E_0 f(0),\\
&-\mu(-1)f_{xx}(-1) + \left(k^2\mu(-1) - \frac{\mu_x}{\mu(-1)}\mu_l\, k\right) f(-1) = -\lambda\frac{\mu_x}{\mu(-1)}E_1 f(-1),\\
&\mu(-1)f_x(-1) - \mu_l\, kf(-1) = -\lambda E_1 f(-1).
\end{aligned}$$

Therefore, we use

$$\begin{aligned}
(\mathbf{A})_{1,j} &= \mu(0)(\mathbf{D_1^x})_{1,j} + \mu_r k(\mathbf{D_0^x})_{1,j},\\
(\mathbf{A})_{2,j} &= -\mu(0)(\mathbf{D_2^x})_{1,j} + \left(k^2\mu(0) + \frac{\mu_x}{\mu(0)}\mu_r k\right)(\mathbf{D_0^x})_{1,j},\\
(\mathbf{A})_{N,j} &= -\mu(1)(\mathbf{D_2^x})_{N+1,j} + \left(k^2\mu(-1) - \frac{\mu_x}{\mu(-1)}\mu_l k\right)(\mathbf{D_0^x})_{N+1,j},\\
(\mathbf{A})_{N+1,j} &= \mu(-1)(\mathbf{D_1^x})_{N+1,j} - \mu_l k(\mathbf{D_0^x})_{N+1,j},\\
(\mathbf{B})_{1,j} &= E_0(\mathbf{D_0^x})_{1,j},\\
(\mathbf{B})_{2,j} &= \frac{\mu_x}{\mu(0)}E_0(\mathbf{D_0^x})_{1,j},\\
(\mathbf{B})_{2,j} &= -\frac{\mu_x}{\mu(-1)}E_1(\mathbf{D_0^x})_{N+1,j},\\
(\mathbf{B})_{N+1,j} &= -E_1(\mathbf{D_0^x})_{N+1,j}.
\end{aligned}$$

We solve the generalized eigenvalue problem using MATLAB's "eig" command.

6.3.1 Finite Difference Method

We now present a finite difference method for solving the eigenvalue problem (3.36). This method was used in an unpublished work by Daripa and Ding [23] and we present it here for comparison with our Chebyshev method.

Previously, a finite difference method to solve the problem (3.27) has been pre-

sented in [30] in which both functions h and f were discretized. This method was used to find upper bounds for the eigenvalues but was not used for computation. Below, we present a method where, instead of solving the second order system defined by $(3.27)_1$ and $(3.27)_2$ using the method presented in [30], we solve the fourth order equation in $f(x)$ (see equation (3.36)). This method was found to be better for computation than the one in [30] and hence provides a better comparison for the Chebyshev method.

We can rewrite equation $(3.36)_1$ in terms of σ as

$$\frac{\mu}{Pe}f_{xxxx} + \frac{3\mu_x}{Pe}f_{xxx} + \left(-\frac{2}{Pe}k^2\mu - \sigma\mu\right)f_{xx} + \left(-\sigma\mu_x - \frac{3}{Pe}k^2\mu_x\right)f_x + \left(\left(\sigma + \frac{k^2}{Pe}\right)k^2\mu - k^2\mu_x\right)f(x) = 0. \tag{6.23}$$

The four boundary conditions for f in terms of σ are:

$$\left.\begin{aligned} &\mu(-1)f_x(-1) = \left(\mu_l\, k - \tfrac{E_1}{\sigma}\right) f(-1), \\ &-\mu(0)f_x(0) = \left(\mu_r\, k - \tfrac{E_0}{\sigma}\right) f(0), \\ &\mu(-1)f_{xx}(-1) = \left\{k^2\mu(-1) - \tfrac{\mu_x}{\mu(-1)}\left(\mu_l\, k - \tfrac{E_1}{\sigma}\right)\right\} f(-1), \\ &\mu(0)f_{xx}(0) = \left\{k^2\mu(0) + \tfrac{\mu_x}{\mu(0)}\left(\mu_r\, k - \tfrac{E_0}{\sigma}\right)\right\} f(0). \end{aligned}\right\} \tag{6.24}$$

The stability problem is then defined by (6.23) and (6.24). This problem is discretized over the domain $(-1, 0)$ using $M + 1$ uniformly spaced nodes with uniform step size $d = L/M$. We use first order accurate approximation for the end point derivatives

and second order approximation for the interior point derivatives, namely,

$$\begin{cases} f_x(-L) = \frac{f_{M-1}-f_M}{d},\ f_x(0) = \frac{f_0-f_1}{d}, \\ f_x(i) = \frac{f(i-1)-f(i+1)}{2d}, \\ f_{xx}(i) = \frac{f(i-1)-2f(i)+f(i+1)}{d^2}, \\ f_{xxx}(i) = \frac{f(i-2)-2f(i-1)+2f(i+1)-f(i+2)}{2d^3}, \\ f_{xxxx}(i) = \frac{f(i-2)-4f(i-1)+6f(i)-4f(i+1)+f(i+2)}{d^4}, \end{cases}$$

where i is any one of the interior discretization points. The equation (6.23) is discretized using these formulas. Using these finite difference approximations in the boundary conditions given in equations (6.24) leads to

$$\begin{cases} \frac{f(0)-f(1)}{d} = -\frac{1}{\mu(0)}(\mu_r k - \frac{E_0}{\sigma})f(0) \\ \frac{f(M-1)-f(M)}{d} = \frac{1}{\mu(-1)}(\mu_l k - \frac{E_1}{\sigma})f(M) \\ \frac{f(0)-2f(1)+f(2)}{d^2} = \frac{1}{\mu(0)}\left\{k^2\mu(0) + \frac{\mu_x}{\mu(0)}\left(\mu_r\, k - \frac{E_0}{\sigma}\right)\right\} f(0) \\ \frac{f(M-2)-2f(M-1)+f(M)}{d^2} = \frac{1}{\mu(-1)}\left\{k^2\mu(-1) - \frac{\mu_x}{\mu(-1)}\left(\mu_l\, k - \frac{E_1}{\sigma}\right)\right\} f(M) \end{cases}$$

which are rewritten as

$$\begin{cases} ((\frac{\mu(0)}{dE_0} + \frac{\mu_r k}{E_0})\sigma - 1)f(0) - \frac{\sigma\mu(0)}{dE_0}f(1) = 0 \\ -\frac{\sigma\mu(-1)}{dE_1}f(M-1) + ((\frac{\mu(-1)}{dE_1} + \frac{\mu_l k}{E_1})\sigma - 1)f(M) = 0 \\ (\sigma(d^2k^2 + \frac{\mu_x}{\mu(0)^2}d^2\mu_r k - 1) - \frac{\mu_x}{\mu(0)^2}d^2E_0)f(0) + 2\sigma f(1) - \sigma f(2) = 0 \\ \sigma f(M-2) - 2\sigma f(M-1) + (\sigma(d^2k^2 - \frac{\mu_x}{\mu(-1)^2}d^2\mu_l k - 1) + \frac{\mu_x}{\mu(-L)^2}d^2E_1)f(M) = 0 \end{cases}$$

Using these finite difference approximations, the discrete analog of the problem defined by (6.23) and (6.24) is given by following system of algebraic equations.

$$\mathbf{A}\mathbf{f} = 0, \tag{6.25}$$

where $\mathbf{f}$ is the vector with entries $f_0, f_1, f_2, ..., f_M$ and $\mathbf{A}$ is a square matrix whose entries, now denoted by $\mathbf{A}_{ij}$, $i, j = 1, 2, ..., (M+1)$, are given by

$$\mathbf{A}_{11} = (\tfrac{\mu(0)}{dE_0} + \tfrac{\mu_r k}{E_0})\sigma - 1, \quad \mathbf{A}_{12} = -\tfrac{\sigma\mu(0)}{dE_0},$$
$$\mathbf{A}_{21} = \sigma(d^2k^2 + \tfrac{\mu_x}{\mu(0)^2}d^2\mu_r k - 1) - \tfrac{\mu_x}{\mu(0)^2}d^2E_0, \quad \mathbf{A}_{22} = 2\sigma, \quad \mathbf{A}_{23} = -\sigma,$$
$$\mathbf{A}_{i,i-2} = (\tfrac{\mu}{d^4Pe} + \tfrac{3\mu_x}{2d^3Pe}), \quad \mathbf{A}_{i,i-1} = (-\tfrac{4\mu}{d^4Pe} - \tfrac{3\mu_x}{d^3Pe} - \tfrac{\sigma\mu Pe+2k^2\mu}{d^2Pe} - \tfrac{\mu_x\sigma Pe+3\mu_x k^2}{2dPe}),$$
$$\mathbf{A}_{i,i} = (\tfrac{6\mu}{d^4Pe} + \tfrac{2(\sigma\mu Pe+2k^2\mu)}{d^2Pe} + (\sigma + \tfrac{k^2}{Pe})k^2\mu - k^2\mu_x),$$
$$\mathbf{A}_{i,i+1} = (-\tfrac{4\mu}{d^4Pe} + \tfrac{3\mu_x}{d^3Pe} - \tfrac{\sigma\mu Pe+2k^2\mu}{d^2Pe} + \tfrac{\mu_x\sigma Pe+3\mu_x k^2}{2dPe}),$$
$$\mathbf{A}_{i,i+2} = (\tfrac{\mu}{d^4Pe} - \tfrac{3\mu_x}{2d^3Pe}), \quad \forall i \in [3, M-1]$$
$$\mathbf{A}_{M,M-1} = \sigma, \quad \mathbf{A}_{M,M} = -2\sigma, \quad \mathbf{A}_{M,M+1} = \sigma(d^2k^2 - \tfrac{\mu_x}{\mu(-1)^2}d^2\mu_l k - 1) + \tfrac{\mu_x}{\mu(-L)^2}d^2E_1,$$
$$\mathbf{A}_{M+1,M} = -\tfrac{\sigma\mu(-1)}{dE_1}, \quad \mathbf{A}_{M+1,M+1} = (\tfrac{\mu(-1)}{dE_1} + \tfrac{\mu_l k}{E_1})\sigma - 1.$$

6.3.2 Comparison of the Numerical Methods

We first solved the eigenvalue problem using the finite difference method above, but this method was slow when the mesh size was small. However, the pseudo-spectral Chebyshev method runs much faster and converges much more quickly than the finite difference method. Consider Figure 6.1. For some values of the parameters, we plot the dispersion relation given by the finite difference method using 20, 30, and 40 internal nodes and the Chebyshev method using 20, 30, 40, and 50 internal nodes. In the legend, M denotes the number of internal nodes. For the Chebyshev method, the four curves are indistinguishable. For the finite difference method, the values of $\sigma(k)$ increase as the number of nodes increase, and they converge to the value given by the Chebyshev method. Therefore, the Chebyshev method has already converged for $M = 20$. Additionally, the finite difference method confirms that our results are correct.

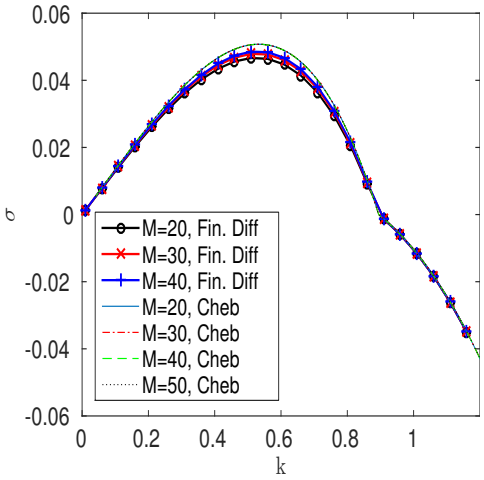

Figure 6.1: Plots of σ versus k for different values of M, the number of nodes in our discretization, and for each of the two numerical methods: pseudo-spectral Chebyshev method and Finite Difference method.

6.4 Variable Viscosity Radial Flow

We now show how to use the Chebyshev method to solve the eigenvalue problem for variable viscosity radial flow. Recall that the equation can be written in terms of $\lambda = 1/\sigma$ as

$$-\Big(\left(\zeta R_2^2(0) + R_0^2(\tau)\right) \mu f'(\zeta) \Big)' + \left(\frac{n^2 R_2^4(0)}{4(\zeta R_2^2(0) + R_0^2(\tau))} \right) \mu f(\zeta) = \frac{Q n^2 R_2^2(0)}{4\pi(\zeta R_2^2(0) + R_0^2(\tau))} \mu' \lambda f(\zeta), \tag{6.26}$$

which holds for $\zeta_1 < \zeta < 1$. As in the previous two cases, we map the interval $[-1, 1]$ to the interval $[\zeta_1, 1]$ using the affine map $\zeta = \frac{1-\zeta_1}{2}(y+1) + \zeta_1$. Therefore, our collocation points are $\zeta_i = \frac{1-\zeta_1}{2}(y_i + 1) + \zeta_1$. Additionally, since $\frac{d}{d\zeta} = \frac{2}{1-\zeta_1}\frac{d}{dy}$, we let $\mathbf{D}_{\mathbf{k}}^{\zeta} = \left(\frac{2}{1-\zeta_1}\right)^k \mathbf{D}_{\mathbf{k}}$.

We require that equation (6.26) hold at each collocation point, ζ_i, which gives a system of $N+1$ equations. Let $\mathbf{V}$ and $\mathbf{V}'$ be the matrices defined by (6.13). Let $\mathbf{X}$

be the diagonal matrix

$$(\mathbf{X})_{i,j} = \begin{cases} \zeta_{i-1}, & j = i, \\ 0, & \text{otherwise.} \end{cases}$$

Then the condition that (6.26) holds for each ζ_i is given by the matrix equation

$$\begin{aligned} &- \left(R_2^2(0)\mathbf{X} + R_0^2(\tau)\mathbf{I}\right)\mathbf{V}\mathbf{D}_{\mathbf{2}}^{\zeta}\mathbf{a} - \Big[\left(R_2^2(0)\mathbf{X} + R_0^2(\tau)\mathbf{I}\right)\mathbf{V}' + R_2^2(0)\mathbf{V}\Big]\mathbf{D}_{\mathbf{1}}^{\zeta}\mathbf{a} \\ &+ n^2 R_2^4(0)\mathbf{I}\Big(4\left(R_2^2(0)\mathbf{X} + R_0^2(\tau)\mathbf{I}\right)\Big)^{-1}\mathbf{V}\mathbf{D}_{\mathbf{0}}^{\zeta}\mathbf{a} \\ =&\lambda Q n^2 R_2^2(0)\mathbf{I}\Big(4\pi\left(R_2^2(0)\mathbf{X} + R_0^2(\tau)\mathbf{I}\right)\Big)^{-1}\mathbf{V}'\mathbf{D}_{\mathbf{0}}^{\zeta}\mathbf{a} \end{aligned}$$

where $\mathbf{I}$ is the $(N+1)\times(N+1)$ identity matrix. Let $\mathbf{A} = -\left(R_2^2(0)\mathbf{X} + R_0^2(\tau)\mathbf{I}\right)\mathbf{V}\mathbf{D}_{\mathbf{2}}^{\zeta} - \Big[\left(R_2^2(0)\mathbf{X} + R_0^2(\tau)\mathbf{I}\right)\mathbf{V}' + R_2^2(0)\mathbf{V}\Big]\mathbf{D}_{\mathbf{1}}^{\zeta} + n^2 R_2^4(0)\mathbf{I}\Big(4\left(R_2^2(0)\mathbf{X} + R_0^2(\tau)\mathbf{I}\right)\Big)^{-1}\mathbf{V}\mathbf{D}_{\mathbf{0}}^{\zeta}$ and $\mathbf{B} = Qn^2 R_2^2(0)\mathbf{I}\Big(4\pi\left(R_2^2(0)\mathbf{X} + R_0^2(\tau)\mathbf{I}\right)\Big)^{-1}\mathbf{V}'\mathbf{D}_{\mathbf{0}}^{\zeta}$. Then we have the generalized eigenvalue problem $\mathbf{A}\mathbf{a} = \lambda\mathbf{B}\mathbf{a}$. However, we must enforce the boundary conditions by amending the first and last rows of $\mathbf{A}$ and $\mathbf{B}$, which correspond to $\zeta_0 = 1$ and $\zeta_N = \zeta_1$, respectively. The boundary conditions can be rewritten as

$$\begin{aligned} &\frac{2R_2^4(\tau)}{R_2^2(0)}\mu(1)f'(1) + nR_2^2(\tau)\mu_o f(1) = \lambda E_2 f(1), \\ &\frac{2R_1^4(\tau)}{R_2^2(0)}\mu(\zeta_1)f'(\zeta_1) - nR_1^2(\tau)\mu_i f(\zeta_1) = -\lambda E_1 f(\zeta_1). \end{aligned}$$

Therefore, the first and last rows of $\mathbf{A}$ and $\mathbf{B}$ are

$$\begin{aligned} (\mathbf{A})_{1,j} &= \frac{2R_2^4(\tau)}{R_2^2(0)}\mu(1)(\mathbf{D}_{\mathbf{1}}^{\zeta})_{1,j} + nR_2^2(\tau)\mu_o(\mathbf{D}_{\mathbf{0}}^{\zeta})_{1,j}, \\ (\mathbf{A})_{N+1,j} &= \frac{2R_1^4(\tau)}{R_2^2(0)}\mu(\zeta_1)(\mathbf{D}_{\mathbf{1}}^{\zeta})_{N+1,j} - nR_1^2(\tau)\mu_i(\mathbf{D}_{\mathbf{0}}^{\zeta})_{N+1,j}, \\ (\mathbf{B})_{1,j} &= E_0(\mathbf{D}_{\mathbf{0}}^{\zeta})_{1,j}, \\ (\mathbf{B})_{N+1,j} &= -E_1(\mathbf{D}_{\mathbf{0}}^{\zeta})_{N+1,j}. \end{aligned}$$

We solve the generalized eigenvalue problem using MATLAB's "eig" command.

7. CONCLUSIONS AND FUTURE WORK

In this dissertation, we have studied the linear stability of multi-layer Hele-Shaw flows. In doing so, we have added to the understanding of both radial and rectilinear flows. In the rectilinear geometry, we first studied three-layer variable viscosity flows in the absence of diffusion. We proved that for increasing viscous profiles, there is a countably infinite number of real eigenvalues and the associated eigenfunctions are complete in a certain Sobolev space. We then did an in-depth study of the special case of an exponential viscous profile. We found a sequence of numbers which interlace with the eigenvalues, thus providing both upper and lower bounds.

In chapter 3, we studied the effect of diffusion on the stability of three-layer variable viscosity rectilinear flows using the non-dimensionalized version of the mathematical formulation given in [29]. This led to a system of coupled, second order ODEs. We were able to prove analytically that the maximum value of the growth rate could be made arbitrarily small by large enough diffusion. Additionally, some numerical calculations showed that by choosing optimal viscous profiles, drastic stabilization can be attained by a modest amount of diffusion.

In chapters 4 and 5, we turned our attention to flows in the radial geometry. In chapter 4, we investigate constant viscosity flows with an arbitrary number of fluid layers. We formulated the eigenvalue problem, including exact solutions for two and three layer flows. We also found upper bounds which depend simply on the physical parameters. Using these upper bounds, we were able to show that using many layers of fluid with small viscous jumps can be used to stabilize the flow.

In chapter 5, we studied variable viscosity radial flows - the first study of its kind. We formulated the eigenvalue problem that governs the growth rate by using

a change of variables that freezes the basic solution. We then found upper bounds using the variational form. We also characterized the eigenvalues and eigenfunctions by defining a new measure and using a corresponding Hilbert space to achieve self-adjointness of the differential operator. Finally, we studied the problem numerically. In chapter 6, we described the numerical method used in the previous section.

There is a broad range of problems in this area that are still open and can be the topic of future studies. To start, there are several questions that arise from the above work that are worthy of a more in-depth look. One such topic is how to find the exact growth rate of a particular interface from the eigenvalues of the problem. For variable viscosity radial flows (see chapter 5), it would be useful to establish a more precise relationship between the growth rate in the transformed coordinate system and the growth rate in the physical coordinate system. Recall that for diffusion in rectilinear flow (see chapter 3), the growth rate was governed by an eigenvalue problem of the form

$$Af = \lambda Bf, \tag{7.1}$$

where A is a second order differential operator and B is a fourth order differential operator, both of which depend on the Peclet number Pe. In the limit as $Pe \to \infty$ (which coincides with the diffusion coefficient going to zero), B becomes a zeroth order differential operator, and thus the problem is second order. This limit is a singular perturbation problem and is worthy of further study. Also, problems of the type given in (7.1) are called linear operator pencils. These types of problems have been studied by many people including Markus [51]. Operator pencils with the eigenvalue in the boundary conditions have been studied by Mennicken and Möller [52], Möller and Zinsou [54], and Tretter [72], among others. However, these results are for pencils in which the order of A is greater than the order of B. Therefore, our

problem is unique and is worthy of exploration.

There are also many extensions to our stability work that would be of practical importance. For radial Hele-Shaw flows, we could change the variable viscosity equations to include the effects of diffusion. For both radial and rectilinear flows, it would be interesting to study the stability for several different physical phenomena including Non-Newtonian fluids in the intermediate layer, the effect of using surfactants in the intermediate layer which causes variable interfacial tension, and variable injection rates. All of these things have been shown to affect the stability of the problem, and in some cases enhance it, but there is a lack of rigorous stability results. It would also be worthwhile to study the non-linear stability of multi-layer Hele-Shaw flows. For a single fluid with variable viscosity, the non-linear stability has been studied by Daripa and Hwang [25]. However, no such non-linear work has been done in the multi-layer case.

Finally, it would be fruitful to perform some numerical simulations as a comparison to the stability results we have obtained. Although there is a vast literature on free boundary problems, including simulations of Hele-Shaw flows with various properties, there is little numerical work on multi-layer Hele-Shaw flows. From the above list of possible projects, there is clearly much room for future endeavors in this field.

REFERENCES

[1] T. Al-Housseiny and H. Stone, *Controlling viscous fingering in tapered Hele-Shaw cells*, Phys. Fluids, 25 (2013), 042110.

[2] M. Awasthi, R. Asthana, and G. Agrawal, *Pressure corrections for viscous potential flow analysis of radial fingering in Hele-Shaw cell*, J. Engrg. Math., 83 (2013), pp. 131–142.

[3] J. Bataille, *Stability of a radial immiscible drive*, Revue Inst. Pétrole, 23 (1968), pp. 1349-1364.

[4] B. Bazaliy and A. Friedman, *The Hele-Shaw problem with surface tension in a half-plane: A model problem*, J. Differential Equations, 216 (2005), pp. 387–438.

[5] J. Boyd, *Chebyshev and Fourier Spectral Methods*, Dover Publications, New York, 2001.

[6] C. Carasso and G. Pasa, *An optimal viscosity profile in the secondary oil recovery*, Rairo-Math. Model. Num., 32 (1998), pp. 211–221.

[7] C. Carasso and G. Pasa, *A modified green's function to estimate the interface stability in oil recovery*, Comput. Methods in Appl. Mech. Eng., 190 (2000), pp. 1197–1207.

[8] S. Cardoso and A. Woods, *The formation of drops through viscous instability*, J. Fluid Mech., 289 (1995), pp. 351–378.

[9] C. Chen, Y. Huang, and J. Miranda, *Radial Hele-Shaw flow with suction: Fully nonlinear pattern formation*, Phys. Rev. E, 89 (2014), 053006.

[10] R. Chuoke, P. Van Meurs, and C. Van Der Poel, *The stability of slow, immiscible, viscous liquid-liquid displacements in a permeable media*, Trans. AIME, 216 (1959), pp. 188–194.

[11] R. Churchill, *Expansions in series of non-orthogonal functions*, Bull. Amer. Math. Soc., 48 (1942), pp. 143–150.

[12] P. Coussot, *Saffman-Taylor instability in yield-stress fluids*, J. Fluid Mech., 380 (1999), pp. 363–376.

[13] L. Cummings, S. Howison, and J. King, *Two-dimensional Stokes and Hele-Shaw flows with free surfaces*, European J. Appl. Math, 10 (1999), pp. 635–680.

[14] M. Dallaston and S. McCue, *New exact solutions for Hele-Shaw flow in doubly connected regions*, Phys. Fluids, 24 (2012), 052101.

[15] H. Darcy, *Les Fontaines Publiques de la Ville de Dijon*, Dalmont, Paris, 1856.

[16] P. Daripa, *Hydrodynamic stability of multi-layer Hele-Shaw flows*, J. Stat. Mech., 12 (2008), P12005.

[17] P. Daripa, *Studies on stability in three-layer Hele-Shaw flows*, Phys. Fluids, 20 (2008), 112101.

[18] P. Daripa, *On estimates for short wave stability and long wave instability in three-layer Hele-Shaw flows*, Physica. A, 390 (2011), pp. 3069–3076.

[19] P. Daripa, *On stabilization of multi-layer Hele-Shaw and porous media flows in the presence of gravity*, Transport Porous Med., 95 (2012), pp. 349–371.

[20] P. Daripa, *Some useful upper bounds for the selection of optimal profiles*, Physica. A, 391 (2012), pp. 4065–4069.

[21] P. Daripa and X. Ding, *A numerical study of instability control for the design of an optimal policy of enhanced oil recovery by tertiary dispalcement processes*, Transport Porous Med., 93 (2012), pp. 673–703.

[22] P. Daripa and X. Ding, *Universal stability properties for multi-layer Hele-Shaw flows and application to instability control*, SIAM J. Appl. Math., 72 (2012), pp. 1667–1685.

[23] P. Daripa and X. Ding, *Harnessing diffusion with impermeable interfaces for extreme stabilization*, Unpublished manuscript, Texas A&M University, College Station, 2013.

[24] P. Daripa and X. Ding, *Selection principle of optimal profiles for immiscible multi-fluid Hele-Shaw flows and stabilization*, Transport Porous Med., 96 (2013), pp. 353–367.

[25] P. Daripa and H. Hwang, *Nonlinear Saffman-Taylor instability for Hele-Shaw flows*, J. Differential Equations, 245 (2008), pp. 1819–1837.

[26] P. Daripa and G. Pasa, *New bounds for stabilizing Hele-Shaw flows*, Appl. Math. Lett., 18 (2005), pp. 1293–1303.

[27] P. Daripa and G. Pasa, *On the growth rate for three-layer Hele-Shaw flows: Variable and constant viscosity cases*, Int. J. Engg. Sci, 43 (2005), pp. 877–884.

[28] P. Daripa and G. Pasa, *A simple derivation of an upper bound in the presence of a viscosity gradient in three-layer Hele-Shaw flows*, J. Stat. Mech., 1 (2006), P01014.

[29] P. Daripa and G. Pasa, *Stabilizing effect of diffusion in enhanced oil recovery and three-layer Hele-Shaw flows with viscosity gradient*, Transport Porous Med., 70 (2007), pp. 11–23.

[30] P. Daripa and G. Pasa, *On diffusive slowdown in three-layer Hele-Shaw flows*, Quart. Appl. Math., LXVIII (2010), pp. 591–606.

[31] E. Dias and J. Miranda, *Influence of inertia on viscous fingering patterns: Rectangular and radial flows*, Phys. Rev. E, 83 (2011), 066312.

[32] E. Dias and J. Miranda, *Determining the number of fingers in the lifting Hele-Shaw problem*, Phys. Rev. E, 88 (2013), 043002.

[33] E. Dias and J. Miranda, *Wavelength selection in Hele-Shaw flows: A maximum-amplitude criterion*, Phys. Rev. E, 88 (2013), 029901.

[34] P. Drazin and W. Reid, *Hydrodynamic Stability*, Cambridge Univ. Press., Cambridge, 1981.

[35] M. Ehrnstroem, J. Escher, and B. Matioc, *Well-posedness, instabilities, and bifurcation results for the flow in a rotating Hele-Shaw cell*, J. Math. Fluid Mech., 13 (2011), pp. 271–293.

[36] J. Escher and B. Matioc, *The parabolicity of the Muskat problem: Well-posedness, fingering, and stability results*, Z. Anal. Anwend., 30 (2011), pp. 193–218.

[37] J. Fontana, E. Dias, and J. Miranda, *Controlling and minimizing fingering instabilities in non-Newtonian fluids*, Phys. Rev. E, 89 (2014), 013016.

[38] A. Friedman and Y. Tao, *Nonlinear stability of the Muskat problem with capillary pressure at the free boundary*, Nonlinear Anal., 53 (2003), pp. 45–80.

[39] L. Galin, *Unsteady filtration with a free surface*, Dokl. Akad. Nauk. S.S.S.R., 47 (1945), pp. 246–249.

[40] C. Gin and P. Daripa, *Stability results for multi-layer radial Hele-Shaw and porous media flows*, Phys. Fluids, 27 (2015), 012101.

[41] C. Gin and P. Daripa, *A study of a non-standard eigenvalue problem and its application to three-layer immiscible porous media and Hele-Shaw flows with exponential viscous profile*, J. Math. Fluid Mech., 17 (2015), pp. 155–181.

[42] S. Gorell and G. Homsy, *A theory of the optimal policy of oil recovery by the secondary displacement process*, SIAM J. Appl. Math., 43 (1983), pp. 79–98.

[43] A. He, J. Lowengrub, and A. Belmonte, *Modeling an elastic fingering instability in a reactive Hele-Shaw flow*, SIAM J. Appl. Math., 72 (2012), pp. 842–856.

[44] S. Hill, *Channelling in packed columns*, Chem. Eng. Sci., 19 (1952), pp. 247–253.

[45] G. Homsy, *Viscous fingering in porous media*, Annu. Rev. Fluid Mech., 19 (1987), pp. 271–311.

[46] S. Howison, *Cusp development in Hele–Shaw flow with a free surface*, SIAM J. Appl. Math., 46 (1986), pp. 20–26.

[47] E. Ince, *Ordinary Differential Equations*, Dover Publications, New York, 1956.

[48] H. Kim, T. Funada, D. Joseph, and G. Homsy, *Viscous potential flow analysis of radial fingering in a Hele-Shaw cell*, Phys. Fluids, 21 (2009), 074106.

[49] S. Li, J. Lowengrub, J. Fontana, and P. Palffy-Muhoray, *Control of viscous fingering patterns in a radial Hele-Shaw cell*, Phys. Rev. Lett., 102 (2009), 174501.

[50] S. Li, J. Lowengrub, and P. Leo, *A rescaling scheme with application to the long-time simulation of viscous fingering in a Hele-Shaw cell*, J. Comput. Phys., 225 (2007), pp. 554–567.

[51] A. Markus, *Introduction to the Spectral Theory of Polynomial Operator Pencils*, American Mathematical Soc., Providence, 1988.

[52] R. Mennicken and M. Möller, *Non-Self-Adjoint Boundary Eigenvalue Problems*, North-Holland Mathematics Studies, Vol. 192, Elsevier, Amsterdam, 2003.

[53] J. Miranda and M. Widom, *Radial fingering in a Hele-Shaw cell: A weakly nonlinear analysis*, Phys. D, 120 (1998), pp. 315–328.

[54] M. Möller and B. Zinsou, *Asymptotics of the eigenvalues of a self-adjoint fourth order boundary value problem with four eigenvalue parameter dependent boundary conditions*, J. Funct. Space. Appl., 2013 (2013), 280970.

[55] N. Mungan, *Improved waterflooding through mobility control*, Canad. J. Chem. Engng., 49 (1974), pp. 32–37.

[56] M. Nagel and F. Gallaire, *A new prediction of wavelength selection in radial viscous fingering involving normal and tangential stresses*, Phys. Fluids, 25 (2013), 124107.

[57] Q. Nie and F. Tian, *Singularities in Hele–Shaw flows*, SIAM J. Appl. Math., 58 (1998), pp. 34–54.

[58] Q. Nie and F. Tian, *Singularities in Hele-Shaw flows driven by a multipole*, SIAM J. Appl. Math., 62 (2001), pp. 385–406.

[59] G. Pasa, *An existence theorem for a control problem in oil recovery*, Numer. Func. Anal. Opt., 17 (1996), pp. 911–923.

[60] L. Paterson, *Radial fingering in a Hele–Shaw cell*, J. Fluid Mech., 113 (1981), pp. 513–529.

[61] E. Paune, M. Siegel, and J. Casademunt, *Effects of small surface tension in Hele-Shaw multifinger dynamics: An analytical and numerical study*, Phys. Rev. E, 66 (2002), 046205.

[62] P. Polubarinova-Kochina, *On the motion of the oil contour*, Dokl. Akad. Nauk. S.S.S.R., 47 (1945), pp. 254–257.

[63] P. Saffman, *Viscous fingering in Hele–Shaw cells*, J. Fluid Mech., 173 (1986), pp. 73–94.

[64] P. Saffman and G. Taylor, *The penetration of a fluid into a porous medium or Hele-Shaw cell containing a more viscous liquid*, Proc. R. Soc. Lond. Ser. A, 245 (1958), pp. 312–329.

[65] P. Schmid and D. Henningson, *Stability and Transition in Shear Flows*, Springer, New York, 2001.

[66] M. Siegel, R. Caflisch, and S. Howison, *Global existence, singular solutions, and ill-posedness for the Muskat problem*, Comm. Pure Appl. Math., 57 (2004), pp. 1374–1411.

[67] M. Siegel, S. Tanveer, and W. Dai, *Singular effects of surface tension in evolving Hele–Shaw flows*, J. Fluid Mech., 323 (1996), pp. 201–236.

[68] C. Tan and G. Homsy, *Stability of miscible displacements in porous-media - rectilinear flow*, Phys. Fluids, 29 (1986), pp. 3549–3556.

[69] S. Tanveer, *Surprises in viscous fingering*, J. Fluid Mech., 409 (2000), pp. 273–308.

[70] S. Tanveer and X. Xie, *Analyticity and nonexistence of classical steady Hele-Shaw fingers*, Comm. Pure Appl. Math., 56 (2003), pp. 353–402.

[71] L. Trefethen, *Spectral Methods in MATLAB*, Society for Industrial and Applied Mathematics, Philadelphia, 2000.

[72] C. Tretter, *Nonselfadjoint spectral problems for linear pencils $N - \lambda P$ of ordinary differential operators with λ-linear boundary conditions: Completeness results*, Integral Equations Operator Theory, 26 (1996), pp. 222–248.

[73] E. Tzimas, A. Georgakaki, C. Garcia Cortes, and S. Peteves, *Enhanced oil recovery using carbon dioxide in the european energy system*, Technical report, European Commission, 2005.

[74] A. Uzoigwe, F. Scanlon, and R. Jewett, *Improvement in polymer flooding: The programmed slug and the polymer-conserving agent*, J. Petrol. Tech., 26 (1974), pp. 33–41.

[75] J. Walter, *Regular eigenvalue problems with eigenvalue parameter in the boundary condition*, Math. Z., 133 (1973), pp. 301–312.

[76] S. Wilson, *Measurement of dynamic contact angles*, J. Colloid Interface Sci., 51 (1975), pp. 532-534.

[77] R. Wooding, *Growth of fingers at an unstable diffusing interface in a porous medium or Hele–Shaw cell*, J. Fluid Mech., 39 (1969), pp. 477–495.

[78] J. Ye and S. Tanveer, *Global existence for a translating near-circular Hele-Shaw bubble with surface tension*, SIAM J. Math. Anal, 43 (2011), pp. 457–506.

[79] ——, *Global solutions for a two-phase Hele-Shaw bubble for a near-circular initial shape*, Complex Var. Elliptic Equ., 57 (2012), pp. 23–61.